F1BEC File Copy

AD-A115183

AFWAL-TR-79-3095
VOLUME I

ADVANCED RESIDUAL STRENGTH DEGRADATION RATE MODELING FOR ADVANCED COMPOSITE STRUCTURES
VOLUME I - TASK I: PRELIMINARY SCREENING

D. E. Pettit
K. N. Lauraitis
J. M. Cox

Lockheed-California Company

Burbank, California

August 1979
Final Report for 1 August 1977 to 29 June 1979

Approved for public release; distribution unlimited

FLIGHT DYNAMICS LABORATORY
AIR FORCE WRIGHT AERONAUTICAL LABORATORIES
AIR FORCE SYSTEMS COMMAND
WRIGHT-PATTERSON AIR FORCE BASE, OHIO 45433

Best Available Copy

20060921112

NOTICE

When Government drawings, specifications, or other data are used for any purpose other than in connection with a definitely related Government procurement operation, the United States Government thereby incurs no responsibility nor any obligation whatsoever; and the fact that the government may have formulated, furnished, or in any way supplied the said drawings, specifications, or other data, is not to be regarded by implication or otherwise as in any manner licensing the holder or any other person or corporation, or conveying any rights or permission to manufacture use, or sell any patented invention that may in any way be related thereto.

This report has been reviewed by the Office of Public Affairs (ASD/PA) and is releasable to the National Technical Information Service (NTIS). At NTIS, it will be available to the general public, including foreign nations.

This technical report has been reviewed and is approved for publication.

George P. Sendeckyj

GEORGE P. SENDECKYJ, Aerospace Engineer
Fatigue, Fracture & Reliability Group

Davey L. Smith

DAVEY L. SMITH, Chief
Structural Integrity Branch

FOR THE COMMANDER

Ralph L Kuster

"If your address has changed, if you wish to be removed from our mailing list, or if the addressee is no longer employed by your organization please notify AFWAL/FIBEC, *W-PAFB, OH 45433 to help us maintain a current mailing list".*

Copies of this report should not be returned unless return is required by security considerations, contractual obligations, or notice on a specific document.

SECURITY CLASSIFICATION OF THIS PAGE (When Data Entered)

REPORT DOCUMENTATION PAGE

READ INSTRUCTIONS BEFORE COMPLETING FORM

1. REPORT NUMBER: AFWAL-TR-79-3095 Volume I	2. GOVT ACCESSION NO.
	3. RECIPIENT'S CATALOG NUMBER
4. TITLE (and Subtitle): Advanced Residual Strength Degradation Rate Modeling for Advanced Composite Structures	5. TYPE OF REPORT & PERIOD COVERED: Final Report 1 Aug. 77 to 21 June 79
	6. PERFORMING ORG. REPORT NUMBER: LR 28360-10
7. AUTHOR(s): D. E. Pettit, K. N. Lauraitis, J. M. Cox	8. CONTRACT OR GRANT NUMBER(s): F33615-77-C-3084
9. PERFORMING ORGANIZATION NAME AND ADDRESS: Lockheed-California Company, Division of Lockheed Aircraft Corporation, Burbank, California 91520	10. PROGRAM ELEMENT, PROJECT, TASK AREA & WORK UNIT NUMBERS: Project No. 2401, Work Unit 24010117
11. CONTROLLING OFFICE NAME AND ADDRESS: Flight Dynamics Laboratory, Air Force Wright Aeronautics Laboratory, Air Force Systems Command, Wright-Patterson AFB, Ohio, 45433	12. REPORT DATE: Aug 1979
	13. NUMBER OF PAGES: 279
14. MONITORING AGENCY NAME & ADDRESS (if different from Controlling Office)	15. SECURITY CLASS. (of this report): Unclassified
	15a. DECLASSIFICATION/DOWNGRADING SCHEDULE

16. DISTRIBUTION STATEMENT (of this Report)

Approved for public release: distribution unlimited

17. DISTRIBUTION STATEMENT (of the abstract entered in Block 20, if different from Report)

18. SUPPLEMENTARY NOTES

19. KEY WORDS (Continue on reverse side if necessary and identify by block number)

composites, graphite/epoxy, impact damage, damaged holes, fatigue, damage propagation, residual strength

20. ABSTRACT (Continue on reverse side if necessary and identify by block number)

This report presents the results of the first task of a three task program directed at the study of relationship between damage propragation and residual static strength of composite laminates. In Task I: Preliminary screening, two laminates a 24-Ply 67% 0° fiber and a 32-Ply quasi-isotropic laminate of T300/5208 graphite/epoxy material were selected for study. Two damage types were studied, a low velocity impact condition (i.e., simulated tool drop) and a badly drilled hole. An initial study was conducted for each damage type to determine the detailed damage introduction parameters resulting in the selection of one set of impact

(Continued on next page)

and one set of poor drilling conditions. Baseline static tension and static compression tests were conducted on each of the four damage/laminate conditions. Stress vs life (S-N) fatigue data were then generated at range ratio R = -1 for each of the four conditions. The damage growth characteristics were monitored on each fatigue specimen using a modified Holscan ultrasonic unit. A subset of the damaged hole specimens was also evaluated in static compression and fatigue (R = -1) using TBE enhanced X-ray methods to monitor damage growth and to assess any detremental effect of TBE on subsequent behavior of the damage.

The results indicate significant reduction in initial static tension and compression strengths for the damaged hole condition in both laminates. Impact damage resulted in a decrease in the static compression strengths of both laminates, 24-ply data were similar to the damaged hole results while 32-ply data showed a smaller reduction in strength than produced by the damaged hole. In tension the 24-ply laminate showed no loss of strength due to the impact damage while the 32-ply laminate showed a slight loss in strength for the largest damage sizes in the population. Under R = -1 fatigue 24-ply impact damaged specimens and 32-ply and 24-ply damaged hole specimens all exhibited typical S-N behavior with relatively consistent damage growth. Thirty-two ply impact damaged specimen fatigue behavior was erratic with specimens frequently failing away from the damage sites, supporting the static test results which indicated the selected damage size was at the threshold level for significant effect on the laminate behavior. Fatigue damage growth results also showed that the specimen stabilization method under compression loading can have a significant effect on S-N behavior of a specimen. Damage (at certain load values) would propragate to the supports and then stop for a period of time prior to failure. Based on the results of this task the damaged hole condition was selected for further evaluation in tasks II and III using the Holscan ultrasonic unit for damage monitoring.

PREFACE

This report has been issued in three volumes. Results of the work completed under Task I, Preliminary Screening, are reported in this volume, Volume I. Volumes II and III encompass the last two tasks of the investigation into the delamination growth and residual strength behavior of initially damaged graphite/epoxy laminates. Volume II includes the results of Task II - Damage Growth and Residual Strength Degradation Prediction and Task III - Effect of Fatigue Loading/Environment Perturbations. The tabulated data for these tasks are available in Volume III - Appendixes.

The work reported herein was accomplished under Contract F33615-77-C-3084, Project 2401, Work Unit 24010117, sponsored by the Flight Dynamics Laboratory of the Air Force Wright Aeronautical Laboratories, Air Force Systems Command, Wright-Patterson AFB, Ohio 45433. Dr. G. P. Sendeckyj, AFWAL/FIBE, was the Air Force Program Monitor.

The program which was conducted by the Structures and Materials Department of the Lockheed-California Company, was directed by the Co-Principal Investigators, Mr. D. E. Pettit and Ms. K. N. Lauraitis of the Fatigue and Fracture Mechanics Laboratory. Analytical and conceptual assistance was provided by Dr. J. T. Ryder of the same laboratory. The support and contributions of the Materials Laboratory personnel, Mr. W. E. Krupp, Group Engineer, Mr. R. C. Young, Specimen Fabrication, Mr. S. Krystkowiak, Fractography, and the Fatigue and Fracture Mechanics Laboratory Personnel, Mr. J. M. Cox, Data Reduction, Mr. D. Diggs, Mr. P. Mohr, Mr. F. Pickel, Mr. W. Renslen, Mr. L. Silvas and Mr. C. Spratt in the area of Mechanical Testing are gratefully acknowledged.

TABLE OF CONTENTS

Volume I

TABLE OF CONTENTS - Continued

Volume I

TABLE OF CONTENTS - Continued

Volume I

TABLE OF CONTENTS - Continued

Volume I

TABLE OF CONTENTS - Continued

Volume I

TABLE OF CONTENTS

Volume II

TABLE OF CONTENTS - Continued

Volume II

TABLE OF CONTENTS - Continued

Volume II

TABLE OF CONTENTS - Continued

Volume II

TABLE OF CONTENTS

Volume III

LIST OF ILLUSTRATIONS

Volume I

LIST OF ILLUSTRATIONS - Continued

LIST OF ILLUSTRATIONS - **Continued**

Volume I

LIST OF ILLUSTRATIONS - Continued

Volume I

LIST OF ILLUSTRATIONS - Continued

Volume I

LIST OF ILLUSTRATIONS - Continued

Volume I

LIST OF ILLUSTRATIONS - **Continued**

Volume I

LIST OF ILLUSTRATIONS

Volume II

LIST OF ILLUSTRATIONS - continued

Volume II

LIST OF ILLUSTRATIONS - continued

Volume II

LIST OF ILLUSTRATIONS - continued

Volume II

LIST OF ILLUSTRATIONS - continued

Volume II

LIST OF ILLUSTRATIONS - continued

Volume II

LIST OF ILLUSTRATIONS - continued

Volume II

LIST OF ILLUSTRATIONS - continued

Volume II

LIST OF ILLUSTRATIONS - continued

LIST OF ILLUSTRATIONS - continued

LIST OF ILLUSTRATIONS - continued

LIST OF ILLUSTRATIONS - continued

LIST OF ILLUSTRATIONS - continued

LIST OF ILLUSTRATIONS - continued

LIST OF TABLES

Volume I

LIST OF TABLES - Continued

Volume I

LIST OF TABLES

Volume II

LIST OF TABLES - continued

Volume II

LIST OF TABLES - continued

Volume II

LIST OF TABLES - continued

Volume II

SECTION I

INTRODUCTION

1.1 TECHNICAL BACKGROUND

The introduction of advanced composite materials into aircraft structural applications in recent years has necessitated the development of analytical methodologies to assure the same level of structural reliability found in comparable metal structures. Composite materials, however, are not well suited to a simple extrapolation of analysis methods used in metals. This is a result of the differences between the basic characteristics of composites and metals. For example, composites are strongly anisotropic by nature and contain major microscopic inhomogeneities reflecting the matrix/interface/fiber nature of the material. In addition first ply failures may occur very early relative to the total laminate failure load. Also the interlaminar strength in the thickness direction is totally different in strength level and micromechanics characteristics relative to the other directions.

Related to the basic differences in material characteristics is the question of what constitutes a defect or damage in a composite. For example, delaminations, matrix cracking, fiber breakage and matrix voids can readily occur in composite materials. From the standpoint of tension residual strength in the presence of a damage zone, energy may be absorbed by a variety of micromechanisms including fiber debond or stress relaxation, fiber breakage, plastic deformation and/or cracking of the matrix, delamination, etc. Under compression loading the damage form which reduces the structural stiffness may become the damage type of major concern, i.e., delaminations may become of greater importance and have a much different effect on the residual strength than is observed in tension. This type of behavior presents a unique aspect of composite behavior; that is, for different loading conditions different forms of damage in the laminate may constitute the damage of concern

which, unlike metals where most types of defect could conservatively be considered as cracks, may have entirely different initial characteristics and possibly propagate in a different manner.

Associated with the difficulties in defining the exact nature of damage and its effect on service life is the added problem of developing adequate nondestructive inspection methods to detect the damage and analysis methods to define its severity. The development of methods for defining, detecting, evaluating, and analyzing these types of damage in a framework consistent with current durability and damage tolerance requirements is the problem area addressed in the current program. Specifically, the objectives of the current program are (1) to develop a statistically valid data base defining the growth behavior of damage regions in graphite/epoxy composite material (2) develop an analysis methodology that is capable of predicting (a) the growth of damage zones under fatique loading and (b) the resulting residual strength of the structure with a given fatigue induced damage zone size and configuration, (3) determine the mechanisms of fatigue induced damage formation and propagation and (4) define the threshold damage sizes which will not propagate and the associated damage zone criteria.

1.2 PROGRAM OVERVIEW

The current program is composed of three major tasks: TASK I: Preliminary Screening is designed to screen the static and fatigue induced damage growth characteristics of two damage types. Based on these results a single damage condition is to be selected for study in Tasks II and III. TASK II: Damage Growth and Residual Strength Degradation Prediction develops statistically significant data sets of the static and fatigue life behavior and of the fatigue induced damage growth and residual strength behavior. Based on these data a model for predicting the damage growth characteristics and the subsequent residual strength will be developed. In TASK III: Effect of Fatigue Loading/Environment Perturbations, three variations in the loading/environmental parameters will be studied to evaluate the applicability of the model over a range of loading/environmental conditions and provide an update for the model if required.

This report presents the results of the Task I: Preliminary Screening, phase of the program, which provides the required preliminary data on the effects of initial damage conditions on static tension behavior, static compression behavior and on the fatigue damage propagation characteristics of advanced composite materials. Sections 2 and 3 of this report provide general background information covering 1) Selection of material, laminates, specimen design, damage types and NDI methods and 2) panel and specimen fabrication, methods of damage introduction and control of initial damage dimensions. Test procedures are outlined in Section 4 and results of static tests are presented in Section 5 which includes an evaluation of several types of compression restraints. Stress vs. life data for the two selected laminate types are given in Section 6 and damage growth measurement methods and results are discussed in Section 7. In addition to the selected Holscan ultrasonic C-scan damage tracking selected for this program, a subset of static and fatigue tests was conducted to evaluate the effect of the opaque dye additive TBE used in X-ray enhancement in subsequent damage development. These results are presented in Section 8.

Section 9 presents a summary of the major results of Task I and the general damage type and NDI method selected for use in subsequent tasks. An overview of the next task, Task II: Damage Growth and Residual Strength Degradation Prediction, is presented in Section 10.

SECTION 2

TASK I OVERVIEW

In Task I, two laminates were evaluated containing two different damage types. The static tension and compression properties were determined as was the damage growth behavior under fatigue loading. The following sections present the rationale employed in selecting the material laminates, specimen configuration, damage types and NDI methods to be used. The final section presents the detailed Task I test matrix.

2.1 MATERIAL/LAMINATE SELECTION

The material selected for use in this program was T300/5208. Two laminates were selected based on the following considerations:

a. Laminate must be representative of those commonly used in aircraft structures.

b. Interlaminar shear and tensile normal stresses should be minimized to prevent premature edge delamination.

c. Symmetry about the mid-plane should be maintained to avoid warping under load or due to fabrication stresses.

d. Both fiber and matrix dominated failures should be investigated.

e. Laminate thickness must be such that adequate bond strength can be obtained.

f. Laminates which are and are not delamination prone under fully reversed fatigue loading (R = -1) should be investigated.

Typical laminates for aircraft structures are frequently selected from the $0_i/\pm45_j/90_k$ or $0_i/\pm45_j$ orientation families. The 0° direction is generally oriented parallel to the principal axial loading direction; ±45 plies provide shear strength and stiffness or buckling resistance, and when needed, 90° plies

provide additional strength in the transverse direction, reduce the Poisson's ratio and can be used to mitigate some of the free edge stresses.

The selection of laminate stacking sequence was governed by three considerations: symmetry, tab bond strength requirements, and free-edge effects. Laminates of twenty-four or more plies impose severe strength requirements on the tab bond, so surface plies were selected to be oriented at 0°. Angle plies terminating at a free-edge induce interlaminar shear and normal stresses due to differences in Poisson ratios. The magnitude and sign of these stresses are functions of the lamina orientations, thicknesses, stacking sequence, and external and thermal stresses. Interlaminar normal tension stresses of sufficient magnitude can cause edge delamination that reduces both static and fatigue strengths. Stacking the laminate so that the normal stresses are compressive generally increases the fatigue strength over that of a laminate with tensile normal stresses. However, cyclically applied loading with reversing direction results in reversal of the sign of the normal stress. Consequently, for fatigue coupons subjected to compressive loading,laminae must be stacked to minimize normal stresses and thus their effects on fatigue strength.

A Lockheed computer program, SIGMZ, based on the method of Pagano and Pipes(1), which approximates the interlaminar stresses, was used as an aid in selecting the stacking sequences. Laminate ultimate strengths were calculated using the Lockheed program HYBRID. The results for tensile and compressive loading of the two laminates A, $(0/45/90/-45_2/90/45/0)_{2s}$, and B, $(0/45/0_2/-45/0_2/45/0_2/-45/0)_s$ are given in Table I.

Both of these 32 and 24 ply laminates meet the criteria expressed in considerations a through f. In compliance with f, data in Reference 2 have shown that laminate A is prone to delamination under both tension-tension and tension-compression fatigue loading while laminate B coupons have revealed no early delaminations during fatigue under either tension-tension or tension-compression fatigue. In fact the failure modes of these two laminates appear to differ in unnotched fatigue tests.

2.2 SPECIMEN DESIGN

Details of the specimen used in this program are presented in Figure 1. Features of this configuration leading to its selection are outlined below.

TABLE I. INTERLAMINAR NORMAL STRESSES AT FREE EDGES OF TEST COUPONS

	$(0/45/90/-45/-45/90/45/0)_{2s}$				$(0/45/0_2/-45/0_2/45/0_2/-45/0)_s$			
	Tension		Compression		Tension		Compression	
$\sigma_x{}^a$ MPa(ksi)	84.1(12.2)		-84.1(12.2)		538 (78)		-538 (-78)	
ΔT, °C (°F)	0 (0)	111 (200)	0 (0)	111 (200)	0 (0)	111 (200)	0 (0)	111 (200)
$\sigma_y{}^0$, MPa(psi)	1.43 (-208)	27.3 (3960)	1.33 (193)	9.94 (1442)	-32.1 (-4660)	-6.55 (-950)	22.2 (3220)	33.0 (4790)
$\sigma_y{}^{45}$, MPa(psi)	32.3 (4985)	34.4 (4985)	-32.2 (-4669)	-32.8 (-4754)	64.2 (9320)	13.2 (1910)	-44.4 (-6440)	-66.0 (-9580)
$\sigma_y{}^{90}$, MPa(psi)	-63.2 (-9174)	-94.4 (-13700)	63.1 (9150)	53.7 (7794)	-	-	-	-
$\sigma_z{}^{max}$, MPa(psi)	.32 (46)	1.70 (246)	.006 (9)	.38 (55)	0	0	.28 (40)	.34 (50)
$\sigma_z{}^{min}$, MPa(psi)	-.069 (-10)	.28 (41)	-.32 (-46)	-.34 (-49)	-.34 (-50)	-.07 (-10)	0	0

a - σ = 84.1 MPa(12.2 ksi) is the limiting stress for first ply failure, $\sigma_{90}{}^{tu}$, when ΔT is assumed to be 111°C (200°F) and σ_x = 538 MPa (78 ksi) is 2/3 of ultimate strength

FIGURE 1.

3-INCH WIDE SPECIMEN CONFIGURATION, DRAWING TL1038

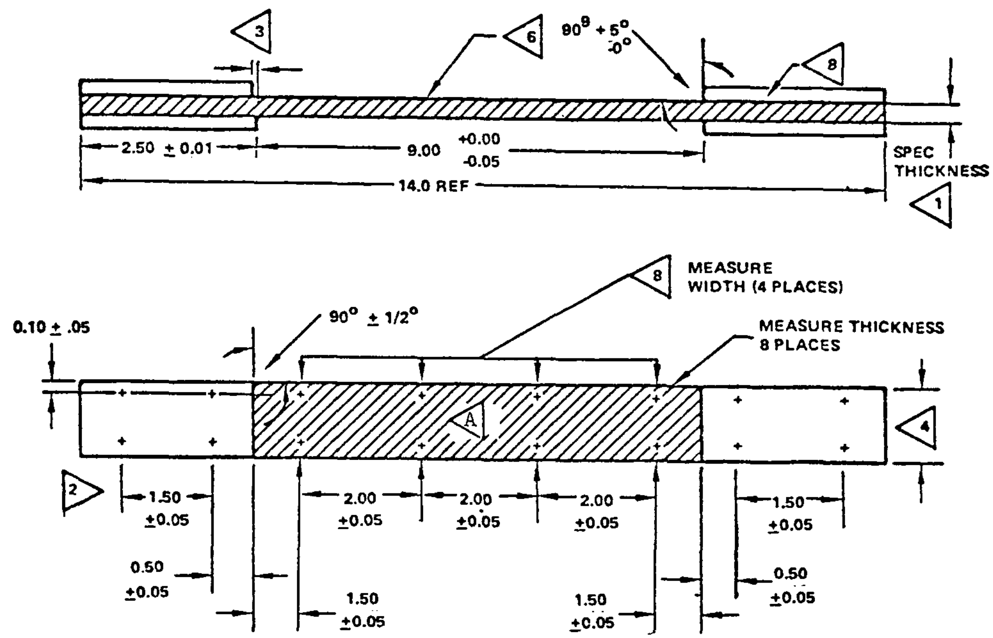

9 SPECIMENS TO BE FLAT OVER THE ENTIRE 14.0 INCH LENGTH WITHIN 0.01 INCHES, MEASURE AND RECORD ACTUAL FOR ALL SPECIMENS.

8 TAB EDGES TO BE PARALLEL TO SIDES OF SPECIMEN WITHIN 0.02 INCHES. OVERHANG NOT TO EXCEED 0.15

7 THE TAB AND SPECIMEN BONDING SURFACES TO BE THOROUGHLY SOLVENT CLEANED USING METHYL-ETHYL-KETONE PRIOR TO BONDING. A 350°F CURING ADHESIVE IS TO BE USED AND MUST COVER ENTIRE SURFACE UNIFORMLY'

6 WATER SPRAY MIST TO BE USED DURING SAWING OPERATIONS AND SOLUBLE OIL DURING GRINDING. MACHINED SURFACES TO BE RMS 50 OR BETTER. NO EDGE DAMAGE OR FIBER SEPARATION SHOULD BE VISIBLE

5 MEASURE SPECIMEN WIDTH 4 PLACES. WIDTH MUST NOT VARY BY MORE THAN 0.004 INCHES.

4 SPECIMEN WIDTH TO BE 3.00 $^{+0.00}_{-0.02}$ INCHES.

3 MISMATCH OF TABS FROM SIDE TO SIDE NOT TO EXCEED 0.01 INCHES.

2 TABS TO BE CUT FROM AN 6 PLY LAMINATE FABRICATED FROM PREPREG OF 1581 GLASS FABRIC IN A 350°F CURING EPOXY. TAB PLUS ADHESIVE THICKNESS MUST NOT VARY SIDE TO SIDE OR END TO END BY MORE THAN 0.01 INCH AS MEASURED 8 PLACES.

1 SPECIMEN THICKNESS TO BE WITHIN ±0.003 INCHES OF THE AVERAGE OF 8 THICKNESS MEASUREMENTS.

A Damage site, centered in specimen width and length.

NOTE: ALL MEASUREMENTS TO BE MADE USING A FLAT-HEADED MICROMETER.
ALL DIMENSIONS IN INCHES (1 IN. = 25.4 MM)

- The geometry can be used for static tension and compression tests as well as for either tension-tension or tension-compression fatigue tests.

- Adequate specimen length is important in composite specimens in order to obtain uniform stress conditions within the test section. Additionally, the selected length aids in minimizing end effects which could affect the damage propagation behavior without making the length too long to be able to control buckling in compression.

- The specimen size is sufficient to provide a good probability of including point-to-point variations in material and layup properties, as well as large enough to be more representative of aircraft structures.

- Variations in test results due to the discontinuity at the specimen edge will vary with laminate, material, and fabrication practice, but in general, will diminish as width is increased. The 3-inch (76mm) width was chosen to minimize the free edge effects which are usually on the order of a laminate thickness (References 3 and 4) so that these do not influence the damage propagation behavior.

- The specimen is wide enough such that a region exists where the stress distribution is not greatly influenced by the initial damage zone size at several flaw diameters away from the damage (References 5 and 6).

- Dimensions are convenient for fabrication and machining; tolerances required to obtain the necessary precision in test results are achievable without extraordinary measures.

The same specimen size and configuration was used for all tests including the static tension and compression tests in order to avoid any effects due to width or length differences.

2.3 SELECTION OF DAMAGE TYPE

A large number of possible defects and/or damage types may occur in composites due either to material defects, fabrication damage, or service induced damage. A questionnaire previously circulated throughout industry surveying the types of flaws that were anticipated and their relative criticality obtained the results presented in Reference 7 and are reproduced in Table II. For the current program, basic material flaws such as prepreg variations outside of limits, etc., which can be controlled by proper Q.C. are not considered,

TABLE 11.- SCORES OF FLAWS IN GRAPHITE/EPOXY IN RESPONSE TO QUESTIONNAIRE 1

Index of effects	Flaw type	Likelihood of occurrence: Frequent	Intermediate	Infrequent	Dropped[a]
25	External delamination, loose fibers, disbonding		x		
25	Internal delamination, blister		x		
66	Oversized hole	X			
38	Hole exit side broken fibers, breakout	X			
32	Tearout or pull-through in countersinks			0	
62	Prepreg variabilities exceeding preset levels	X			
9	Resin-starved bearing surface				0
14	Resin-rich or fiber-starved areas	X			
19	Excessive porosity, voids		x		
10	Scratch, fiber breakage, damage done in handling				0
22	Dent, no fiber breakage, damage done in handling	X			
9	Fiber breakaway from impact surface				0
31	Edge delamination, splintering	X			
10	Overtorqued fastener				0
7	Split tow, fiber separation				0
17	Edge notch or crack			0	
19	Corner notch or crack			0	
13	Mislocated hole - not required			0	
28	Mislocated hole - resin refilled, redrilled		x		
27	Wrinkles, waviness, miscollimation	X			
28	Marcelled fibers	X			
29	Reworked areas	X			
20	Missing ply or plies			0	
24	Foreign particle, contamination, inclusion	X			
25	Out-of-round hole	X			
9	Wrong material				0
21	Misoriented ply			0	
15	Ply overlap	X			
19	Ply underlap, gap		x		
13	First ply failure or separation		x		
27	Improper fastener seating	X			
21	Variable cure, temperature inhomogeneities in oven		x		
24	Figure 8 hole			0	
25	Nonuniform bond joint thickness			0	
9	Off-axis drilled hole (i.e., not perpendicular to surface)				0
25	Countersink on wrong side of laminate		x		
25	Mislocated cocured assemblies in same tool		x		
15	Tool impressions	X			
9	Burned drilled holes from high-speed drilling				0
21	Pills and fuzz balls			0	
3	Undersized fasteners				0
25	Grossly nonuniform agglomerations of hardener agents			0	
20	Misfitting parts cutting fibers in fillets, poor seating		x		
16	Metal-graphite/epoxy mating surfaces not shear balanced				0
20	Overwarpage of parts from poor tooling				
30	Process control coupon thickness not constant or misrepresentative				0

Index of Effects = (likelihood scores) x (criticality scores) on a scale of 0 to 100 as follows:

100 = (very frequent flaw) x (most crucial effects)
56 = (fairly common experience) x (critical flaw)
25 (occasional occurrence) x (possibly critical flaw)
6 = (rare, low likelihood) x (minor effects)

[a]Dropped or eliminated when index scored less than 10 or flaw is design error

There were 281 scores in the "frequent," X, category, 249 in the "intermediate," x, category, and 203 in the "infrequent," 0, category.

the primary emphasis being placed on manufacturing type damage which can be introduced in a controlled manner that permits more meaningful statistical analysis of the results.

The first damage type selected for study was that of a poorly drilled hole which results in multiple delaminations in the hole. This damage condition was selected over an alternative damage of a surface cut or gouge since it represents a condition likely to occur because large numbers of holes are required in a structure and it provides an analogous case to the corner crack at a hole in metal structures. In addition, the case of a surface cut is being studied in detail by NASA and has been examined by Sendeckyj et al[8] who indicates a relatively simple analysis may be adequate for predicting the residual strength for this damage case.

A second dangerous damage which can occur in composites is that which can result from low velocity impact of dropped tools, etc., since this type of damage could occur in any location, often shows no indications of damage on the impacted surface and may not show much damage on the side opposite the impact[9,10]. As a result, second damage type studied was that produced by dropping an impactor on the panel.

2.4 EVALUATION AND SELECTION OF NDI METHOD FOR DAMAGE MONITORING

The detection of damage in composites by NDI methods must, as for the analysis, be considered in the context of the condition that the method is designed to detect and the type of damage to which this would correspond. Methods most commonly used for the inspection of composites are ultrasonic C-scan, x-ray, Moiré, brittle lacquer, acoustic imaging, photoelastic casting, penetrant, thermography, acoustic emission and laser holography.

At the present state-of-the-art, most NDI methods which provide adequate damage detail cannot be used continuously without introducing the adverse conditions of: (a) inserting a foreign substance and an accompanying unknown effect (i.e. penetrant and TBE enhanced X-ray), (b) a water bath environment (ultrasonics and acoustic imaging), or (c) temperature excursions (thermography). In the current program the major criteria for the selection of NDI methods were fourfold; (a) to select a method which provides the most detailed information

as to the size, shape and most importantly, the type of damage which is present, (b) to select a system which introduces the minimum number of potential external factors into the specimen damage growth behavior, (c) to select a system which can be readily used in a laboratory environment and, (d) to provide a tie between the indications of the method selected with the type of damage size indications that would be measured using a normal service NDI method.

A review of current literature shows that of the variety of NDI methods available, few provide detailed information on the type of damage present. One class of methods which has been used provides information only on the extent of surface distortion by monitoring displacements in the thickness direction. These methods include laser holography and Moiré methods. While some report limited success using these methods[11], no quantitative correlation between strength and the holographic indications could be found, probably due to the lack of definition of the specific type of damage which resulted in the NDI indication.

X-ray methods have been used by many, but it is usually necessary to use an opaque additive dye, such as TBE (tetrabromoethane) to enhance the resulting x-ray[8,12,13]. This method appears to offer the potential of being able to define considerable detail of the actual types of damage which are occurring. Added information on the number of delaminations, etc, which lie above one another can also be obtained by carefully varying the exposures and the x-ray angle on multiple shots and comparing the results. This method provides photos which can be input for computer enhancement analysis. On the negative side, TBE is a hazardous material to work with in that it is extremely toxic and constitutes a health hazard due to inhalation and skin contact, thus making its use outside of a controlled laboratory situation highly unlikely. More importantly, questions exist as to its effect on the subsequent material behavior[12]. From a chemical viewpoint, the potential to plasticize the epoxy is real. In the current program where the fatigue tests may run for a considerable period of time, the effect could be magnified. In addition, only those damage areas that intersect a surface where the TBE can infiltrate the damage zone will be seen. Thus, damage limited to the inside region with no

path to the free surface can not be observed. Thus while the method provides considerable detail (assuming all damage areas are wetted and penetrated by the TBE), the serious question of its effect on subsequent material behavior must be resolved before it can be used with confidence.

Acoustic emission has also been used[12] and, while being one of the few methods that has the potential of detecting fiber breakage, is not capable of giving more than a general level of activity type of information and provides only limited definition of the source type and location.

Application of acoustic imaging methods had also been shown to have the potential to detect and define certain types and extent of damage in composite materials[15,16]. Unlike radiography, any small inclusion or discontinuity in a material will scatter acoustic energy; hence cracks and defects can produce substantial acoustic signal variations. The main disadvantage of this method is that an acoustic transfer medium (water) must be in contact with the specimen. This is the same disadvantage of normal C-scan ultrasonics.

Another method, ultrasonic C-scan[8,11], has been used in the past with mixed results. For C-scan this results from the "go,no-go" type of instrument normally used which results in only an indication of a loss of energy equal to a preset standard and provides only a plan area view of the damage with no detail as to damage type. In addition, results obtained by Sendeckyj show that immersion of samples containing near surface delaminations from holes can result in the loss of the thru-transmission ultrasonic damage indication due to water intrusion into the delamination[17]. Thus the two main limitations with traditional ultrasonic C-scan methods are a lack of detailed information from normal go,no-go C-scan results and the potentially adverse effects of sample immersion in a water bath.

Evaluation of alternate ultrasonic techniques, however, showed an alternate method to be available which minimized the usual limitations of normal ultrasonic procedures. The system selected for use was a specially modified Holscan System 400 produced by Holosonics Inc. This unit is a pitch-catch type of ultrasonic system as opposed to a thru-transmission type.

The system consists of a basic Holosonic System 400 with the following modifications:

a) The "flex arm" transducer mount was replaced with a digital mechanical scanner control interfaced with the System 400 electronics. This overcomes the basic system limitation of requiring a manual hand scanning of the specimen and enables the addition of a recall memory capability. In addition, this mounting system permits a larger selection of transducers with the needed characteristics for use in the current program.

b) A digital memory, real time image display electronic processor and dual mode scope was interfaced with the System 400 electronics to provide a digital memory storage unit to retain and provide subsequent display of the data in C-scan and associated B-scan format as well as 3-D isometric format. This provides a major tool to assess composite damage characteristics in that measurement of the ply level at which damage occurs can be determined as can the extent of the damage at each level.

c) A vertical mounting and coupling system was attached to the transducer/digital scanner. Inclusion of this system provides a system which can be used on test specimens mounted in the test frame, thus eliminating the necessity to remove and reinstall specimens each time they are to be examined. This provides a major improvement also in that the specimen is not immersed in water for extended periods such as occur during normal C-scan, the water contact being limited to the 1/2 inch (13mm) diameter water column directly in front of the scanning transducer. In addition, only a single scan is required, the data then being available in the memory for further analysis.

Preliminary results obtained with this type of system have been found to be quite good for characterizing impact damage in composites as previously discussed in Reference 18. A full discussion of the final system is presented in Reference 18.

A second NDI method was also evaluated in TASK I, that of enhanced X-ray. This method offers the potential of being able to define the types of damage which are occurring, but the effects of the TBE or similar enhancing fluids are not known. As a result this method was included as a separate subset of tests to assess the magnitude of any effect, if present.

2.5 TASK I TEST PLAN

The Task I test matrix is presented in Table III. Item 1 tests (Table III) consisted of standard quality control tension tests using duplicate specimens from each of the test panels fabricated. Item 2 tests consisted of ten replicate tests in tension and ten replicate tests in compression using the fatigue supports for each of the four laminate/damage conditions. These tests were conducted to failure without interruption.

A subset of static compression tests was included in Item 3 to evaluate the inherent local buckling characteristics of the damaged laminate. This characteristic behavior is of importance since normal constrained compression testing may yield compressive failure values which are unrealistically high compared to the restraint conditions of a typical structure. These tests thus supply additional specimen stability data to verify or give direction to the modification of the guides required in the subsequent R = -1 fatigue testing to assure that the specimen response simulates that of actual structure as closely as possible.

The tests shown in Table III as Item 4 were designed to provide the basic S-N curve for each of the four laminate/damage conditions while also providing the basic fatigue induced damage growth characteristics for each of the laminate/damage conditions. For these tests, three replicates were tested at each of six stress levels to define the general R = -1 S-N characteristics for each of the four laminate/damage conditions. The damage growth was monitored by use of a Holosonics Series 400 Holscan unit, as described in Section 2.4.

A subset of both static compression and fatigue tests was conducted to provide a statistically based answer as to the effect of TBE on subsequent material behavior, as shown in Items 5 and 6 in Table III. No significant effect of TBE has been reported in static tension (reference 8). Therefore a series of specimens were tested in compression by loading duplicate specimens to each of three strain levels, removing them and running ultrasonic analysis of the damage and then conducting TBE enhanced X-ray analysis. The specimens were then reloaded to failure. In this manner a set of six

TABLE III. PROPOSED TASK I TEST MATRIX

Item	Test Type	Laminate/Damage Conditions	Replicates	Data Required	Total Number Of Test Specimens
1.	Panel Quality Control	2 laminates, no damage = 2	2 per panel x 5 panels per laminate	Quality control tensile data	20
2.	Initial Static Tension and Compression Strength Determinations.	2 laminates x 2 damage = 4	10 replicates x 4 conditions x 2 test types	Residual Strength	80
3.	Column Buckling Tests	2 laminates x 2 damage = 4	1 each x 4 column length x 4 conditions	Buckling conditions	16
4.	Base S-N Fatigue Tests	2 laminates x 2 damage = 4	3 replicas x 6 stress levels x 4 conditions	Base S-N data and damage propagation data	72
5.	Initial Static Compression Strength Determination	2 laminates x 2 damage = 4	2 replicas x 3 stress levels x 4 conditions	Damage growth and effect of TBE	24
6.	S-N Fatigue Tests	2 laminates x 2 damage = 4	3 replicas x 3 stress levels x 4 conditions	Damage growth and affect of TBE on damage growth	36
					248

specimen results per laminate/damage conditions were available for comparison with the 10 reference sets of data. In addition, added data on damage growth under static loading were made available for subsequent analysis.

The subset of fatigue tests to examine the effect of TBE additions on the subsequent fatigue behavior consisted of running triplicate specimens at three of the six stress levels examined in Item 4 of Table IV. These tests were conducted using the same procedures as the Item 4 tests except that following each ultrasonic examination, a set of TBE enhanced X-rays was taken. From these results both a direct comparison of the TBE enhanced X-ray and ultrasonic inspection results was obtained and a data base for examining the effect of the TBE on the fatigue behavior was established.

The number of coupons selected to be tested at each test condition was chosen to adequately insure a large enough data set for obtaining statistically meaningful and reliable distributions of fatigue life and static residual strength. The number of test points at any particular condition needed to insure adequate statistical confidence (at least 90% and preferably 95% or better) depends upon the dispersion of the data. The particular distribution function (binomial, Poisson, multinomial, normal, Weibull or other) chosen to represent data dispersion also affects the confidence that can be applied to the same data set. The most common distribution used in analyses of composite data is the Weibull distribution (Reference 19), $P(x) = \exp [- ((x-e)/(v-e))^{k}]$, where e, v, and k are constants. With these thoughts in mind, the number of test specimens at each test condition required for acceptable confidence of the data dispersion and probability of survival of any one coupon was considered. For this preliminary TASK I study, a sample size of 10 coupled with the double random specimen selection procedure was selected to provide adequate statistical significance for a meaningful indication of mean data trends.

The results of the Task I tests thus provide, a) a data base for the selection of the stress riser (damage type) to be used in the Task II and III study, b) the basic fatigue induced damage propagation characteristics of the damage zone over a range of stress levels, c) the basic tension and compression

static strength and static damage formation characteristics for the four laminate/damage conditions, and d) data on the column buckling characteristics for four laminate/damage conditions.

SECTION 3

SPECIMEN FABRICATION AND QUALITY CONTROL

All material procurement, panel fabrication and specimen fabrication were controlled to conform to the program Quality Control Plan requirements as presented in Reference 20. The following sections present a summary of the requirements and the results of each phase of the specimen fabrication sequence.

3.1 MATERIAL QUALITY CONTROL RESULTS

Following approval of the Quality Control Plan, one material batch of T300/5208 material was procured for TASK I from Narmco Materials, Inc. The material (Batch number 1015) was found to meet all requirements of the Quality Control Plan and the material was accepted. All material qualification tests were conducted by both Narmco Materials Inc., and the Lockheed California Company Quality Control Division and were reported in Reference 20.

Two 12 by 12 inch (305 x 305mm) cure cycle trial panels were intially made to verify the fabrication procedure given in the Quality Control Plan [20]. One panel was fabricated of each of the two lay-ups selected for study, a 24 ply 67% 0° fiber laminate $(0/+45/0_2/-45/0_2/+45/0_2/-45/0)_s$ and a 32 ply 25% 0° fiber quasi-isotropic laminate $(0/+45/90/-45_2/90/+45/0)_{2s}$. Acid digestion, fiber fraction determination by density measurement and metallographic examination of the two preliminary 12 by 12 inch (305 x 305mm) cure trial panels showed the percent fiber volumes to be 64.0% for the 24 ply material (panel #1SY1156) and 62.9% for the 32 ply material (panel #2SY1156). Ultrasonic evaluation and metallographic sections (see Figures 2 and 3) show the panels to be free of significant void formation or other major defects. Unfortunately, during the 11-day Lockheed Plant shutdown from December 24, 1977 to January 3, 1978, the freezer in

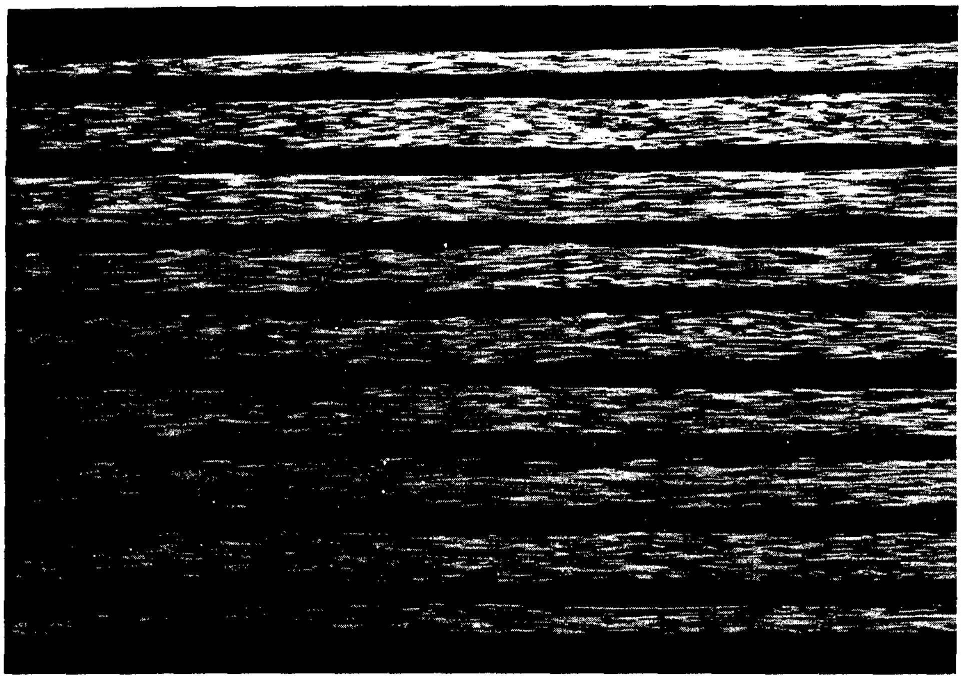

(a) Outer Area of Panel 2519-1-2, 25X

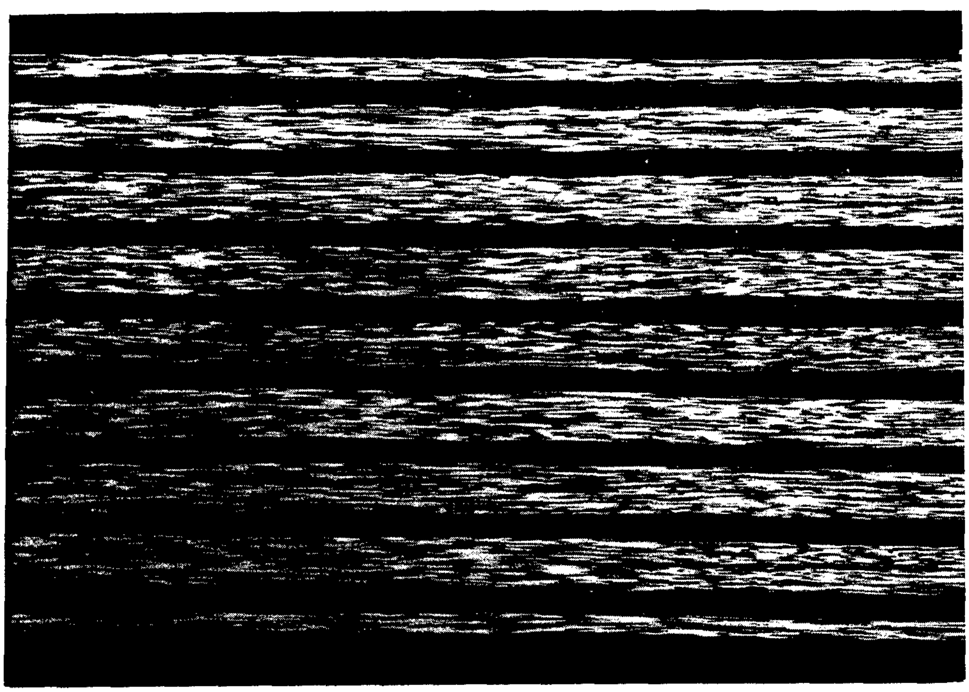

(b) Center Area of Panel 2519-2-3, 25X

Figure 2. Typical Metallographic Sections of Panel 1SY1156, 24 ply T300/5208

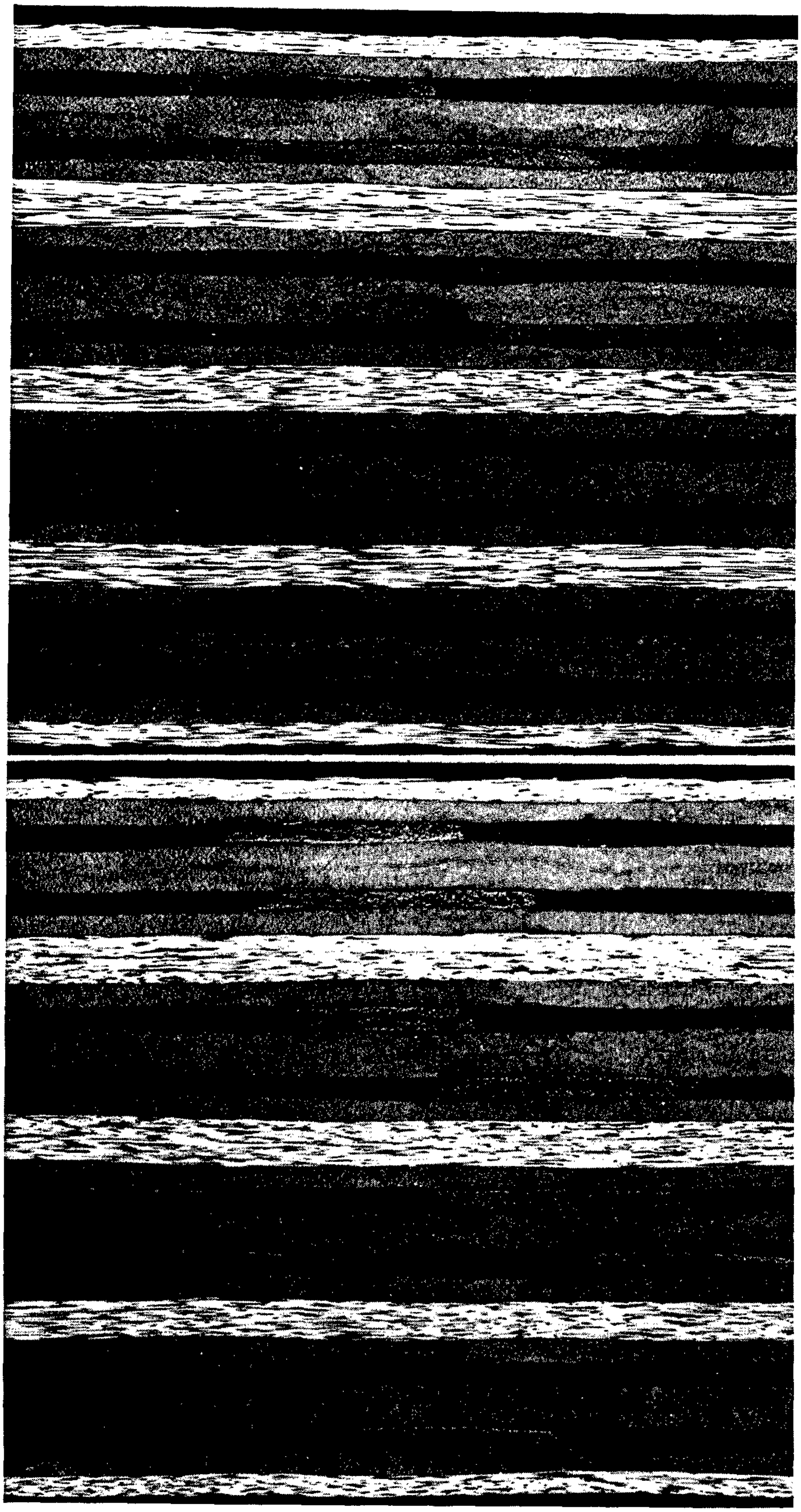

(a) Outer Area of Panel

2520-1-1, 25X

(b) Center Area of Panel

2520-2-1, 25X

Figure 3. Typical Metallographic Sections of Panel 2SY1156, 32 Ply T300/5208

which this batch of T300/5208 material was stored failed, resulting in a rise in temperature in the freezer to above freezing and the condensation of moisture in the freezer. Following discussions by phone with the Air Force Technical Monitor, it was concluded that the material should not be used for the balance of this program. As a result, a new lot of material was ordered to replace the questionable quality material.

The material replacing that lost in the freezer failure was received and qualification testing performed. The Narmco Quality Control Test Results (21) are presented in Table IV and the Lockheed Quality Control Test Results (22) are presented in Table V. Narmco Batch #1079 was found to meet all requirements and the material was accepted.

3.2 PANEL FABRICATION

Subsequent to material acceptance, panel fabrication was initiated as per the previously approved Quality Control Plan. One preliminary impact study panel 20 x 25-in. (508 x 635mm) was fabricated for each of the 32 and 24 ply layups. Five 35 x 46 in. (889 x 1168mm) panels of each of the 32 ply quasi-isotropic laminate and the 24-ply 67% 0° laminate were then fabricated. A summary of the laminate panel numbers and the material code letter which was assigned to each panel is shown in Table VI. All panels received a standard production ultrasonic C-scan inspection using a 1/4-inch (6mm) diameter teflon disc standard, the results of which are summarized in Table VI. Resin and void content results for each panel are given in Appendix A.

3.3 PRELIMINARY DAMAGE DEVELOPMENT STUDY

3.3.1 Impact Damage Study

A key part of the specimen fabrication is the method of introducing the initial damage. Results at Lockheed (Reference 23) have shown narrow specimens, 1.8-inch (46mm) wide, fail under low velocity impact in a manner which is not representative of the type of damage which occurs in 6-inch (152mm) wide panels under the same conditions. The 1.8 inch (46mm) wide specimens typically failed due to back ply failure across the entire specimen width. In contrast, a six-inch (152mm) wide

TABLE IV. Summary of the Narmco Quality Control Tests for Rigidite 5208-T300
Certified Test Report No. 34776

TESTING RESULTS

ITEM # 1
MATERIAL: Rigidite 5208-T300 12"
Batch # 1079

Roll	Amount	Resin Content	Areal Fiber Weight	Mfg. Date	Test Date
10	24.2	41	144 grams/sq.meter	1-12-78	1-17-78
11	26.2	42	144		
12	25.7	41	144		
13	25.4	42	143		
14	25.6	40	144		
15	21.5	42	144		
16	21.5	41	144		
17	26.7	43	144		

Flow:	22%
Volatiles:	0.2%
Gel Time:	19.53 min. @ 350°F.
Tack:	Acceptable
Specific Gravity:	1.58/1.58/1.58: 1.58 g/cc avg.
Cured Fiber Volume:	66/66/66: 66% average
RT Long. Tensile Strength:	218,360/244,290/255,560: 239,400 psi avg.
RT Long. Tensile Modulus:	20.43/21.96/21.49: 21.29 x 10^6 psi avg
RT Long. Flex Strength:	282,390/292,310/271,330: 282,010 psi avg.
180°F. Long. Flex Strength:	273,050/298,270/247,490: 272,940 psi avg.
RT Long. Flex Modulus:	23.25/22.74/22.15: 22.71 x 10^6 psi avg.
180°F. Long. Flex Modulus:	24.30/23.16/21.95: 23.13 x 10^6 psi avg.
RT Short Beam Shear:	18,000/17,830/17,830: 17,890 psi avg.
180°F. Short Beam Shear:	15,040/14,840/15,670: 15,190 psi avg.
Cured Ply Thickness:	0.0047"
Discrepancy Sheets:	Attached

TABLE V. SUMMARY OF LOCKHEED QUALITY CONTROL TESTS FOR NARMCO RIGIDITE 5208-T300 MATERIAL BATCH #1079 [22]

Material Property	Specification Requirements C-22-1379/111	Measured Property	Accepted
	UNCURED PROPERTIES		
1. Areal Fiber Weight (4 req)	139 - 149 g/m^2	143 g/m^2	x
		144 "	x
		145 "	x
		144 "	x
		Ave. 144 "	
2. Infrared Spectrophotometric Anal. (1 req)	Conformance to file spectrogram	-	x
3. Volatiles (2 req) 60± 5 min at 350°F	2% Maximum	0.3% edge	x
		0.35% center	x
4. Dry resin content (4 req)(Soxhlet)	38 - 44%	43.1% left	x
		43.4% left center	x
		43.1% right center	x
		44.0% right	x
5. Resin Flow at 350°F and 85 psi (2 req)	15 - 29%	19.0%	x
		18.9%	x
6. Gel Time at 350°F (2 req)	For information only	20.0 minutes	-
		20.3 minutes	-
7. Fiber Orientation	0°	-	x
	CURED LAMINATES		
1. Cured Fiber Volume, 16 ply panel (3 req)	60 - 68%	62.3	x
		65.0	x
		65.4	x
		Ave. 64.2	
2. Cured Fiber Volume, 8 ply panel (3 req)	60 - 68%	64.5	x
		64.5	x
		65.2	x
		Ave. 64.7	
3. Specific Gravity, 16 ply panel (3 req)	1.55 - 1.62	1.57	x
		1.57	x
		1.58	x
		Ave. 1.57	

TABLE V. SUMMARY OF LOCKHEED QUALITY CONTROL TESTS FOR NARMCO RIGIDITE 5208-T300 MATERIAL BATCH #1079[22] (Continued)

Material Property	Specification Requirements C-22-1379/111	Measured Property	Accepted
4. Specific Gravity, 8 ply panel (3 req)	1.55 - 1.62	1.57	x
		1.57	x
		1.58	x
		Ave. 1.57	
5. Tensile Strength, longitudinal at $75^{o}F$ (3 req)	170 ksi min.	227	x
		119	x
		223	x
		Ave. 216 ksi	
6. Elastic Modulus, longitudinal at $75^{o}F$ (3 req)	$20 \cdot 10^{6}$ psi min.	$20.6 \cdot 10^{6}$	x
		$20.0 \cdot 10^{6}$	x
		$21.0 \cdot 10^{6}$	x
		Ave. $20.5 \cdot 10^{6}$	
7. Flexural Strength at $75^{o}F$ (3 req)	210 ksi min.	255	x
		245	x
		264	x
		Ave. 254 ksi	
8. Flexural Modulus at $75^{o}F$ (3 req)	$18 \cdot 10^{6}$ psi min.	18.0	x
		18.1	x
		18.2	x
		Ave. $18.1 \cdot 10^{6}$ psi	
9. Flexural Strength at + $180^{o}F$ (3 req)	200 ksi min.	224	x
		238	x
		231	x
		Ave. 231 ksi	
10. Flexural Modulus at + $180^{o}F$ (3 req)	$16 \cdot 10^{6}$ psi min.	$18.4 \cdot 10^{6}$	x
		$19.7 \cdot 10^{6}$	x
		$20.0 \cdot 10^{6}$	x
		Ave. $19.4 \cdot 10^{6}$ psi	
11. Short Beam Shear Strength at 75^{o} (3 req)	13 ksi min.	16.7	x
		15.6	x
		16.7	x
		Ave. 16.3 ksi	

TABLE V. SUMMARY OF LOCKHEED QUALITY CONTROL TESTS FOR NARMCO RIGIDITE 5208-T300 MATERIAL BATCH #1079 [22] (Continued)

Material Property	Specification Requirements C-22-1379/111	Measured Property	Accepted
12. Short Beam Shear Strength at + 180°F (3 req)	12 ksi min	13.2	x
		13.6	x
		13.4	x
		Ave. 13.4 ksi	
13. Thickness per ply, 16 ply panel (5 req)	0.0046 - 0.0056 inch	0.0048	x
		0.0048	x
		0.0050	x
		0.0048	x
		0.0051	x
		Ave. 0.0049 inch	
14. Thickness per ply, 8 ply panel (5 req)	0.0046 - 0.0056 inch	0.0050	x
		0.0051	x
		0.0050	x
		0.0050	x
		0.0051	x
		Ave. 0.0050 inch	

TABLE VI. SUMMARY OF PANEL IDENTIFICATION CODES

Laminate Type	Panel Number	Assigned Panel Code	C-Scan Inspection Results
32-ply quasi-isotropic	2TY 1228	A	No indications
	1TY 1228	B	
	2TY 1227	C	
	1TY 1230	D	
	1TY 1229	E	No indications
24-ply 67% 0° Fibers	1TY 1238	H	No indications
	1TY 1236	J	
	2TY 1236	K	
	2TY 1234	L	
	1TY 1234	M	No indications

specimen exhibited internal delaminations. As a result, all impacting was performed on 14.0 x 37-inch (356 x 940mm) sub-panels rather than smaller specimen blanks.

A preliminary impact study panel 20 x 24 inches (508 x 610mm) was fabricated in both layups with the Task I panels. These small panels were used to set the initial impact conditions to be used in developing the impact damage on the actual test specimens. For these tests, a simple drop tower consisting of a Teflon guide tube mounted in a support frame was used. The impactors consisted of a one-inch (25mm) diameter steel cylinder with interchangeable impact heads, one with a one-inch (25mm) diameter hemispherical head and one with a No. 2 standard Phillips screwdriver point, and adjustable weight. Drop heights were preset by use of location pins which extend through the Teflon guide tube. Impactor velocity at impact, the deflection dynamics of the specimen and impactor, and the rebound velocity of the impactor were monitored by a high speed motion picture camera. Triplicate drops were made for each of four mass/heights with each of the two impactor head configurations at locations defined by a three-inch (76mm) square grid on the panel. The test panels were supported during the impacting by a 3/8-inch (10mm) thick section of HRH10-3/16-3.5 honeycomb core material. This support method was selected since tests have indicated [23] this provides a reproducible support system for low velocity impact testing. A typical drop test set-up is shown in Figure 4.

Triplicate impacts were made for each of eight sets of impact conditions for each of the two test laminates. Resulting damage was evaluated using standard ultrasonic C-scan methods to determine those impact conditons that resulted in damage in the desired size range. Subsequently detailed characterization of the resulting damage was conducted using the Holscan unit. A summary of the impact conditions is presented in Tables VII and VIII.

3.3.1.1 Evaluation of Impact Damage Conditions (32 Ply Quasi-Isotropic Material)

First, an examination of the ultrasonic C-scan results shown in Figure 5 for the 32 ply panel 2TY-1222 was made. Impact conditions 1 and 4 (impact locations 1-3 and 10-12) were found to be below the damage producing threshold for these impact conditions and material. Impact condition 6 (location 16-18)

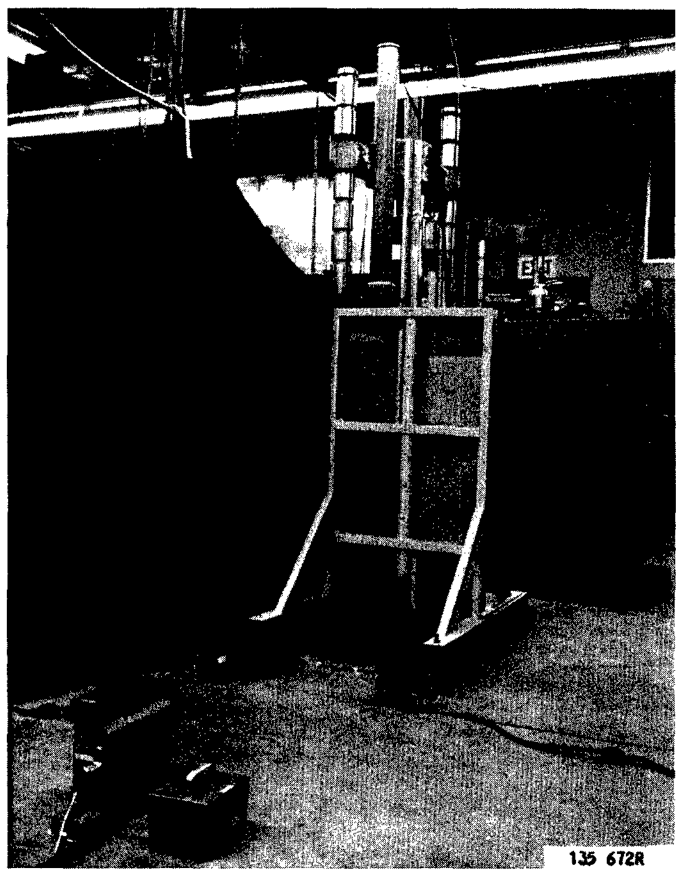

Figure 4. Typical Tool Drop Simulation Set Up

TABLE VII. IMPACT PARAMETERS FOR 32 PLY QUASI-ISOTROPIC LAMINATE
(Panel 2TY-1222)

Location	Run Number	Drop Height, m	(inch)	Impact Head Type*	Impact Mass kg	(slug)	Impact Velocity m/sec	(ft/sec)	Kinetic Energy E_K J	(ft-lb)	Apparent Damage Size, x by y mm	(inch)
1	37	1.24	(48.8)	1	0.240	(0.016)	4.02	(13.2)	1.94	(1.43)	0	0
2	38	1.24	(48.8)	1	0.240	(0.016)	3.96	(13.0)	1.87	(1.38)	0	0
3	39	1.24	(48.8)	1	0.240	(0.016)	4.11	(13.5)	2.02	(1.49)	0	0
4	40	0.48	(18.8)	1	0.590	(1.040)	2.44	(8.0)	1.75	(1.29)	17.8 x 19.0	(0.70 x 0.75)
5	41	0.48	(18.8)	1	0.590	(1.040)	2.50	(8.2)	1.84	(1.36)	17.5 x 17.3	(0.69 x 0.68)
6	42	0.48	(18.8)	1	0.590	(1.040)	-	-	-	-	18.3 x 18.3	(0.72 x 0.72)
7	43	0.73	(28.8)	1	0.590	(1.040)	3.29	(10.8)	3.20	(2.36)	20.8 x 23.1	(0.82 x 0.91)
8	44	0.73	(28.8)	1	0.590	(1.040)	3.23	(10.6)	3.08	(2.27)	21.6 x 22.4	(0.85 x 0.88)
9	45	0.73	(28.8)	1	0.590	(1.040)	3.35	(11.0)	3.31	(2.44)	20.3 x 22.6	(0.80 x 0.89)
10	46	0.73	(28.8)	1	0.240	(0.016)	3.23	(10.6)	1.25	(0.92)	0	0
11	47	0.73	(28.8)	1	0.240	(0.016)	3.47	(11.4)	1.44	(1.06	0	0
12	48	0.73	(28.8)	1	0.240	(0.016)	3.35	(11.0)	1.34	(0.99)	0	0
13	49	1.24	(48.8)	2	0.248	(0.017)	4.14	(13.6)	2.13	(1.57)	13.7 x 13.2	(0.54 x 0.52)
14	50	1.24	(48.8)	2	0.248	(0.017)	4.14	(13.6)	2.13	(1.57)	10.4 x 11.4	(0.41 x 0.45)
15	51	1.24	(48.8)	2	0.248	(0.017)	4.24	(13.9)	2.22	(1.64	12.4 x 12.7	(0.49 x 0.50)
16	52	0.73	(28.8)	2	0.248	(0.017)	3.17	(10.4)	1.25	(0.92)	2.5 x 1.2	(0.10 x 0.05)
17	53	0.73	(28.8)	2	0.248	(0.017)	3.35	(11.0)	1.40	(1.03)	3.0 x 5.3	(0.12 x 0.21)
18	54	0.73	(28.8)	2	0.248	(0.017)	3.26	(10.7)	1.32	(0.97)	10.2 x 8.9	(0.40 x 0.35)
19	55	0.73	(28.8)	2	0.598	(1.041)	3.23	(10.6)	3.01	(2.27)	16.5 x 16.5	(0.65 x 0.65)
20	56	0.73	(28.8)	2	0.598	(1.041)	-	-	-	-	17.3 x 16.8	(0.68 x 0.66)
21	57	0.73	(28.8)	2	0.598	(1.041)	3.54	(11.6)	3.69	(2.72)	19.8 x 20.0	(0.78 x 0.79)
22	58	0.48	(18.8)	2	0.598	(1.041)	2.96	(9.7)	2.58	(1.90)	14.7 x 14.5	(0.58 x 0.57)
23	59	0.48	(18.8)	2	0.598	(1.041)	2.59	(8.5)	1.98	(1.46)	15.2 x 15.2	(0.60 x 0.60)
24	60	0.48	(18.8)	2	0.598	(1.041)	2.47	(8.1)	1.80	(1.33)	14.0 x 14.7	(0.55 x 0.58)

* 1 = 1-inch (25mm) diameter round head
2 = 2 Phillips Head Screwdriver point

TABLE VIII. IMPACT PARAMETERS FOR 24 PLY 67% 0° FIBER LAMINATE
(Panel 1TY-1222)

Location	Run Number	Drop Height, m	(inch)	Impact Head Type*	Impact Mass kg	(slug)	Impact Velocity m/sec	(ft/sec)	Kinetic Energy E_K J	(ft/lb)	Apparent Damage Size, x by y mm	(inch)
1	31	0.477	(18.8)	1	0.240	(0.016)	2.65	(8.7)	0.84	(0.62)	8.9 x 10.7	(0.35 x 0.42)
2	32	0.477	(18.8)	1	0.240	(0.016)	2.65	(8.7)	0.84	(0.62)	0	0
3	33	0.477	(18.8)	1	0.240	(0.016)	2.74	(9.0)	0.89	(0.66)	0	0
4	34	0.732	(28.8)	1	0.164	(0.011)	3.26	(10.7)	0.87	(0.64)	8.1 x 13.2	(0.32 x 0.52)
5	35	0.732	(28.8)	1	0.164	(0.011)	3.32	(10.9)	0.91	(0.67)	10.2 x 14.2	(0.40 x 0.56)
6	36	0.732	(28.8)	1	0.164	(0.011)	3.26	(10.7)	0.87	(0.64)	10.7 x 15.2	(0.42 x 0.60)
7	61	0.477	(18.8)	1	0.164	(0.011)	2.68	(8.8)	0.59	(0.435)	0	0
8	62	0.477	(18.8)	1	0.164	(0.011)	2.53	(8.3)	0.53	(0.39)	0	0
9	63	0.477	(18.8)	1	0.164	(0.011)	2.56	(8.4)	0.54	(0.40)	5.6 x 6.4	(0.22 x 0.25)
10	64	0.477	(18.8)	1	0.240	(0.016)	2.53	(8.3)	0.77	(0.565)	0	0
11	65	0.477	(18.8)	1	0.240	(0.016)	2.50	(8.2)	0.75	(0.55)	7.6 x 14.2	(0.30 x 0.56)
12	66	0.477	(18.8)	1	0.240	(0.016)	2.53	(8.3)	0.77	(0.565)	7.9 x 12.2	(0.31 x 0.49)
13	67	0.477	(18.8)	2	0.248	(0.017)	2.65	(8.7)	0.87	(0.64)	7.4 x 12.2	(0.29 x 0.49)
14	68	0.477	(18.8)	2	0.248	(0.017)	2.59	(8.5)	0.83	(0.61)	7.4 x 10.2	(0.29 x 0.40)
15	69	0.477	(18.8)	2	0.248	(0.017)	2.65	(8.7)	0.87	(0.64)	7.1 x 13.0	(0.28 x 0.51)
16	70	0.732	(28.8)	2	0.172	(0.012)	3.17	(10.4)	0.87	(0.64)	7.6 x 10.2	(0.30 x 0.40)
17	71	0.732	(28.8)	2	0.172	(0.012)	3.23	(10.6)	0.89	(0.66)	7.9 x 11.4	(0.31 x 0.45)
18	72	0.732	(28.8)	2	0.172	(0.012)	3.29	(10.8)	0.94	(0.69)	7.1 x 14.7	(0.28 x 0.58)
19	73	0.477	(18.8)	2	0.172	(0.012)	2.53	(8.3)	0.56	(0.41)	6.6 x 10.2	(0.26 x 0.40)
20	74	0.477	(18.8)	2	0.172	(0.012)	2.65	(8.7)	0.60	(0.445)	5.8 x 10.2	(0.23 x 0.40)
21	75	0.477	(18.8)	2	0.172	(0.012)	2.59	(8.5)	0.58	(0.425)	5.3 x 9.6	(0.21 x 0.38)
22	76	0.477	(18.8)	1	0.590	(1.040)	2.53	(8.3)	1.88	(1.39)	15.7 x 21.3	(0.62 x 0.84)
23	77	0.477	(18.8)	1	0.590	(1.040)	2.53	(8.3)	1.88	(1.39)	13.0 x 18.5	(0.51 x 0.73)
24	78	0.477	(18.8)	1	0.590	(1.040)	2.65	(8.7)	2.07	(1.53	14.0 x 20.6	(0.55 x 0.81)

* 1 = 1-inch (25mm) diameter round head
2 = 2 Phillips Head Screwdriver point

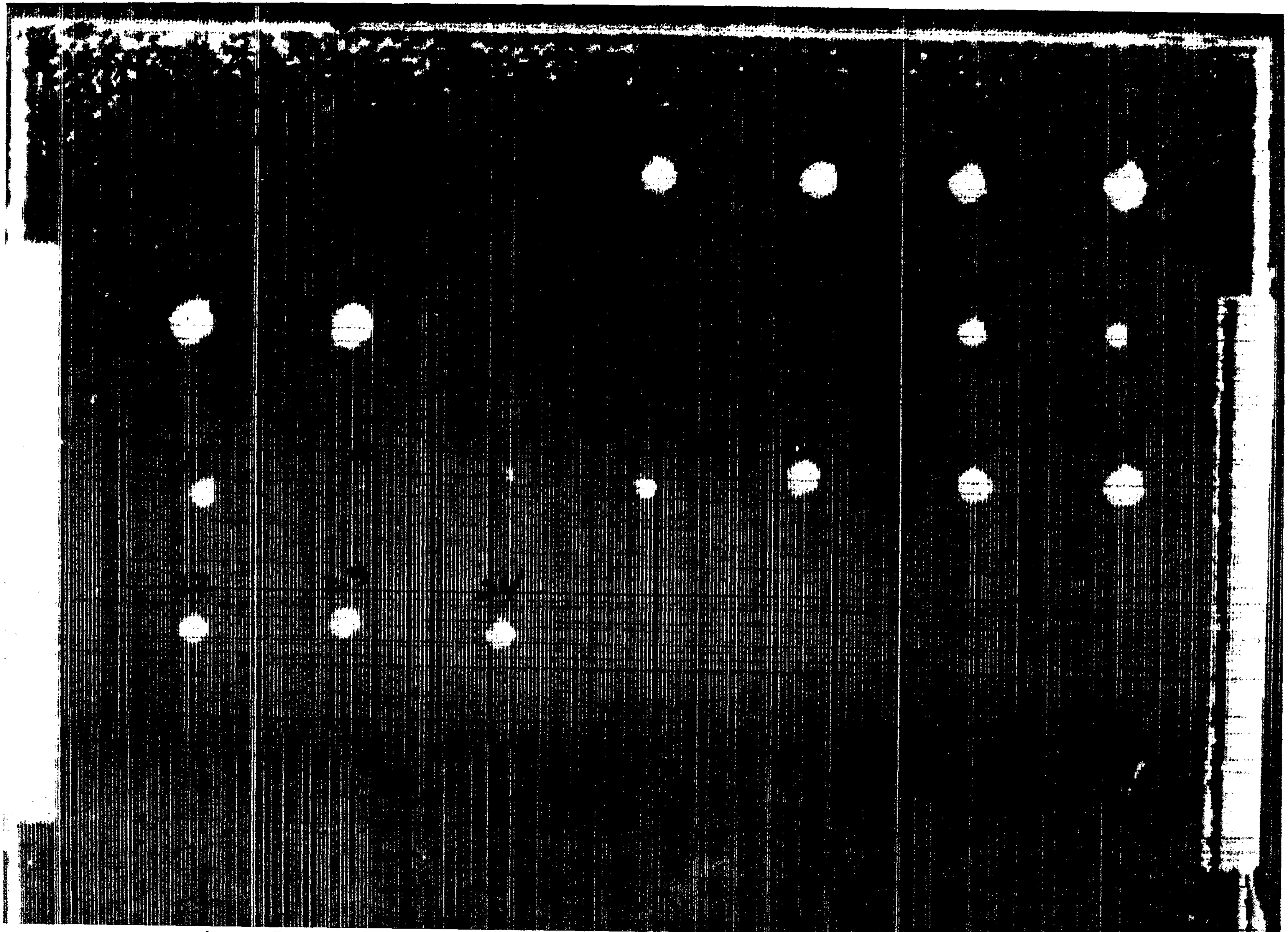

Figure 5. Ultrasonic C-Scan Results of the Preliminary Impact Damage Study on the 32-Ply Quasi-Isotropic Laminate

was also eliminated from consideration due to the generally small and highly variable damage size observed. Of the remaining five impact conditions, conditions 3 (location 7-9) resulted in damage areas with the dimension X in the specimen width direction greater than 0.80 inch (20 mm). These initial damage sizes are considered too large for the current program since they would allow insufficient room for damage growth measurement during test. Since impacts 7 and 8 (locations 19-21 and 22-24 respectively) were generated under similar conditions and the resulting damage areas were only slightly different, condition 8 was retained and condition 7 eliminated. The remaining three impact conditions, 2, 5 and 8 (locations 4-6, 13-15, and 22-24 respectively) were thus selected for further examination using the Holscan system to characterize the damage present. These three damage conditions represent one due to a blunt impactor (condition 2) and two using a more pointed Phillips head screw driver point (conditions 5 and 8).

Detailed Holscan evaluations were conducted on a representative damage location of each of the three selected conditions. The results shown in Figures 6 - 11 show multiple delamination and intraply cracking in essentially all plies between the 4th ply and the 28th ply for all three of the impact conditions. In addition, impact conditions 5 and 8 were found to result in a slight puncture $\sim$ 2-3 plies deep on the impact surface.

3.3.1.2 Evaluation of Impact Damage (24 Ply Material)

Preliminary analysis based on ultrasonic C-scan results shown in Figure 12 show impact conditions 1, 3, and 4 (a verification of condition 1) to be unsuitable due to lack of consistent damage development. This indicates that these conditions represent a threshold level for damage development under the test conditions examined. Of the remaining five conditions, condition 7 was eliminated because the resulting damage was considered too small, the dimension X in the specimen width being less than 1/4 inch (6 mm). The four remaining damage conditions produced reasonably consistent damage size, X, in the range of 0.28 to 0.6 in. (7 to 15 mm). A representative damage site for each of these four conditions was selected and subjected to a detailed Holscan analysis. This

Figure 6.

Site No. 4 Viewed from Impact Side,
32-Ply Panel No. 2TY-1222

0° Fiber Orientation ⟶

C-SCAN RESULTS

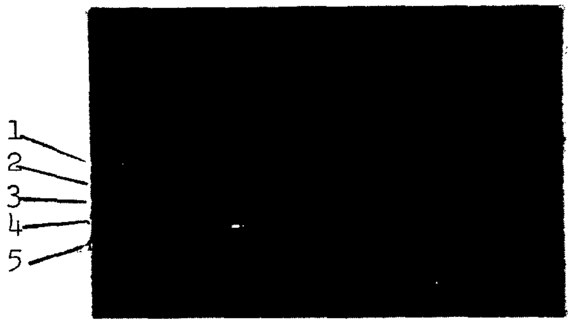

Scope

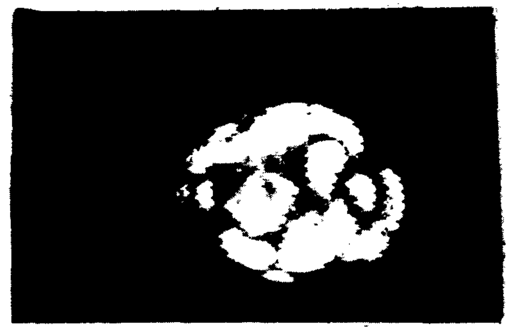

TV, 2X

B-SCAN RESULTS

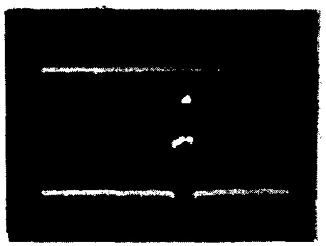

1

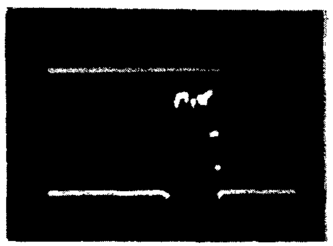

2

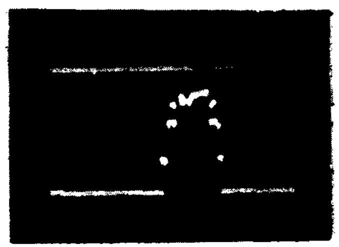

3

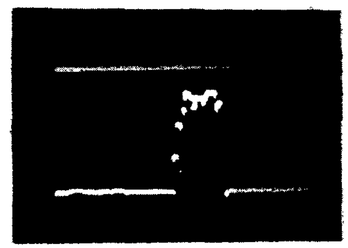

4

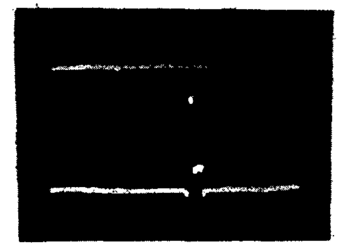

5

Σ

Figure 7.

Site No. 4 Viewed from Back Side,
32-Ply Panel No. 2TY-1222

0° Fiber Orientation ⟶

C-SCAN RESULTS

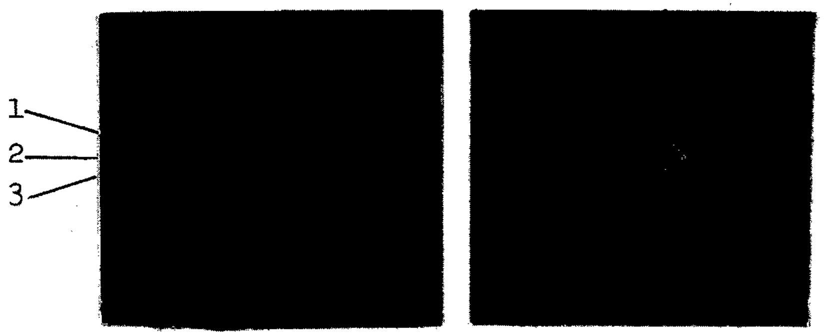

Scope

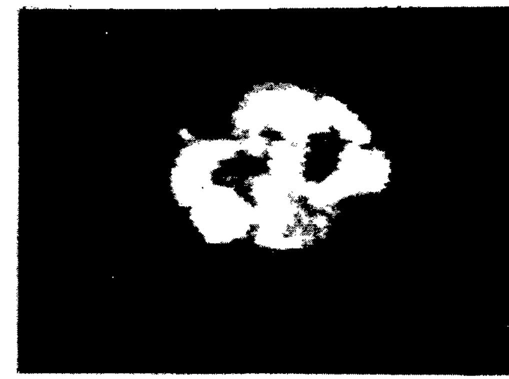

TV, 2X

B-SCAN RESULTS

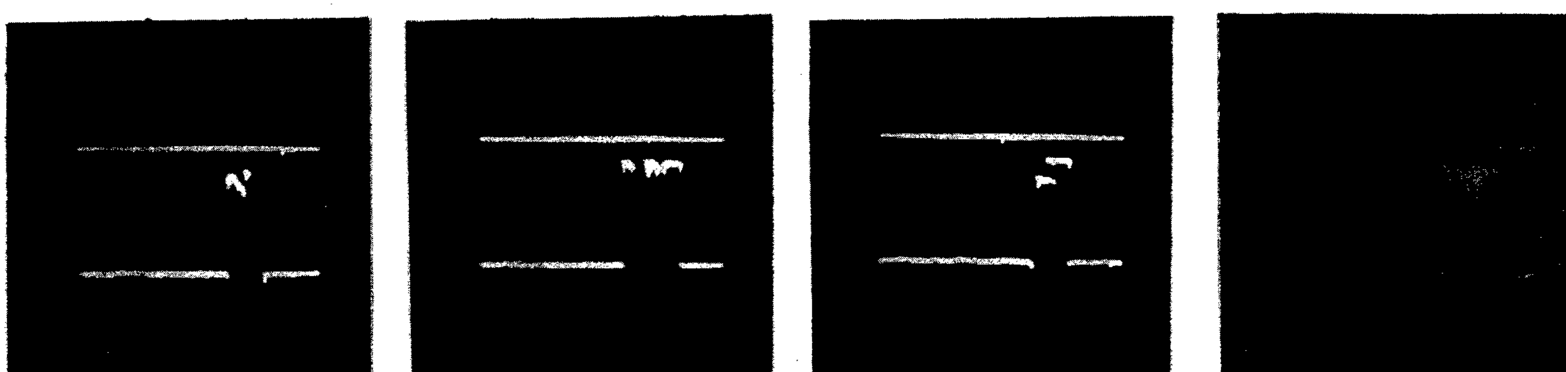

1 2 3 Σ

Figure 8.

Site No. 15 Viewed from Back Side
32-Ply Panel No. 2TY-1222

0° Fiber Orientation ⟶

C-SCAN RESULTS

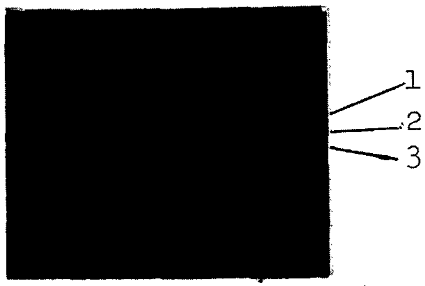

Scope

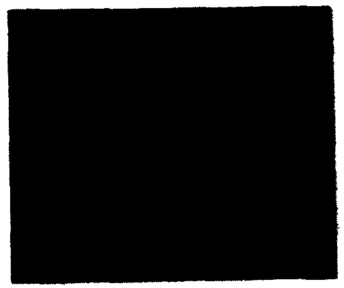

TV - 2X

B-SCAN RESULTS

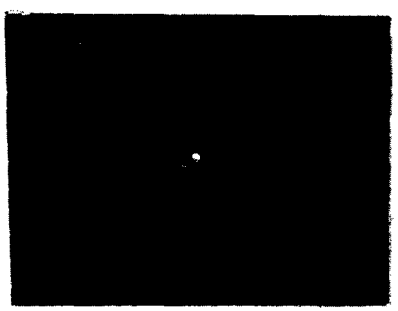

1

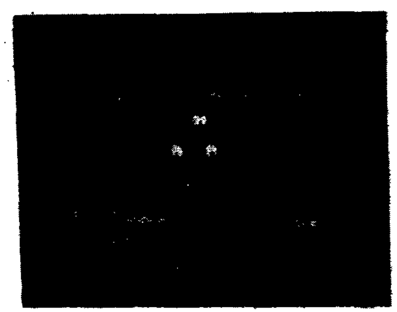

2

3

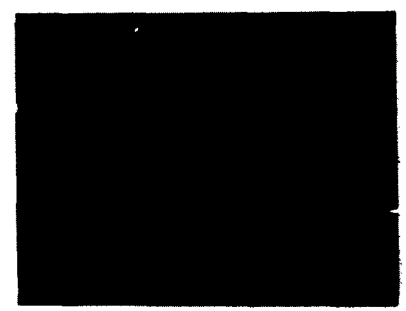

ΣB

Figure 9.

Panel No. 2TY-1222, 32 Ply

Site No. 15 Viewed from Impact Side

0° Fiber Orientation →

C-SCAN RESULTS

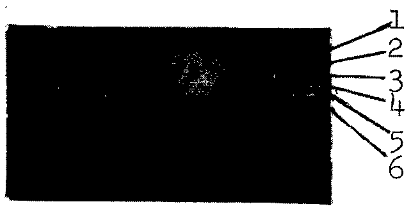

Scope

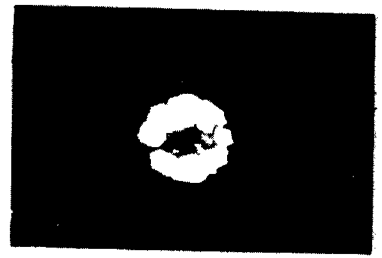

TV

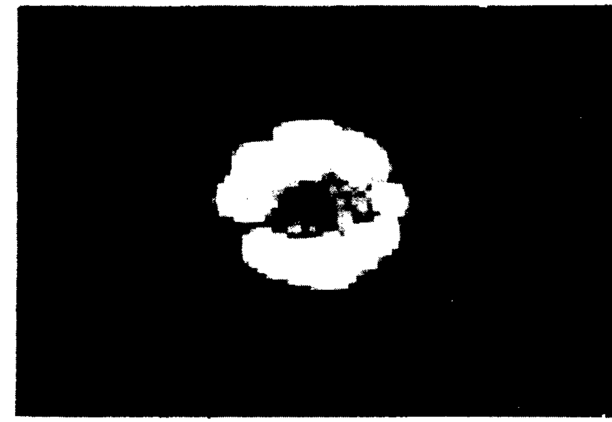

TV, X2

B-SCAN RESULTS

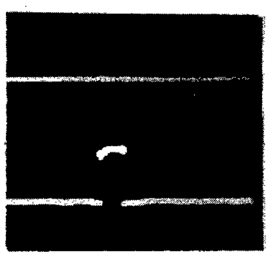

1

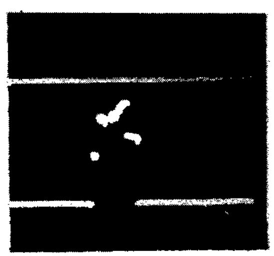

2

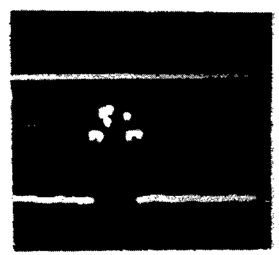

3

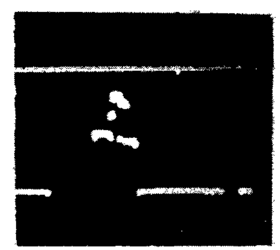

4

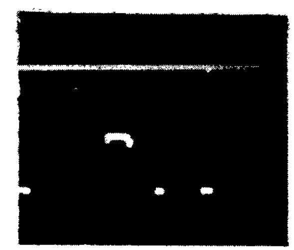

5

6

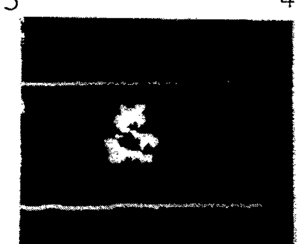

Σ

Figure 10.

Site No. 22 Viewed from Impact Side,
32-Ply Panel No. 2TY-1222

0° Fiber Orientation →

C-SCAN RESULTS

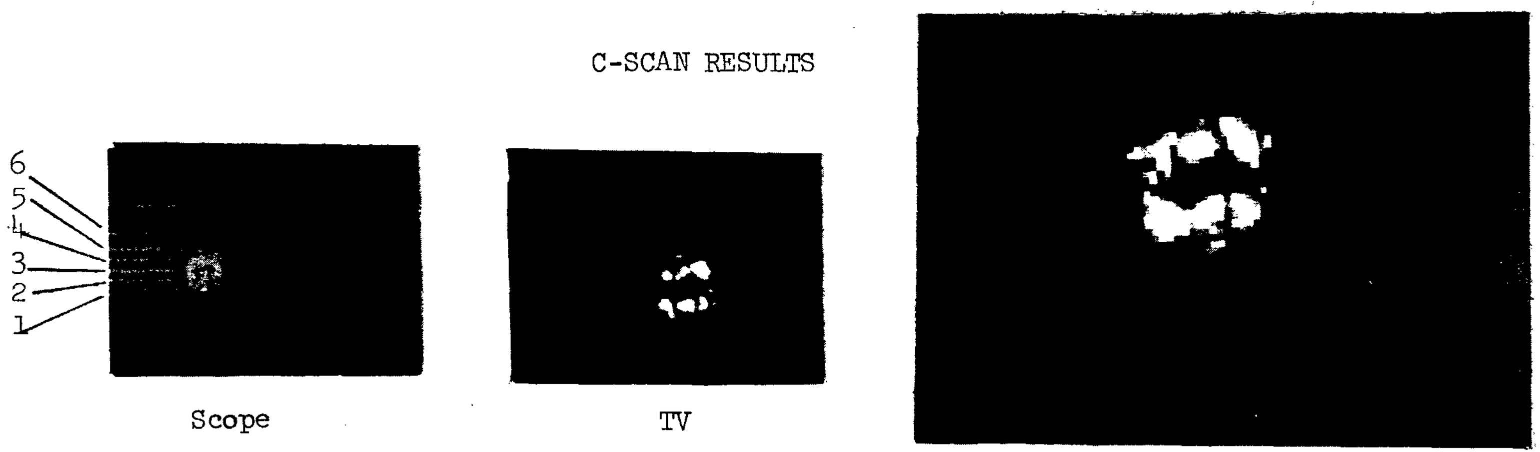

Scope   TV   TV, 2X

B-SCAN RESULTS

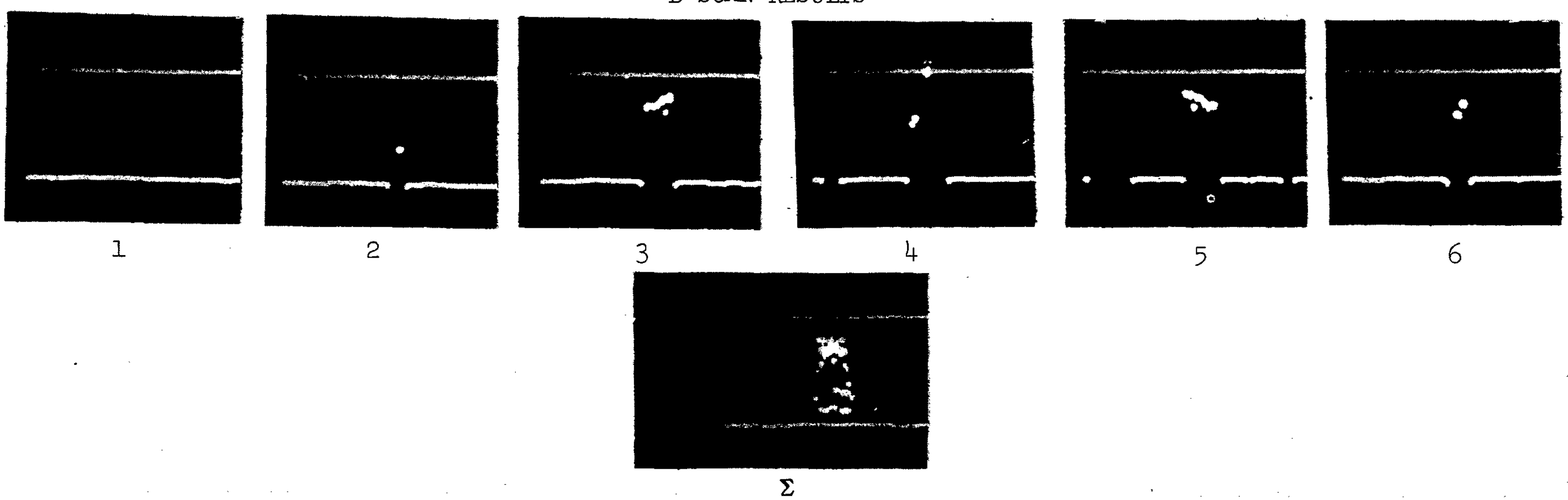

Figure 11.

Site No. 22 Viewed from Back Side,
32-Ply Panel No. 2TY-1222
0° Fiber Orientation ↑

C-SCAN RESULTS

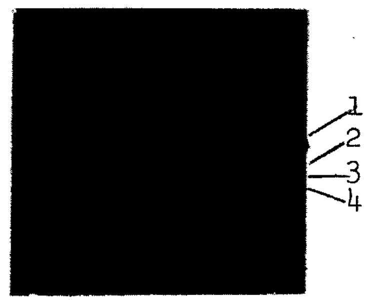

Scope

B-SCAN RESULTS

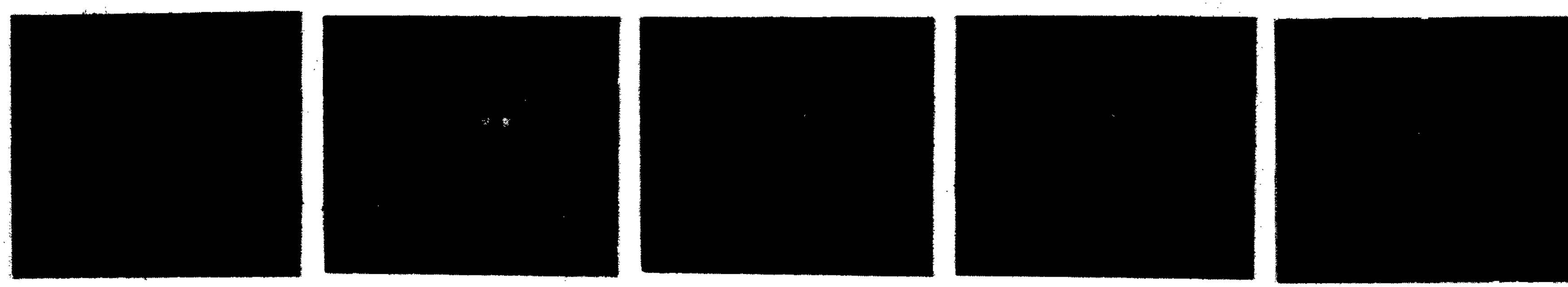

1 2 3 4 Σ

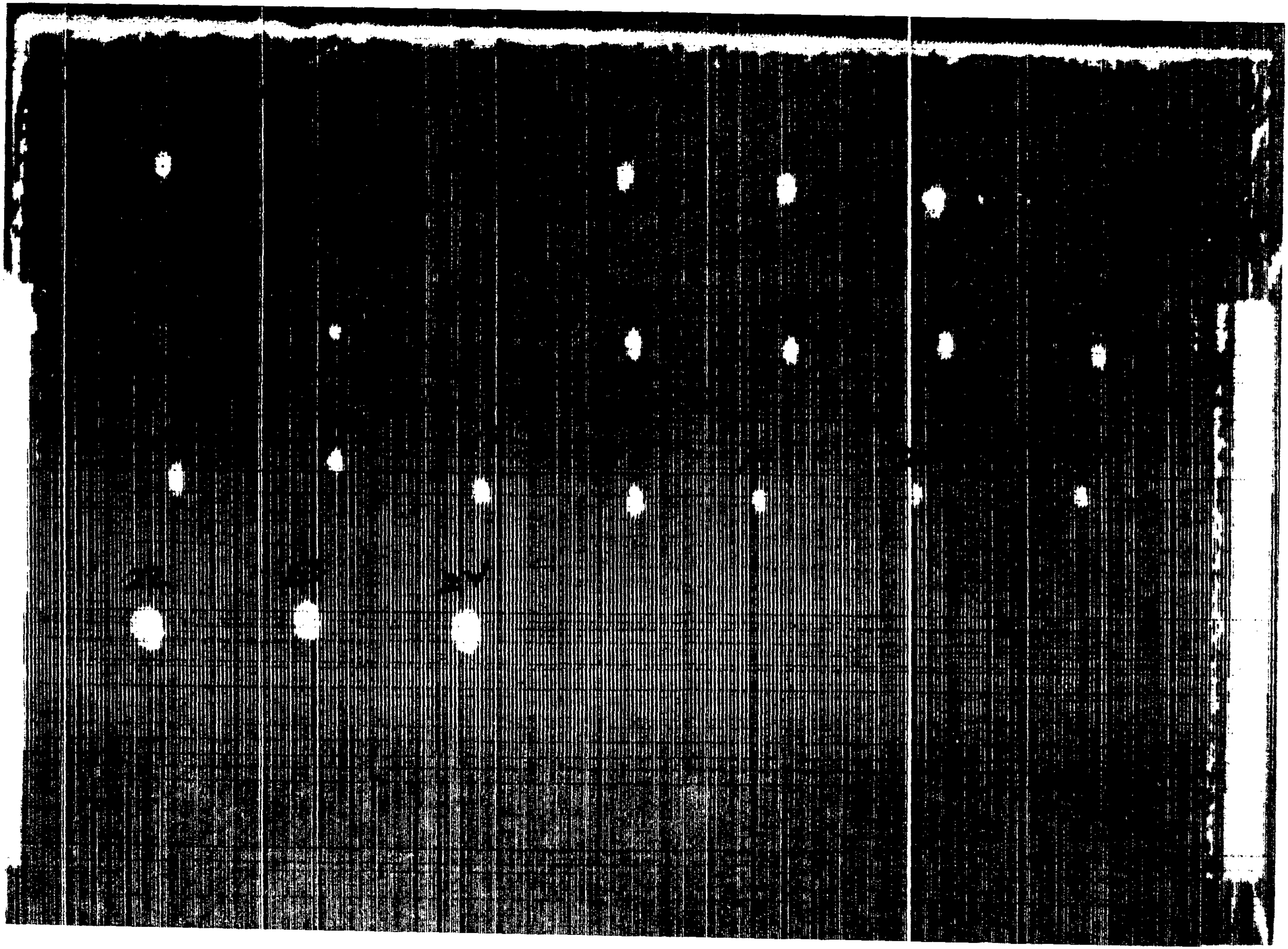

Figure 12. Ultrasonic C-Scan Results of the Preliminary Impact Damage Study on the 24 Ply 67% 0° Fiber Laminate

selection represents two conditions (2 and 8) with the 1-inch (25 mm) diameter hemispherical impact head and two conditions (5 and 6) with the No. 2 Phillips head screwdriver point impact head.

Detailed Holscan examinations shown in Figures 13-20 revealed multiple delaminations and intraply cracking located primarily in plies 4 through 20, very similar to that which was observed in the 32 ply material. However, no surface puncture marks were observed for impact locations which were impacted with the No. 2 Phillips head screwdriver.

3.3.1.3 Final Selection of Impact Conditions

Based on these results, the following impact conditions were agreed upon with the approval of the Air Force Technical Monitor for use in the remainder of the program.

32 Ply Material

Impactor: 0.017 Slug (0.248 Kg) mass with No. 2 Phillips head screwdriver point

Drop Height: 18.8 inches (0.48 meter)

24 Ply Material

Impactor: 0.034 Slug (0.490 Kg) mass with 1-inch (25.4 mm) diameter round head

Drop Height: 18.8 inches (0.48 meter)

3.3.2 Damaged Hole Drilling Study Results

Based on previous machining experience with composite materials, nine sets of hole drilling parameters were selected for evaluation. One hole was drilled in both the 24 ply and in the 32 ply material for each of the nine drilling conditions listed in Table IX. The Holscan unit was then used to characterize the resulting damage for each condition. Results of the Holscan inspection are presented in Figures 21 and 22 for the 32 ply and the 24 ply material respectively. Based on these results, three drilling conditions, numbers 1, 3 and 5 were selected for further evaluation. These three conditions were selected since they resulted in a damaged region which was

Figure 13.

Site No. 6 Viewed from Back Side,
24-Ply Panel No. 1TY-1222

0° Fiber Orientation ⟶

C-SCAN RESULTS

Scope TV

B-SCAN RESULTS

1 2 3 4 & 5 Σ

Figure 14.

Site No. 6 Viewed from Back Side
24-Ply Panel No. 1TY-1222

0° Fiber Orientation →

C-SCAN RESULTS

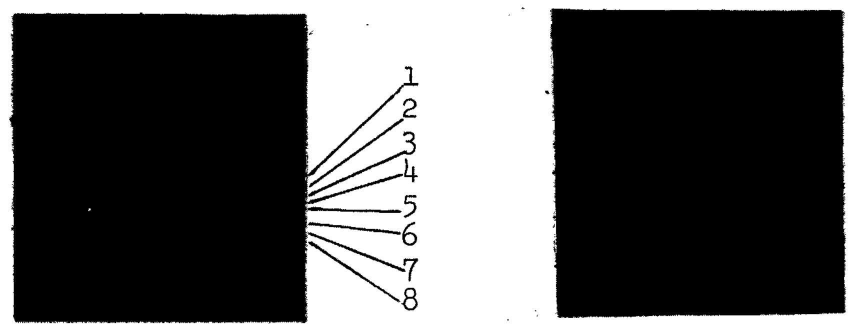

Scope

B-SCAN RESULTS

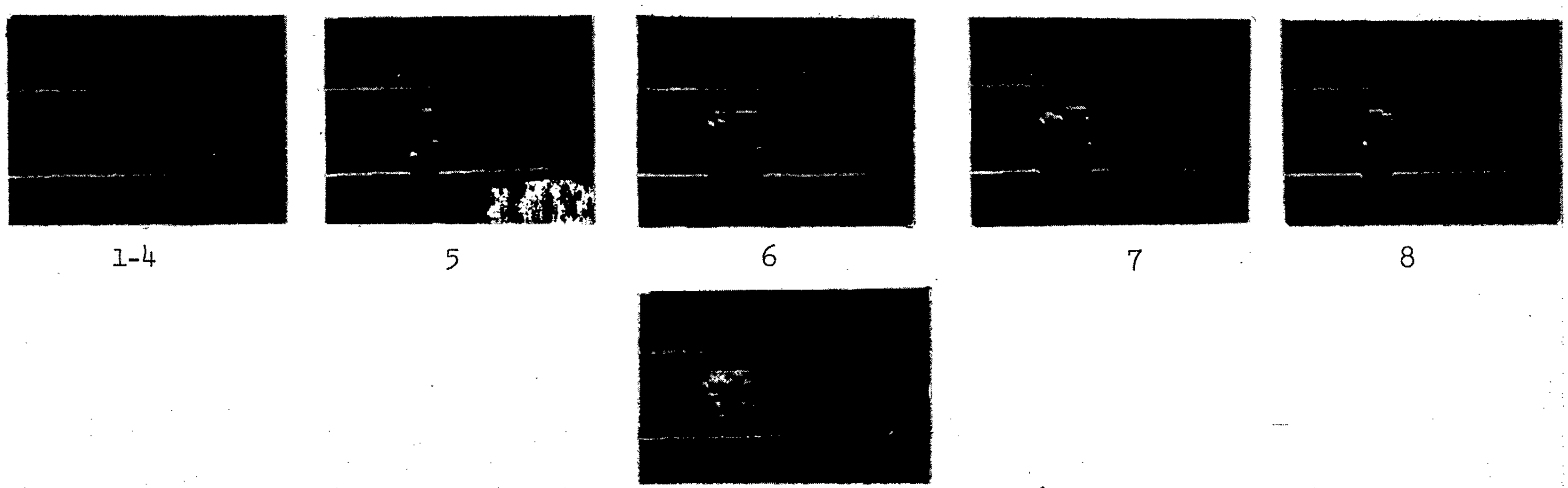

Figure 15.

Site No. 13 Viewed from Impact Side
24-Ply Panel No. 1TY-1222

0° Fiber Orientation ⟶

C-SCAN RESULTS

Scope

B-SCAN RESULTS

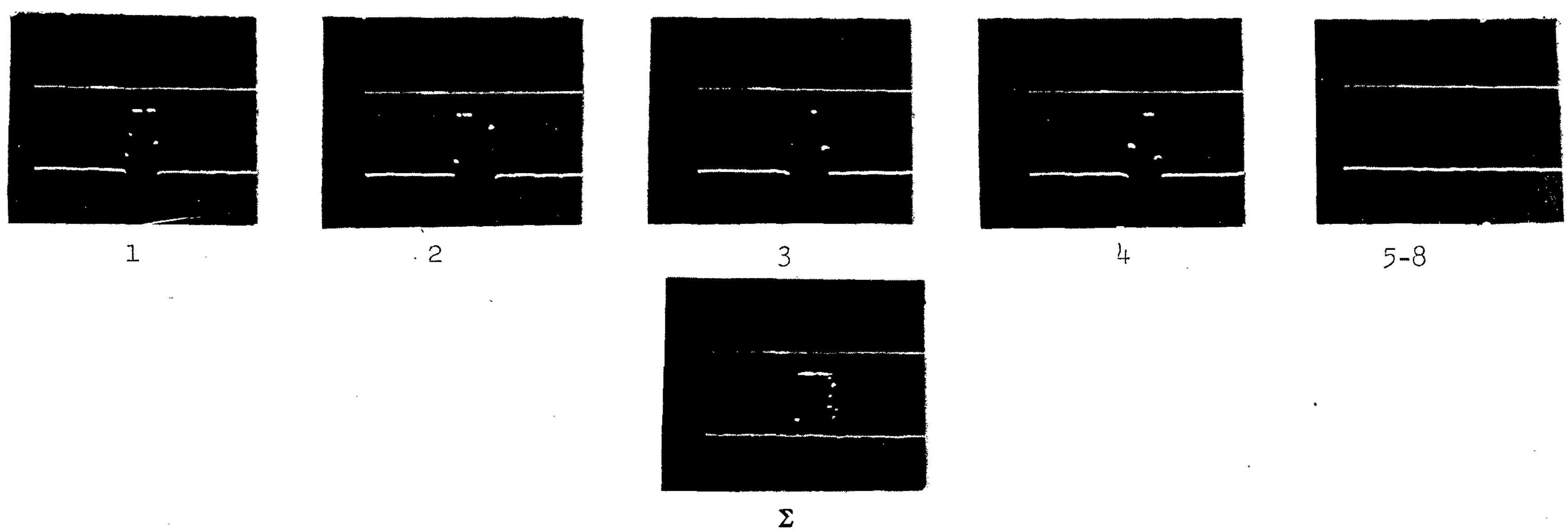

Figure 16

Site No. 13 Viewed from Back,
24-Ply Panel No. 1TY-1222

0° Fiber Orientation ⟶

C-SCAN RESULTS

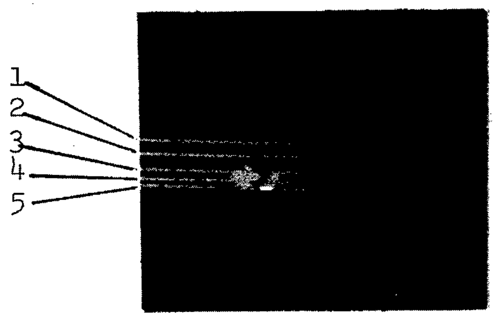

Scope

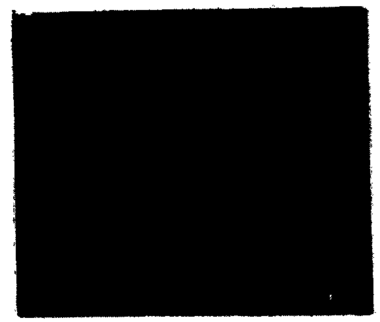

TV

B-SCAN RESULTS

1

2

3

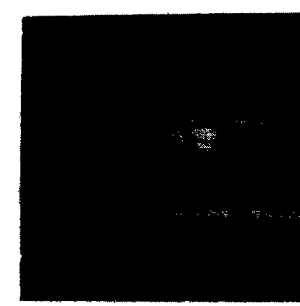

Σ

Figure 17

Site No. 17 Viewed from Impact Side
24-Ply Panel No. 1TY-1222

0° Fiber Orientation ↑

C-SCAN RESULTS

Scope

TV

B-SCAN RESULTS

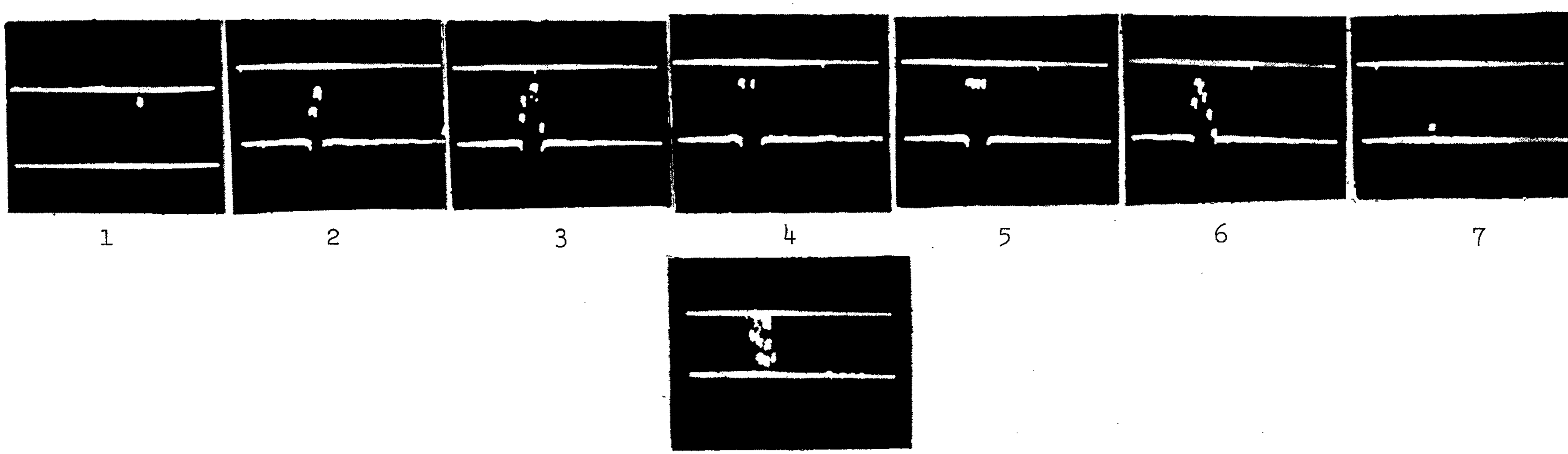

Figure 18

Site No. 17 Viewed from Back Side,
24-Ply Panel No. 1TY-1222

0° Fiber Orientation ↑

C-SCAN RESULTS

Scope TV

B-SCAN RESULTS

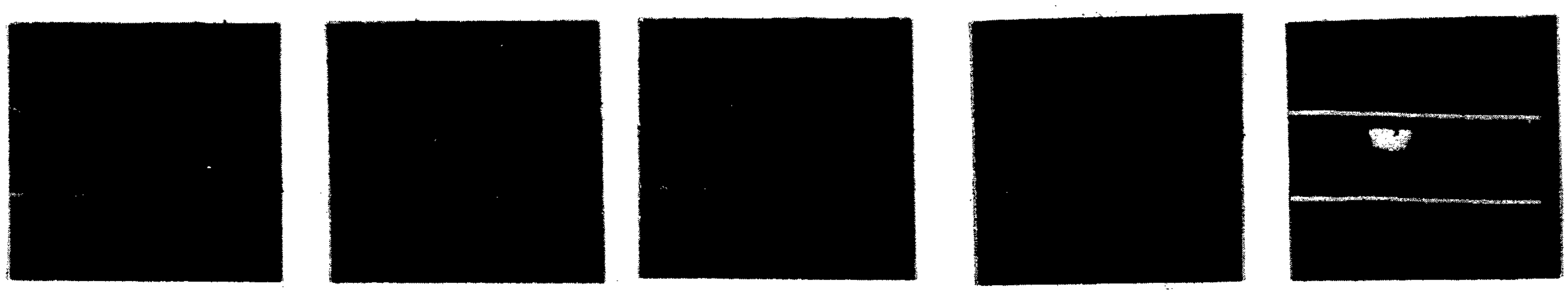

1 2 3 4 Σ

Figure 19

Site No. 24 Viewed from Impact Side
24-Ply Panel No. 1TY-1222

0° Fiber Orientation ↑

C-SCAN RESULTS

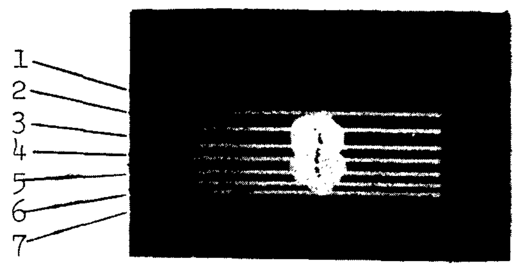

Scope

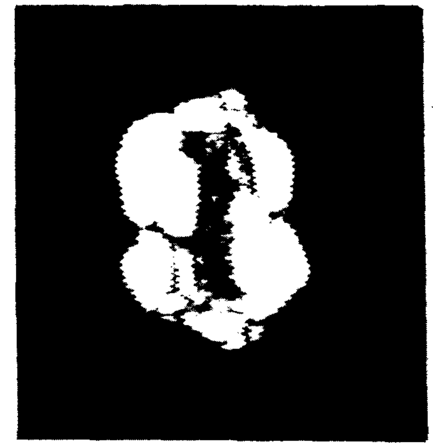

TV, 2X

B-SCAN RESULTS

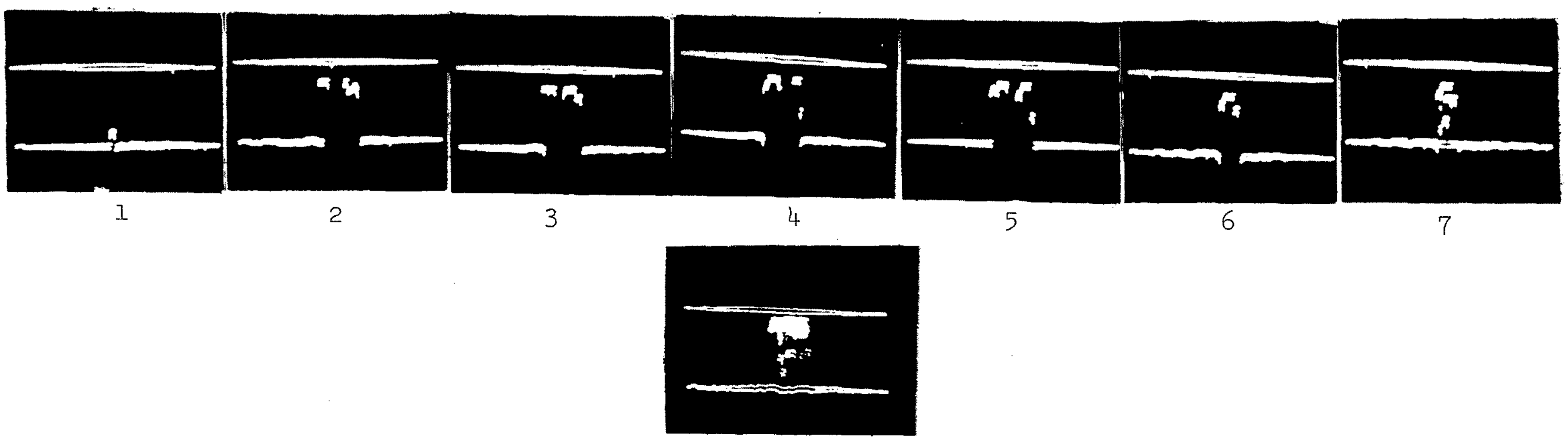

Figure 20

Site No. 24 Viewed from Back Side,
24-Ply Panel No. 1TY-1222

0° Fiber Orientation ⟶

C-SCAN RESULTS

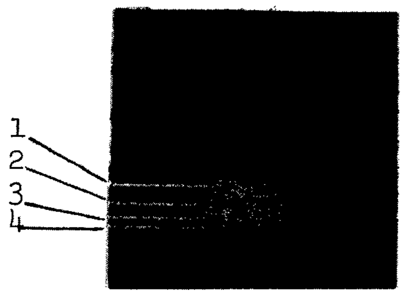

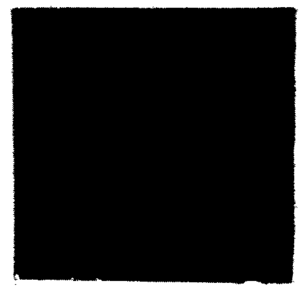

Scope

TV

B-SCAN RESULTS

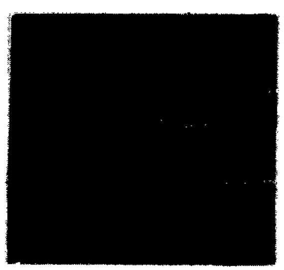

1

2

3

4

Σ

TABLE IX. PRELIMINARY DAMAGED HOLE DRILLING PARAMETERS

Condition *	Drill Bit Type**	Drill Speed		Drill Feed Rate		Hole Location No.
		rpm	rad/s	inch/revolution	mm/360 rad	
1	Standard High Speed Drill	2000	12,000	0.004	0.102	25
2		1065	6,390	0.001	0.025	27
3		600	3,600	0.004	0.102	29
4	Standard Cobalt Drill	2000	12,000	0.004	0.102	31
5		1065	6,390	0.004	0.102	33
6		600	3,600	0.001	0.025	35
7	#5330 Tip Carbide Drill	2000	12,000	0.008	0.204	37
8		1065	6,390	0.008	0.204	39
9		600	3,600	0.008	0.204	41

* All drilling conditions used an Aluminum back-up plate with a central 0.625 inch (15.88 mm) diameter hole opposite the drill bit.

** All holes were drilled with 3/8 inch (9.52 mm) diameter drill

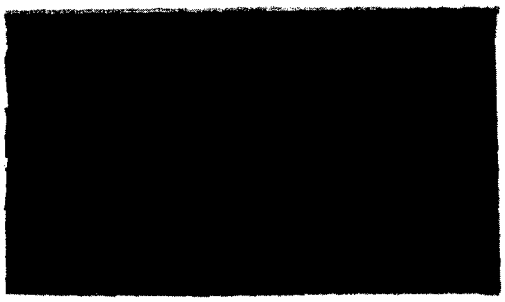

Hole #25

Hole #31

Hole #27

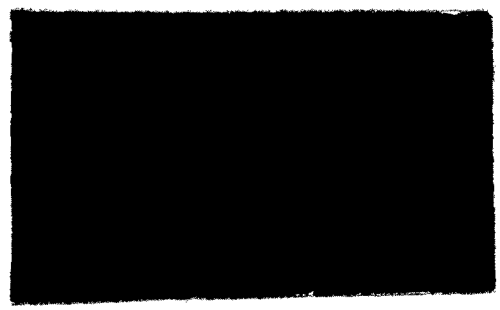

Hole #33

Hole #29

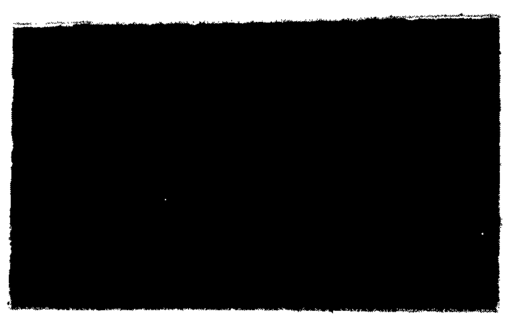

Hole #35

No damage, Holes #37, 39 and 41.

Figure 21. Ultrasonic C-Scan Results for 32-Ply Laminate Hole Study

Hole #25

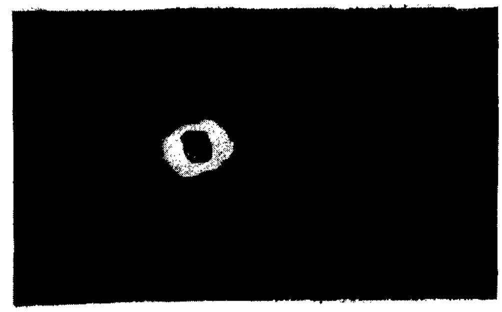

Hole #27

Hole #29

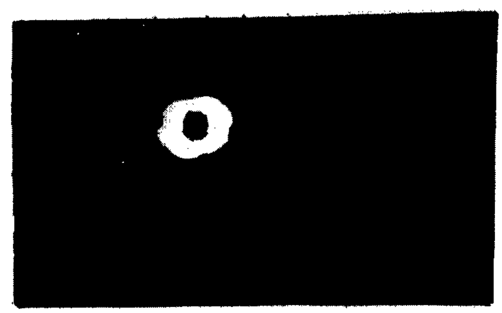

Hole #31

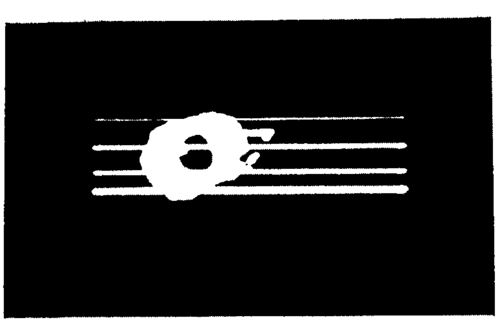

Hole #33

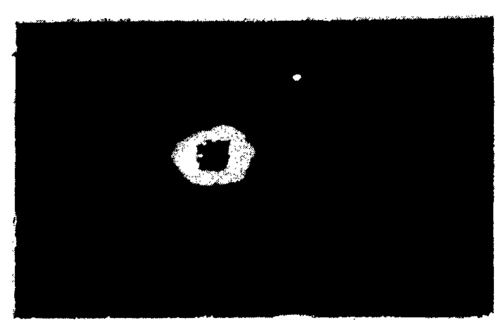

Hole #35

No significant damage in holes #37, 39, and 41.

Figure 22. Ultrasonic C-Scan Results for 24 Ply Laminate Hole Study

reasonably uniform about the hole without gross surface indications. A total of three holes were then prepared using each of the three drilling methods and the resulting damage characterized using the Holscan.

The results of hole damage characterization are shown in Figures 23-25 for the 32 ply material and Figures 26-28 for the 24 ply material. The results show the damage to again be primarily located in the region of the internal ply levels, similar to that shown for the impact damage condition. All three drilling methods seem to indicate similar damage extents and locations for each of the two laminates. Method 5, however, showed somewhat inconsistent results in the 32 ply material as shown in Figure 25. As a result, drilling method number 3 using a standard 3/8 inch (9.5 mm) high speed drill was selected for use in the balance of the program.

3.4 SPECIMEN RANDOMIZATION AND FABRICATION

Following panel fabrication and inspection, a master panel layout was developed for each panel as shown in Figure 29. A random sampling procedure was then used to select which coupons from each panel will have impact damage. Essentially the procedure is double random in that coupons for each test condition are randomly selected from each panel fabricated, and randomly assigned to a test condition and a test type. Randomization was accomplished using software programs developed at the Lockheed-California Company and based upon unbiased, Monte Carlo random number generators. A random number sequence was generated from 1 to 30 (the number of specimen blanks per panel) and a table of selection order vs. specimen number generated for each panel. The sequence orders 1 - 15 were assigned to contain impact damage and sequence orders 16 - 30 assigned to contain a damaged hole. A typical result is illustrated in Table X. Next, four random number tables were generated, one for each laminate and damage type to be studied. The panels of each laminate were then randomized by test as illustrated in Table XI. Randomization was conducted in sets of five (the number of panels per condition) to assure that all test panels were represented in a test type equally to eliminate any local statistically possible variations that would bias the sample in terms of a single panel.

Monitor C-Scan | Scope, C-Scan | Cumulative B-Scan

Hole #25

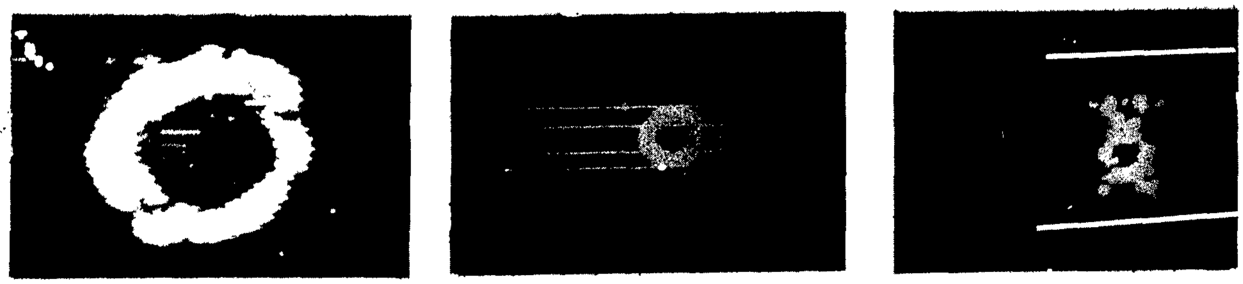

Hole #30

Hole #38

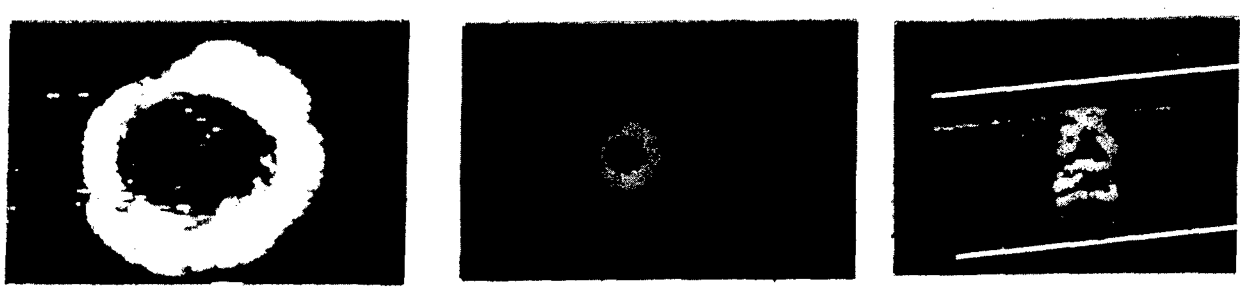

Figure 23. Variability of Hole Damage for Drilling Method No. 1 in 32-Ply Laminate

Monitor C-Scan | Scope, C-Scan | Cumulative B-Scan

Hole #29

Hole #32

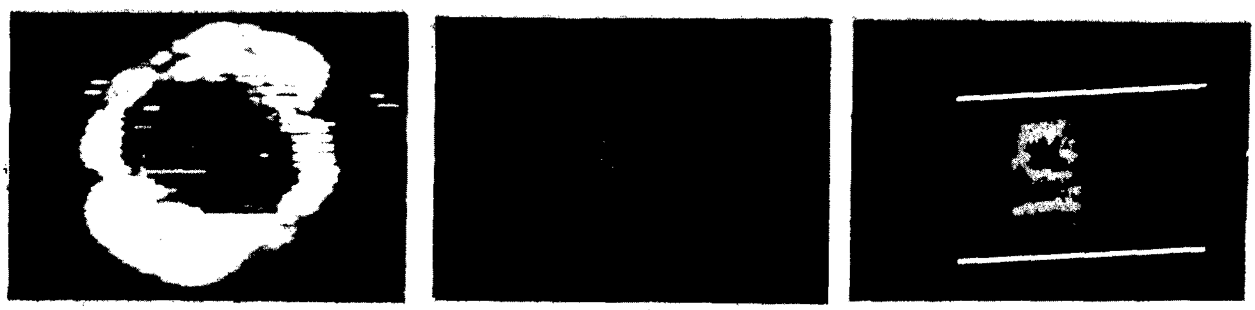

Hole #40

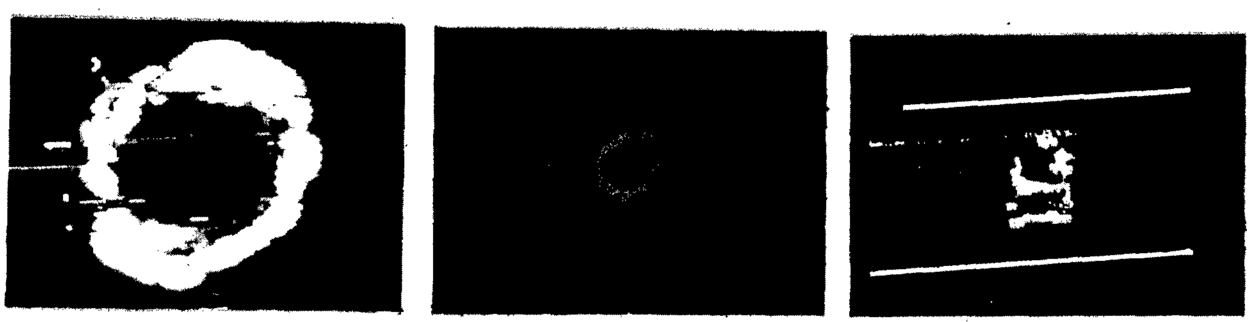

Figure 24. Variability of Hole Damage for Drilling Method No. 3 for 32-Ply Laminate

Monitor C-Scan | Scope, C-Scan | Cumulative B-Scan

Hole #26

Hole #33

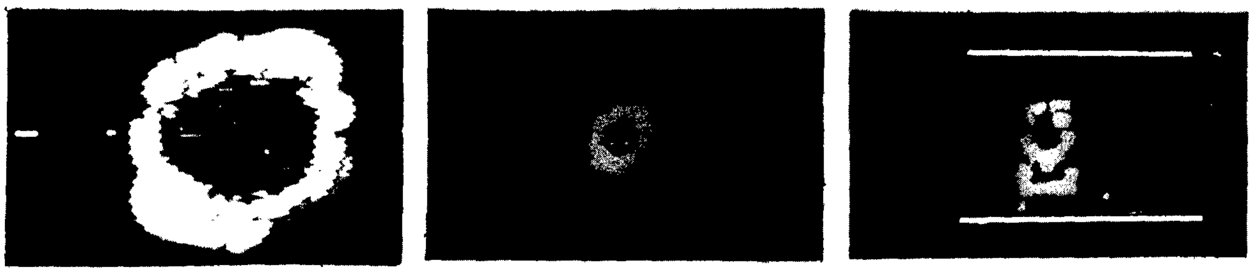

Hole #34

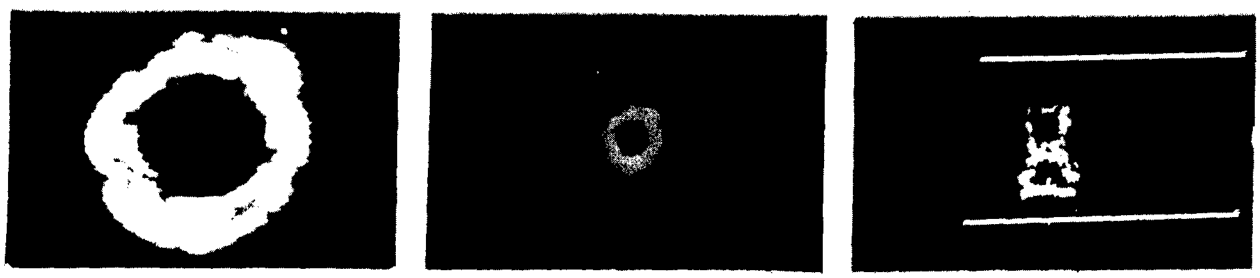

Figure 25. Variability of Hole Damage for Drilling Method No. 5 for 32-Ply Laminate

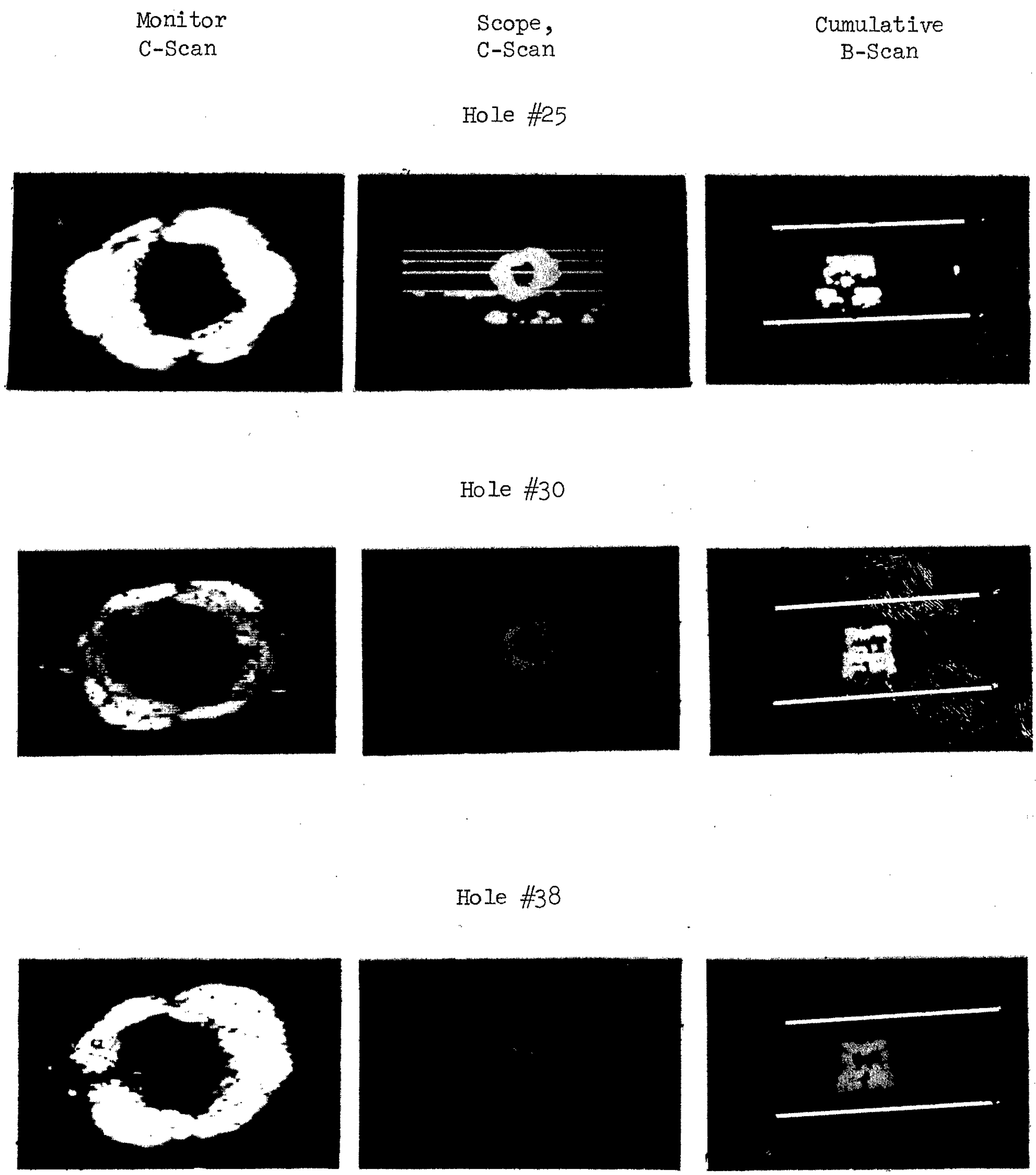

Figure 26. Variability of Hole Damage for Drilling Method No. 1 for 24-Ply Laminate

Monitor C-Scan | Scope, C-Scan | Cumulative B-Scan

Hole #29

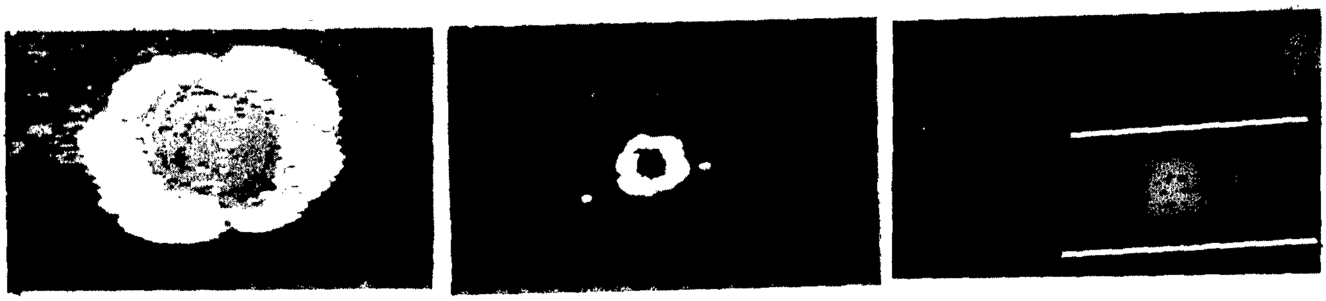

Hole #32

Hole #40

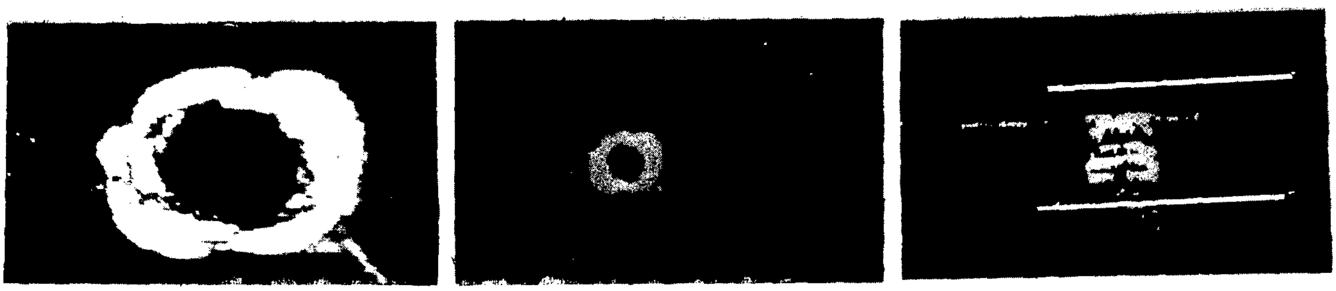

Figure 27. Variability of Hole Damage for Drilling Method No. 3 for 24-Ply Laminate

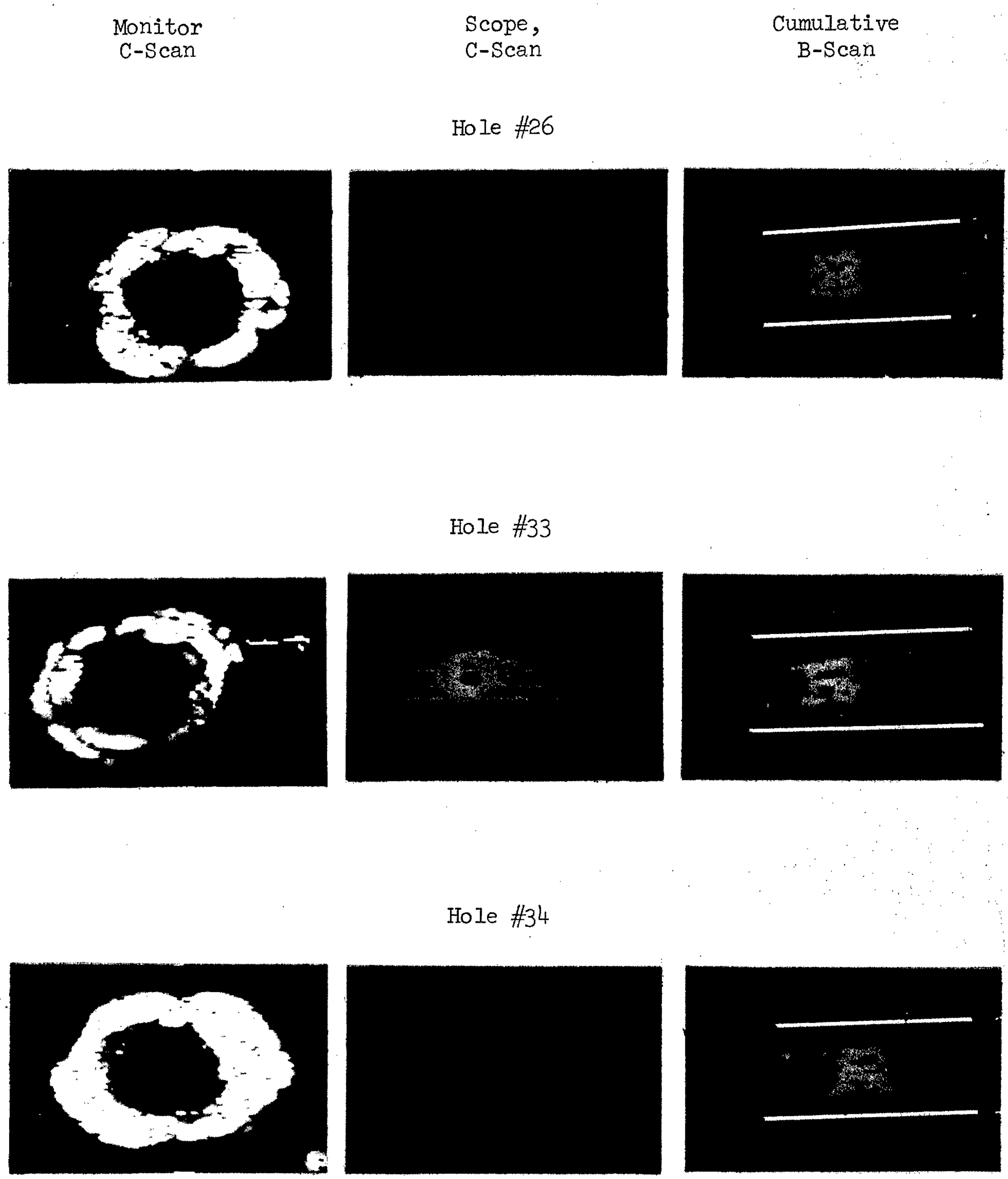

Figure 28. Variability of Hole Damage for Drilling Method No. 5 for 24-Ply Laminate

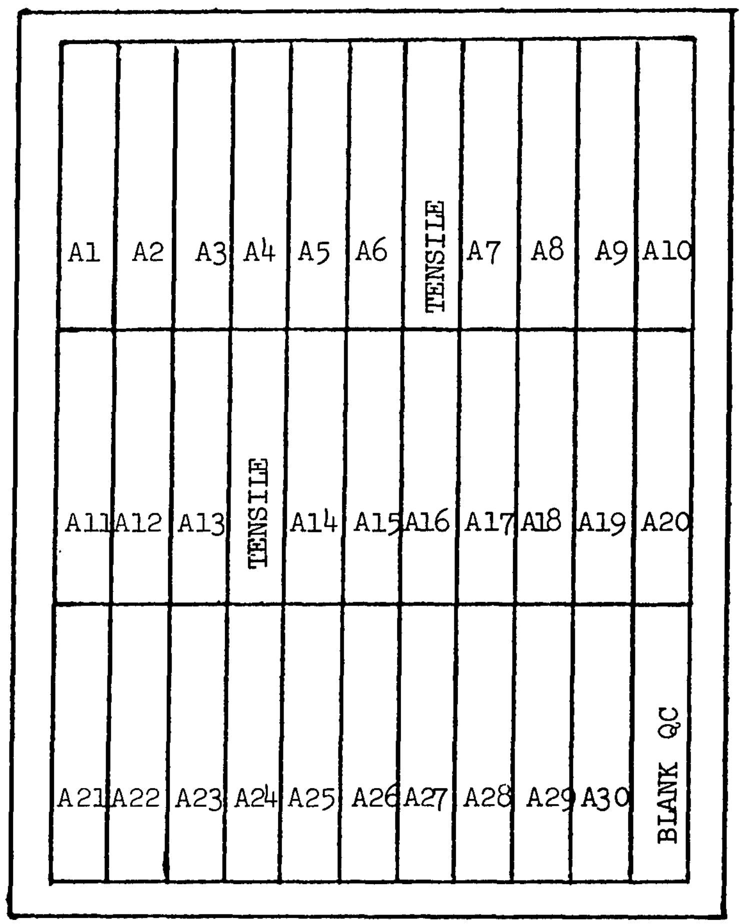

Figure 29. Typical Master Panel Layout as Prepared for Each Panel.

TABLE X. TYPICAL RANDOMIZATION OF SPECIMEN SEQUENCES

Panel Number: 2SY1179, Code "A"

	Sequence Number	Corresponding Specimen Number
Specimens to Contain Impact Damage	1	A-27
	2	A-1
	3	A-6
	4	A-2
	5	A-15
	6	A-20
	7	A-3
	8	A-9
	9	A-11
	10	A-12
	11	A-30
	12	A-4
	13	A-10
	14	A-7
	15	A-14
Specimens to Contain Damaged Holes	16	A-24
	17	A-5
	18	Etc.
	19	
	20	
	21	
	22	
	23	
	24	
	25	
	26	
	27	
	28	
	29	
	30	

TABLE XI. ILLUSTRATION OF RANDOMIZATION OF PANELS BY TEST

Damage Type: Impact

Laminate: 32 Ply

Panel Designations:	Code		Panel #:
	A (1)		______
	B (2)		______
	C (3)		______
	D (4)		______
	E (5)		______

Test Type	Number of Specimens Required	Panel	Corresponding Specimen No.
Static Tension	10	2	B-4 (First Spec. from Panel B)
		3	C-27 (First Spec. from Panel C)
		5	E-3 (First Spec. from Panel E)
		1	A-18 (First Spec. from Panel A)
		2	B-29 (Second Spec. from Panel B)
		1	A-6 (Second Spec. from Panel A)
		4	D-25 Etc.
		3	C-11
		5	E-10
		3	C-26
Static Compression	10	4	D-3
		5	
		2	
		etc.	etc.
Column Buckling	4	2	B-1
		etc.	etc.
Base S-N Tests	18	2	D-4
		etc.	etc.
TBE Static Compression	6	4	D-2
		etc.	etc.
TBE S-N Fatigue	9	1	A-6
Total Req.	57	etc.	etc.
Available Replacements	18	1	A-2
		4	D-29
		etc.	etc.

Following the selection of the impact specimen locations, each panel was laid out to locate the center of these specimens. Each site was then impacted using the selected impact conditions. Following the introduction of the impact damage, the panels were examined by ultrasonic C-scan to provide a permanent record of the exact impact damage sizes and locations. Initial impact damage details are given by specimen number in Appendix B. Specimens of the configuration previously shown in Figure 1 were then machined from the panels, tabs bonded on the specimen blanks, and the specimens measured and inspected by the Quality Control Laboratory. Specimen blanks which were to contain damaged holes were then returned to the shop for final hole drilling using the selected procedures. Initial damage dimensions of badly drilled holes were extremely consistent. Typical damage areas are also presented in Appendix B. All specimens were measured and stabilized in controlled laboratory air, 70 ± 3°F, 40 ±10% RH upon completion of fabrication for two weeks minimum prior to testing. All specimens were identified using the following numbering system.

A A - 12

panel identification code

sub-panel location in panel

specimen location in the panel/sub-panel

SECTION 4

EXPERIMENTAL PROCEDURES

4.1 STATIC TENSION TEST PROCEDURES

All tests were conducted in a 100 kip (445 kN) MTS closed loop Universal test machine equipped with three-inch hydraulic grips. Test procedures matched those used for normal ASTM E-8 static tension tests. A one-inch (25 mm) extensometer was attached across the damage zone on each specimen. For selected tests, a second 1/2-inch (13 mm) extensometer was attached one inch (25 mm) away from the damage area for comparison of the stress-strain results from the damaged and undamaged areas. All tests were conducted in room temperature laboratory air.

For the specimens with the damaged hole, the extensometer attached to the specimen surface across the hole was found to give accurate results for the early loading portion of the test, but as the specimen approached higher loads the material above and below the hole was found to exhibit out-of-plane displacements (i.e., the damage area "raised up") which caused the extensometer to slip. As a result, load-displacement curves were also recorded for all damaged hole specimens as a back-up system. A modified extensometer system is now being designed for use in Phase II and III to eliminate this problem.

4.2 STATIC COMPRESSION TEST PROCEDURES

Evaluation of the effect of compressive load bearing behavior of the damaged laminates was conducted in three phases. First a cursory examination of the column buckling behavior of each of the four damaged laminate conditions was conducted. Next a fatigue buckling support was designed and fabricated and a single compression test run for each damage/laminate condition and the results compared with the column buckling data to determine the relative

effectiveness of the fatigue guides. Finally, a full set of compression tests was conducted for each of the four damage/laminate conditions using the fatigue buckling supports.

The compression and column buckling tests were conducted using the same 100 kip (445 kN) MTS closed-loop test machine used for the tension tests. A continuous record of the applied load vs. stroke was recorded for each specimen. Tests were run at a "static" stroke rate of between 0.01 and 0.02 in./min (0.25 and 0.5 mm/min) and in laboratory air [70 $\pm$ 3°F (21 $\pm$ 2°C), 40$\pm$10% RH].

A complete set of test fixtures developed at Lockheed was used which permits compression testing of composite laminate specimens under controlled conditions in either the fully-restrained mode, under column compression at various controlled bay lengths, or which can be used with the fatigue buckling guides. The specimen-supporting fixtures are designed for use with the MTS hydraulically actuated grips installed in the 100 kip (445 kN) MTS test machine. A full description of these test fixtures is given in Reference 24 and 25.

Briefly, a close-fitting steel shell surrounds each grip, providing a mount for transverse adjustment screws that prevent destabilizing motion of the platens and specimen. The grips are rigidly mounted to the machine base and test head, precise alignment having first been achieved with the aid of spherically surfaced seats.

The fixture used to provide specimen support for testing to "compression ultimate" stress consists of two rigid guides or platens similar in gross form to those of ASTM 695 Federal Test Standard 406, on the inner surfaces of which are located a set of extendable auxiliary platens which provide support over the full length of the test specimen. The auxiliary platens have a tapered overlap in the width dimension so that no critical length of the specimen is left unsupported. A detailed description is given in Reference 25.

Pin-end column test conditions are provided using the same general test arrangement as described above, but with the smooth auxiliary platens of the specimen support fixture replaced with pin-locating platens as shown in Figure 30. Five different sets of platens are available. These provide pin-end

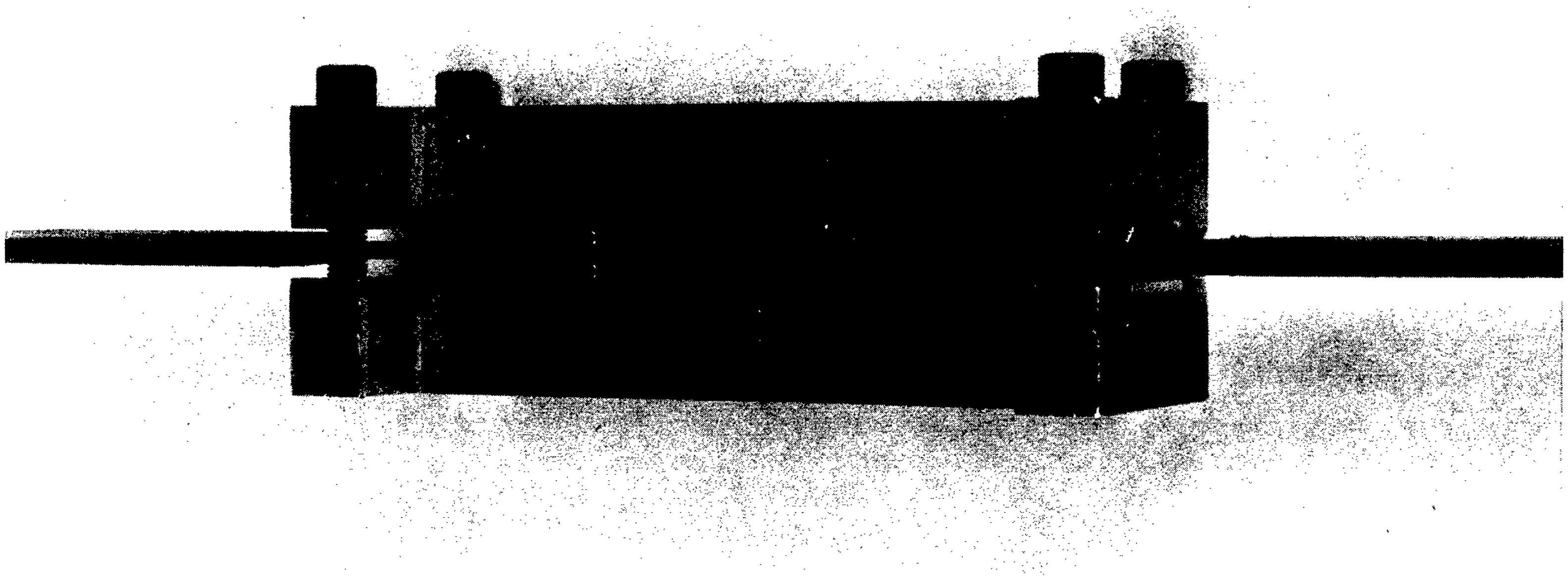

136217R

Figure 30. Composite Specimen Column Test Fixture

test lengths of 2.383, 1.570, 1.170, 0.776 and 0.580 inches, (60.5, 39.9, 29.7, 19.7 and 14.7 mm) obtained with 3, 5, 7, 11 and 15 bays respectively. The 3 and 7 bay lengths were used.

4.3 FATIGUE TEST PROCEDURES

Room temperature fatigue tests were conducted in vertical closed-loop electro-hydraulic test machines at a range ratio of -1.0 and at a frequency of 5 Hz until failure or 2×10^6 cycles was achieved. Each of the closed-loop electro-hydraulic fatigue machines is equipped with a peak and valley load monitoring system which allows the monitoring of the load signal maximum peak, maximum valley, and minimum peak and minimum valley with an accuracy of ±1.0 percent of full-scale reading. Maximum peak and valley loads are monitored continuously and can be preset to sound an alarm or stop the test in the event of any loading deviation. Since previous work(2) has shown that early failures may result due to initial loading at normal fatigue loading rates, the following test start procedure was adopted. Loading for the first ten cycles of a specimen's life was conducted at a frequency of 0.05 Hz. Following NDI inspection, assuming no significant growth, the frequency was increased to 5 Hz and the test continued to failure at 5 Hz. Damage zone size measurements and damage characterization examinations were made periodically during each test using the modified Holscan 400 Ultrasonic NDI system previously described in Section 2.4.

Due to the large compressive component to be experienced during these tests, the method of test specimen support is a major concern since unrealistic supporting conditions such as full face plate buckling guides are not representative of aircraft structure loading. Thus the test support must be carefully designed such that minimum external constraint due to the support is induced.

The fatigue support design used for the current test program is shown in Figure 31. This configuration was designed to allow localized deflection normal to the plane of the specimen while still providing adequate constraint to prevent extensive gross buckling.

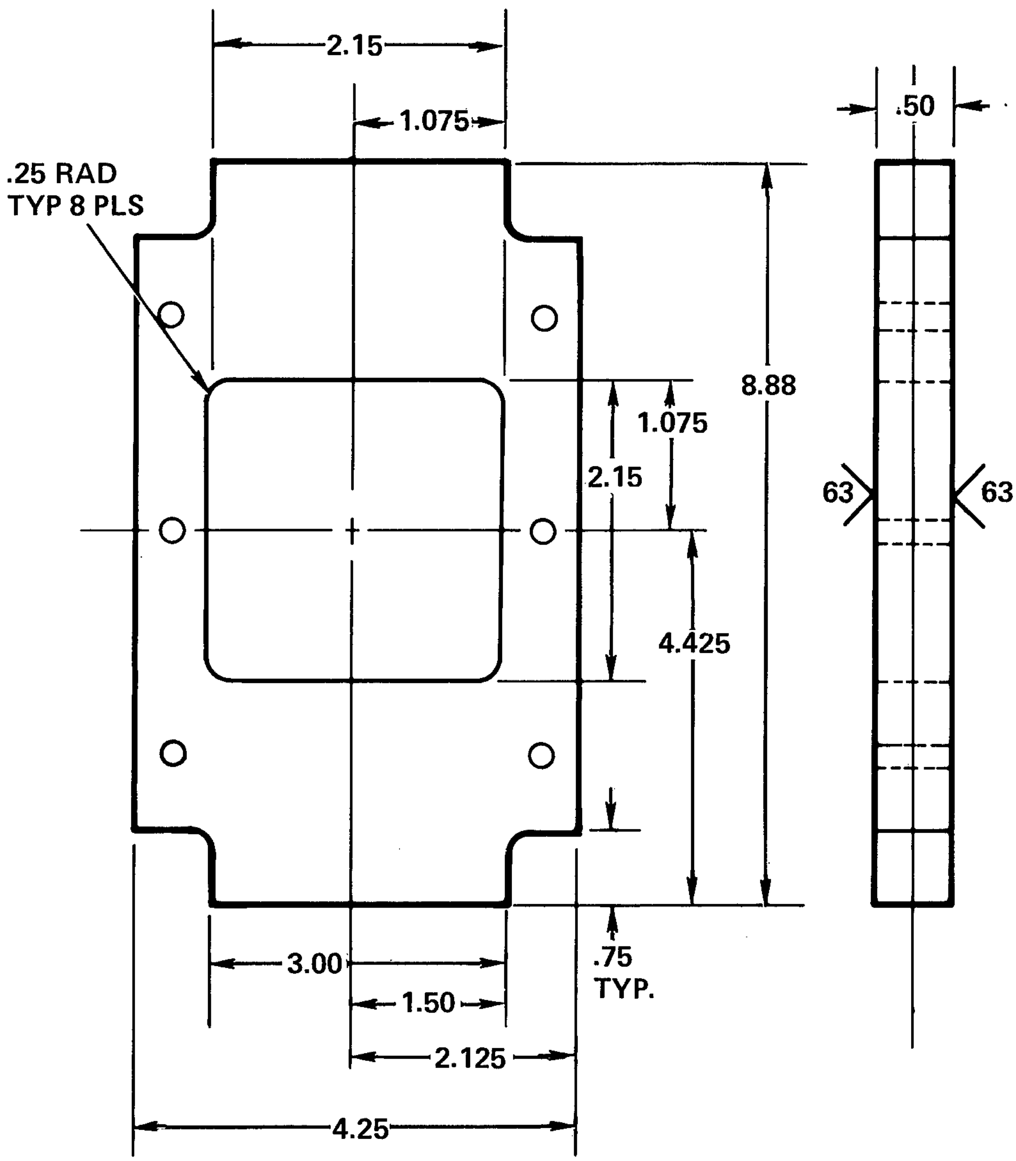

NOTE: All Dimensions in Inches (1 in. = 25.4 mm).

Figure 31. Fatigue Buckling Guide Design

SECTION 5

STATIC TEST RESULTS

The first data developed on the damaged laminates were those of static tension, compression column buckling, and static compression strength. Once these limiting stress levels were obtained, fatigue testing was conducted. This section presents the results of these static tests.

5.1 STATIC TENSION TEST RESULTS

All static tension tests were conducted in room temperature laboratory air using the procedures described in Section 4.2. Ten replicate tests were conducted for each of the four damage/laminate conditions. In addition, 1.0 inch (25.4 mm) wide duplicate quality control tension specimens were removed from random locations in each panel and tested in the undamaged condition to provide a static strength reference level and to indicate any significant panel to panel variation in the base panel strength level. Results of these tests are presented in the following section.

5.1.1 QUALITY CONTROL TENSILE TEST RESULTS

Standard Quality Control tension tests were conducted on duplicate 1-inch wide x 10.5-inch long (25mm x 267mm) tension specimens selected from random locations in each of the five panels of 32 ply and of 24 ply material. The results are presented in Tables XII and XIII for the 32 ply and 24 ply material, respectively.

The 32 ply material exhibited the typical two stage slope shown schematically in Figure 32 that is typical for quasi-isotropic laminates. Examination of the results shown in Table XII indicates the range of all values to be approximately ± 10% or less, a range not unusual for a data set involving several processing runs[2]. While the duplicate results from within a panel appear to be less than approximately ± 5% for 4 of the 5 panels, panel No.

TABLE XII. TENSION TEST RESULTS FOR 32 PLY QUASI-ISOTROPIC T300/5208, UNDAMAGED 1-INCH (25.4 mm) WIDE

Specimen ID	Average Area, A		Ultimate Load, P_{ult}		Ultimate Stress, σ_{ult}		Ultimate Strain, ϵ_{ult}, mm/mm, in 1 inch (25.4 mm)	Slope Deviation Stress, σ_y		Slope Deviation Strain, ϵ_y, mm/mm in 1 inch (25.4 mm)	Initial Apparent Modulus, E_1		Secondary Apparent Modulus, E_2		Failure Location, Distance from Tab	
	$inch^2$	mm^2	kip	KN	ksi	MPa		ksi	MPa		$psi \cdot 10^6$	GPa	$psi \cdot 10^6$	GPa	inch	mm
2TY-1228-AA	0.1605	104	13.3	59.2	82.7	570	0.0104	57.3	395	0.0068	8.42	58.0	7.10	49.0	2.0	49
2TY-1228-AC	0.1606	104	12.6	56.0	78.6	542	0.0102	53.5	369	0.0066	8.11	55.9	6.92	47.7	0.5	12
1TY-1228-BA	0.1533	102	12.5	55.6	78.8	543	0.0102	55.6	383	0.0068	8.18	56.4	6.98	48.1	0.8	20
1TY-1228-BB	0.1530	102	12.4	55.2	78.0	538	0.0099	57.9	399	0.0070	8.27	57.0	6.95	47.9	1.5	38
2TY-1227-CA	0.1622	105	13.3	59.2	82.0	565	0.0104	49.3	340	0.0060	8.22	56.7	7.29	50.3	*	*
2TY-1227-CC	0.1526	98.4	12.4	55.2	81.3	561	0.0103	53.7	370	0.0068	7.90	54.5	6.95	47.9	1.0	25
1TY-1230-DA	0.1654	107	11.4	50.7	69.2	477	0.0089	53.2	367	0.0067	7.94	54.7	6.80	46.9	2.5	64
1TY-1230-DB	0.1663	107	12.0	53.4	72.4	499	0.0097	51.1	352	0.0066	7.74	53.4	6.56	45.2	3.0	76
1TY-1229-EB	0.1667	108	13.5	60.0	80.9	558	0.0108	49.2	339	0.0062	7.94	54.7	6.91	47.6	1.5	38
1TY-1229-EC	0.1650	106	11.6	51.6	70.4	485	0.0093	54.5	376	0.0069	7.90	54.5	6.57	45.3	1.0	25
Average					77.4	534	0.0100	53.5	369	0.0066	8.06	55.6	6.90	47.6		
					+ 5.3	+ 36	+ 0.0008	+ 4.4	+ 30	+ 0.0004	+ 0.36	+ 2.4	+ 0.39	+ 2.7		
					- 7.0	- 57	- 0.0011	- 4.3	- 30	- 0.0006	- 0.16	- 2.2	- 0.34	- 2.4		

* Specimen Shattered

TABLE XIII. TENSION TEST RESULTS FOR 24 PLY 67% 0° FIBER T300/5208, UNDAMAGED 1-INCH (25.4 mm) WIDE

Specimen ID	Average Area, A		Ultimate Load P_{ult}		Ultimate Stress, σ_{ult}		Ultimate Strain ϵ_{ult}, mm/mm in 1 inch (25.4 mm)	Apparent Modulus of Elasticity, E		Failure Location Distance from tab	
	inch^2	mm^2	lb.	KN	ksi	MPa		psi·10^6	GPa	inch	mm
1TY-1236-JA	0.1261	81.3	17,600	78.3	139.6	962	0.0092	14.9	103	0	0
1TY-1236-JB	0.1237	79.8	17,160	76.3	138.7	956	0.0093	15.2	105	1.8	46
1TY-1238-HA	0.1216	78.4	17,520	77.9	144.1	993	0.0094	15.4	106	0	0
1TY-1238-HB	0.1227	79.2	18,580	82.6	151.4	1044	0.0095	15.6	108	0.4	10
2TY-1236-KB	0.1233	79.5	19,060	84.8	154.6	1066	0.0096	15.7	108	0	0
2TY-1236-KC	0.1217	78.5	17,600	78.3	144.6	997	0.0094	15.2	105	0	0
1TY-1234-MB	0.1260	81.3	17,900	79.6	142.1	980	0.0094	15.5	107	0	0
1TY-1234-MC	0.1206	77.8	18,100	80.5	150.1	1035	0.0098	15.0	103	0	0
2TY-1234-LA	0.1230	79.3	19,000	84.5	154.5	1065	0.0097	15.6	108	0	0
2TY-1234-LB	0.1237	79.8	19,050	85.7	154.0	1062	0.0097	14.9	103	0	0
Average					147.4	1016	0.0095	15.3	106		
					+ 7.2	+ 50	+0.003	+ 0.4	+ 2		
					- 8.7	- 60	-0.003	- 0.4	- 3		

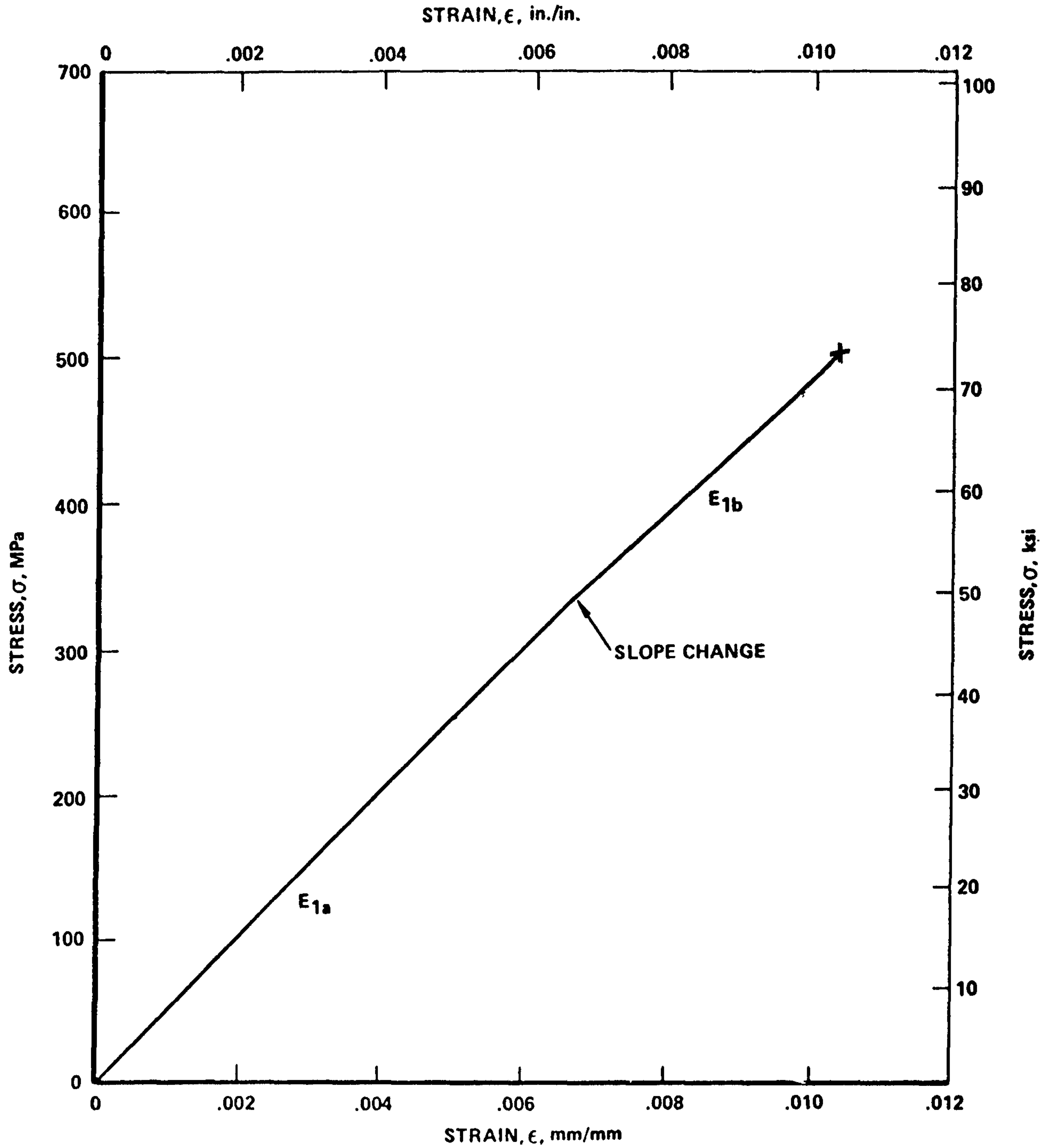

Figure 32. Typical Stress-Strain Curve Measured for the 32 Ply Quasi-Isotropic Laminate

1TY-1229 (Code "E") shows scatter between the two results on the order of the total range for all 5 panels. As a result of the small data sample size per panel it is not possible to determine if small panel to panel variation is real or only isolated points of the larger distribution reflected by the results for the 5 panel set.

The 24 ply 67% 0° fiber tensile results showed a linear to fracture curve such as shown in Figure 33 which is typical for this high percentage of 0° fiber laminate. The scatter of the resulting data shown in Table XIII was quite small, typically of the order ± 6% or less for all measured values. Note that in Table XIII many of the specimens are reported to have failed near the tab. This indicates that while failure may have occurred over some distance, the failure did extend down to the top of the tab, thus resulting in a "0" entry in Table XIII. The significance of these near tab failures is not fully known. It should be noted that the two failures, specimens 1TY-1236-JB and 1TY-1238-HB represent the lowest data point and one of the higher data points of the set. A recent study by Ryder[2] on this same 67% 0° fiber laminate of T300/934 also exhibited a number of tension test failures near the tab on a much larger data set. Following a statistical evaluation of these results it was concluded that the near tab failures did not compose a different data population than those that failed away from the tab region.

5.1.2 Static Tension Test Results for 24 Ply 67% 0° Fiber, T300/5208 Laminate Specimens containing Impact Damage

Results of these tests are presented in Table XIV. Examination of Table XIV shows generally very little variation in the results. Of the two exceptions (specimens LC-28 and MA-4), MA-4 was found to have been initially loaded to 33,000 lb (147 kN) when a system failure resulted in a hydraulic pressure dump which unloaded the specimen. On reloading to failure, a significant change in the specimen modulus was noted, final failure occurring at a very low load. For this reason the results for specimen MA-4 were eliminated from the averaging and are considered invalid. No test procedure anomaly could be found in the test records for specimen LC-28 which was retained in

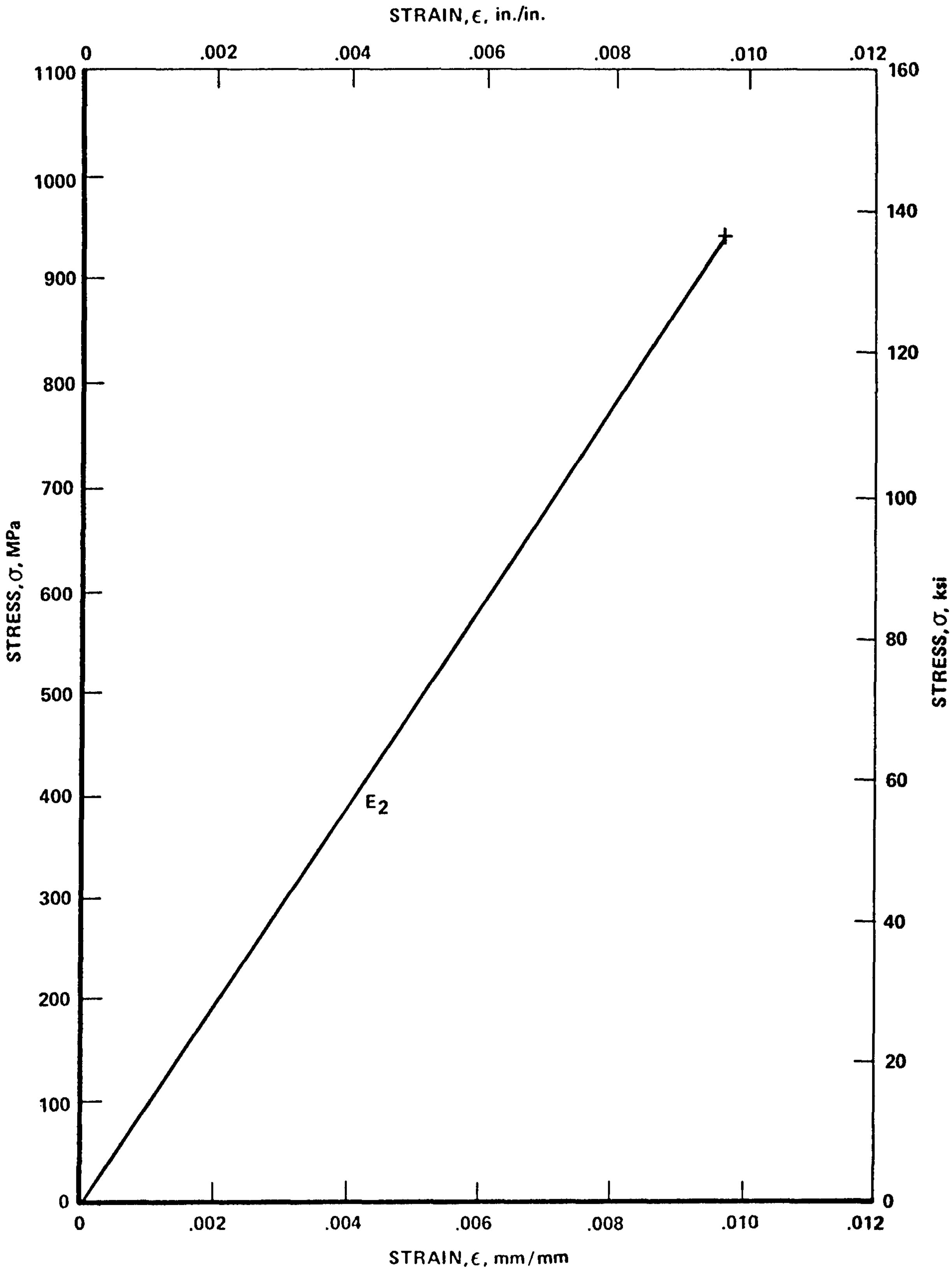

Figure 33. Schematic of the Typical Stress Strain Curve Measured for the 24 Ply 67% 0° Fiber Laminate

TABLE XIV. TENSION TEST RESULTS FOR 24 PLY 67% 0° FIBER T300/5208 SPECIMENS CONTAINING IMPACT DAMAGE

Specimen ID	Average Area, A		Ultimate Load, P_{ult}		Apparent Ultimate Stress, σ_{ult}		Apparent Ultimate Strain ϵ_{ult}, mm/mm in 1 inch (25.4 mm)	Apparent Modulus of Elasticity E_D		C-Scan Apparent Damage Size X·Y	
	$inch^2$	mm^2	kip	KN	ksi	MPa		$psi \cdot 10^6$	GPa	in. x in.	mm x mm
1TY-1238-HB-18	0.3668	237	53.5	238	145.8	1005	0.0099	14.3	98.6	.46 x .66	12 x 17
-HC-30	0.3637	235	56.0	249	154.0	1062	0.0101	15.0	103	.45 x .69	11 x 18
1TY-1236-JA-4	0.3754	242	59.2	263	157.7	1087	0.0112	13.6	93.8	.44 x .63	11 x 16
-JB-16	0.3728	240	57.0	254	152.9	1054	0.0103	14.0	96.5	.45 x .65	11 x 17
2TY-1236-KA-6	0.3688	238	59.2	263	160.5	1106	0.0110	14.2	97.9	.48 x .71	12 x 18
-KB-12	0.3664	236	58.0	258	158.3	1091	0.0107	14.6	101.0	.45 x .65	11 x 17
2TY-1234-LB-15	0.3709	239	55.0	245	148.3	1022	0.0105	13.9	95.8	.47 x .78	12 x 20
-LC-28	0.3694	238	46.2	206	125.1	862	0.0092	13.0	89.6	.41 x .71	10 x 18
1TY-1234-MA-8	0.3733	241	56.1	250	150.3	1036	0.0104	14.0	96.5	.45 x .71	11 x 18
-MA-4	0.3730	241	39.5 *	176	105.9 *	730	0.0085 *	11.5*(14.8)**	(79.3)*(102)**	.45 x .69	11 x 18
Average					150.3	1036	0.0104	14.1	97.0		
					+ 10.2	+ 70	+0.0008	+0.9	+6.0		
					- 25.2	-174	-0.0012	-1.1	-7.4		

* Second loading, loaded to 33,000 lb and unloaded previously, data not included in average.

** First loading

the data set. A comparison of these results in Table XIV with the basic quality control tensile test results presented in Table XIII shows no significant decrease in the tensile strength of the damaged laminates although some reduction ($\approx 7\%$) in the apparent modulus across the damage zone is observed. Extensometer results obtained across the damage region compared with those obtained away from the damage on the edge of the specimen indicated only slightly higher modulus values for the former as shown in Table XV.

Review of the Holscan records of the initial damage showed no consistent correlation with the static strength of the impact damaged specimens. Typical results are shown in Figure 34 for specimen KA-6 (highest static strength of 160.5 ksi (1106 MPa), JB-16 (typical mid-range static strength of 152.9 ksi (1054 MPa)), and LC-28 (lowest static strength of 125.1 ksi (862 MPa)). The impact damage characteristics are seen to be virtually the same for all three specimens. In addition, no correlation was found between static strength of the damaged laminate specimens with panel fiber volume content or undamaged static strength.

Examination of the failed specimens revealed three distinctive types of fracture. Specimens JA-4, KA-6, and LB-15 failed along $\approx 45°$ angles intersecting in the damage zone. A typical failure is shown in Figure 35a.

A slightly different form of the 45° fracture path occured for specimen MA-8 (fig. 35b) where the 45° fracture appears to pass through the upper and lower edge of the impact damage region. Note that these failures occur over the entire range of static strengths and are not indicative of high or low values.

A second fracture type was observed as shown in Figure 36 for specimens KB-12, HB-18 and JB-16. These specimen failures showed extensive longitudinal cracking with some breakage occurring normal to the loading direction. Again this failure type did not appear to be typical of either high or low failure stresses but rather spans the entire range of observed values. Thus, there seems to be no preference as to the occurrence of a Type 1 or Type 2 failure mode based on panel or on observed failure stress.

TABLE XV. COMPARISON OF STRAIN RESULTS FROM EXTENSOMETERS LOCATED ACROSS THE IMPACT DAMAGE SITE AND ACROSS UNDAMAGED MATERIAL IN 24 PLY 67% 0° FIBER T300/5208

	1-Inch (24.5 mm) Extensometer Across Damage			0.5-Inch (12.7 mm) Extensometer Across Undamaged Region		
	Apparent Ultimate Strain ϵ_{ult_D}	Apparent Modulus of Elasticity E_D		Ultimate Strain ϵ_{ult}	Modulus of Elasticity, E	
Specimen Number		$psi \cdot 10^6$	GPa		$psi \cdot 10^6$	GPa
1TY-1236-JB-16	0.0103	14.0	96.5	0.0104	14.5	100.0
2TY-1236-KB-12	0.0107	14.6	100.7	0.0107	14.6	100.7
2TY-1234-LB-15	0.0105	13.9	95.8	0.0099	14.6	100.7

→ 0°

TV Monitor, 2X

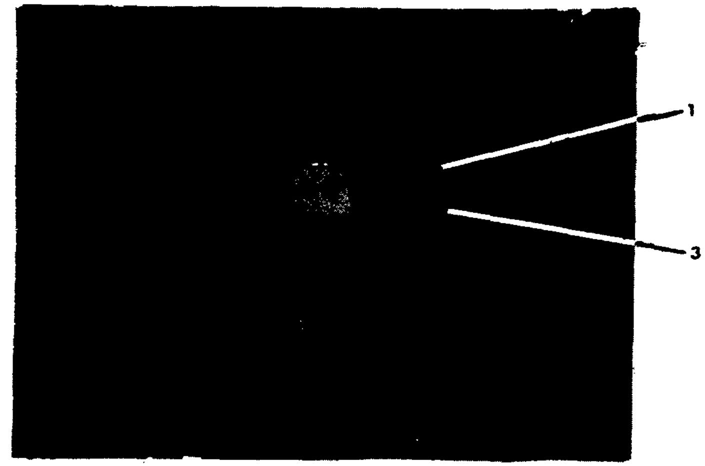

Scope

Section 1 B-Scan

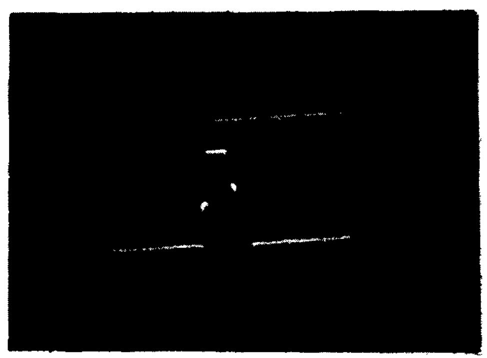

Section 2 B-Scan

Total B-Scan

(A) KA-6, 1106 MPa (160.5 ksi) Failure Stress

Figure 34a. Typical Impact Damage, 24 Ply 67% 0° Fiber T300/5208 Laminate

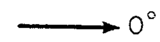

TV Monitor, 2X

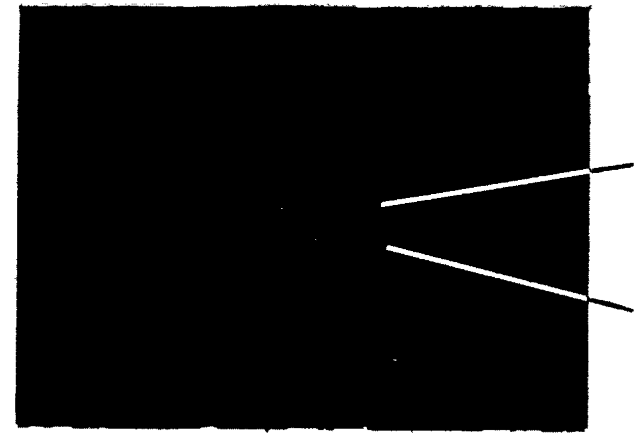

Scope

Section 1 B-Scan

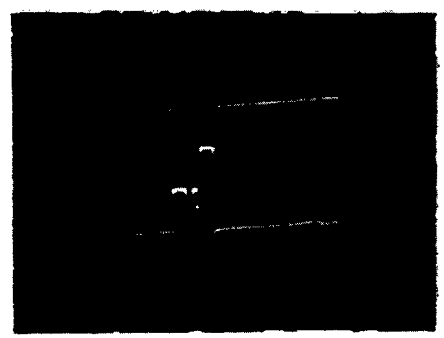

Section 3 B-Scan

Total B-Scan

(B) JB-16, 1054 MPa (152.9 ksi) Failure Stress

Figure 34b. Typical Impact Damage, 24 Ply 67% 0° Fiber T300/5208 Laminate

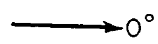

TV Monitor, 2X

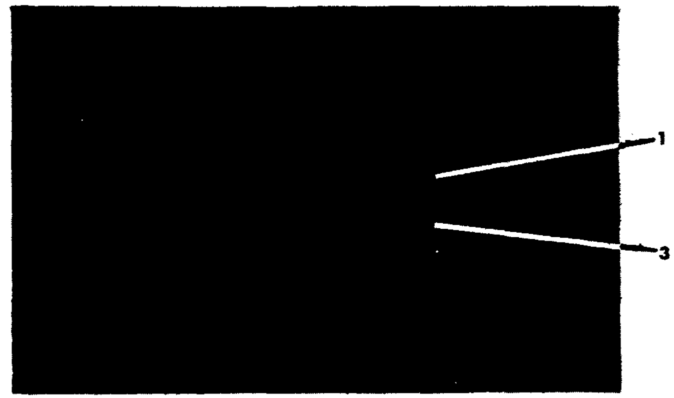

Scope

Section 1 B-Scan

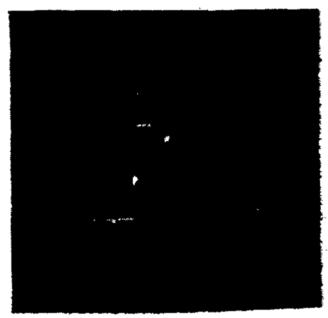

Section 2 B-Scan

Total B-Scan

(C) LC-28, (125.1 ksi) 862 MPa Failure Stress

Figure 34c. Typical Impact Damage, 24 Ply 67% 0° Fiber T300/5208 Laminate

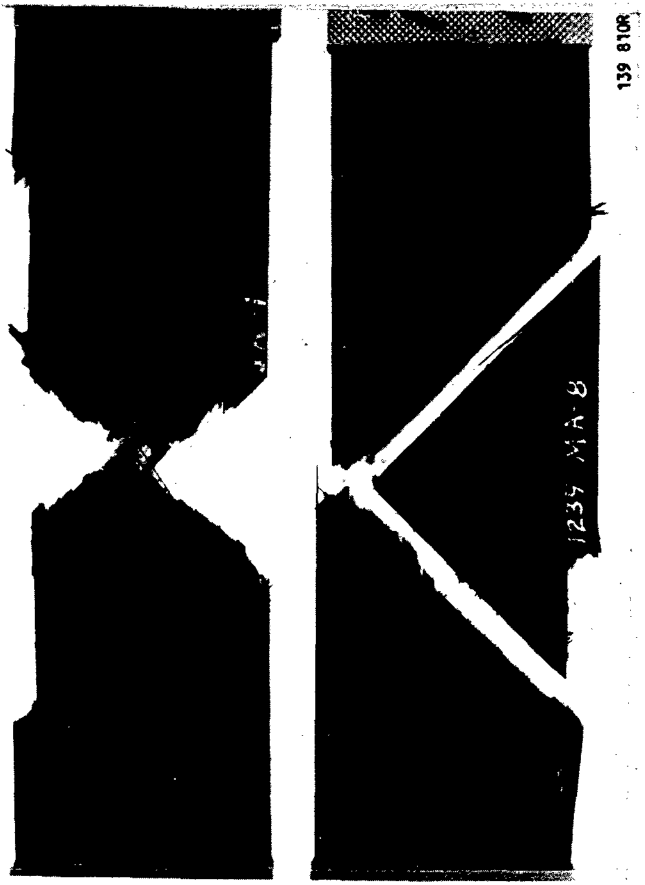

a b

Figure 35. Typical Type 1 Tension Failure of Impact Damaged 24 Ply 67% 0° Fiber Laminate

Figure 36. Typical Type 2 Tension Failure Mode of Impact Damaged 24 Ply 67% 0° Fiber Laminate

Occurrence of the remaining (Type 3) failure mode was, however, typical only of the two lowest failure stress values. The Type 3 failure mode, shown in Figure 37, was observed only in specimen MA-4 and LC-28. Both of these failures exhibited extensive delamination, a characteristic not observed in either the Type 1 or Type 2 failures. While specimen MA-4 had anomalous loading history in the form of a previous load cycle to > 80% of the subsequent fracture load, no similar anomalous load history was found for LC-28. Note however, that LC-28 exhibited the lowest modulus value of the nine test specimens, a drop in modulus being the major difference observed between the first and second loading of specimen MA-4. However, since no significant anomaly in the history of LC-28 can be identified, the data point is not eliminated at this point in time. The effect of this data point on the statistical distribution is discussed in the subsequent section.

5.1.3 Static Tension Test Results for 24 Ply 67% 0° Fiber T300/5208 Laminate Specimens Containing Damaged Holes

Results of these tests are presented in Table XVI. Comparison of these results with the undamaged tensile test results (Table XIII) shows a drop of over 50% in static strength for the 3/8 inch (9.5 mm) diameter damaged hole specimens, the scatter in the static strength value for the damaged hole specimens being less than ± 7%. The initial modulus values listed in Table XVI were obtained from the 1-inch (25.4 mm) gage length extensometer located across the hole and show a marked drop in the initial gross values of greater than 40% compared to the unnotched tension specimens. Examination of the Holscan results showed the damage in all the holes to be very consistent, the typical damage zone extending ~ 0.08 inch (2 mm) around the 0.375 inch (9.5 mm) diameter hole. Typical C-scan results for the range of static strengths are shown in Figure 38 and show no identifiable variation with failure loads. As previously noted, extensometer slippage occurred prior to fracture, so the failure strains given in Table XVI are average values based on the load vs deflection record.

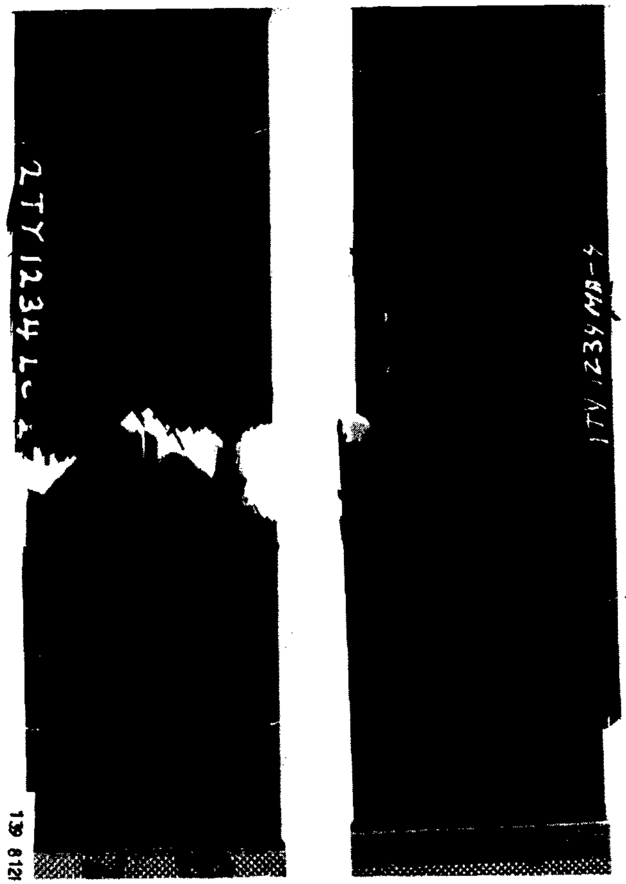

LC-28
862 MPa
(125.1 ksi)

MA-4
730 MPa
(105.9 ksi)

LC-28

MA-4

Figure 37. Type 3 Failure Modes observed in Low Strength Tension Failures of Impact Damaged 24 Ply 67% 0° Fiber Laminates

TABLE XVI. 24 PLY 67% 0° FIBER T300/5208 DAMAGED HOLE TENSION TEST RESULTS

Specimen Number	Average Thickness, B		Gross Area, A		Failure Load, P_u		Gross Area Failure Stress σ_u		Initial Gross Average Modulus E		Estimated Strain at Failure ϵ_u
	inch	mm	inch^2	mm^2	kip	KN	ksi	MPa	psi · 10^6	GPa	mm/mm
HA-9	0.1219	3.10	0.3654	236	26.70	119	73.1	504	8.14	56.1	0.0079
HC-29	0.1210	3.07	0.3628	234	27.15	121	74.8	516	8.77	60.5	0.0074
JC-26	0.1230	3.12	0.3683	238	25.00	111	67.9	468	7.99	55.1	0.0074
JC-28	0.1238	3.14	0.3708	239	24.55	109	66.2	456	8.22	56.7	0.0070
KB-19	0.1226	3.11	0.3674	237	25.50	113	69.4	478	8.57	59.1	0.0071
KC-23	0.1226	3.11	0.3676	237	25.05	111	68.1	469	7.75	53.4	0.0077
LA-5	0.1238	3.14	0.3709	239	25.75	114	69.4	478	8.11	55.9	0.0075
LC-27	0.1230	3.12	0.3685	238	25.00	111	67.8	467	7.96	54.9	0.0074
MA-3	0.1247	3.17	0.3737	241	26.70	119	71.4	492	7.78	53.6	0.0080
MA-6	0.1251	3.18	0.3748	242	25.90	115	69.1	476	8.34	57.5	0.0073
Average							69.7	480	8.16	56.3	0.0075
							+ 5.1	+ 36	+ 0.61	+ 4.2	+ 0.0005
							- 3.5	- 24	- 0.41	- 2.9	- 0.0005

NOTE: See Appendix B for typical initial damage dimensions.

TV Monitor, X2

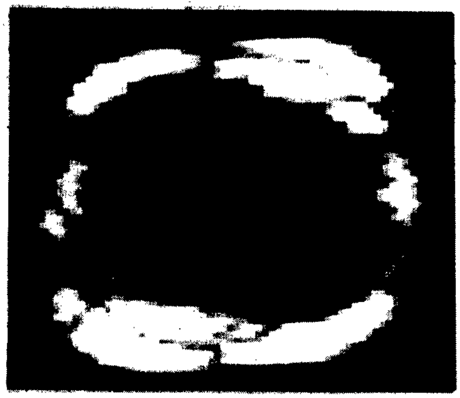

HC-24

σ_u = (74.8 ksi) 516 MPa

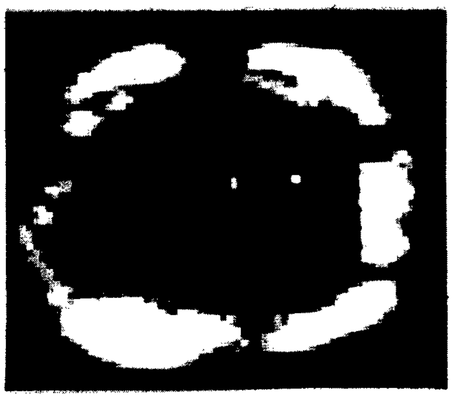

MA-3

σ_u = (71.4 ksi) 492 MPa

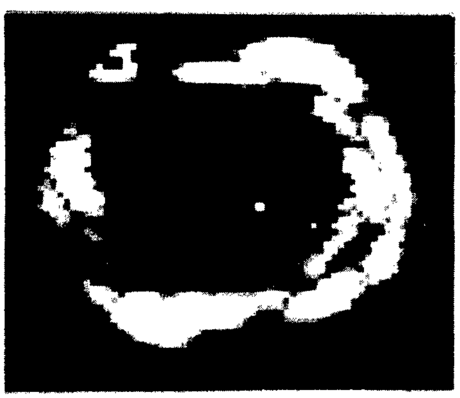

LA-5

σ_u = (69.4 ksi) 478 MPa

JC-28

σ_u = (66.2 ksi) 456 MPa

Figure 38. Typical C-Scan Hole Damage Sizes in Tension Test Specimens of 24 Ply 67% 0° Fiber Laminate

A two parameter Weibull data fit* is shown in Figure 39 for the damaged hole and impact damaged tension result. The values for the shape parameter $k = 24.699$ with a characteristic value $v = 71.087$ were obtained for the damaged hole specimen data. Correlation between the $k = 22.611$ obtained for the baseline tension specimens is reasonably good for this small sample size. This indicates that the postulate of Whitney, et al[26] that the main difference in specimens containing a hole or notch should be a translation of the results with the same shape parameter, k, holds reasonably well for this laminate.

Two sets of Weibull curves are shown in Figure 39 for the 24 ply Impact damaged specimens. The open circles (9 point set) and dashed line represent the Weibull fit for the data set including the results of specimen LC-28. The filled circles (8 point set) and solid line represent the same data with LC-28 excluded. Note that if the results of LC-28 are excluded the 2-parameter Weibull data fit is greatly improved from $k = 12.07$ to $k = 28.33$ which is similar to that observed for the undamaged tension results ($k = 22.61$). Note also that the characteristic value $v = 156.0$ ksi for the impact damaged results is slightly higher than the $v = 150.5$ ksi value observed for the undamaged tension data.

Figure 40 shows typical fracture characteristics of the damaged hole specimens tested in tension. Note that a typical feature of all the failures is a fracture path roughly normal to the loading direction for a distance approximately 1/2 to 3/4 inch (12 - 19 mm) from the hole for most specimens followed by fracture along 45° planes to the specimen edges. This final fracture along 45° planes often resulted in triangular pieces being completely broken out of the specimen on one or both sides. As shown in Figure 40b, relatively little delamination accompanies the failure.

5.1.4 Static Tension Test Results for 32 Ply Quasi-Isotropic T300/5208 Laminate Specimens Containing Impact Damage

Results of these tests are presented in Table XVII. Since a number of the specimens were observed to fail away from the impact damage site, the results

* All fits were made in standard English units.

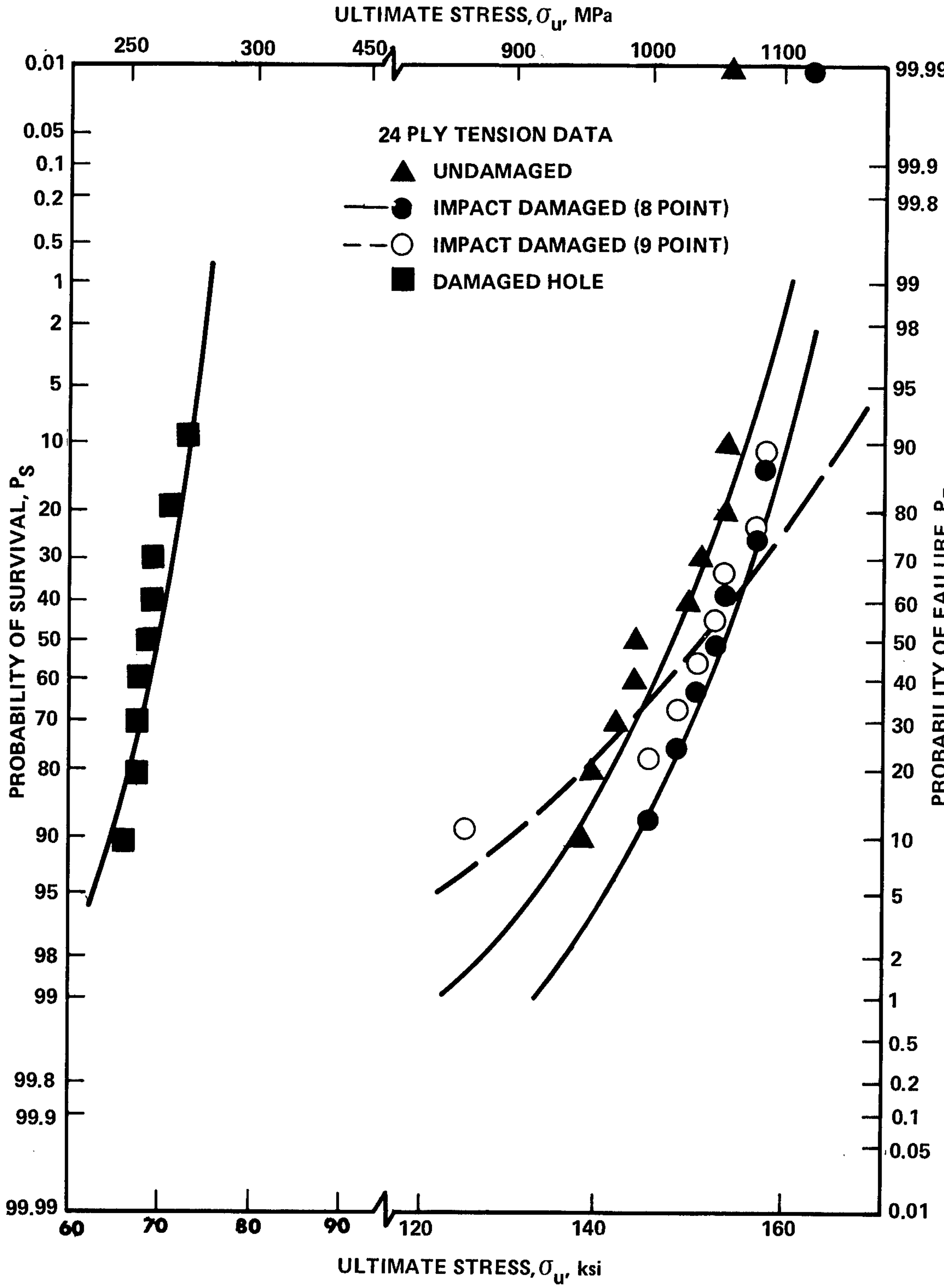

Figure 39. Comparison of the 2-Parameter Weibull Distributions for Tenaion Test Results of Undamaged, Impact Damaged, and Damaged Hole 24-Ply Laminates

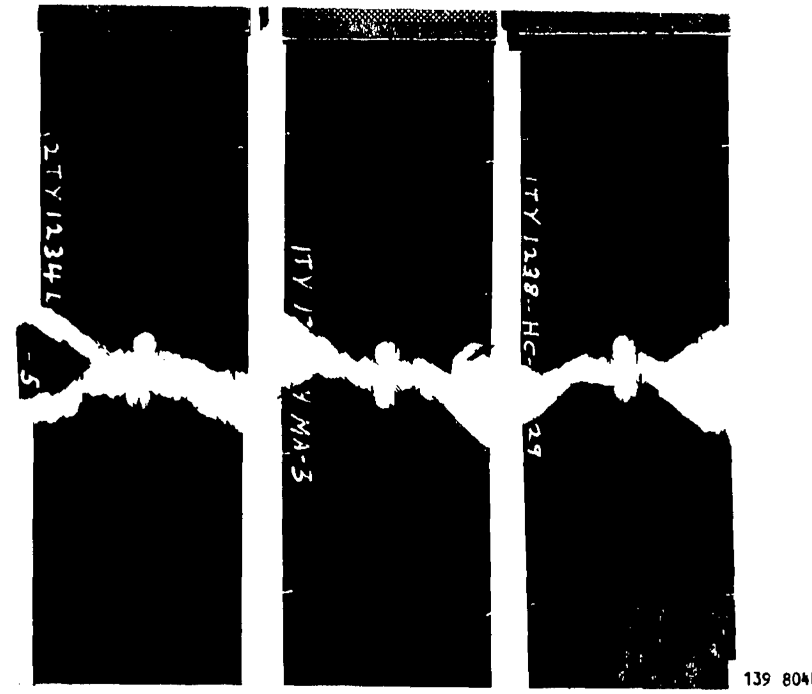

LA-5 MA-3 HC-29

a) Front View

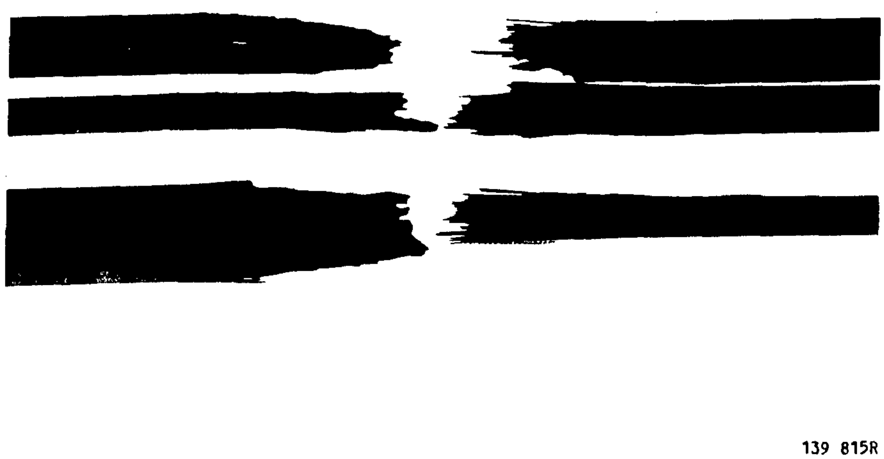

HC-29

MA-3

LA-5

b) Edge View

Figure 40. Typical Fracture Characteristics of Damaged Hole 24-Ply Laminates Tested in Tension

TABLE XVII. TENSION TEST RESULTS FOR 32 PLY QUASI-ISOTROPIC SPECIMENS CONTAINING IMPACT DAMAGE

Specimen ID	Average Area, A		Ultimate Load P_{ult}		Ultimate Stress σ_{ult}		Apparent Ultimate Strain ϵ_{ult_D}, mm/mm in 1 inch (25.4 mm)	Slope Deviation Stress σ_y		Slope Deviation Strain ϵ_y, mm/mm in 1 inch (25.4 mm)	Initial Apparent Modulus, E_{1D}		Secondary Apparent Modulus, E_{2D}		Apparent C-Scan Damage Size X·Y		Comments
	$inch^2$	mm^2	kip	KN	ksi	MPa		ksi	MPa		$psi \cdot 10^6$	GPa	$psi \cdot 10^6$	GPa	in. x in.	mm x mm	
2TY-1228-AB-16	0.4829	312	34.5	153	71.4	492	0.0094	41.4	285	0.0064	6.68	44.2	6.32	43.6	.39 x .36	10 x 9	*
2TY-1228-AB-18	0.4816	311	33.7	150	70.0	483	0.0095	52.1	359	0.0069	7.55	52.0	6.60	45.5	.36 x .36	9 x 9	Failed 3 inch (76 mm) from damage area
1TY-1128-BA-4	0.4786	309	32.2	143	67.3	464	0.0087	50.9	351	0.0068	7.49	51.6	6.60	45.5	.44 x .41	11 x 10	Failed 3.5 inch (85 mm) from damage area
1TY-1128-BC-29	0.4724	305	36.2	161	76.6	528	0.0101	57.2	394	0.0071	8.06	55.6	6.50	44.8	.21 x .26	5 x 7	Failed 1 inch (25.4 mm) from damage area
2TY-1227-CA-2	0.4796	309	32.3	144	67.3	464	**	46.4	320	0.0071	7.64	52.6	**	**	.37 x .39	9 x 10	*
2TY-1227-CB-11	0.4830	312	33.4	149	69.2	477	0.0098	49.7	343	0.0065	7.65	52.7	5.83	40.2	.22 x .22	6 x 6	Failed 3 inch (76 mm) from damage area
1TY-1230-DA-3	0.4979	321	30.0	133	60.3	415	**	44.7	308	0.0069	7.33	50.5	**	**	.49 x .44	12 x 11	*
1TY-1230-DB-16	0.5007	323	32.2	143	64.3	443	0.0089	51.9	358	0.0069	7.52	51.8	6.48	44.7	.41 x .41	10 x 10	*
1TY-1229-EB-17	0.5008	323	29.0	129	57.9	399	0.0080	47.9	330	0.0064	7.48	51.6	5.98	41.2	.55 x .60	14 x 15	*
1TY-1229-EB-19	0.4957	320	31.5	140	63.5	438	0.0088	48.4	334	0.0065	7.45	51.4	6.50	44.8	.36 x .38	9 x 10	*
Average					See Text			49.1 + 8.1 - 7.7	338 + 56 - 53	0.0068 +0.0003 -0.0004	7.48 +0.52 -0.80	51.4 +4.2 -7.2	6.35 +0.25 -0.52	43.8 +1.71 -3.59			

* Failed thru damage zone.

** Extensometer slipped, no data.

were examined in terms of the size of the impact damage. As a first approximation, the damage size measured across the specimen width, X, was used as measured from the Holscan, ultrasonic unit C-scan results. Note that, fortuitously, the damage sizes included in the 10 specimen tension data set contained the two smallest damage sites (specimen BC-29 and CB-11) in the entire 32 ply specimen population.

Figure 41 presents the ultimate strength data in terms of the damage dimension, X, in the width direction. Also shown in Figure 41 are the basic undamaged Q.C. tensile data. The results show a decreasing strength with increasing damage size for damage sizes greater than (~0.4 in.) ~ 11 mm. For damage sizes less than this size, failure generally occurred in regions away from the damage at stress levels which were in the range of failures of the undamaged tensile specimens. Thus the damage conditions selected represents a threshold condition for an effect on the tensile strength. Figure 42 shows the impact damage characteristics for various strengths. No major difference in ply level of damage through the thickness is observed, the major changing parameter being increased extent of damage as indicated on the C-scan presentation. No properties other than ultimate strength and strain at failure showed a significant correlation with damage size. Typical fracture characteristics are shown in Figure 43. The failures are typified by extensive delamination.

A comparison of the initial and secondary modulus values across the damage area (Table XVII) with the undamaged specimens (Table XII) show significantly lower modulus values for these measurements taken across the damage area. Only slight variations in the slope deviation stress and strain values are seen. Table XVIII presents a comparison of the extensometer results across the damage and the region away from the damage. It is of interest to note that the results from the extensometer away from the damage agree reasonably well with the one at the damage site rather than with the 1-inch (25 mm) wide undamaged tension results.

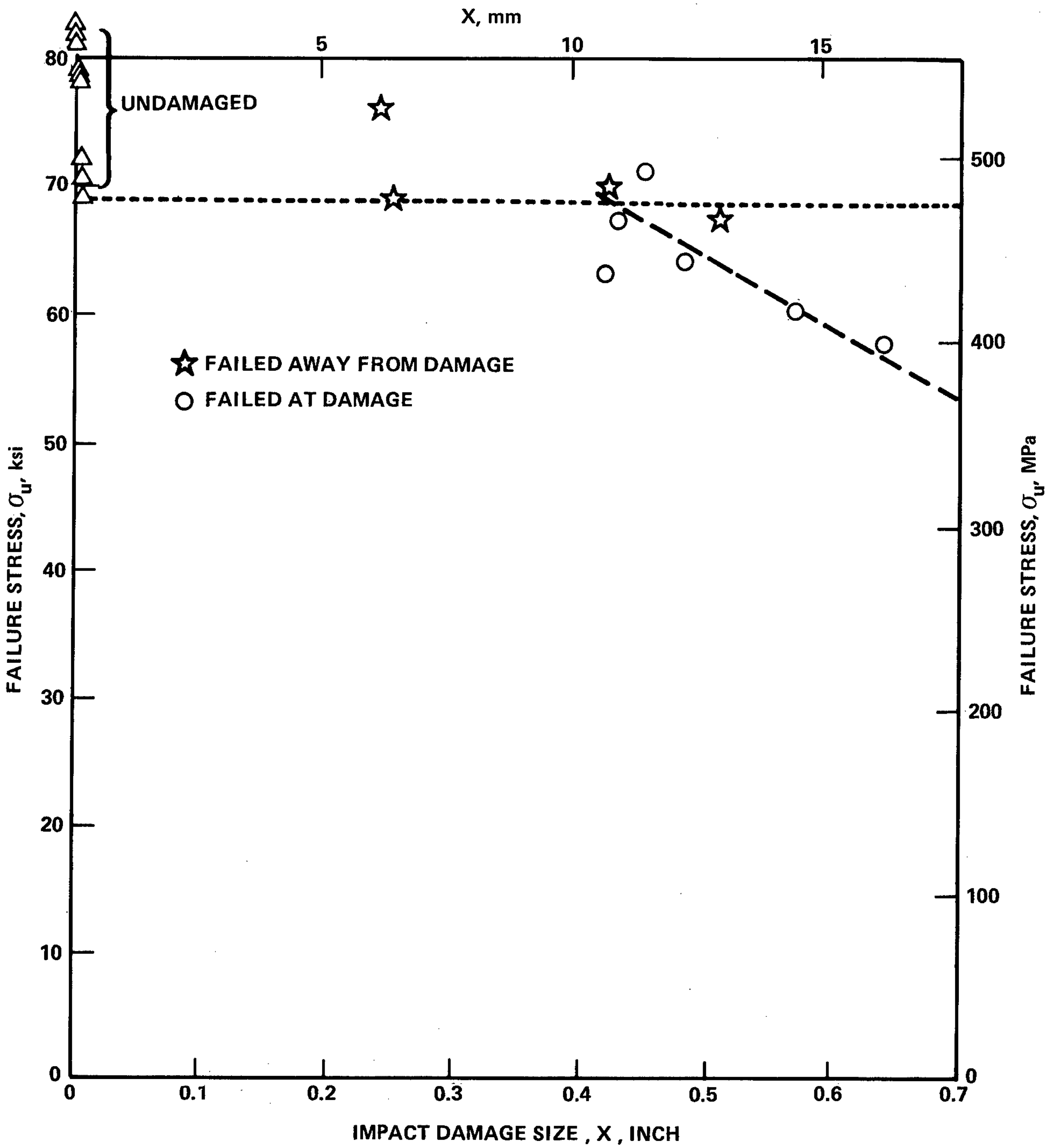

Figure 41. Correlation of Tension Strength with Damage Size for Impact Damaged 32-Ply Laminates.

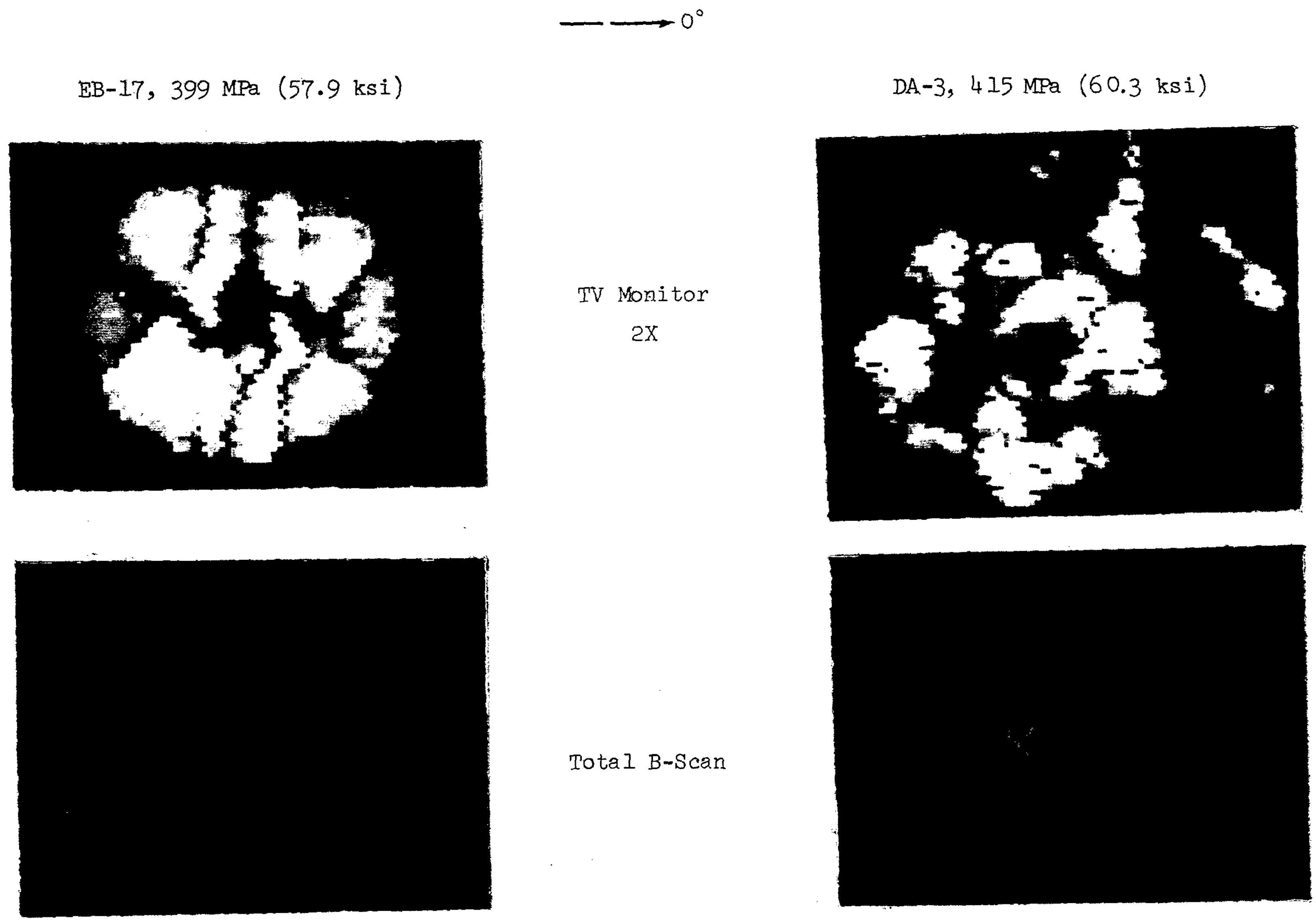

Figure 42a. Damage Size Correlation with Static Tensile Strength for Impact Damaged 32 Ply Quasi-Isotropic Laminates

→ 0°

EB-19, 438 MPa (63.5 ksi)

CA-2, 464 MPa (67.3 ksi)

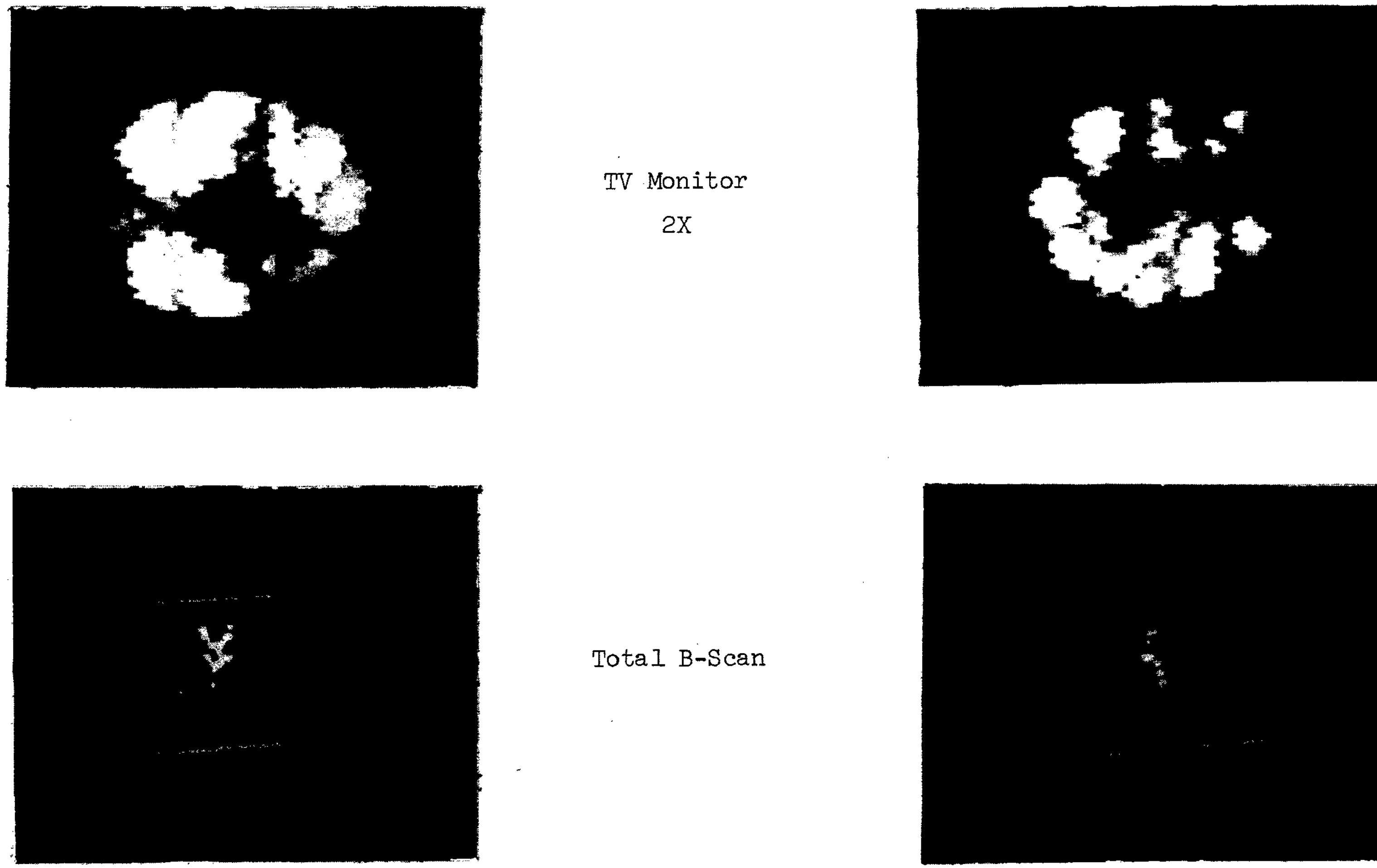

Figure 42b. Damage Size Correlation with Static Tensile Strength for Impact Damaged 32-Ply Quasi-Isotropic Laminates

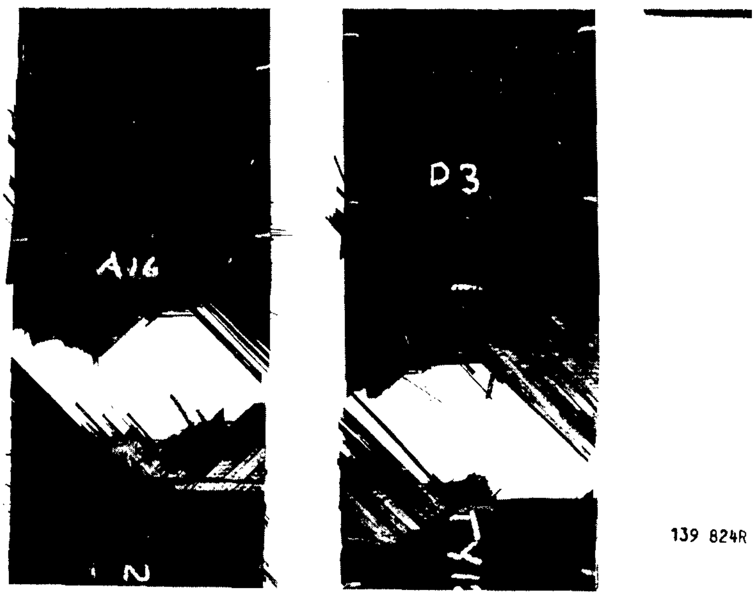

AB-16 DA-3

a) Surface View

DA-3

AB-16

b) Edge View

Figure 43. Typical Fracture Features of Impact Damaged 32-Ply Laminate Tension Test Failures

TABLE XVIII. COMPARISON OF EXTENSOMETER RESULTS FOR THE 32 PLY QUASI-ISOTROPIC MATERIAL

Specimen Number	Apparent Initial Modulus of Elasticity, E_{1a}		Slope Deviation Stress		Slope Deviation Strain in 1 in. (25.4 mm)
	psi · 10^6	GPa	ksi	MPa	ϵ
1TY-1128-BA-4	7.49 *	51.6	50.9	351	0.0068
	(7.68)**	(52.9)	(50.8)	(350)	(0.0067)
2TY-1227-CA-2	7.64 *	52.6	46.4	320	0.0071
	(7.52)	(51.8)	(***)	(***)	(***)
1TY-1230-DA-3	7.33 *	50.5	44.7	308	0.0069
	(7.33)	(50.5)	(***)	(***)	(***)

* Numbers are from the Extensometer placed across the damage zone.

** All values in parentheses ( ) are from 1/2-inch (12.7 mm) extensometer located away from damage area.

*** Extensometer slipped, invalid data.

5.1.5 Static Tension Test Results for 32 Ply Quasi-Isotropic T300/5208 Laminate Specimens Containing a Damaged Hole

Results of these tests are presented in Table XIX. As was previously observed, the basic stress vs strain record showed a two stage essentially linear behavior, but the ultimate stress values decreased nearly 50% relative to the base tension data. Examination of the Holscan results for these specimens again showed a very consistent level of damage to be present in each specimen as can be seen in Appendix B, the typical damage size resulting in an approximately 0.55 inch (14 mm) diameter centered around the 0.375 inch (9.5 mm) hole. A comparison of the two parameter Weibull data fit results for the damaged hole data (k = 24.958, v = 40.9707) and the base undamaged tensile data (k = 14.697, v = 79.9309) as shown in Figure 44, indicates a significant difference in the shape parameter, k, unlike the 24 ply 67% 0° laminate data results. This indicates that for this laminate the simple translation of the distribution curve for specimens containing damaged holes is not applicable. Rather it is observed that the scatter is significantly reduced for the damaged hole specimens compared to the undamaged baseline tension data.

Unlike the impact damaged specimens which showed only a minor decrease in the slope deviation stress, the damaged hole specimens show a major decrease of $\sim$ 50% compared to the baseline tension specimens. In addition, the apparent modulus values also showed significant decreases of $\sim$ 30%.

Typical fracture features are shown in Figure 45. The failures occur predominately in the 90° orientation normal to the applied load. Delamination is minor with some limited 45° fiber pull-out.

5.2 COLUMN BUCKLING TEST RESULTS

Column buckling tests were conducted at two bay lengths and for full-fixity conditions for each of the four damage/laminate conditions. Bay lengths, L' of 2.383 inch (60.5 mm) and 1.170 inch (29.7 mm) were selected for evaluation because results of other programs[25] indicate this range will

TABLE XIX

32 PLY QUASI-ISOTROPIC T300/5208 DAMAGED HOLE TENSION TEST RESULTS

Specimen Number	Average Thickness, B		Average Gross Area, A		Failure Load, P_u		Initial Gross Area Modulus E_1,		Gross Area Failure Stress σ_u		Gross Area Slope Deviation Stress σ_y		Slope Deviation Strain ϵ_y	Secondary Gross Area Modulus E_2		Estimated Failure Strain ϵ_u
	in.	mm	in.^{2}	mm^2	kip	KN	psi · 10^6	GPa	ksi	MPa	ksi	psi	mm/mm	psi · 10^6	GPa	mm/mm
AB-20	0.1599	4.06	0.4796	309	19.2	85.4	5.35	36.9	40.0	276	31.3	216	0.0052	4.74	32.7	0.0077
AC-23	0.1612	4.09	0.4836	312	19.4	86.3	5.44	37.5	40.1	276	20.9	144	0.0039	4.51	31.1	0.0082
BA-5	0.1593	4.05	0.4779	308	20.25	90.1	5.44	37.5	42.4	292	22.0	152	0.0041	4.52	31.2	0.0080
BA-10	0.1594	4.05	0.4783	309	18.65	83.4	5.59	38.5	39.0	269	24.0	165	0.0046	4.75	32.8	0.0076
CC-23	0.1619	4.11	0.4854	313	18.75	83.4	5.63	38.8	38.6	266	25.8	178	0.0049	4.49	31.0	0.0075
CC-29	0.1604	4.07	0.4811	310	20.65	91.8	5.47	37.7	42.9	296	29.1	201	0.0053	4.78	33.0	0.0080
DA-6	0.1661	4.22	0.4934	318	19.10	85.0	4.93	34.0	38.7	267	33.4	230	0.0048	*	*	*
DC-21	0.1626	4.13	0.4876	314	20.0	89.0	5.38	37.1	41.0	283	30.8	212	0.0060	4.81	33.2	0.0080
EB-16	0.1663	4.22	0.4989	322	19.75	87.8	5.32	36.7	39.6	270	25.1	173	0.0048	4.64	32.0	0.0076
EC-21	0.1641	4.17	0.4923	318	19.50	86.7	5.16	35.6	39.6	273	23.4	161	0.0049	4.40	30.3	0.0080
					Average		5.37	37.0	40.2	277	26.6	183	0.0048	4.63	31.9	0.0078
							+0.26	+1.8	+2.7	+19	+6.8	+47	+0.0012	+0.18	+ 1.3	+0.0004
							-0.44	-3.0	-1.6	-11	-5.7	-39	-0.0009	-0.23	- 1.6	-0.0003

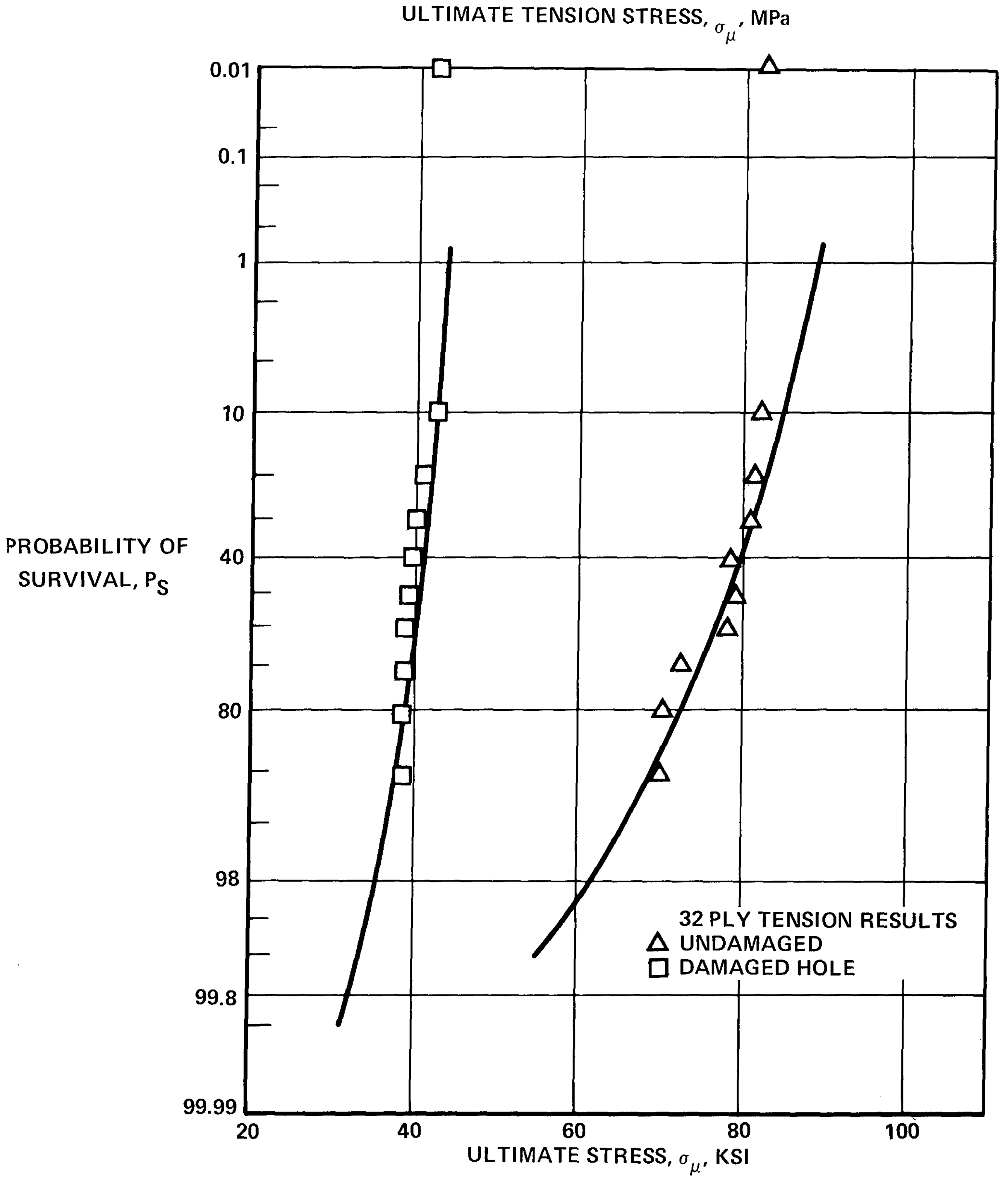

Figure 44. Two Parameter Weibull Curve Fit for Undamaged and Damaged Hole Specimens of 32 Ply Laminate

laminate type at two strain rates. Results are summarized in Table XVI along with Task II room temperature data which are included for comparison. The overall effect of high strain rate for all conditions evaluated and both laminates types was a reduction in the strength of laminates containing damaged holes. Compression strength decreases due to the higher strain rate were insignificant at elevated temperatures for both laminates while at room temperature the reduction was on the order of 15%. Tension strength dropped approximately 8% as a result of high strain rate for all cases except the 32-ply laminate room temperature condition where no change was evident. Elevated temperature produced an increase in tensile strength in all cases, most likely due to a reduction in notch acuity. As expected, compressive strength decreased as a consequence of the increased propensity towards buckling which is evident in the photographs of Figure 42. Tension fractures at elevated temperatures did not differ measurably in appearance from room temperature tests. Typical examples are displayed in Figure 43.

5.6 TENSION AND COMPRESSION DATA FOR UNDAMAGED LAMINATES

Included in the Task II test matrix (Item 9) was a set of baseline material tests to be conducted on 3-inch (76 mm) wide specimens identical to the damaged hole specimens of Figure 17 except that they contained no hole or intentional damage. Four replicates of each laminate per a condition were tested.

The 24-ply and 32-ply laminate undamaged tension and compression test results, at strain rates of 0.005 min^{-1} and 2.3 min^{-1} are presented in Tables XVII and XVIII and comparison with the QC data is shown in Figures 44 and 45. A number of 24-ply specimens tested in tension were machined to a 2.5-inch (64 mm) width since the load required to fail the wider specimens exceeded the 55,000 lb. (245 kn) load capacity of the hydraulic grips.

bracket the elastic instability behavior region and the catastrophic fracture instability region. Full-fixity results indicate the upper-bound maximum compression strength achievable.

5.2.1 24 Ply 67% 0° Fiber Laminate Results

Column buckling test results for the impact damaged and damaged hole specimens are presented in Table XX. The results indicate that, as anticipated, the two pin (L' = 2.383 inch = 60.5 mm) bay length resulted in elastic instability for both damage types. Subsequent Holscan results showed no significant damage extension to have occurred during these tests. Both the 6-pin (L' = 1.170 inch = 29.7 mm) and the full-fixity conditions resulted in fracture at instability. The fracture appearances of the impact damaged and damaged hole specimens are shown in Figure 46.

5.2.2 32 Ply Quasi-Isotropic Laminate Results

Column buckling results for the impact damaged and damaged hole specimens are presented in Table XXI. The impact damage results are somewhat different than those observed in the 24 ply laminate in that both the 2-pin and 6-pin tests resulted in instabilities associated only with limited surface ply failure as shown in Figure 47a. The full-fixity test condition resulted in failure away from the damage site but within the supported test length. This indicates that, similar to the tension results for this damage condition, the damage is near the threshold level for a measurable effect on the static behavior. Damaged hole column buckling results were similar to those observed for the 24 ply laminate, the 2-pin resulting in elastic instability while the 6-pin and full-fixity resulted in fracture at instability. Damaged hole column buckling test failures are shown in Figure 47b.

5.3 STATIC COMPRESSION TEST RESULTS WITH FATIGUE SUPPORTS

The fatigue support design used for the balance of the test program is shown in Figure 31. This configuration was designed to allow localized deflection normal to the plane of the specimen while still providing adequate constraint to prevent extensive gross buckling. One specimen of each damage/

TABLE XX. 24 PLY COLUMN BUCKLING TEST RESULTS

Specimen Number	Damage Type	Damage Size x · y in. x in. (mm x mm)	Support Type	Bay Length L' in. (mm)	Critical Load kip (KN)	Gross Critical Stress ksi (MPa)	Secant Modulus at 35 ksi (241 MPa) psi · 10^6 (GPa)	Average Thickness in. (mm)	Average Area in.^{2} (m^2)	Comments
JB-18	Impact	.42 x .69 (11 x 18)	2-Pin	2.383 (60.5)	9.55 (42.5)	25.5 (175.8)	-	0.1249 (3.2)	0.3745 (241.6)	Elastic
LA-2	Impact	.43 x .69 (11 x 18)	6-Pin	1.170 (29.7)	17.75 (79.0)	48.7 (335.8)	8.70 (60.0)	0.1217 (3.1)	0.3648 (235.4)	Failed thru damage
KB-20	Impact	.37 x .63 (9 x 16)	Full Fixity	~ 0	35.90 (159.7)	98.5 (679.1)	8.65 (59.6)	0.1216 (3.1)	0.3646 (235.2)	Failed thru damage
HA-7	Hole	-	2-Pin	2.383 (60.5)	8.02 (35.7)	21.9 (151.0)	-	0.1224 (3.1)	0.3668 (236.6)	Elastic
LA-8	Hole	-	6-Pin	1.170 (29.7)	17.32 (77.0)	46.8 (322.7)	8.71 (60.1)	0.1238 (3.1)	0.3710 (239.4)	Failed near Tab
KB-13	Hole	-	Full Fixity	~ 0	21.50 (95.6)	58.2 (401.3)	8.91 (61.4)	0.1232 (3.1)	0.3692 (238.2)	Failed

TABLE XVII
TENSION STRENGTH DATA
FOR UNNOTCHED SPECIMENS

Laminate Type	STANDARD STRAIN RATE Specimen ID	σ_{ult} ksi	MPa	HIGH STRAIN RATE Specimen ID	σ_{ult} ksi	MPa
	BB-11	161.2	1111	AC-22	118.5	817
	BC-24	a,b	-	DA-9	166.7	1149
	EB-13	a,b	-	FC-22	152.4	1051
Unnotched	EC-28	157.8	1088	GB-13	145.2	1001
24-Ply	HB-14	a	-			
67% - 0°	IB-18	149.4[b]	1030			
Laminate						
	Mean	156.1	1076		145.7	1005
	Std. Dev.	6.1	42		20.2	139
	Coef. of Var. %	3.9	3.9		13.9	13.9
	JB-13	77.6	535	KA-1	76.0	524
Unnotched	LC-22	78.3	540	PC-28	82.5	569
32-Ply	QB-15	82.7	570	SC-28	78.4	541
Quasi-	RA-9	72.2	498			
Isotropic						
Laminate	Mean	77.7	536		79.0	545
	Std. Dev.	4.3	30		3.3	23
	Coef. of Var. %	5.5	5.5		4.2	4.2

a = Loaded to grip capacity without failure
b = 3 inches wide

NOTE: Specimens Machined to 2.5-inch (64 mm) Width Except Where Noted Otherwise

TABLE XVIII
COMPRESSION STRENGTH DATA
FOR UNNOTCHED SPECIMENS

Laminate Type	STANDARD STRAIN RATE Specimen ID	σ_{ult} ksi	σ_{ult} MPa	HIGH STRAIN RATE Specimen ID	σ_{ult} ksi	σ_{ult} MPa
Unnotched 24-Ply 67% - 0^{o} Laminate	CB-13	85.8	592	AC-23	93.7	646
	CC-29	85.5	590	BA-3	93.5	645
	EA-2	88.3	609	GA-8	86.9	599
	FC-28	93.9	647	GC-28	97.1	669
				IC-26	85.6	590
	Mean	88.4	609		92.5	638
	Std. Dev.	3.9	27		4.9	34
	Coef. of Var. %	4.4	4.4		5.3	5.3
Unnotched 32-Ply Quasi-Isotropic Laminate	NB-12	54.7	377	JA-2	60.3	416
	NC-23	51.3	354	KC-29	63.7	439
	PA-2	58.1	401	MA-9	57.1	394
	QB-18	59.4	410	QA-10	75.9	523
				RB-16	68.2	470
	Mean	55.9	385		65.0	448
	Std. Dev.	3.6	25		7.3	50
	Coef. of Var. %	6.5	6.5		11.3	11.3

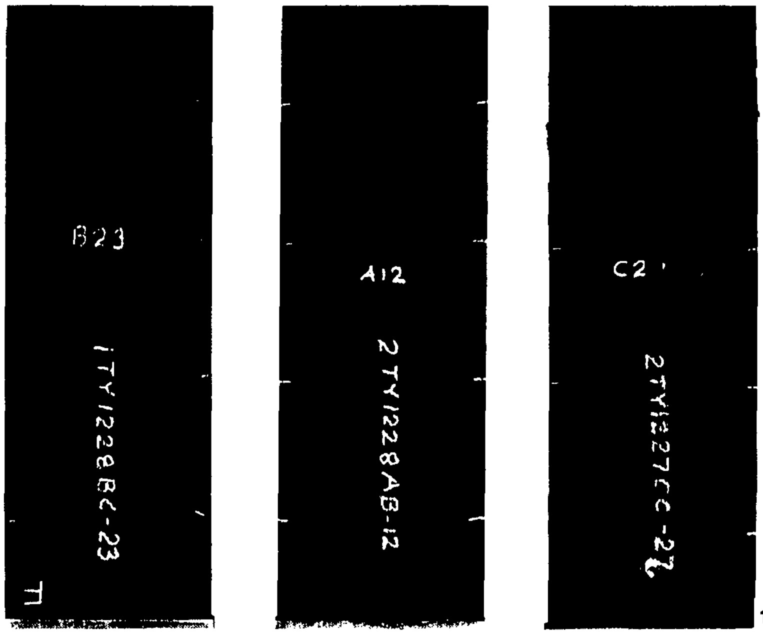

139 801R

BC-23 2-Pin | AB-12 6-Pin | CC-27 Full-Fixity

a) Impact Damaged

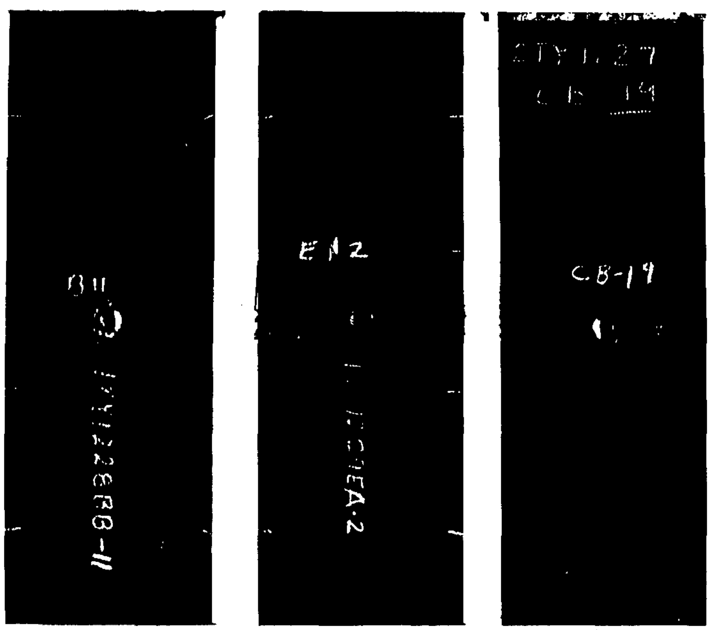

139 803R

BB-11 2-Pin | EA-2 6-Pin | CB-19 Full-Fixity

b) Damaged Hole

Figure 47. Column Buckling Failures, 32-Ply Laminate

laminate type was first tested and, when the results appeared to provide a reasonable approximation of the constraint condition which might be encountered in a structure, the balance of the static compression specimen set was tested with the fatigue guides.

5.3.1 Compression Test Results for Impact Damaged 24 Ply Laminates

Compression test results for the 24 ply laminate containing impact damage are presented in Table XXII. The results show very consistent failure behavior with all specimens failing through the damage region. A comparison of these results with the tension test results for the impact damage (Table XIV) shows a major drop to 1/3 of the static tension strength. A similar drop in the apparent modulus values of $\sim 40\%$ is also observed for the compression results.

Typical fracture characteristics are shown in Figure 48a. All specimens showed extensive internal delamination growth which created extensive "bulging" of both surfaces with some matrix cracking along the surface ply 0° fiber. The extent of the typical internal delamination is shown by the dotted line in Figure 48a. Final fracture occurred through the site supported region under the buckling support.

5.3.2 Compression Test Results for Damaged Hole 24 Ply Laminates

Compression test results for this condition are presented in Table XXIII. As was observed for the impact damaged 24 ply laminate tested in compression, the results are seen to be very consistent. The ultimate strength in compression with the fatigue support is observed to be $\sim 33\%$ lower than the comparable tensile static strength. Apparent modulus values, however, show little difference between the tension and compression results.

Typical fracture features of the damaged hole 24 ply laminate tested in compression were found to be quite similar to the impact damaged laminate results as is shown in Figure 48b. Again extensive internal delaminations and "bulging" of the surfaces were observed. The primary distinguishing feature of the damaged hole specimen failures was the increased tendency to fracture

The sample size was too small to determine whether an effect existed.

There seemed to be an increase in compression strength for both laminates at the higher strain rate while the tension strength appeared to be unaffected for the 32-ply laminate and reduced for the 24-ply laminate.

The linear two stage slope exhibited by the unnotched one-inch (25 mm) wide and the notched three inch (76 mm) 32-ply specimens was also evident in the tension stress-strain record obtained for the 3-inch (76 mm) wide unnotched coupons. However, these wide unnotched 24-ply specimens displayed a tension stress-strain curve more comparable to that of the notched specimens and unlike the fairly linear record of the narrow unnotched coupons. The tensile curve was linear to only approximately 20% of the strength then progressed at a continuously decreasing slope to failure. Compression stress vs. strain records were totally non-linear for both laminates and similar to previously observed behavior.

Low strain rate tension specimens of the 24-ply laminate exhibited the two types of fractures shown in Figure 46a. Either a 45° triangle was split from the center of the specimen or a longitudinal piece was separated from the specimen at a 45° angle at either end. Final fracture was always at a 45° angle and accompanied by almost no delamination. These failures were very similar to those observed for the higher strength impact damaged specimens of Task I. The high strain rate tension failures were very similar to the second mode of failure exhibited by the low strain rate specimens differing by perhaps some slight delamination near the fracture.

Low and high strain rate tension failures of the 32-ply laminates were indistinguishable. Failures occurred away from the tab usually normal to the load direction accompanied by a secondary crack at a 45° angle (Figure 47). Some delamination was present but was not extensive as was the case for the impact failures in Task I. Tension fractures of both the 24-ply and 32-ply

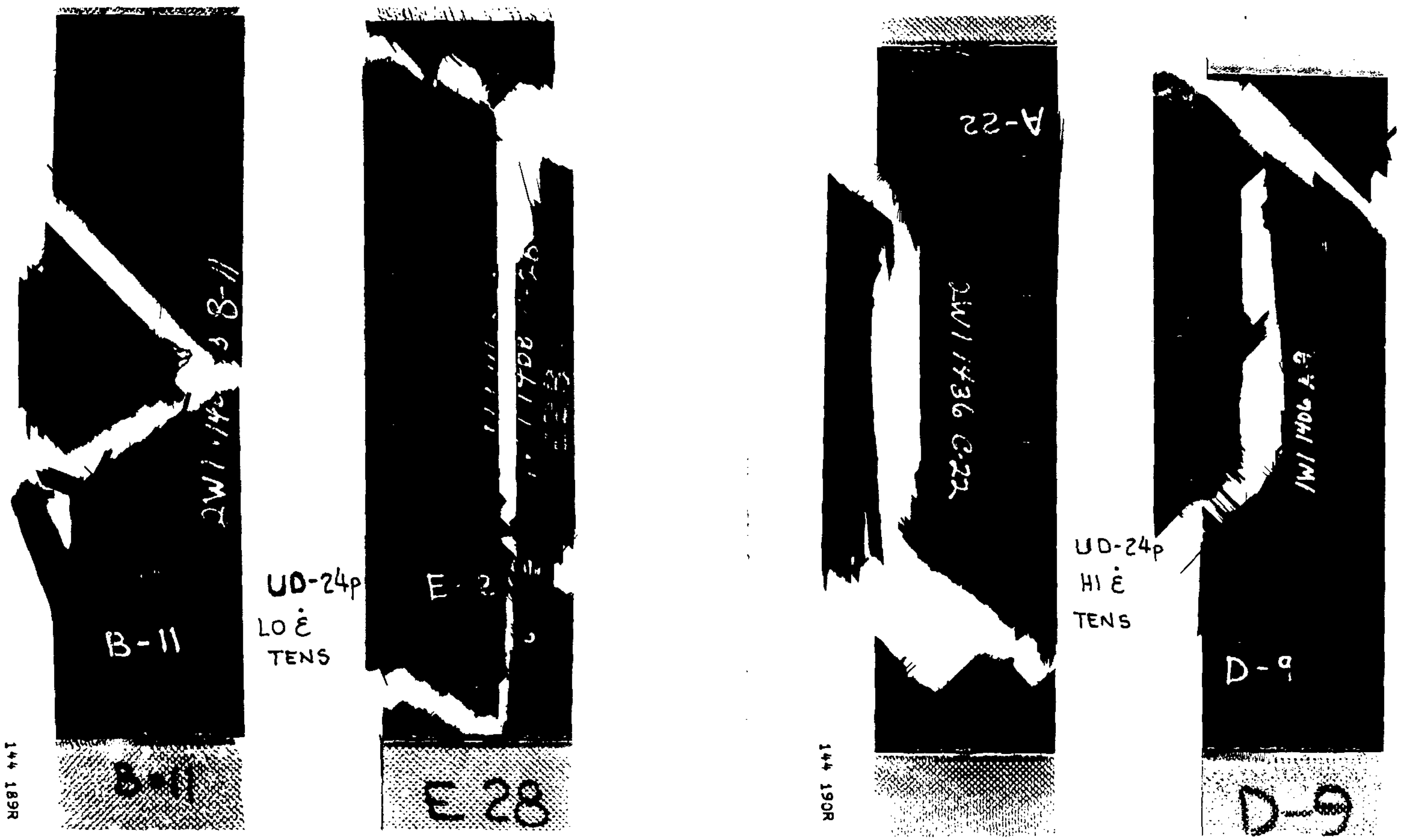

BB-11 EC-28 AC-22 DA-9

a. Strain rate = 0.005 min^{-1} b. Strain rate = 2 min^{-1}

Figure 46: Typical Fractures of Undamaged 24-Ply Laminate **Specimens Tested in Tension at Room Temperature**

TABLE XXIII. 24 PLY DAMAGED HOLE, COMPRESSION RESULTS(WITH FATIGUE SUPPORT)

Specimen Number	Average Thickness		Average Area		Failure Load		Gross Failure Stress		Secant Modulus, at 30 ksi E_s,		Apparent Fracture Strain
	inch	mm	$inch^2$	mm^2	kip	MN	ksi	MPa	psi . 10^6	GPa	mm/mm
HA-6	0.1217	3.09	0.3648	235	16.20	72.1	47.1	325	8.65	59.6	0.0058
HB-16	0.1222	3.10	0.3663	366	17.62	78.4	48.1	332	8.38	57.8	0.0066
JC-27	0.1233	3.13	0.3692	238	18.25	81.2	49.4	341	8.35	57.6	0.0065
JC-24	0.1239	3.15	0.3711	239	17.05	75.8	45.9	316	8.34	57.5	0.0060
KC-27	0.1232	3.13	0.3691	238	16.70	74.3	45.2	312	8.27	57.0	0.0056
KA-7	0.1227	3.12	0.3678	237	15.60	69.4	42.4	292	8.27	57.0	0.0056
LA-3	0.1234	3.13	0.3697	238	16.38	72.9	44.3	304	8.30	57.2	0.0056
LB-18	0.1238	3.14	0.3710	239	17.75	78.9	47.8	330	8.66	59.7	0.0060
MB-18	0.1247	3.17	0.3736	241	17.95	79.8	48.0	331	8.56	59.0	0.0062
MB-12	0.1248	3.17	0.3740	241	16.55	73.6	44.2	305	8.20	56.5	0.0057
Average							46.2	318	8.40	57.9	0.0060
							+ 3.2	+ 23	+0.22	+ 1.8	+0.0006
							- 3.8	- 26	-0.22	- 1.4	-0.0004

NOTE: Typical initial damage dimensions are given in Appendix B.

the surface 0° ply across the specimen width on the drill entry (front) side of the specimen, the back side showing failure features similar to those seen in the impact damaged specimens. It should be noted that, as shown in Reference 1, the damaged holes do tend to show more initial delamination near the back surface.

5.3.3 Comparison of the Compression Test Results for 24 Ply Laminate

A comparison of the two parameter Weibull curve fit to the compression data for the 24 ply laminate containing impact damage and damaged holes is presented in Figure 49. Both the impact damaged and damaged hole specimens yield very similar results, with values of k = 19.97 for the impact damage and k = 20.6 for the damaged hole specimens as shown in Table XXIV. Note that this is similar to the 24 ply undamaged tension value of k = 22.6. In addition, the characteristic values of v = 47.3 for the damaged holes and v = 49.96 for the impact damaged laminates are very close.

Figure 50 presents a comparison of the compression strengths using the fatigue guides with the column buckling results. For both damage conditions, the compression results with the buckling guides yield static strengths that are virtually identical to the 6-pin (L' = 1.170 inch = 29.7 mm) column buckling results.

5.3.4 Compression Test Results for Impact Damaged 32 Ply Laminates

Results of the compression tests on impact damaged 32 ply quasi-isotropic laminate specimens are presented in Table XXV. As shown in Table XXV, several of the specimens failed away from the damage zone. An initial examination showed no correlation between damage size and failure location. Typical load vs deflection curves, such as shown in Figure 51, showed those specimens which failed through the damage region exhibited very little extension beyond the initial instability point while the ones which failed near the tab exhibited much more extensive deflection beyond the instability point. This extension resulted in the buckling support bottoming on the specimen tab. As a result of this bottoming of the fixture, a bending was introduced near the tab moving

wide specimen had some similarity to the fractures of the narrow QC specimens as shown in Figure 48. Longitudinal splitting was not observed in the narrow 24-ply coupons while this failure type dominated in the wide specimens.

Since undamaged compression specimens were tested with the fatigue guide support the obvious failure location was the unsupported length near the tab which occurred for all conditions as shown in Figure 49.

5.7 COMPARISON OF TASK I AND TASK II DATA

The results of the Task I and Task II tension and compression data were represented by two-parameter Weibull statistical distributions (see Figures 50 through 55 and Table XIX) of the type described in Appendix K. The commonly used Weibull distribution is a specific form of the third asymtotic function of the statistical theory of extreme values [27] and can be thought of as a generalization of the exponential probability distribution function.

Interpretation of a comparison of the experimental results by using the Weibull parameters shown in Table XIX often leads to conflicting inferences. This problem results because simple contrast of shape and characteristic value parameters does not always allow easy inference of whether distribution functions are different. For example, the population pairs represented by the first, second and sixth entries of Table XIX are probably different and that of entry five the same, but whether those of entries three and four are truly different is less clear.

Non-parametric statistical procedures were used to solve such problems in discrimination. In essence, differences in the Weibull parameters of two populations is a necessary condition for their distribution to be

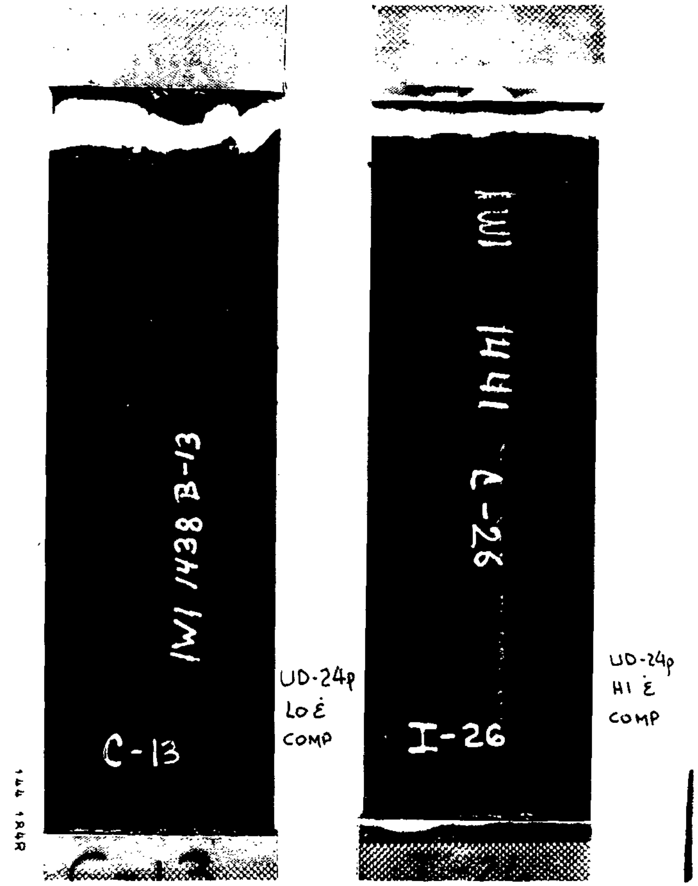

CB-13

$\dot{\epsilon} = 0.005\ \mathrm{min}^{-1}$

IC-26

$\dot{\epsilon} = 2\ \mathrm{min}^{-1}$

a. 24-Ply Laminate

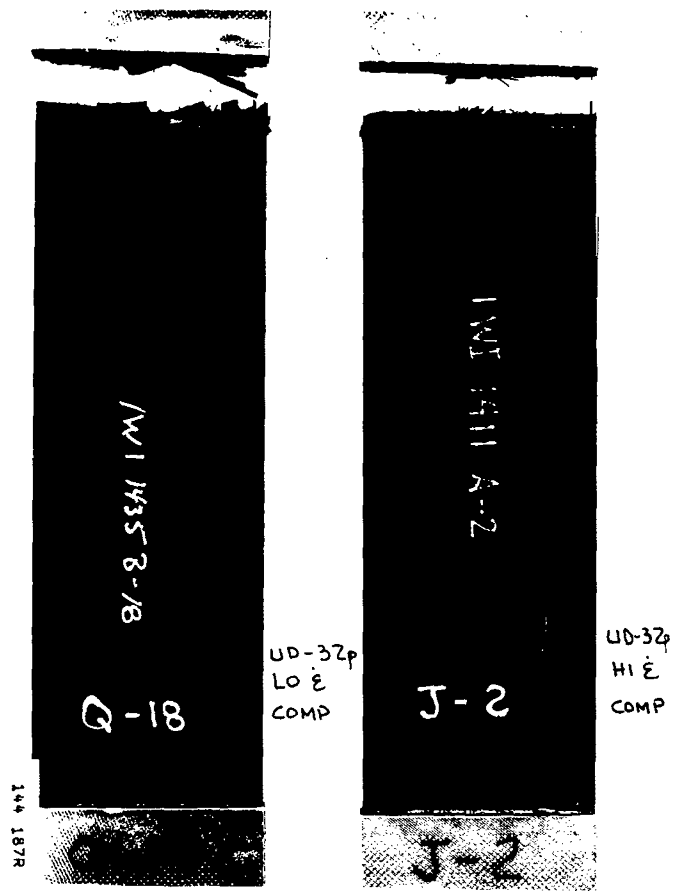

QB-18

$\dot{\epsilon} = 0.005\ \mathrm{min}^{-1}$

JA-2

$\dot{\epsilon} = 2\ \mathrm{min}^{-1}$

b. 32-Ply Laminate

Figure 49: **Typical Fractures of Undamaged Specimens Tested in Compression at Room Temperature**

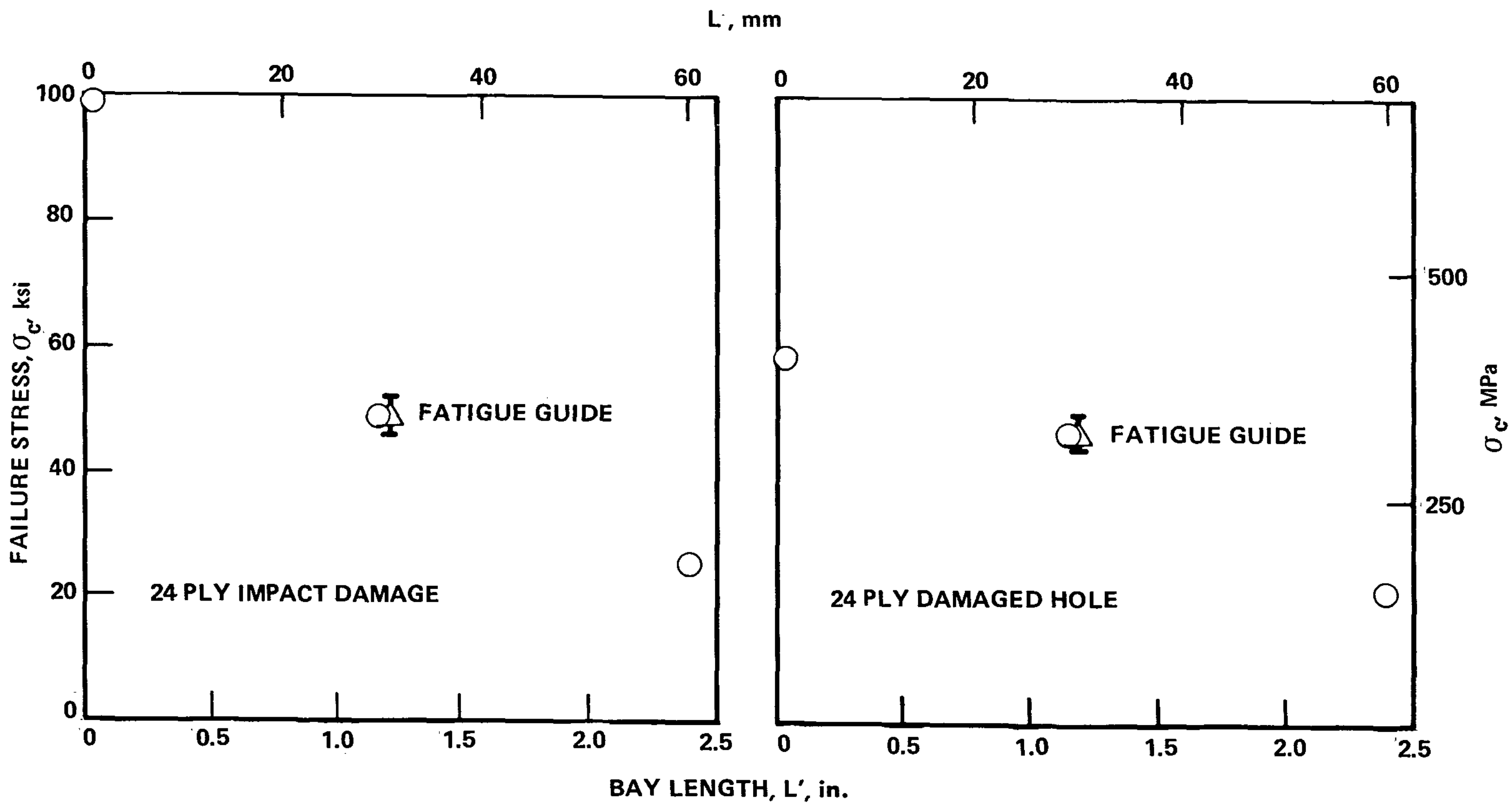

Figure 50. Comparison of Damaged 24-Ply Laminate Column Buckling Results with Compression Test Results Using the Fatigue Support

TABLE XXV. 32 PLY IMPACT DAMAGED LAMINATE COMPRESSION TEST RESULTS (WITH FATIGUE SUPPORTS)

Specimen Number	Average Thickness		Average Area		Failure Load		Gross Failure Stress		Secant Modulus at 35 ksi E_s		Instability Load		Instability Stress		Apparent Instability Strain	Damage Size X · Y		Comments
	inch	mm	$inch^2$	mm^2	kip	KN	ksi	MPa	$psi \cdot 10^6$	GPa	kip	KN	ksi	MPa	mm/mm	in. x in.	mm x mm	
AA-5	0.1596	4.05	0.4787	309	25.50	113	53.3	367	4.85	33.4	24.1	107	50.3	347	0.0117	.43 x .47	11 x 12	A
AC-29	0.1607	4.08	0.4819	311	30.00	133	62.25*	429	4.68	32.3	27.75	123	57.6	397	0.0142	.55 x .52	14 x 13	B
BC-24	0.1581	4.02	0.4742	306	27.55	122	57.2	394	4.66	32.1	25.20	112	53.1	366	0.0128	.37 x .47	9 x 12	A
CA-1	0.1601	4.07	0.4803	310	25.10	112	52.3	361	4.62	31.8	24.75	110	51.5	355	0.0125	.43 x .48	11 x 12	A
CA-7	0.1610	4.09	0.4830	312	26.35	117	54.6	376	4.62	31.8	26.35	117	54.6	376	0.0128	.40 x .43	10 x 11	A
DA-8	0.1664	4.23	0.4991	322	31.60	140	63.3*	436	4.80	33.1	29.5	131	59.1	407	0.0131	.56 x .52	14 x 13	B
DB-20	0.1648	4.18	0.4942	319	29.15	130	59.0*	407	4.83	33.3	28.4	126	57.5	396	0.0138	.22 x .19	6 x 5	B
DC-28	0.1645	4.18	0.4950	319	28.75	128	58.1	400	4.55	31.4	26.5	118	53.4	369	0.0130	.43 x .43	11 x 11	C
EA-3	0.1652	4.20	0.4956	320	28.25	126	57.0*	393	4.77	32.9	28.25	126	57.0	393	0.0138	.43 x .42	11 x 11	B
EB-14	0.1672	4.25	0.5008	323	31.60	140	63.1*	435	4.40	30.3	27.85	124	55.6	383	0.0140	.39 x .47	12 x 12	B
					Average		54.4**	375**	4.68 +0.17 -0.28	32.2 +1.2 -0.8			55.0 + 4.1 - 4.7	379 + 28 - 32	0.0132 +0.0010 -0.0015			

* Specimen failed away from damage area

** Based on Specimens CA-1, CA-7, BC-24 and AA-5 only

A - Failed thru damage

B - Failed near Tab

C - Test stopped prior to final fracture

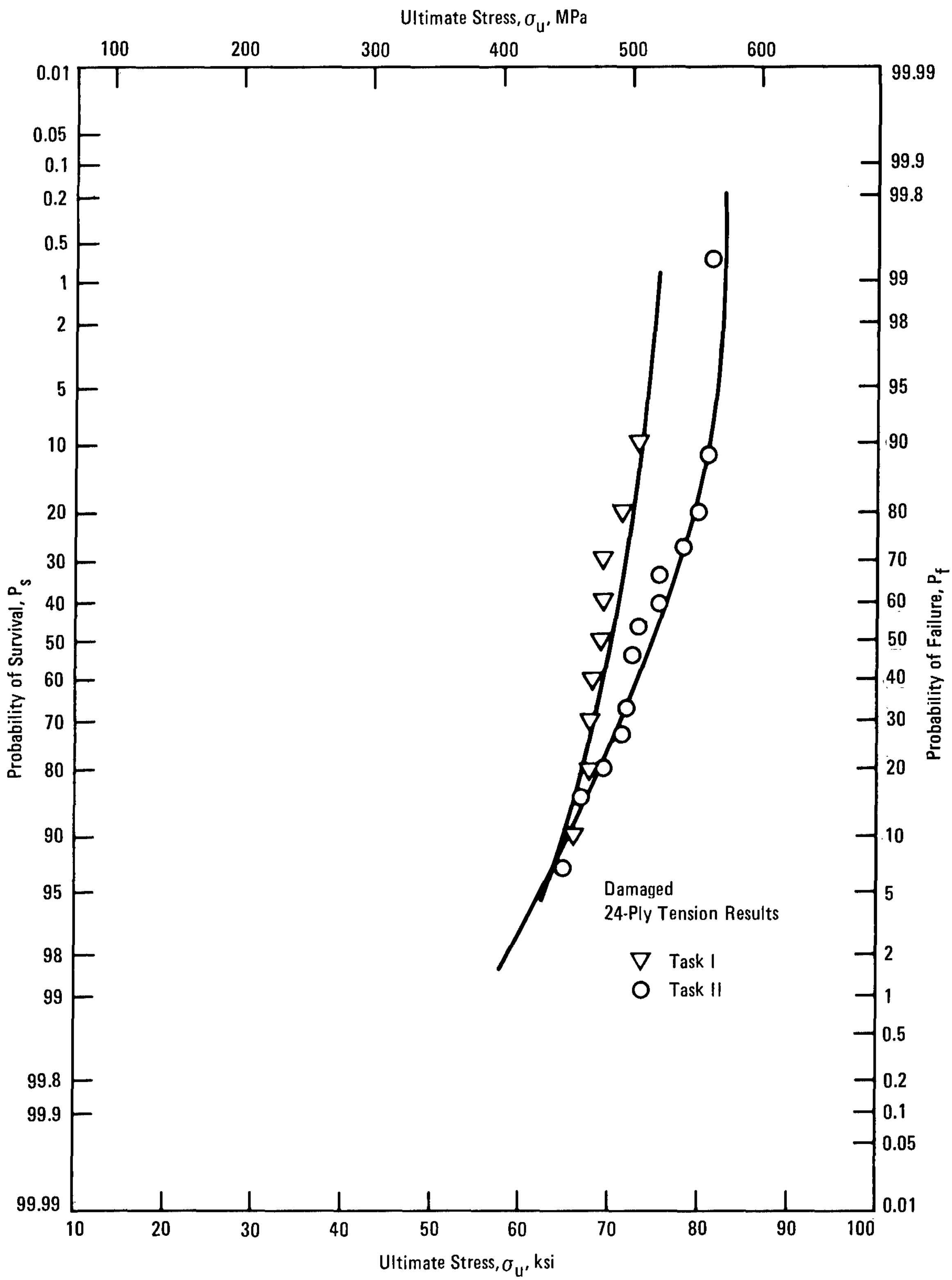

Figure 52: Comparison of Two Parameter Weibull Curve Fit for Damaged Task I and II 24-Ply Tension Data

the final failure to this region. To verify this, specimen DC-28 was unloaded just past the initial instability point. The resulting damage is shown in Figure 52.

As shown in Figure 52, the typical valid fracture characteristics were very similar to those observed in the 24 ply impact damaged specimens in that extensive internal delamination extension occurred with surface cracking along the 0° surface fibers. Specimen DC-28 shows that the initial damage instability involves the breaking loose of the 0° surface ply with some internal delamination extension. As a result, the instability stress values were used in subsequent evaluations rather than the fracture stress values.

5.3.5 Compression Test Results for 32 Ply Laminates Containing a Damaged Hole

Compression test results using the fatigue supports for 32 ply laminate specimens containing a damaged hole are presented in Table XXVI. The results show a slight drop ($\sim$ 10 to 15%) in the static strength and apparent modulus values relative to the tension test results. While the observed scatter in the compression results is somewhat larger than observed in the other laminate, no correlation between the hole damage and the failure stress could be identified. Typical fracture characteristics are shown in Figure 53 and show the same extensive internal delamination extension previously observed in the 24 ply laminate hole data.

5.3.6 Comparision of the Compression Test Results for the 32 Ply Laminate

A comparison of the two parameter Weibull curve fit to the 32 ply impact damaged and damaged hole specimens is presented in Figure 54. Comparison of the K and v values, presented previously in Table XXIV, does not show any consistent pattern such as was observed for the 24 ply material. Comparison with the column buckling results is shown in Figure 55 for both the impact damaged and damaged hole results. For these test conditions, laminates and damage types the effective restraint is somewhat greater than the 6-pin column buckling support.

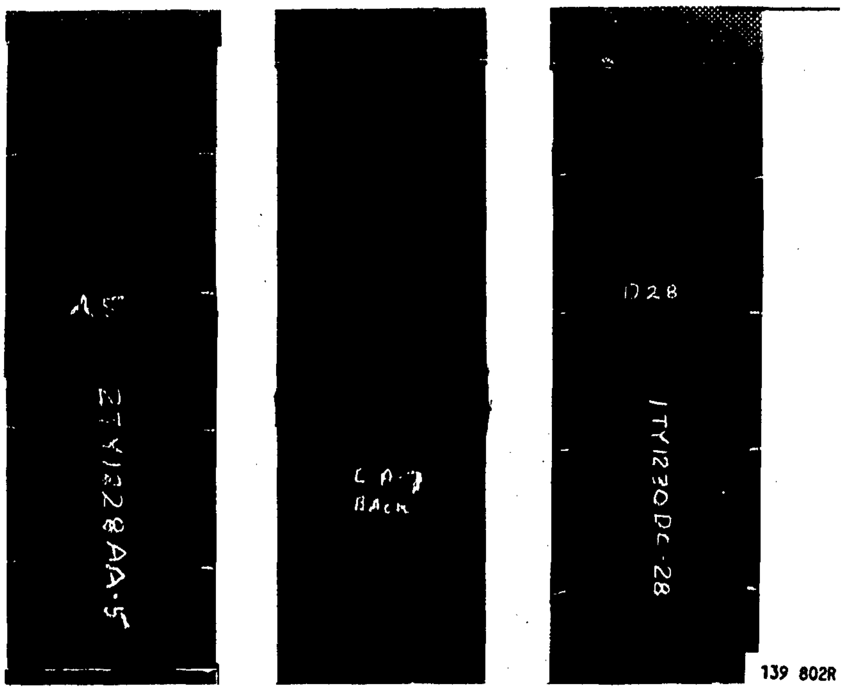

AA-5 CA-7 DC-28

Figure 52. Typical Fracture Features of Impact Damaged 32-Ply Laminate Specimens

TABLE XXVI. 32 PLY DAMAGED HOLE COMPRESSION RESULTS (WITH FATIGUE SUPPORTS)

Specimen Number	Average Thickness		Average Area		Failure Load		Gross Failure Stress		Secant Modulus, at 20 ksi E_s,		Apparent Fracture Strain
	inch	mm	$inch^2$	mm^2	kip	MN	ksi	MPa	$psi \cdot 10^6$	GPa	mm/mm
AA-9	0.1591	4.04	0.4773	308	19.80	88.1	41.5	286	4.91	33.8	0.0093
AB-17	0.1613	4.10	0.4833	312	18.50	82.3	38.2	263	4.84	33.4	0.0087
AC-26	0.1608	4.08	0.4824	311	16.28	72.4	33.7	232	5.00	34.5	0.0071
BC-21	0.1571	3.99	0.4713	304	16.75	74.5	35.5	245	5.08	35.0	0.0076
BB-16	0.1606	4.08	0.4817	311	18.95	84.3	40.2	277	4.92	33.9	0.0087
CB-17	0.1622	4.12	0.4867	314	13.38	59.5	28.3	195	4.74	32.7	0.0062
CB-20	0.1612	4.09	0.4836	312	17.05	75.8	35.3	243	4.90	33.8	0.0077
DB-13	0.1662	4.22	0.4984	322	15.78	70.2	31.7	219	4.63	31.9	0.0073
EA-5	0.1659	4.21	0.4977	321	17.28	76.9	34.7	239	4.69	32.3	0.0078
EC-22	0.1651	4.19	0.4952	319	17.55	78.1	35.4	244	4.78	33.0	0.0078
Average							35.4 + 6.1 - 7.1	244 + 42 - 49	4.85 +0.23 -0.22	33.4 + 1.6 - 1.5	0.0078 +0.0015 -0.0016

NOTE: All fracture across drill entry side, "bulge" on exit side

NOTE: Typical initial damage dimensions are given in Appendix B.

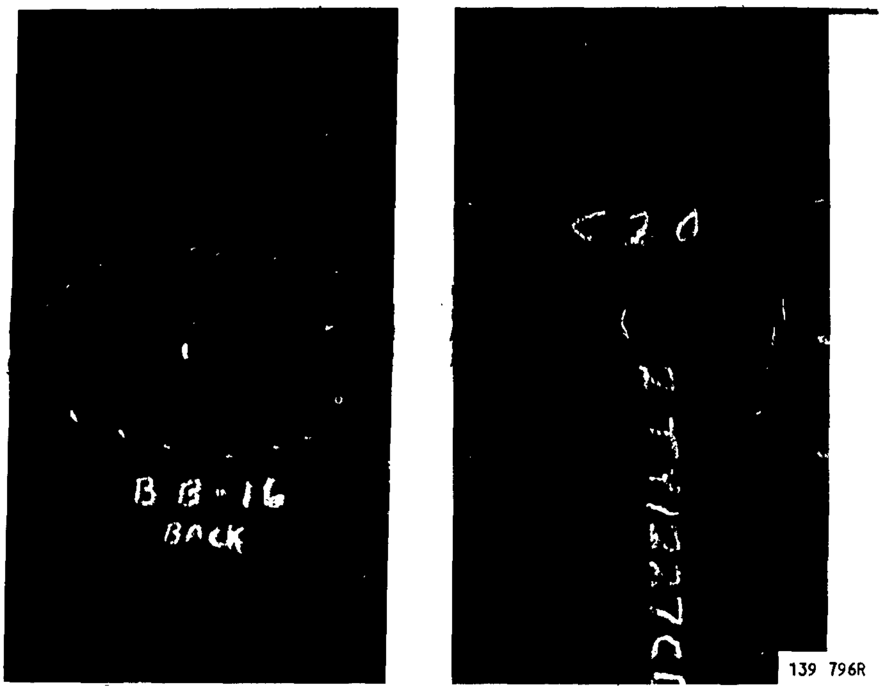

BB-16
Drill Exit Side

CB-20
Drill Entry Side

Figure 53. Typical Fracture Features of Damaged Hole 32-Ply Laminate Specimens

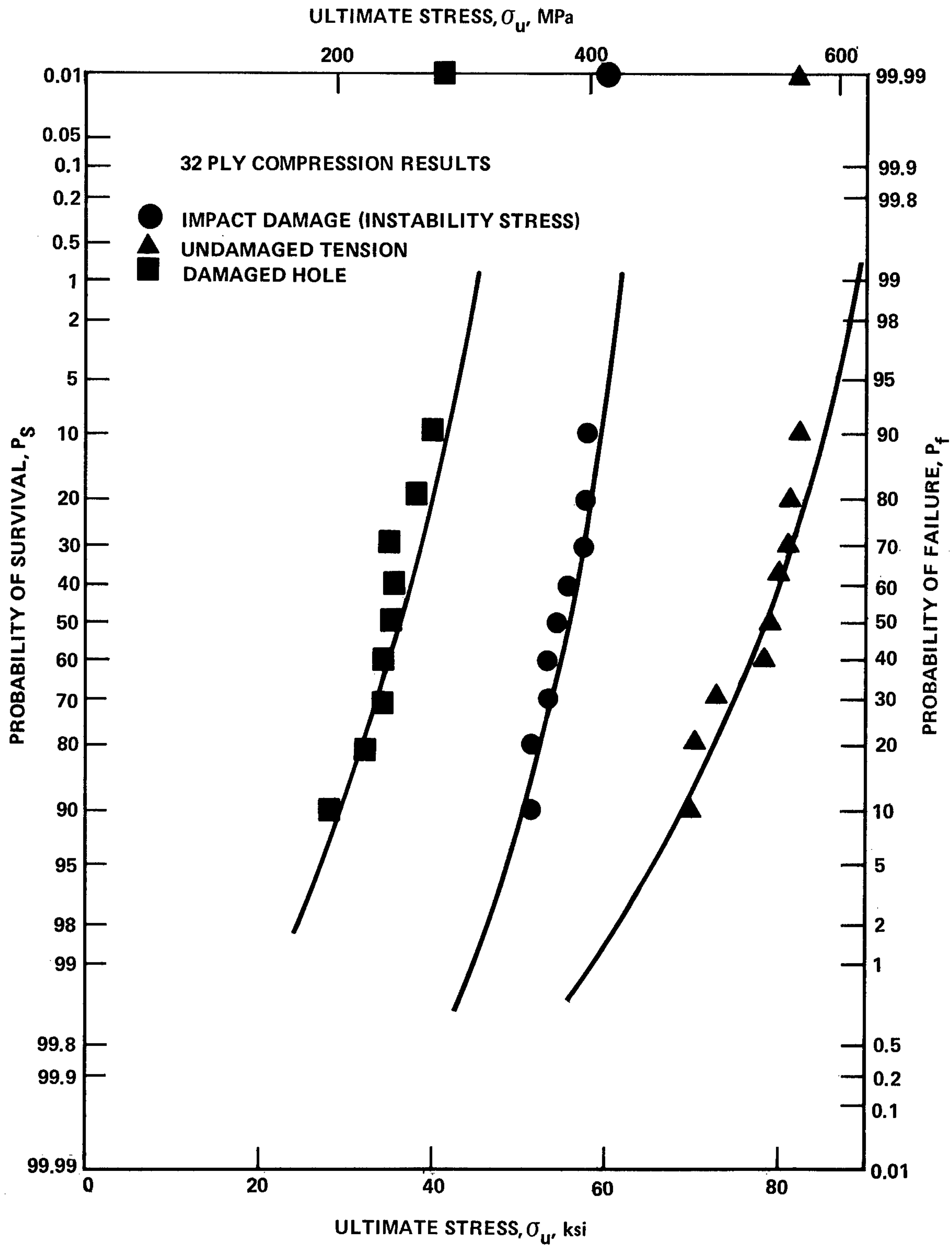

Figure 54. Two Parameter Weibull Data Fits for Damaged 32-Ply Laminate Specimens

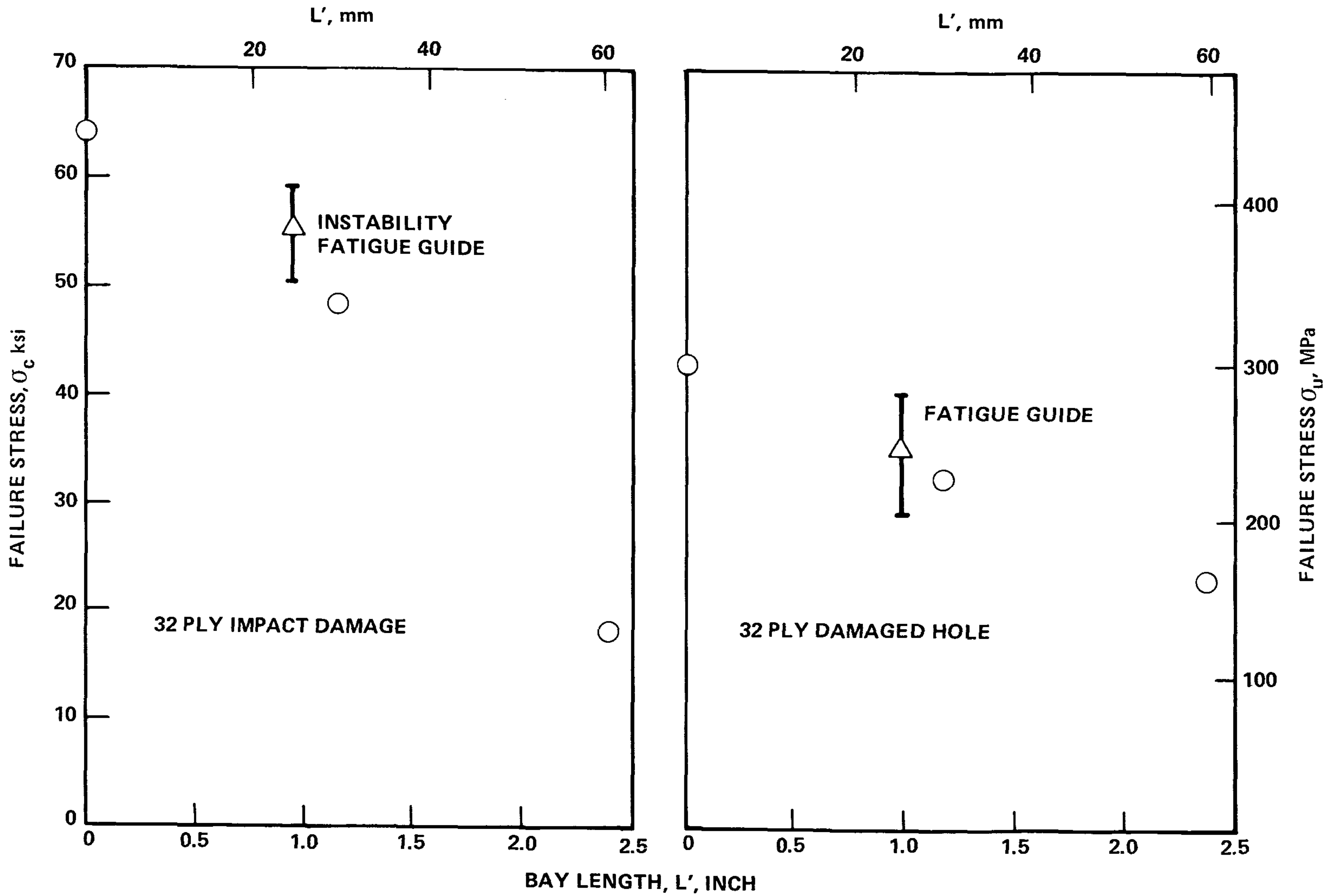

Figure 55. Comparison of Compression Results obtained with the Fatigue Support with the Column Buckling Behavior of Damaged 32-Ply Laminates

5.3.7 Summary of Compression Results

A summary of the two parameter Weibull curve fit parameters is presented in Table XXIV. For the 24 ply results, the shape parameter k varied from 20-28 for essentially all conditions, the major variation being a translation of the curve as shown by changing characteristic value, v. Such was not the case, however, for the 32 ply results where k varied from 8.76 to 24.96 with no apparent consistent trend.

Summaries of the failure stress values and the apparent modulus values are presented in Tables XXVII and XXVIII respectively. The static strength values indicate major degradation of the static compression strength for both impact damage and damaged holes. Similarly the apparent modulus values show a significant drop in compression. Thus, in determining the fatigue loads for the R = -1 fatigue tests, the compression static strength is the determining parameter.

TABLE XXVIII. SUMMARY OF THE APPARENT MODULUS VALUES FOR VARIOUS TEST CONDITIONS

Laminate	Damage Type	Initial Apparent Gross Area Modulus of Elasticity, E_1			
		Tension		Compression	
		ksi	MPa	ksi	MPa
32 Ply Quasi-Isotropic	Damaged Hole	$5.37^{+0.26}_{-0.44}$	$37.0^{+1.8}_{-3.0}$	(B) $4.85^{+0.23}_{-0.22}$	$33.4^{+1.6}_{-1.5}$
	Impact Damage	$7.48^{+0.52}_{-0.80}$	$51.4^{+4.2}_{-7.2}$	(A) $4.68^{+0.17}_{-0.28}$	$32.2^{+1.2}_{-0.8}$
	Undamaged	$8.06^{+0.36}_{-0.16}$	$55.6^{+2.4}_{-2.2}$	-	-
24 Ply 67% 0° Fiber	Damaged Hole	$8.16^{+0.61}_{-0.41}$	$56.3^{+4.2}_{-2.9}$	(C) $8.40^{+0.22}_{-0.22}$	$57.9^{+1.8}_{-1.4}$
	Impact Damage	$14.1^{+0.9}_{-1.1}$	$97.0^{+6.0}_{-7.4}$	(A) $8.55^{+0.26}_{-0.40}$	$59.0^{+1.4}_{-2.8}$
	Undamaged	$15.3^{+0.4}_{-0.4}$	$106.0^{+2.0}_{-3.0}$	-	-

(A) 35 ksi Secant Modulus
(B) 20 ksi Secant Modulus
(C) 30 ksi Secant Modulus

SECTION 6

FATIGUE TEST RESULTS

In the fatigue portion of Task I, tests were conducted to define both the S-N fatigue behavior and the damage growth characteristics for each of the four damage/laminate conditions. For these tests, three replicates were tested at each of six stress levels to define the general R = -1 S-N characteristics for each of the four laminate/damage conditions. Damage growth was monitored by use of a Holosonics Series 400 Holscan unit. The S-N fatigue data are presented in this section, the damage growth data are presented in Section 7.

6.1 FATIGUE RESULTS FOR THE 24 PLY 67% 0° FIBER LAMINATE

Results obtained for the T300/5208 24-ply 67% 0° fiber damaged hole and impact damaged specimens are presented in Figures 56 and 57, respectively, and the results tabulated in Tables XXIX and XXX, respectively. These results indicate the existence of a typical S-N curve for both damage types. Comparison of the results for the two damage types shows a distinct similarity in the S-N curves, the general shapes appearing to be similar. While the impact damaged specimens show a slightly steeper S-N curve, the stress level necessary for minimum growth in $2 \cdot 10^6$ cycles is actually a little lower for the damaged hole specimen than for the impact damaged specimen.

Typical failures at the various stress levels are shown in Figures 58 and 59 for the damaged hole and impact damaged specimens, respectively.

6.2 FATIGUE RESULTS FOR THE 32 PLY QUASI-ISOTROPIC LAMINATE

Fatigue test results for the 32 ply quasi-isotropic specimens containing damaged holes and impact damage are presented in Figures 60 and 61, respectively and are tabulated in Tables XXXI and XXXII. The specimens containing a single damaged hole again exhibit a typical S-N fatigue curve with what appears to be

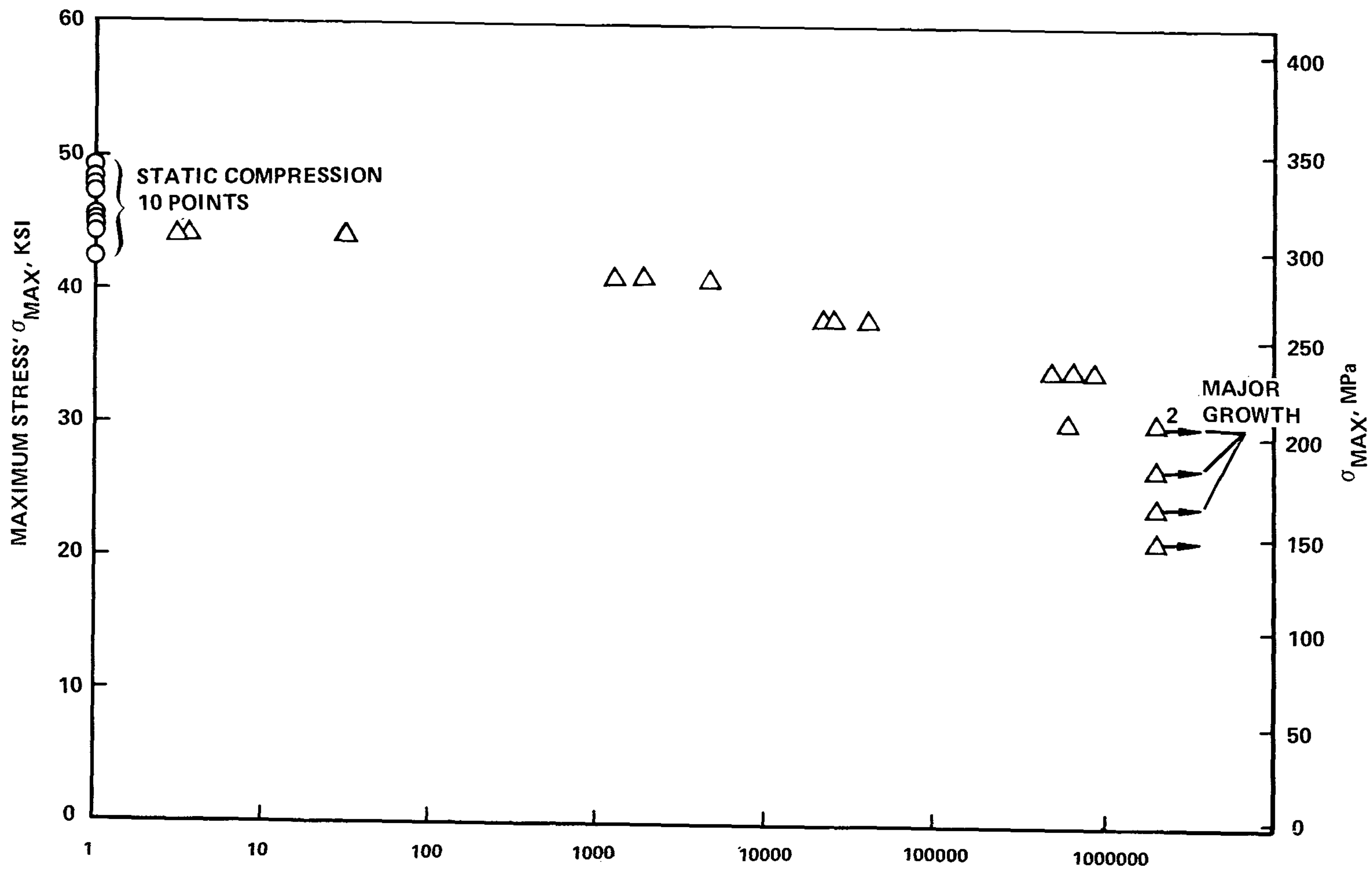

Figure 56. Fatigue Life Data for Damaged Hole Specimens of 24 Ply, 67% 0° Fiber Laminates, R = -1, 5 Hz

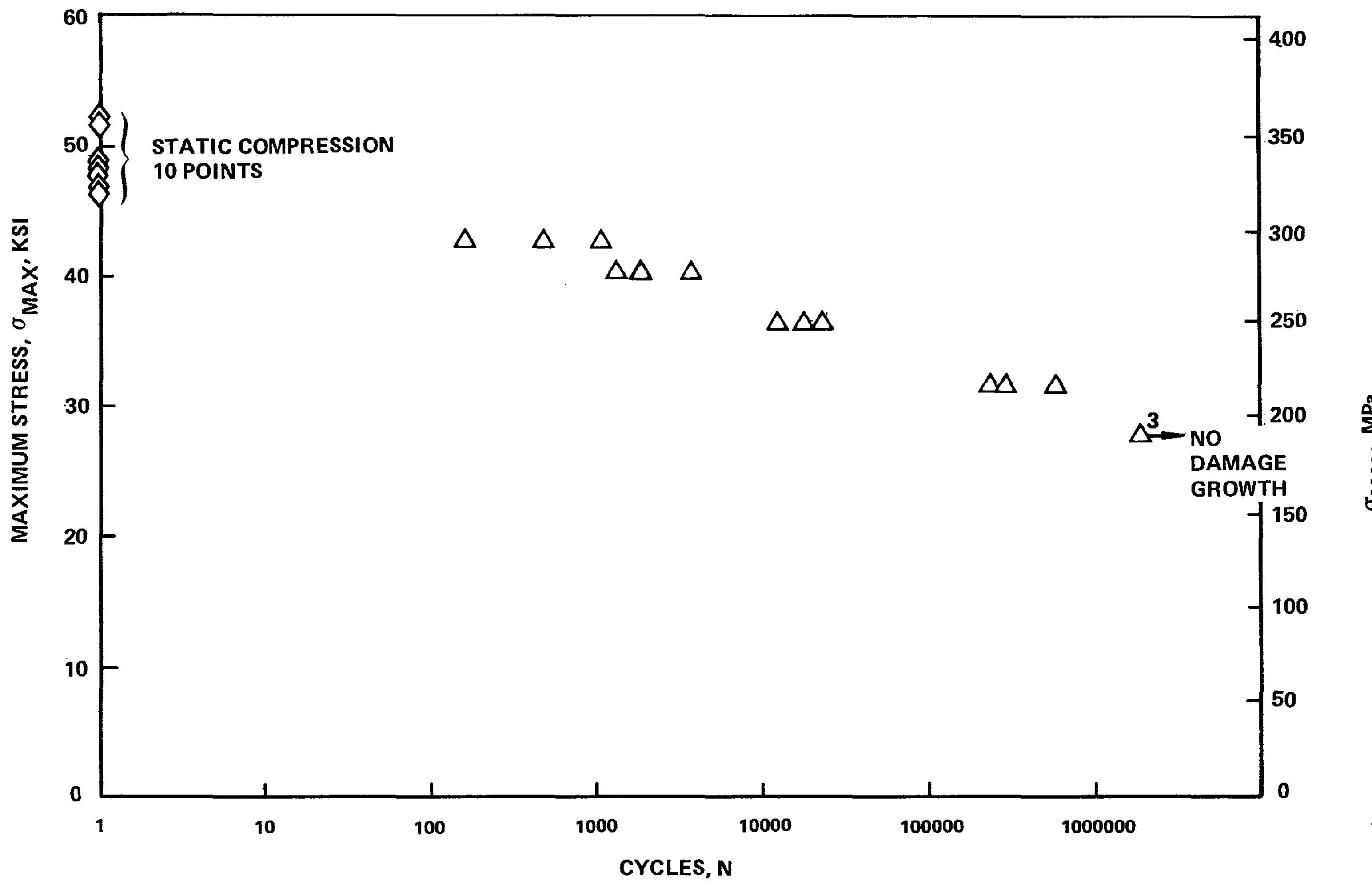

Figure 57. Fatigue Life Data for Impact Damaged 24-Ply, 67% 0° Laminates, R = -1, 5 Hz

TABLE XXIX

FATIGUE TEST RESULTS FOR DAMAGED HOLE SPECIMENS OF 24-PLY 67% 0° FIBER T300/5208 LAMINATE

R = -1, Room Temperature Laboratory Air, 5Hz

Specimen Number	Average Thickness, B		Average Width, W		Maximum Cyclic Stress, σ max		Cycles to Failure, N	Comments
	inch	mm	inch	mm	ksi	MPa		
MB-14	0.1254	3.185	2.997	76.12	44.0	303	3	
KB-17	0.1230	3.124	2.997	76.12	44.0	303	4	
JB-14	0.1253	3.183	2.995	76.07	44.0	303	43	
LB-17	0.1240	3.150	2.997	76.12	41.0	283	1,240	
LA-7	0.1233	3.132	2.996	76.10	41.0	283	1,900	
JB-15	0.1244	3.160	2.994	76.05	41.0	283	4,667	
KA-4	0.1230	3.124	2.997	76.12	38.0	262	23,233	
HA-1	0.1207	3.066	2.996	76.10	38.0	262	25,691	
JC-21	0.1220	3.100	2.995	76.07	38.0	262	40,530	
MC-22	0.1245	3.162	2.997	76.12	34.0	234	498,822	
HA-8	0.1218	3.094	2.984	75.79	34.0	234	626,500	
JA-8	0.1246	3.165	2.996	76.10	34.0	234	855,800	
HA-4	0.1216	3.090	2.996	76.10	30.0	207	375,500	
KB-11	0.1225	3.112	2.997	76.12	30.0	207	2,000,000 DNF*	Major Damage Growth
LC-23	0.1233	3.132	2.997	76.12	30.0	207	2,000,000 DNF*	Major Damage Growth
MC-25	0.1247	3.167	2.997	76.12	26.0	179	2,000,000 DNF*	Major Damage Growth
JC-29	0.1230	3.124	2.996	76.10	23.5	162	2,000,000 DNF*	
KC-29	0.1217	3.091	2.996	76.10	21.0	145	2,000,000 DNF*	Minor Damage Growth

TABLE XXX

FATIGUE TEST RESULTS FOR IMPACT DAMAGED SPECIMENS OF 24 PLY 67% 0° FIBER T300/5208 LAMINATE

R = -1, Room Temperature Laboratory Air, 5 Hz

Specimen Number	Average Thickness, B		Average Width, W		Maximum Cyclic Stress, σ_{max}		Cycles to Failure, N	Comments
	inch	mm	inch	mm	ksi	MPa		
LC-29	0.1235	3.137	2.990	75.95	45.5	314	65	
KB-14	0.1232	3.129	2.998	76.15	45.5	314	169	
MA-10	0.1231	3.127	2.999	76.17	45.5	314	584	
LC-26	0.1234	3.134	2.999	76.17	42.75	295	501	
JA-7	0.1248	3.170	2.999	76.17	42.75	295	906	
MB-15	0.1262	3.205	2.989	75.92	42.75	295	1,085	
HC-25	0.1216	3.089	2.998	76.15	40.5	279	1,328	
MB-16	0.1260	3.200	2.999	76.17	40.5	279	2,720	
KA-3	0.1233	3.132	2.998	76.15	40.5	279	3,980	
KA-10	0.1206	3.063	2.999	76.17	36.8	254	12,090	
HB-14	0.1223	3.106	3.001	76.22	36.8	254	14,062	
LC-22	0.1233	3.132	2.999	76.17	36.8	254	18,444	
HC-22	0.1209	3.071	2.999	76.17	31.5	217	122,360	
LB-12	0.1230	3.124	2.999	76.17	31.5	217	221,367	
JC-22	0.1228	3.119	2.999	76.17	31.5	217	556,000	
MC-26	0.1244	3.160	2.999	76.17	27.6	190	2,213,565 DNF*	No damage growth
JC-30	0.1233	3.132	2.999	76.17	27.6	190	2,000,000 DNF*	" " "
KB-15	0.1229	3.122	2.991	75.97	27.6	190	2,000,000 DNF*	" " "

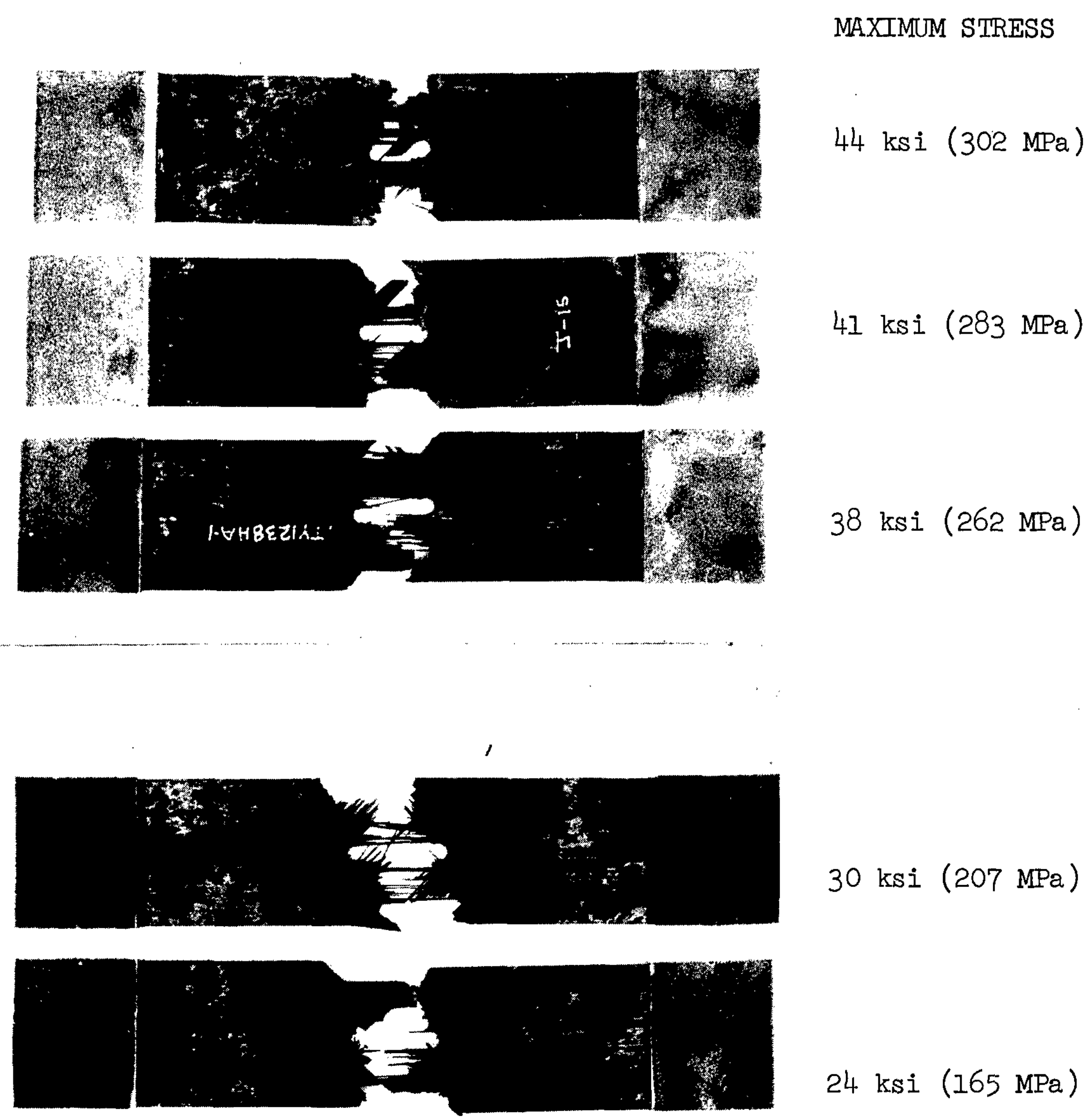

Figure 58. Fatigue Fracture Appearance of Damaged Hole 24-Ply 67% 0° Fiber Specimens

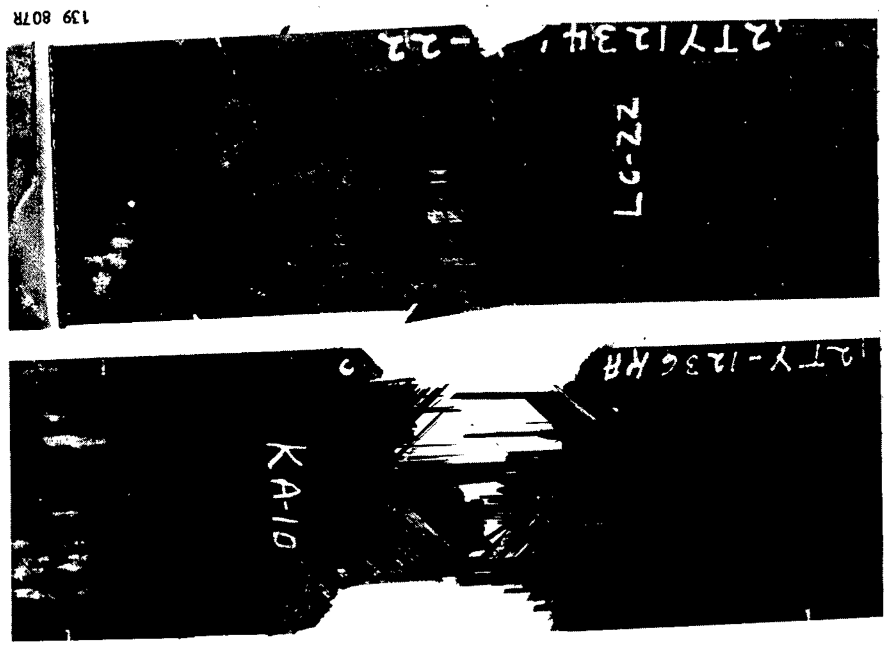

LC-22
18,443 Cycles

KA-10
1290 Cycles

a) Front Surface

KA-10

LC-22

Figure 59. Fracture Appearance of Impact Damaged 24-Ply 67% 0° Fiber Laminates Fatigue Tested at ± 36.8 ksi (254 MPa)

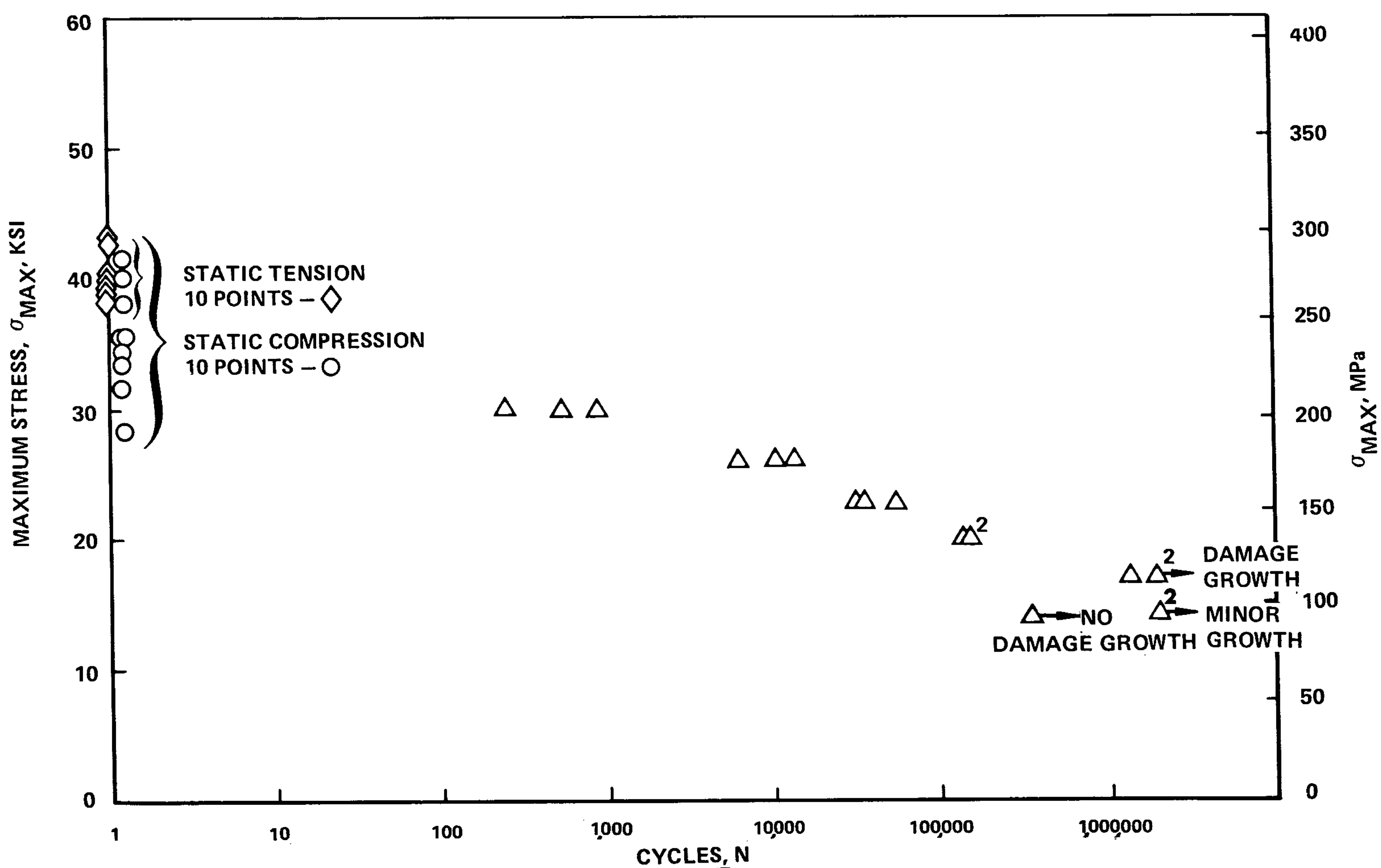

Figure 60. Fatigue Life Data for Damaged Hole 32-Ply Quasi-Isotropic Laminates, R = -1, 5 Hz

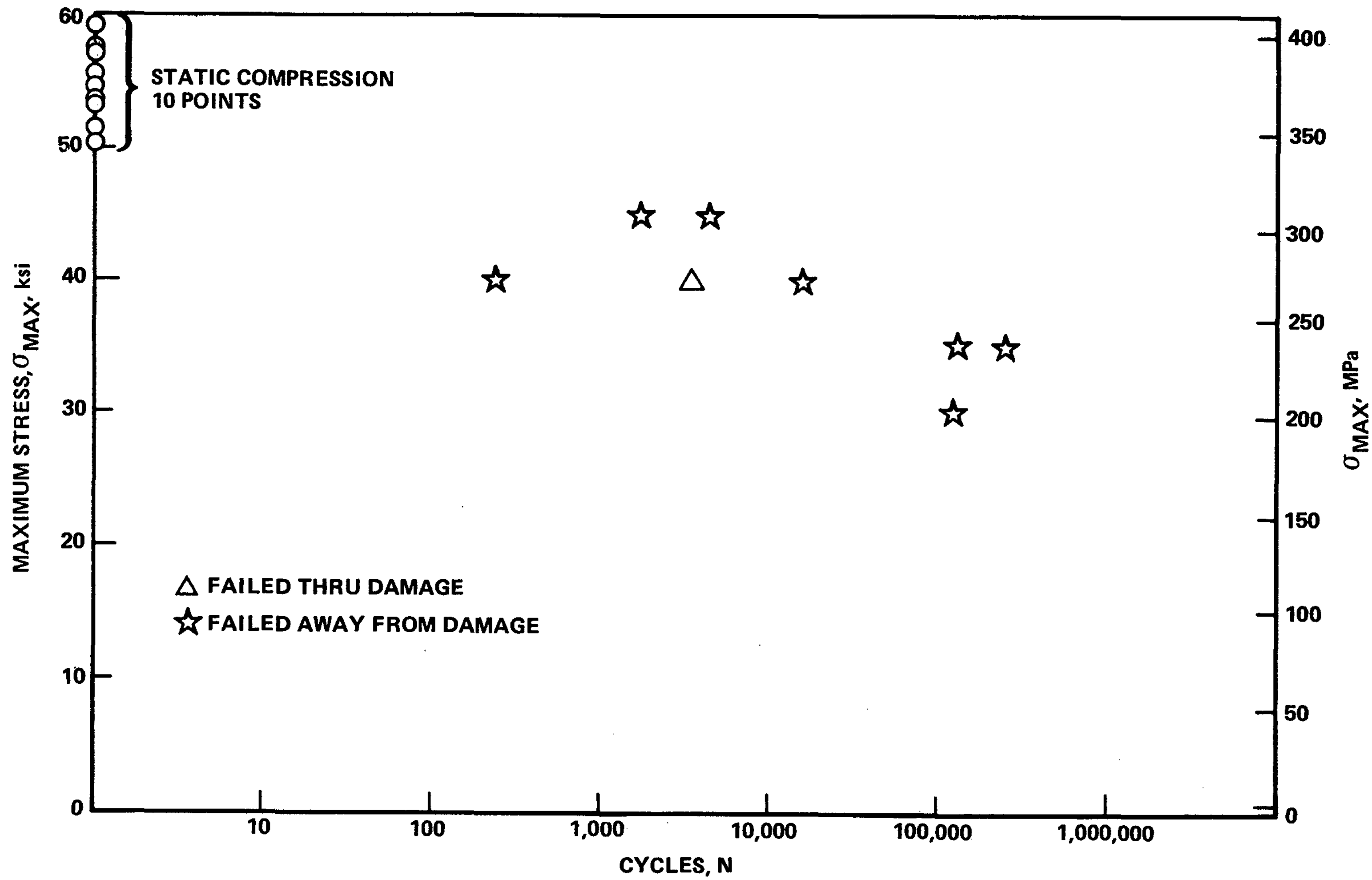

Figure 61. Fatigue Life Data for Impact Damaged Specimens of 32-Ply Quasi-Isotropic Laminates, R = -1,5 Hz

TABLE XXXI

FATIGUE TEST RESULTS FOR DAMAGED HOLE SPECIMENS OF 32-PLY QUASI-ISOTROPIC T300/5208 LAMINATE

R = -1, Room Temperature Laboratory Air, 5 Hz

Specimen Number	Average Thickness, B		Average Width, W		Maximum Cyclic Stress, σ max		Cycles to Failure, N	Comments
	inch	mm	inch	mm	ksi	MPa		
EC-23	0.1649	4.188	2.997	76.12	30.0	207	321	
BB-14	0.1598	4.059	2.999	76.17	30.0	207	540	
AA-6	0.1593	4.046	2.999	76.17	30.0	207	884	
DA-5	0.1654	4.201	2.940	74.68	26.0	179	6,011	
CC-30	0.1599	4.061	2.922	74.22	26.0	179	11,009	
EC-27	0.1658	4.211	2.998	76.15	26.0	179	13,101	
DB-14	0.1656	4.206	2.940	74.68	23.0	158	31,655	
BC-22	0.1578	4.008	2.999	76.17	23.0	158	34,652	
BC-28	0.1589	4.036	3.000	76.20	23.0	158	54,271	
CA-5	0.1611	4.092	2.970	75.44	20.0	138	149,464	
DB-19	0.1648	4.186	2.943	74.75	20.0	138	158,196	
AB-11	0.1595	4.051	2.999	76.17	20.0	138	159,224	
CB-12	0.1612	4.094	2.960	75.18	17.0	117	1,257,106	
EB-18	0.1658	4.211	2.997	76.12	17.0	117	2,000,000 DNF*	Significant damage growth
DC-26	0.1642	4.171	2.940	74.68	17.0	117	2,000,000 DNF*	Significant damage growth
AA-2	0.1588	4.034	2.999	76.17	14.0	96.5	346,532**	No damage growth
EB-11	0.1649	4.188	2.998	76.15	14.0	96.5	2,000,000 DNF	
AA-4	0.1590	4.039	2.971	75.46	14.0	96.5	2,000,000 DNF	Minor damage growth

*DNF = did not fail
** = machine malfunction, invalid failure

TABLE XXXII

FATIGUE TEST RESULTS FOR IMPACT DAMAGED SPECIMENS OF 32-PLY QUASI-ISOTROPIC T300/5208 LAMINATE

R = -1, Room Temperature Laboratory Air, 5 Hz

Specimen Number	Average Thickness, B		Average Width, W		Maximum Cyclic Stress, σ max		Cycles to Failure, N	Comments
	inch	mm	inch	mm	ksi	MPa		
CC-21	0.1596	4.054	2.964	75.28	45.0	310	1,858*	
BB-20	0.1597	4.056	2.989	75.92	45.0	310	4,651*	
DB-18	0.1618	4.109	2.990	75.95	40.0	276	245*	
AC-22	0.1604	4.074	2.990	75.95	40.0	276	3,456	
EA-9	0.1639	4.163	2.969	75.41	40.0	276	16,622*	
BA-6	0 1606	4.079	2.999	76.17	35.0	242	124,810*	
DC-22	0.1640	4.166	2.999	76.17	35.0	242	246,677*	
CA-9	0.1612	4.094	2.989	75.92	30.0	207	127,097*	

* failed away from damage site

relatively small scatter, (i.e., less than an order of magnitude for any of three sets of triplicate specimens). Typical failures are shown in Figure 62.

Results for the impact damaged 32-ply quasi-isotropic specimens did not, however, show consistent damage growth or fatigue S-N behavior. As shown in Figure 61 and Table XXXII, a large number of the failures in the 32-ply impact damaged specimens occurred away from the damage region. Typical failures are shown in Figure 63. These results indicate that the impact conditions used for the 32-ply quasi-isotropic material resulted in damage which is very near the threshold size to cause failure due to fatigue. To assure that the results were not a testing artifact, the following test variables were evaluated; 1) machine alignments were rechecked and found to be accurate, 2) tests were repeated in two additional test machines with the same results, and 3) buckling guide flatness and clearance was rechecked, and the guides were found to be flat and have adequate clearance throughout the load cycle. As a result of these findings, it was concluded that the damage size was near the threshold level to cause failure due to fatigue in this laminate and testing of the 32-ply impact damaged specimens was discontinued. Note that this result is consistent with the static tension results previously presented in Section 5.

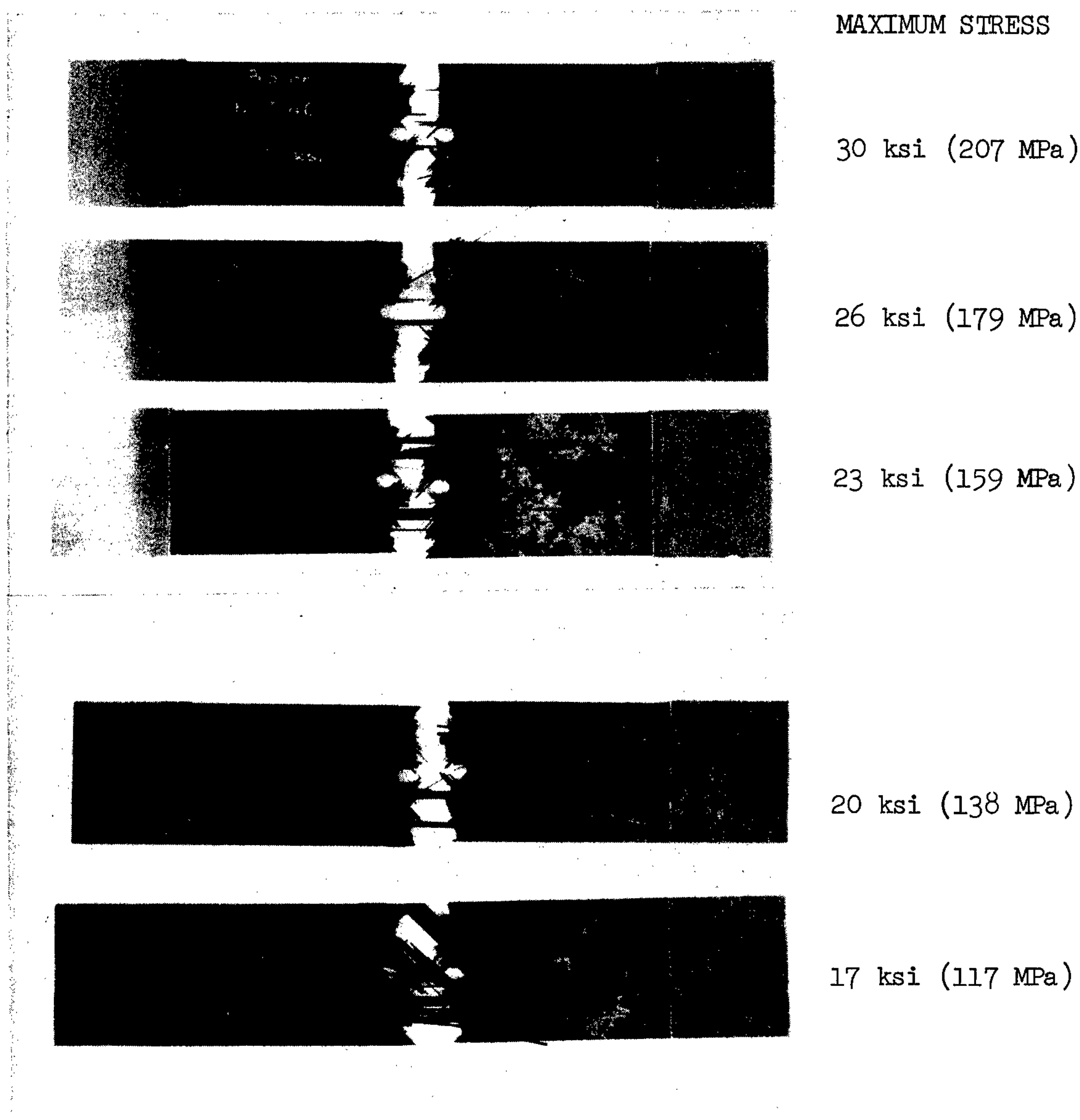

Figure 62. Typical Failures in Damaged Hole 32-Ply Quasi-Isotropic Specimens

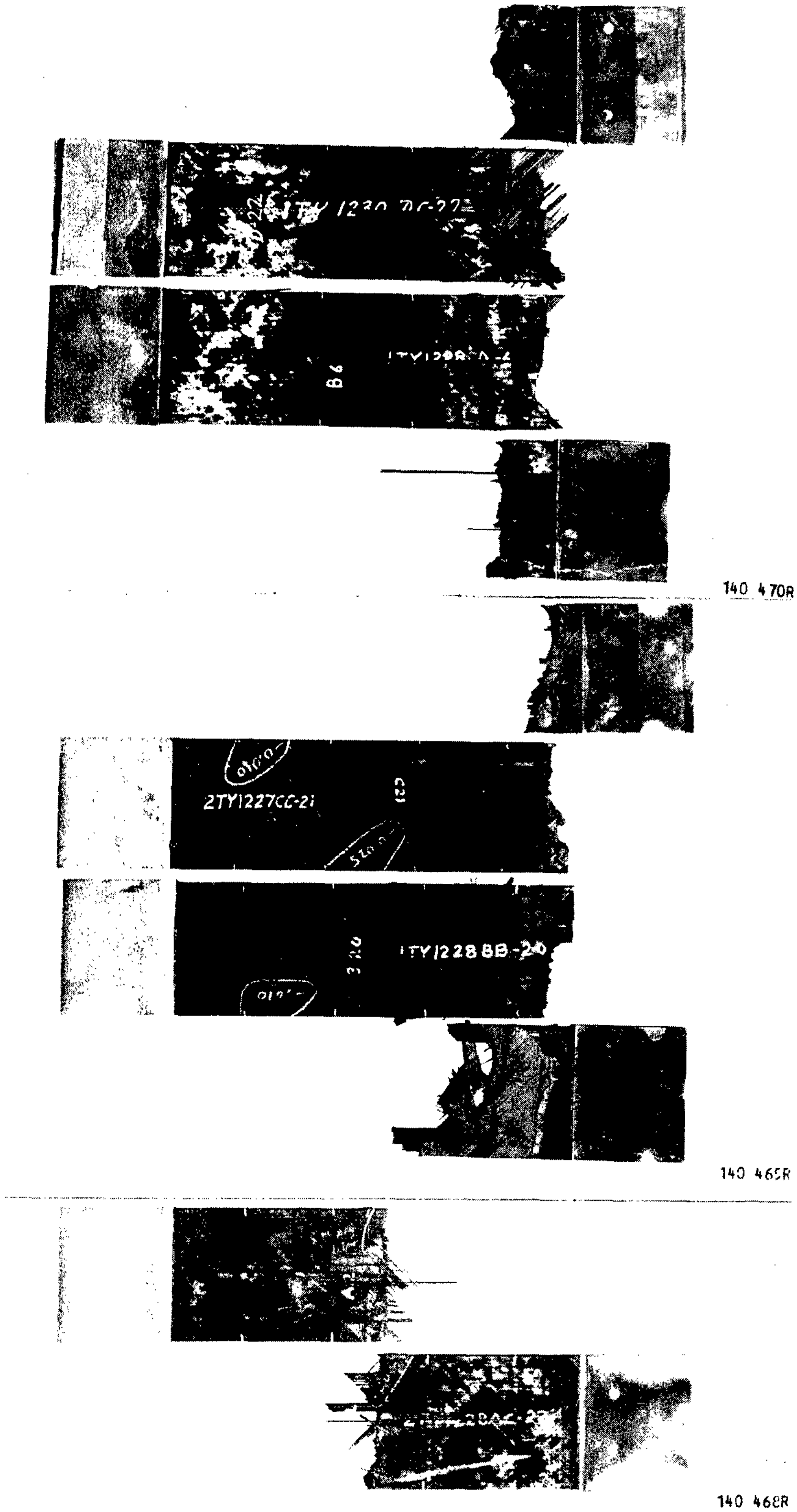

DC-22
σ_{max} = 35ksi (241 MPa)

BA-6
σ_{max} = 35 ksi (241 MPa)

CC-21
σ_{max} = 45 ksi (310 MPa)

BB-20
σ_{max} = 45 ksi (310 MPa)

AC-22 (Valid)
σ_{max} = 40 ksi (276 MPa)

Figure 63. Typical Failures in Impact Damaged 32-Ply Quasi-Isotropic Specimens

SECTION 7

DAMAGE GROWTH RESULTS

Definition of damage growth characteristics in composite materials is considerably more difficult than in metals where a single crack length parameter can be used to characterize the damage. In composite materials the wide variety of potential damage modes, many of which may occur in a single damage region, and their sensitivity to the NDI method used to detect damage make the selection of a meaningful damage parameter or parameters difficult. In this section the damage data available are reviewed, the rationale for the damage parameter selection developed and the results presented for the various damage/laminate conditions.

7.1 BUCKLING GUIDE CONSIDERATIONS

Of major importance in the interpretation of the fatigue/damage growth behavior in composite materials under loading that extends into the compression region is the influence of the method of constraining buckling. Numerous studies[2,14] have shown that the fatigue life under tension-compression fatigue varies with the method used to constrain buckling. Since all methods of support are imperfect attempts to model actual structural response, the limitations must be kept in mind in the interpretation of the results.

For the current program, the main interest is in the damage propagation characteristics. The buckling guide used contains an open rectangular "window" 2.15 x 2.15 inch (54.6 x 54.6 mm) which effectively defines the maximum X or Y direction growth which can occur before encountering the clamping effect of the buckling support. As a result, X and Y data with dimensions larger than this value should be considered beyond the valid range.

7.2 RECORDED DATA AVAILABLE FOR ANALYSIS

A typical set of Holscan data such as shown in Figure 64 consist of the following basic information:

a. A C-scan photo taken from the TV monitor. These data are recorded since the TV-monitor records nine levels of intensity proportional to the acoustic attenuation of the signal. As a result, it provides the maximum amount of C-scan information.

b. A C-scan photo from the memory scope. These data are more typical of standard C-scan results and are based on the attenuation exceeding a specific level, i.e., as a go-no-go record.

c. A cumulative B-scan which shows the levels at which damage is occurring.

In addition to this basic information taken at each inspection interval, a second set of data was taken each time a significant change was observed in the basic damage characteristics. This second data set typically consisted of the following:

d. A photo of the C-scan results with marker lines showing the locations of single pass B-scans through the damage area.

e. Photos of the individual B-scans taken through selected regions of the damage. A typical set of these data is shown in Figure 65.

Since ultrasonic inspection methods such as the Holscan normally present a projection of the total damage area parallel to the specimen surface, the C-scan damage area was selected as a starting point for the reduction of the data. While many possible ways exist to present this volume of data, three damage parameters were selected for comparison and evaluation as a significant damage parameter for damage characterization. These three parameters were:

a. The damage area, A, determined from the C-scan photos as measured using a K&E model 4242 Planimeter to trace around the outer periphery of the damage indication to determine the area of the damage.

b. The maximum damage extension in the specimen width direction, X, as measured from the C-scan photo.

A. TV Monitor C-Scan Results

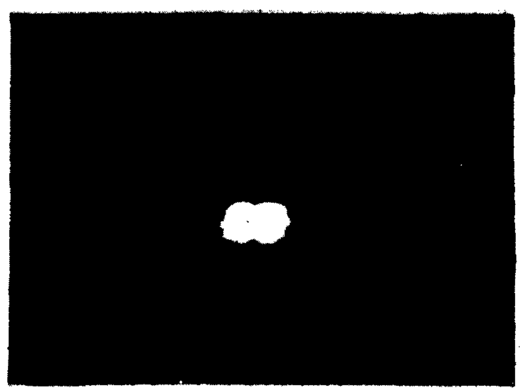

B. Memory Scope C-Scan Results

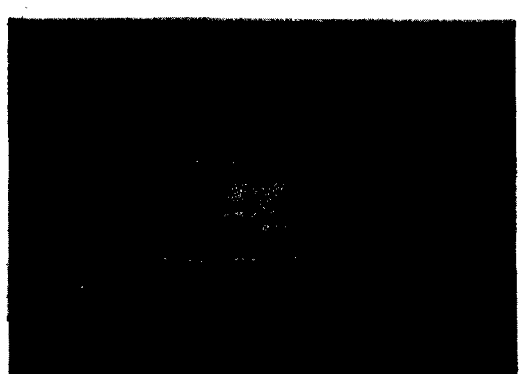

C. Cumulative B-Scan Results

Figure 64. Typical Set of Holscan Data for Each Damage Growth Interval

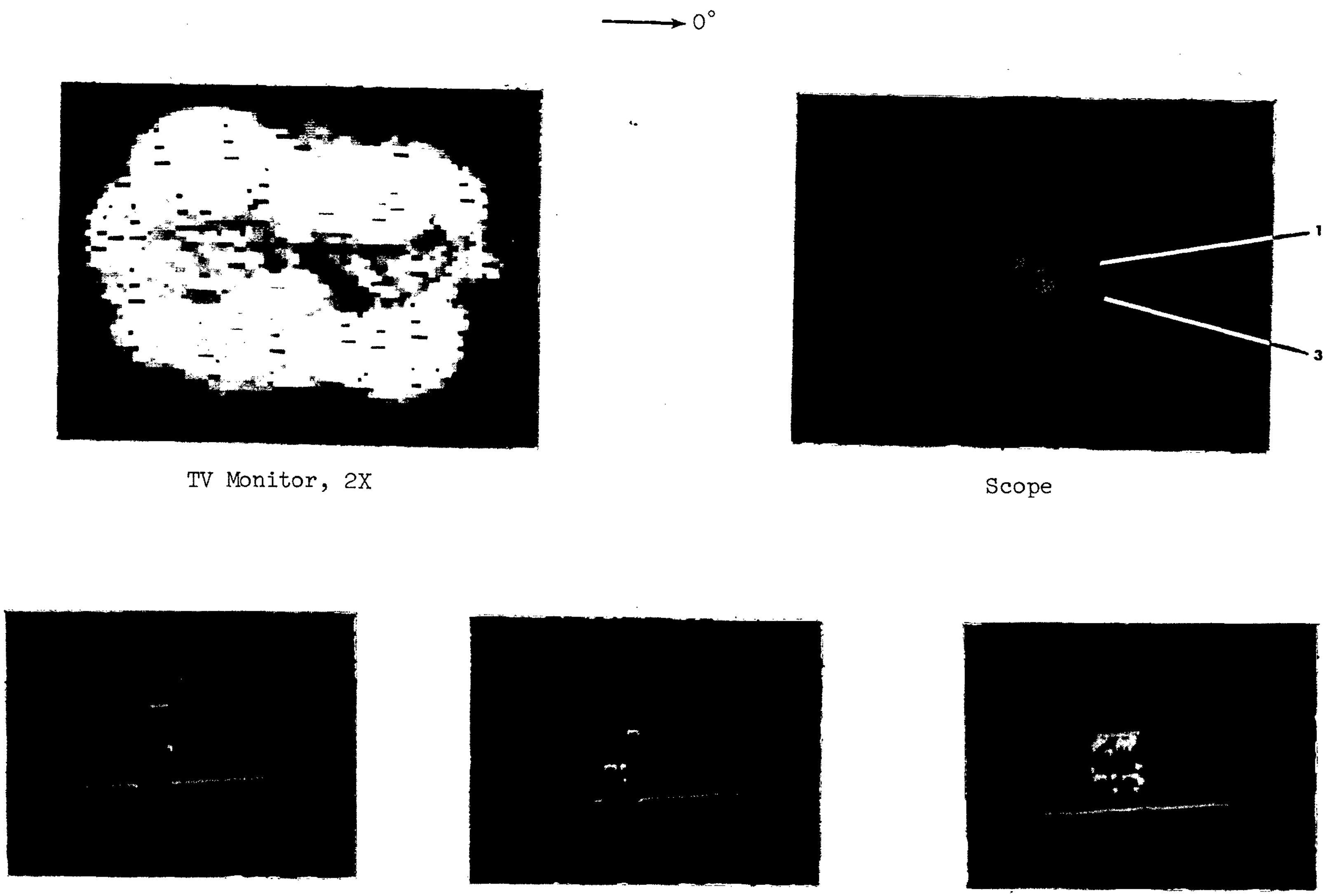

TV Monitor, 2X

Scope

Section 1 B-Scan

Section 3 B-Scan

Total B-Scan

Figure 65. Typical Data Set Showing Single Pass B-Scan Results at Selected Locations Through the Damage.

c. The maximum damage extension in the 0° fiber direction, Y, as measured from the C-scan photos.

Normally the 1X magnification TV monitor photo was used for all measurements except where the damage extended off the TV screen. For these cases the memory scope C-scan was used. A typical illustration of the damage size parameter is shown in Figure 66.

7.3 SYSTEM CALIBRATION AND AREA MEASUREMENT PROCEDURES

In order to assure accurate scale factors for the photo, a special calibration block of the 32-ply quasi-isotropic T300/5208 material was machined with two parallel milled cuts running vertically and two parallel machined cuts running horizontally across the block. The width and spacing of the slots were then measured with a tool makers microscope. The block was then scanned with the Holscan unit and photos taken of the TV monitor C-scan and the memory scope C-scan as shown in Figure 67, and the spacings measured from the photos to obtain the scaling factors. These scans have been repeated periodically to check for variations and have been found to be stable over the course of the program and showed the system to be very stable.

Once the scale factors were obtained, the C-scan photos were measured using a K&E model 4242 Planimeter by tracing around the outer periphery of the damage indication to determine the area of the damage. A transparent scale marked to 0.01 in. (0.25mm) was used to determine the measurement X and Y dimensions. Normally the 1X TV monitor photo was used except where the damage extended off the TV screen. For these cases the memory scope C-scan was used. Repeated measurements by one reader were compared with those of a second reader and the areas found to be reproducible to approximately ± 5%. An initial evaluation of the damage characteristic of each of the damage/laminate types was first conducted by examining the behavior of the X, Y, and area parameter for the three replicate specimens at three selected stress levels. A damage parameter was then selected for use on the remaining specimens.

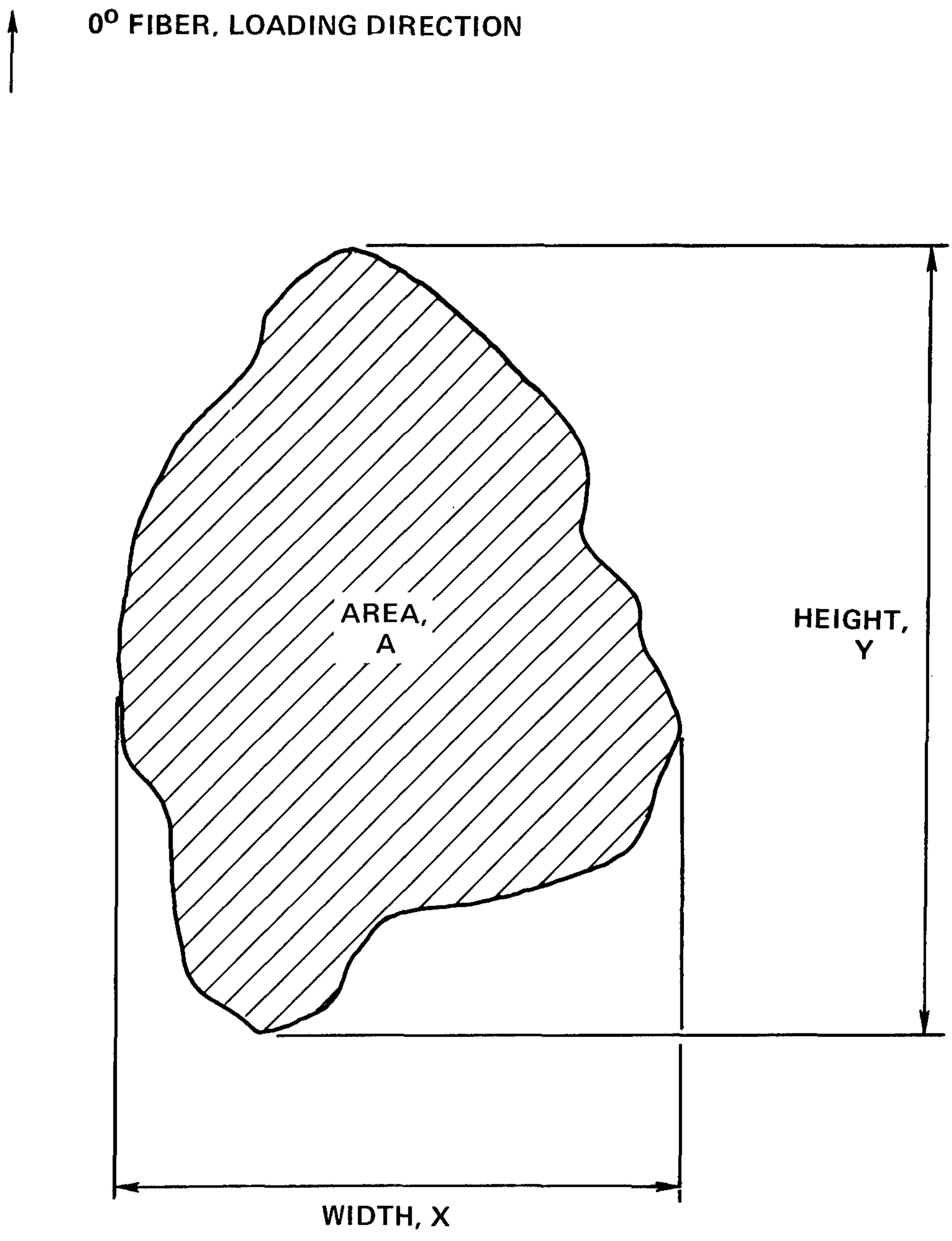

Figure 66. Illustration of the Damage Zone Size Parameters Evaluated

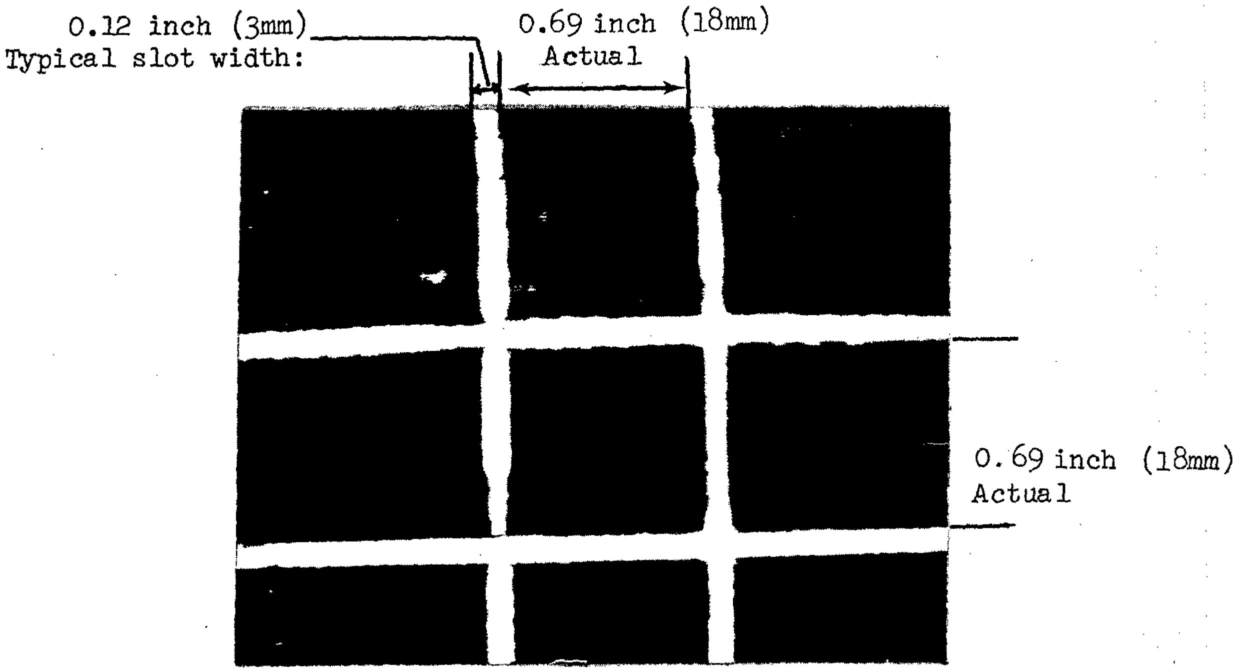

A. TV Monitor Photo, 1X
Scale Factor: 1-inch = 0.70 inch actual
25mm = 18mm actual

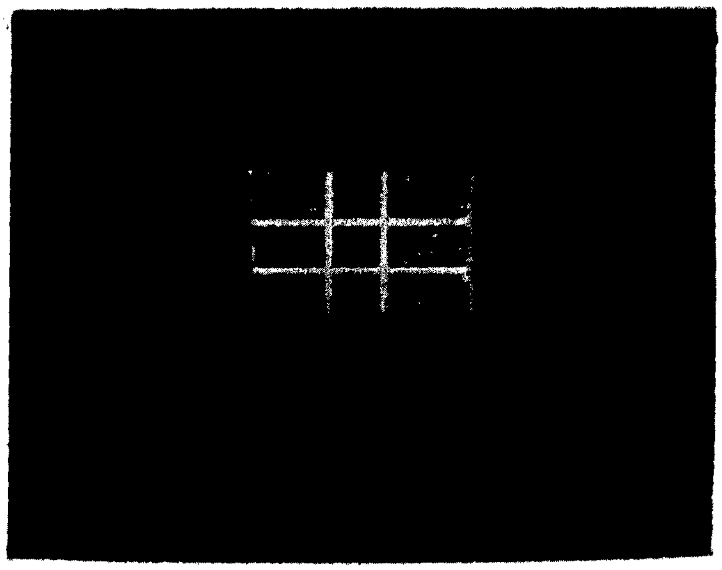

B. Memory Scope Photo
Scale Factor: 1-inch = 2.69 inch actual
25mm =68mm actual

Figure 67. C-Scan Photos of Calibration Block Used

7.4 DAMAGE GROWTH IN 24 PLY LAMINATES WITH A DAMAGED HOLE

Results for the 24 ply 67% 0° fiber laminate containing a damaged hole in the high stress (± 41 ksi, 283 MPa) low lifetime (< 10,000 cycles) region typically showed an initial rapid growth in the width (X) direction which then slowed and progressed at a lower rate to failure, as shown in Figure 68. Note that the shortest life specimen, LB-17, exhibited initial growth which extended rapidly to the fatigue support, the remaining specimens JB-15 and LA-7 exhibiting growth within the open gage section to failure. Results similar to the X dimension growth are also observed for the damage height dimension, except that the initial rapid increase is much smaller, the rate being more consistent over the specimen lifetime.

The damage area parameter, shown in Figure 69, shows the typical general correlation that would be expected from the damage width and height results. The one point of note here is that the limit of the area size corresponding to the X or Y damage dimension exceeding the support size occurs at an area of ~ 2.5 in.^{2} ($16 \cdot 10^{-4}$ m^2) rather than the ~ 4.6 in.^{2} ($30 \cdot 10^{-4}$m^2) total open area of the buckling guide. This is only a reflection of the irregular outer periphery of the damage size.

At an intermediate stress level of 38 ksi (262 MPa), behavior similar to that at the higher stress level is observed as shown in Figure 70. Examination of this set of specimens, however, does show that the specimen HA-1 did exhibit significantly different growth behavior than previously observed at 41 ksi (283 MPa) or for specimens JC-21 or KA-4 tested at the same stress level. As shown in Figure 69, specimen HA-1 exhibited very little growth in the width (X) direction following the initial burst of growth. Instead the damage extended in the loading direction (height, Y) until it encountered the buckling support which then slowed the Y growth rate somewhat. A comparison of the damage appearance of Specimen HA-1 with the more typical appearance illustrated by specimen JC-21 tested at the same stress level is shown in Figure 71 and graphically illustrates the difference in the growth appearance of specimen HA-1. Note in Figure 71 that there does appear to be some damage in the

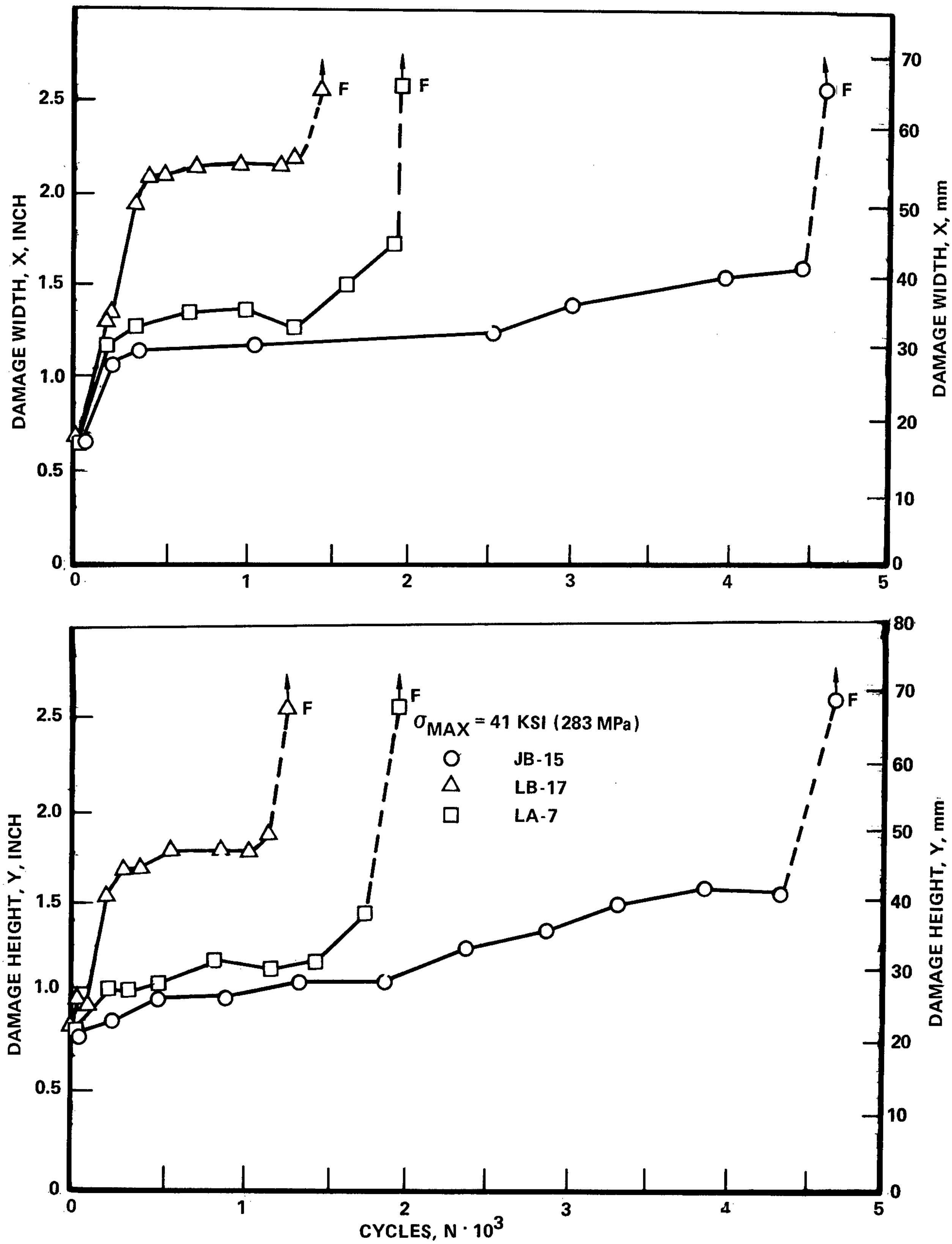

Figure 68. Damage Growth Behavior of 24-Ply 67% 0° Fiber Laminates Containing a Damaged Hole, R = -1, σ_{max} = 41 ksi (283 MPa)

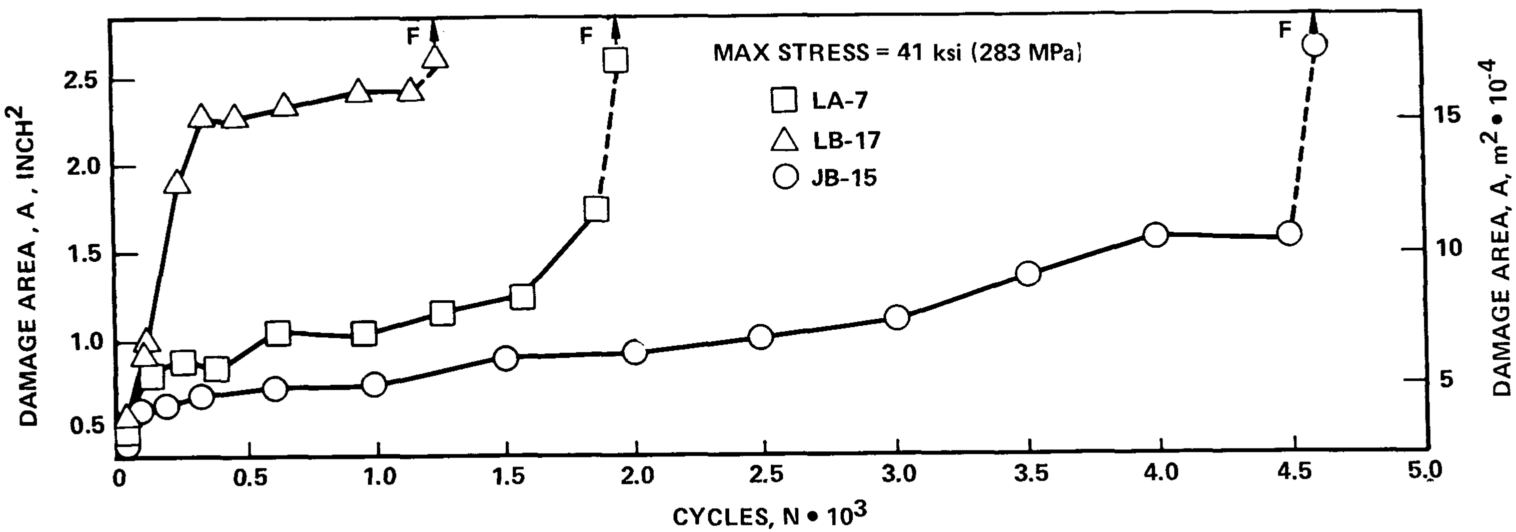

Figure 69. Damage Growth Behavior of Damaged Hole 24-Ply 67% 0° Fiber Specimens, R = -1, σ_{max} = 41 ksi (283 MPa)

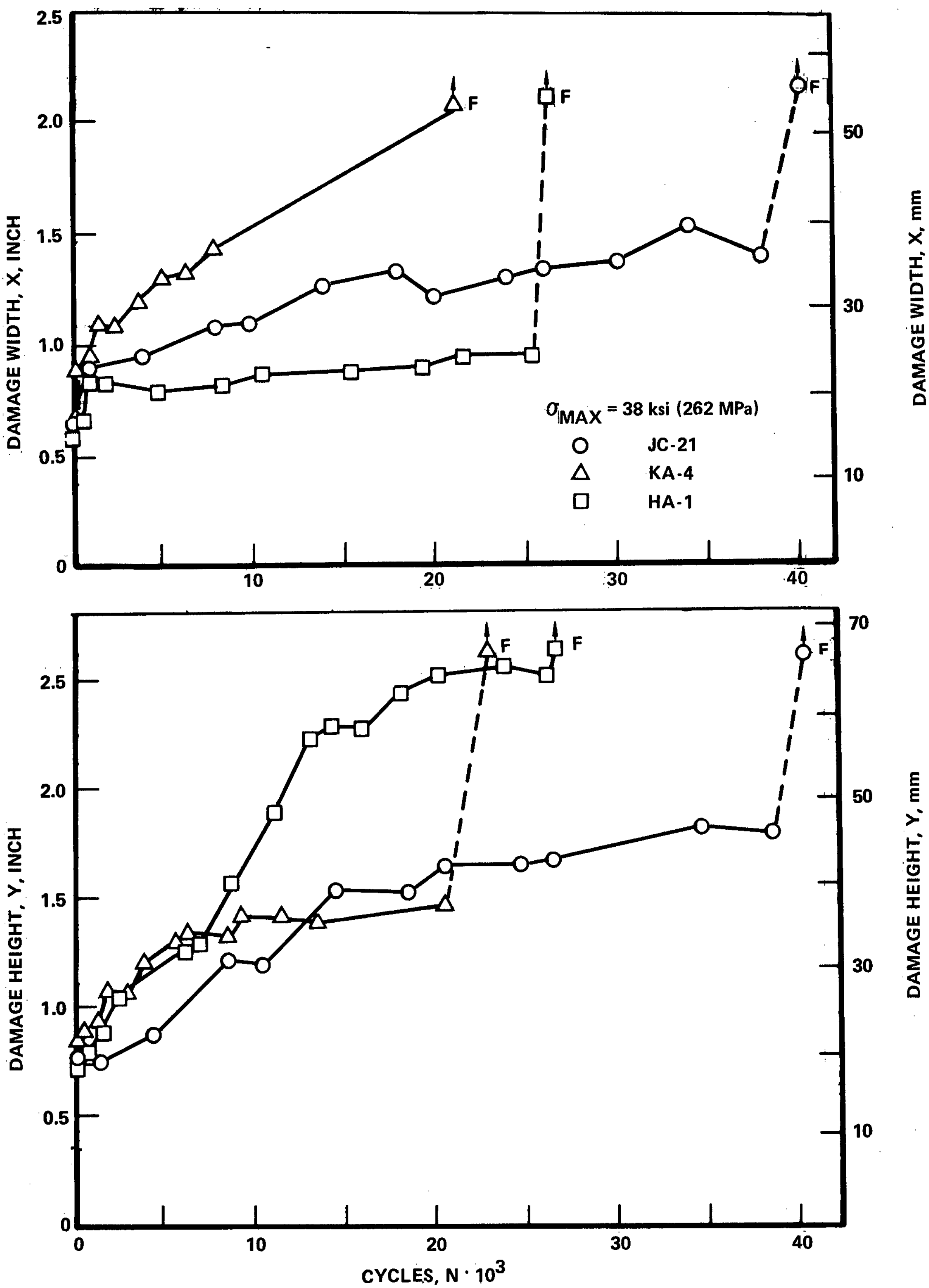

Figure 70. Damage Growth Behavior of Damaged Hole 24-Ply 67% 0° Fiber Specimens, R = -1, σ_{max} = 38 ksi (262 MPa)

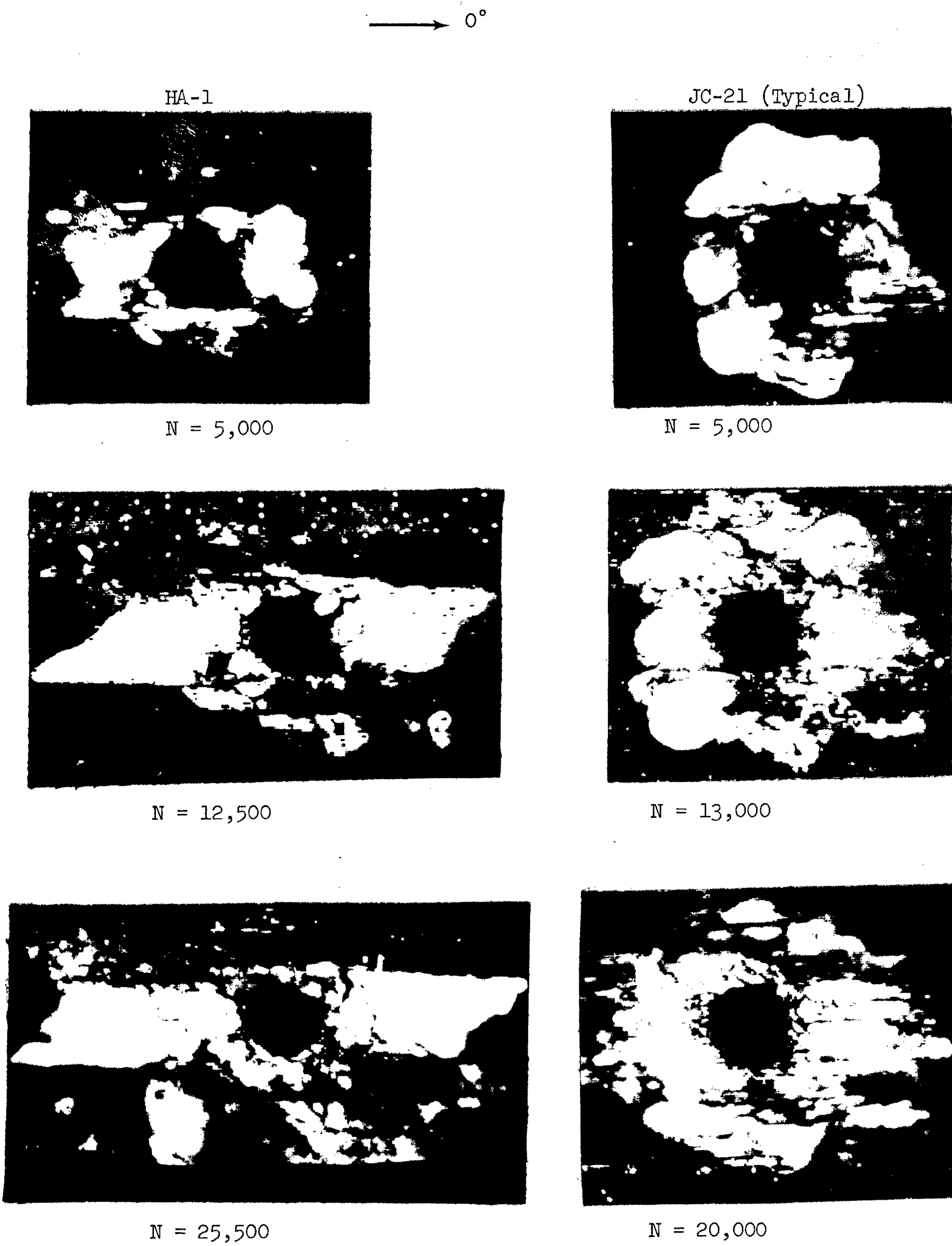

Figure 71. Comparison of the Damage Growth Characteristics of HA-1 with Other Typical Specimens, R = -1, σ_{max} = 38 ksi (262 MPa)

width direction on specimen HA-1, but this damage was very near the surface and not associated with the main damage growth region. If the results are compared on an area basis as shown in Figure 72, the results are somewhat more consistent, the HA-1 area being smaller than for the other two specimens.

At a still lower stress level, the damage in the width direction generally shows a more consistent and significant growth behavior than observed for the damage height direction, as shown in Figure 73. At this lower stress level, the damage width does grow to a size > 1.9 inch (56 mm) where the damage is slowed by the buckling guide. Damage growth in the loading (Y) direction is seen to exhibit a less consistent behavior at this stress level. Trends similar to the width damage growth are shown in Figure 74 for the damage area parameter.

Typical damage propagation sequences are presented in Figures 75 and 76 for maximum stress levels of 34 ksi (234 MPa) and 41 ksi (283 MPa) respectively. It is of interest to note that at 38 ksi (262 MPa) specimen HA-1 showed a damage growth behavior more typical of the lower stress levels while the other two specimens tested at this level (JC-21 and KA-4) showed damage propagation similar to that observed at higher stress levels. Thus it appears that this level provides a transition in the damage growth shape. Representative damage growth results are presented in Appendix C for each test condition. Based on these observations, the damage area parameter, A, appears to be as useful as any other for describing the damage growth in the 24 ply laminate. Damage area growth vs cycles are presented for the balance of the data in Figures 77 through 79

7.5 <u>DAMAGE GROWTH IN 24 PLY LAMINATES WITH AN IMPACT DAMAGE</u>

Initial examination of the impact damage growth data showed very little growth occurring during the first 60-90% of the fatigue life. Damage growth then occurred rapidly in the later portion of the fatigue life. Results using the X, Y, and area parameters at stress levels of 42.75 ksi (295 MPa), 36.8 ksi (254 MPa) and 31.5 ksi (217 MPa) are presented in Figures 80 through 82 respectively. No significant variation of the damage height, Y,

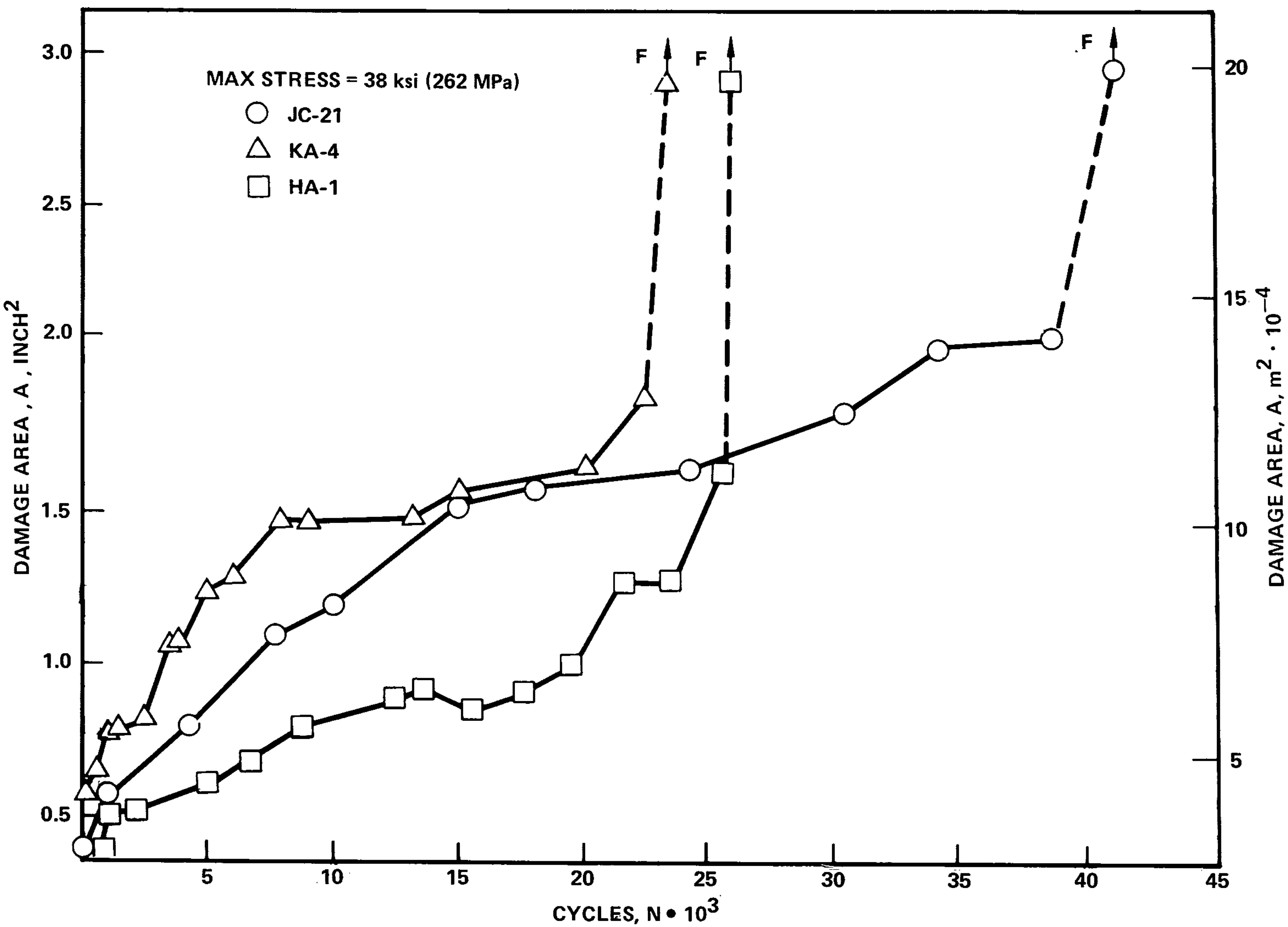

Figure 72. Damage Growth Behavior of Damaged Hole 24-Ply 67% 0° Fiber Specimens, R = -1, σ_{max} = 38 ksi (262 MPa)

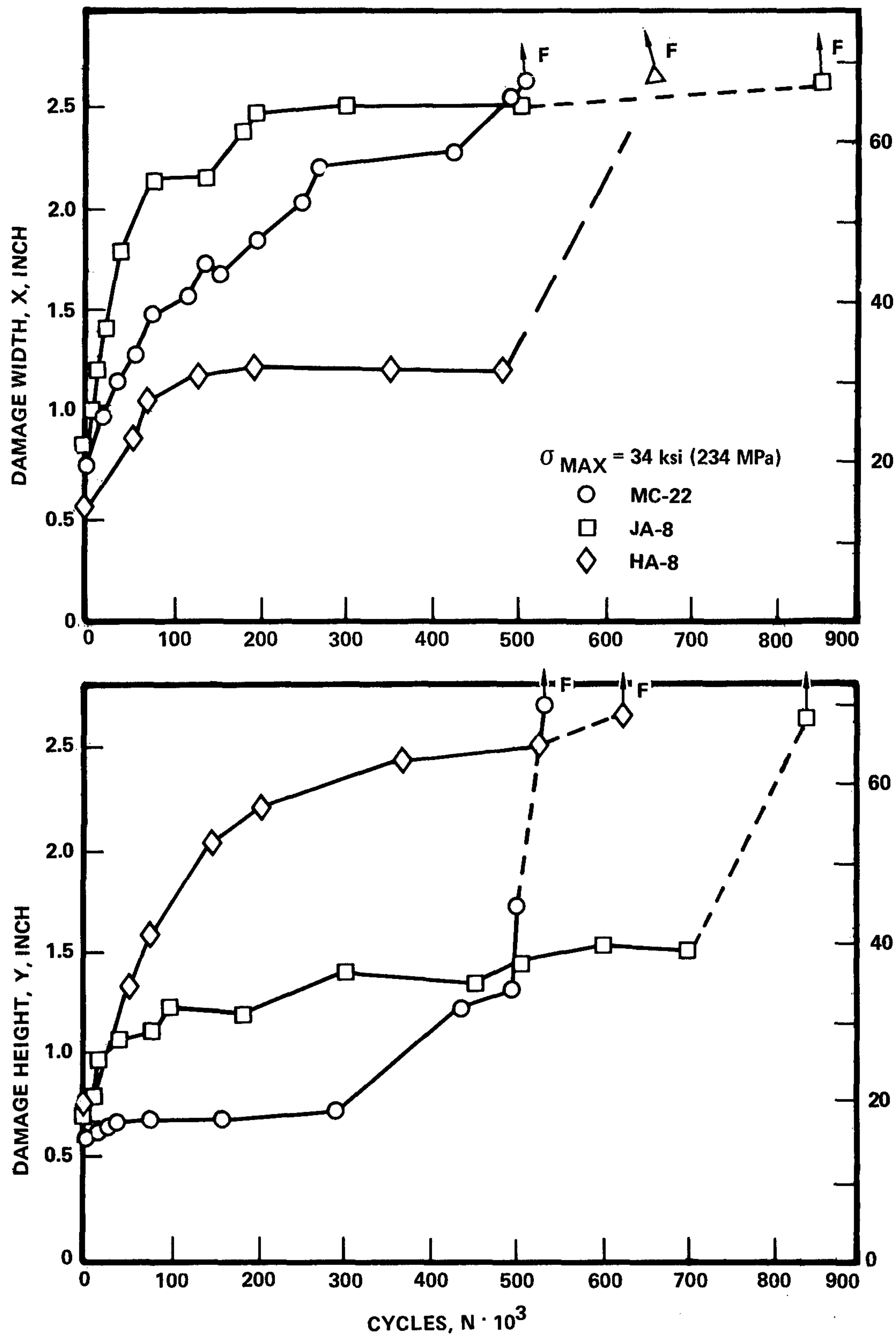

Figure 73. Damage Growth Behavior of Damaged Hole 24-Ply 67% 0° Fiber Specimens, R = -1, σ_{max} = 34 ksi (234 MPa)

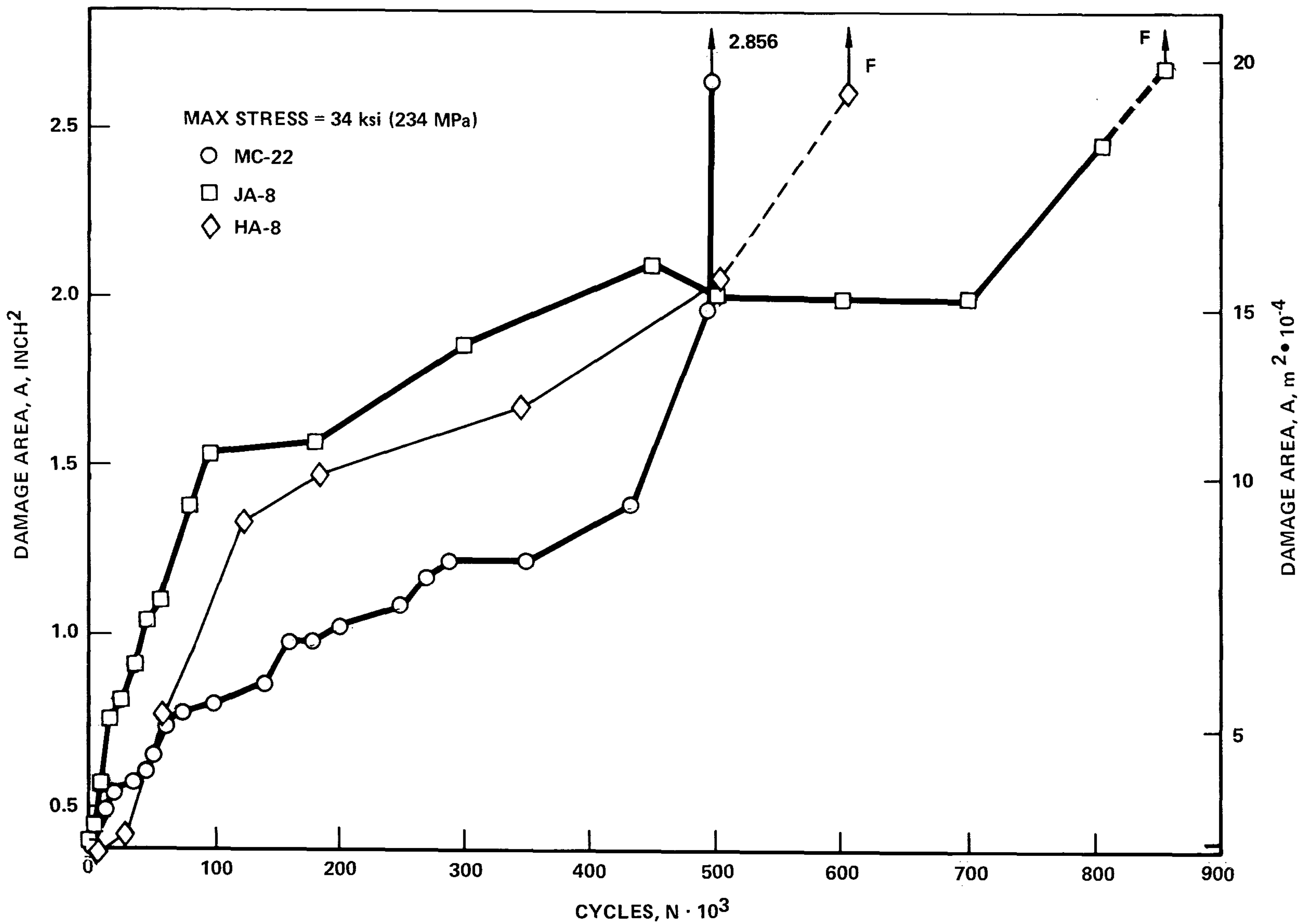

Figure 74. Damage Growth Behavior of Damaged Hole 24-Ply 67% 0° Fiber Specimens, R =-1, σ_{max} = 34 ksi (234 MPa)

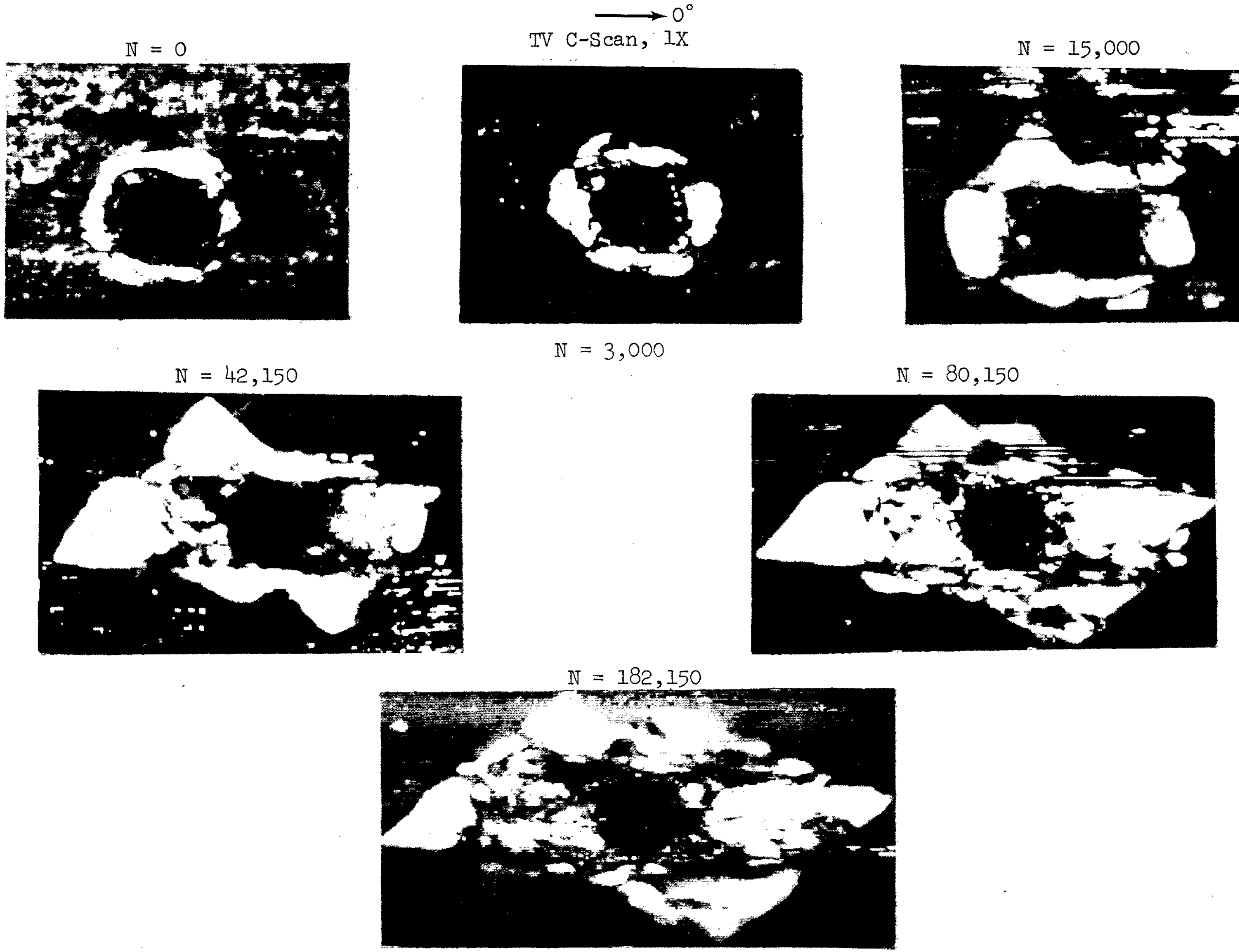

Figure 75a. Typical Damage Growth Characteristics of Damaged Hole 24-Ply 67% 0° Fiber Specimens. Specimen JA-8, σ_{max} = 34 ksi (234 MPa)

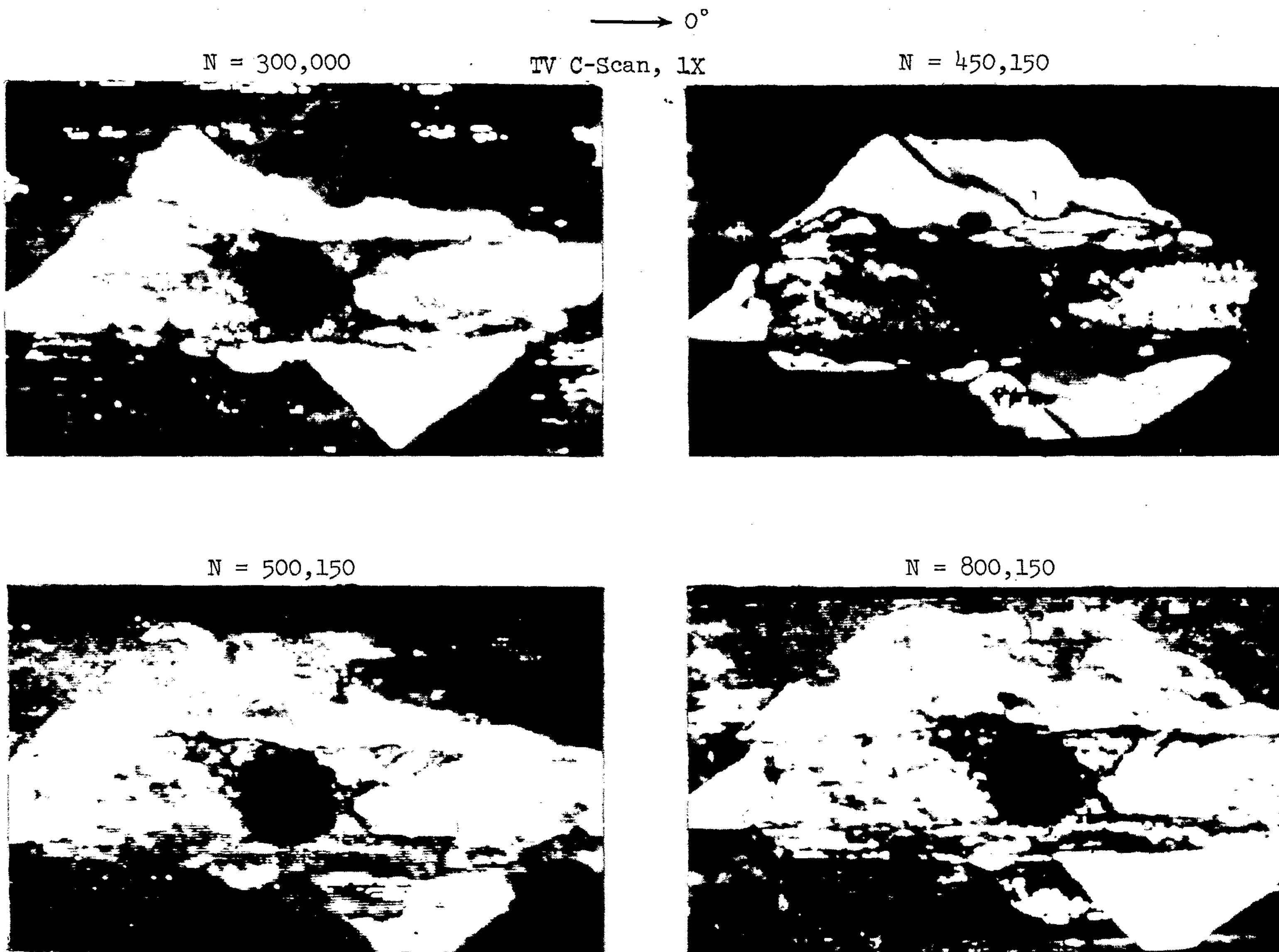

Figure 75b. Typical Damage Growth Characteristics of Damaged Hole 24-Ply 67% 0° Fiber Specimens. Specimen JA-8 σ_{max} = 34 ksi (234 MPa)

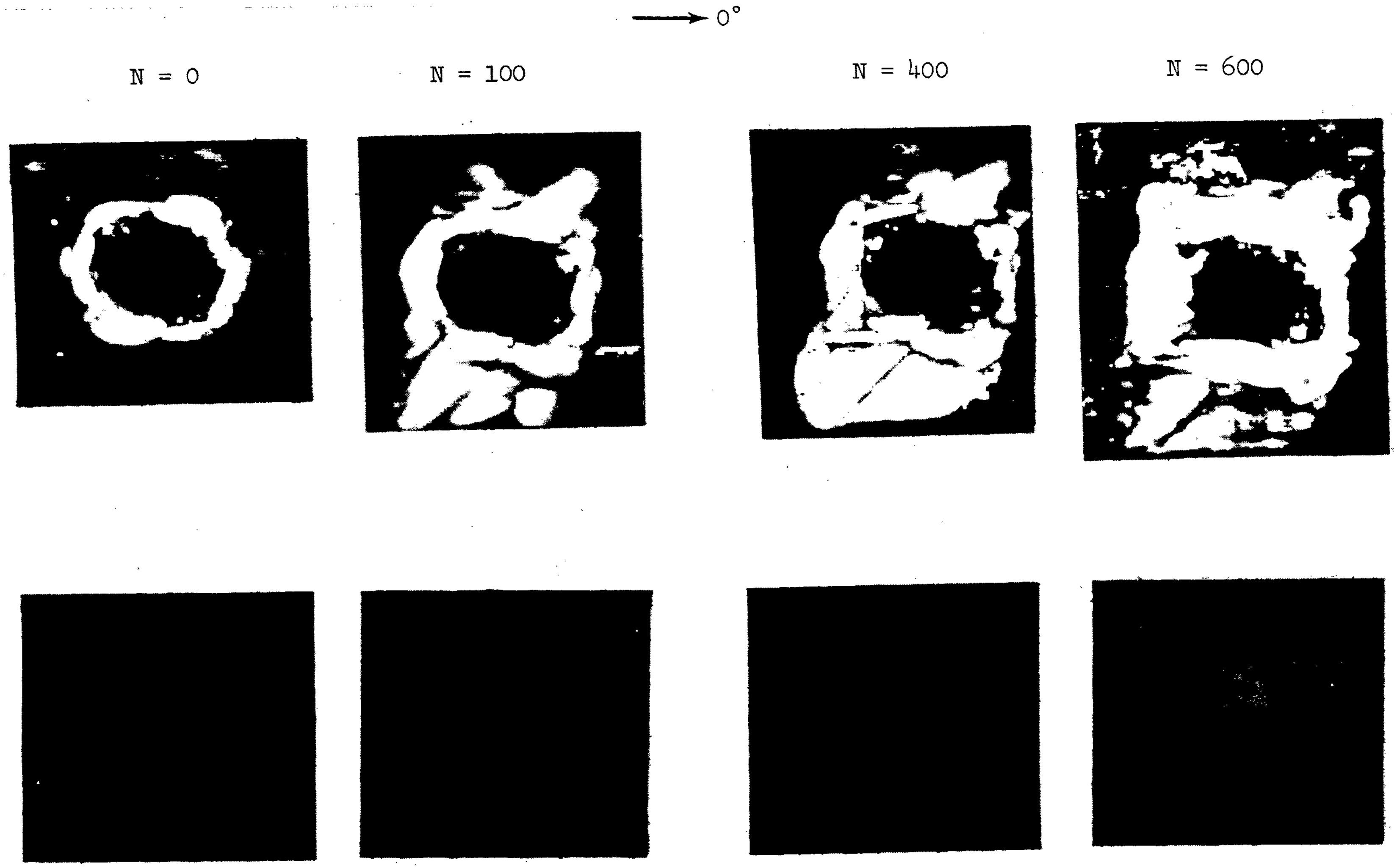

Figure 76a. Typical Damage Growth Characteristics of Damaged Hole 24-Ply 67% 0° Fiber Specimens. Specimen IA-7, σ_{max} = 41 ksi (283 MPa)

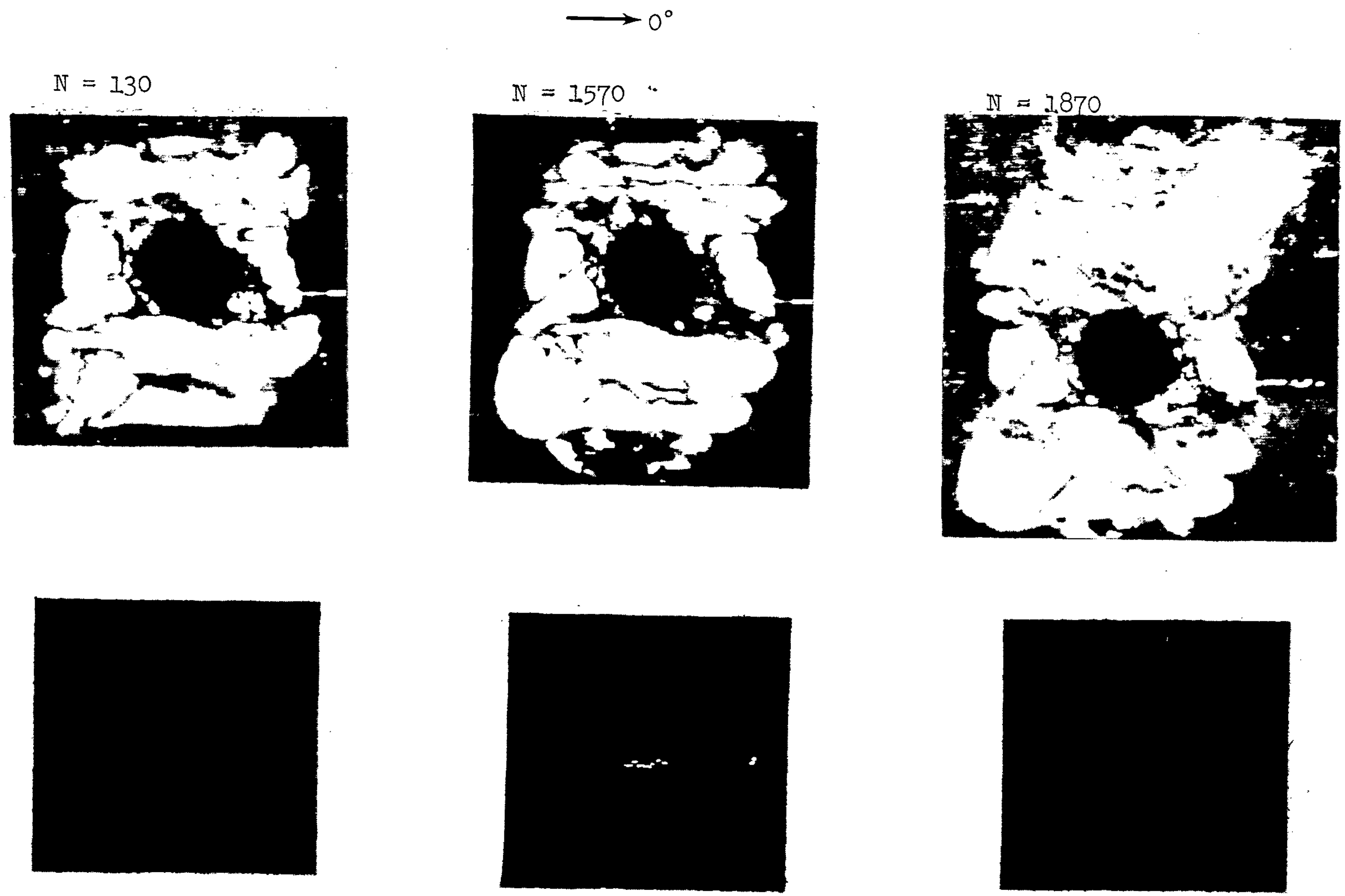

Figure 76b. Typical Damage Growth Characteristics of Damaged Hole 24-Ply 67% 0° Fiber Specimens. Specimen LA-7, σ_{max} = 41 ksi (283 MPa)

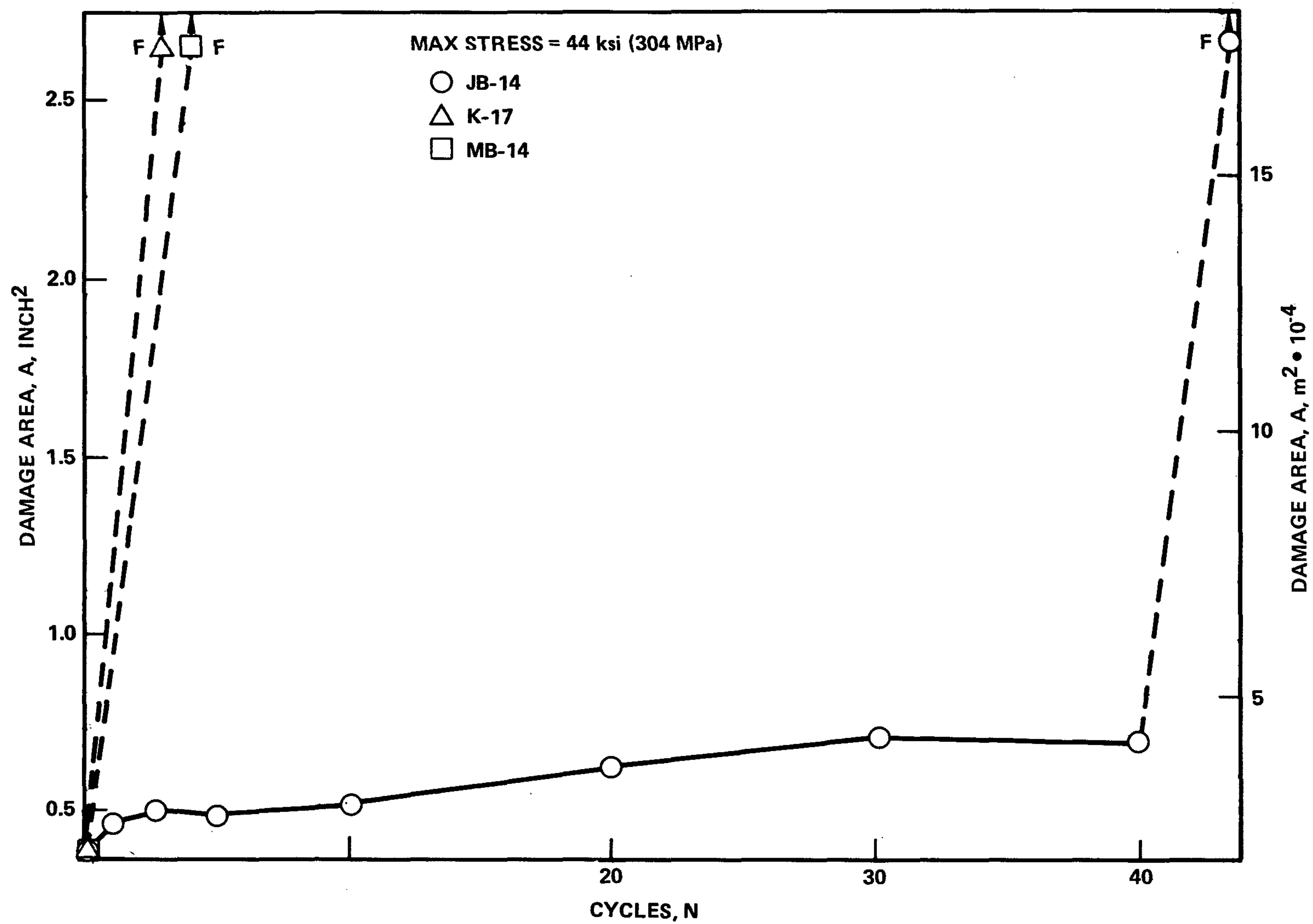

Figure 77. Area Damage Growth Behavior of Damaged Hole 24-Ply 67% 0° Fiber Specimens, R = -1, σ_{max} = 44 ksi (304 MPa)

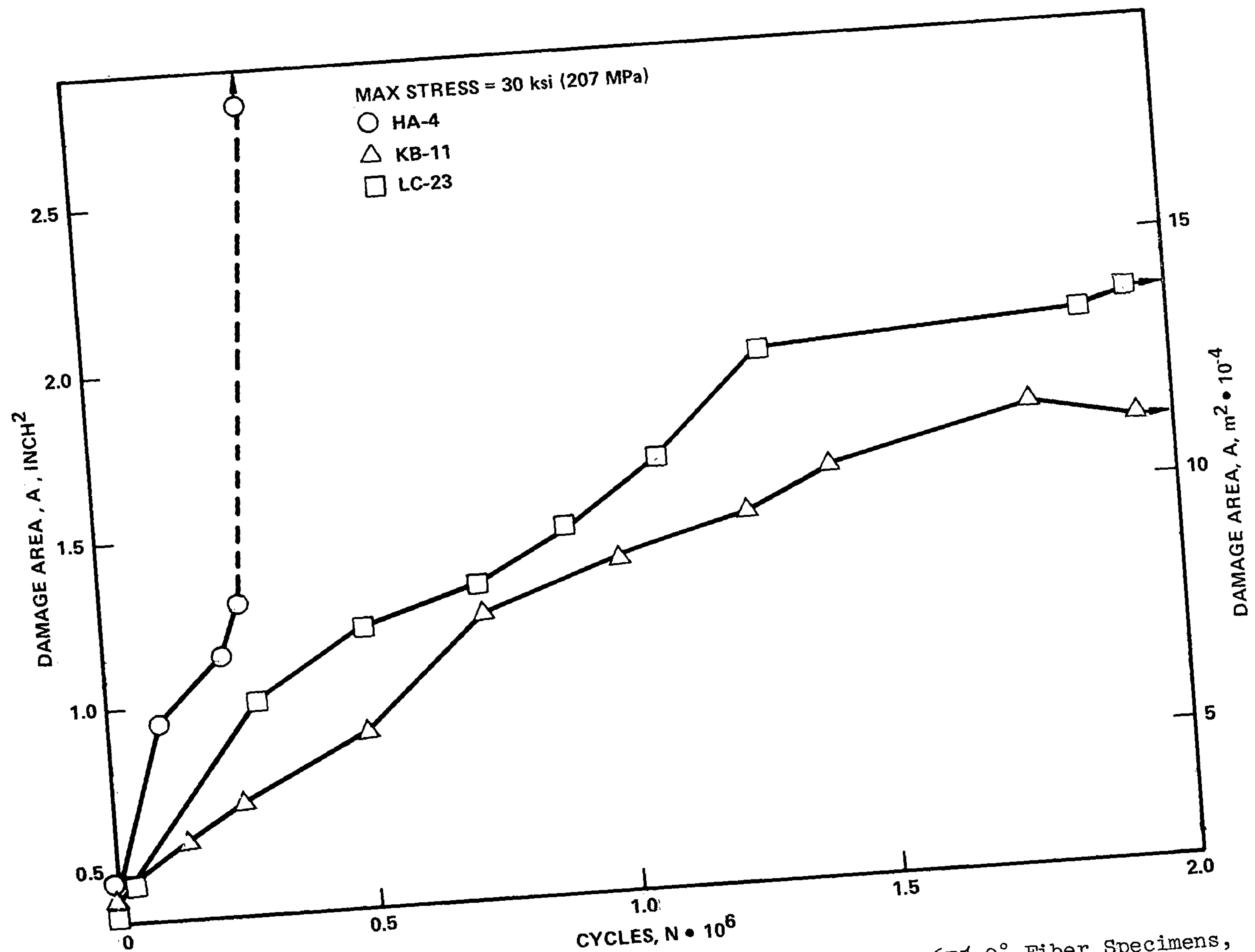

Figure 78. Area Damage Growth Behavior of Damaged Hole 24-Ply 67% 0° Fiber Specimens, $R = -1$, $\sigma_{max} = 30$ ksi (207 MPa)

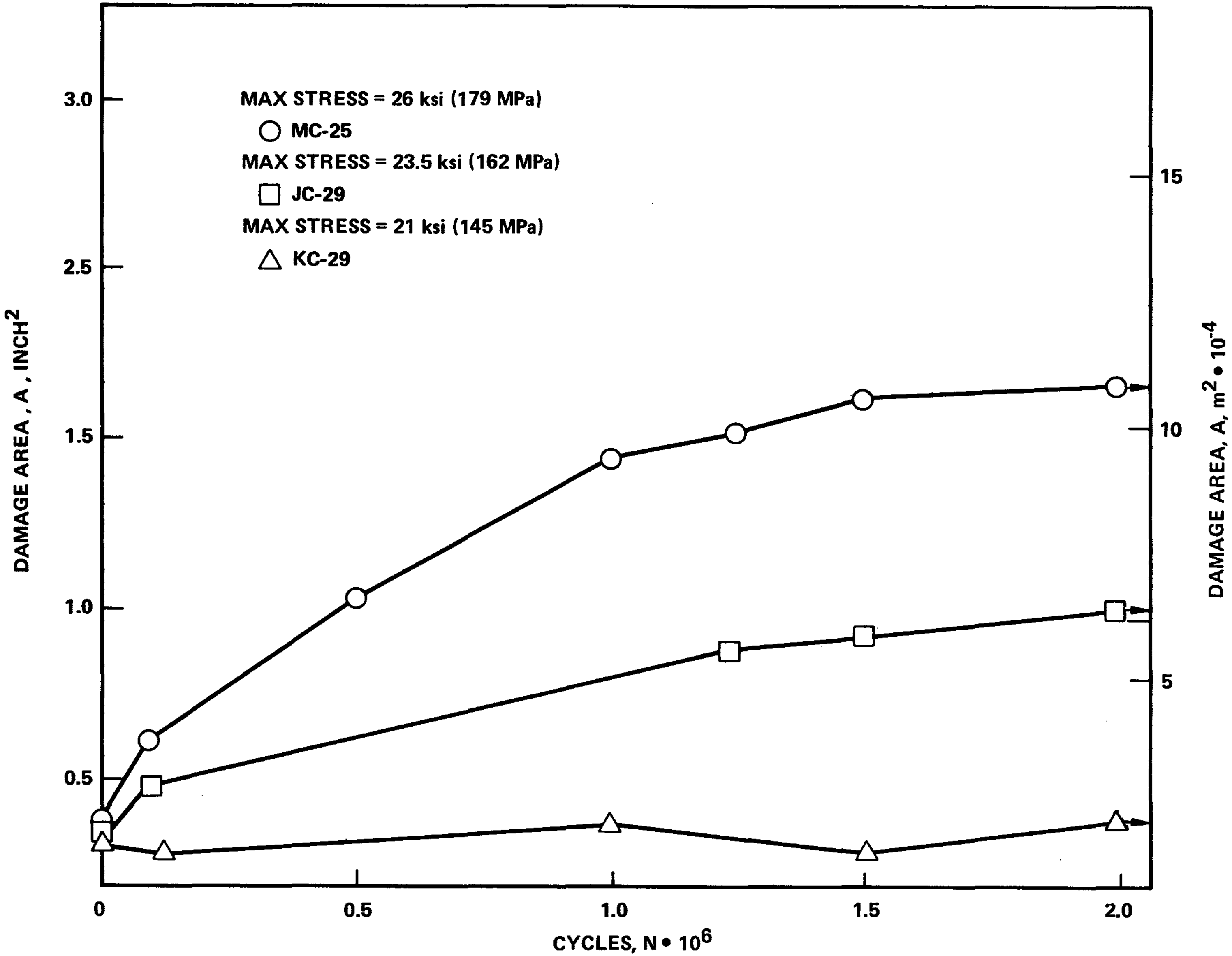

Figure 79. Area Damage Growth Behavior of Damaged Hole 24-Ply 67% 0° Fiber Specimens, $R = -1$, $\sigma_{max} = 26$ ksi (179 MPa), 23.5 ksi (162 MPa) and 21 ksi (145 MPa)

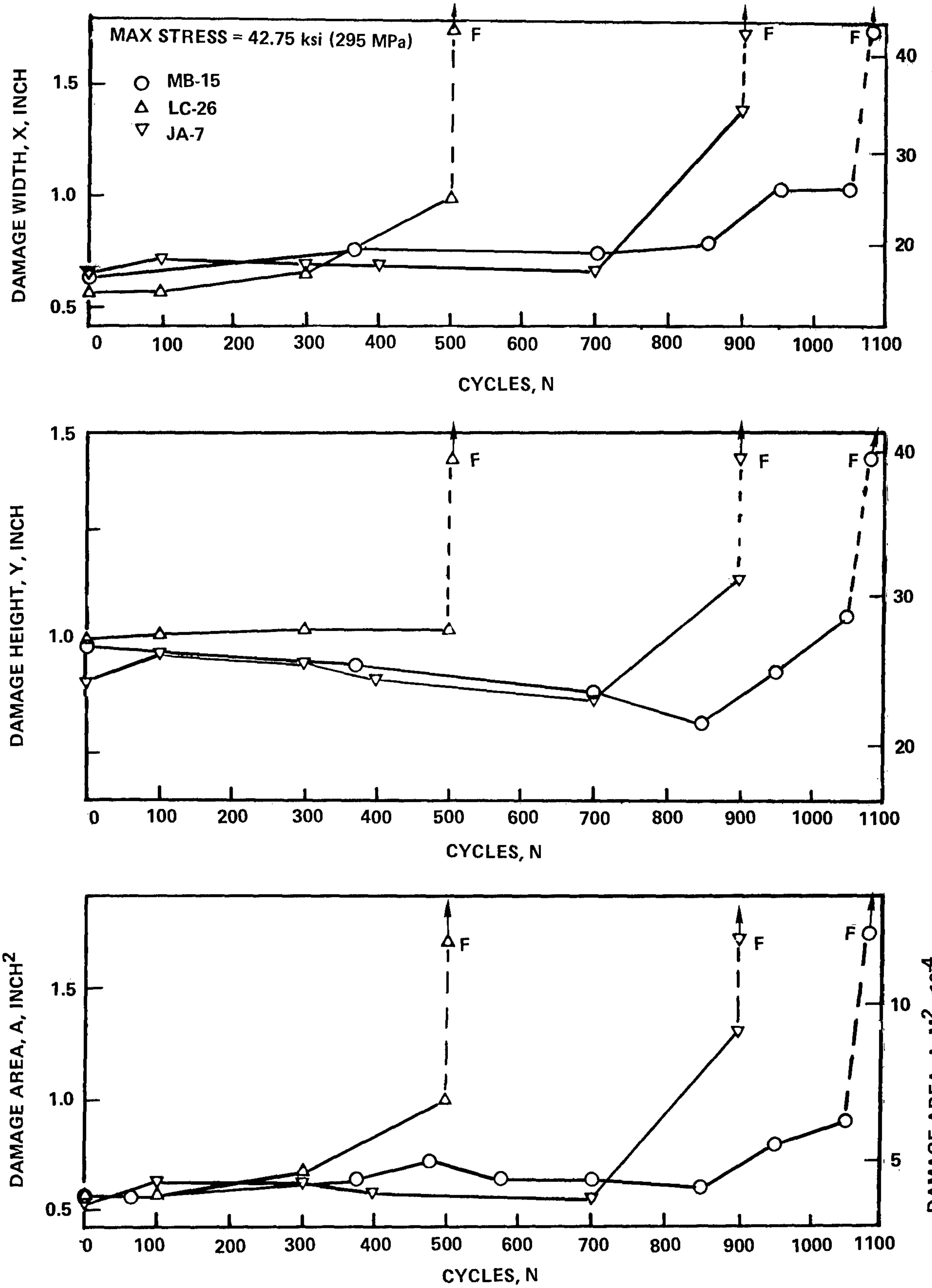

Figure 80. Damage Growth Behavior of Impact Damaged 24-Ply 67% 0° Fiber Specimens, R = -1, σ_{max} = 42.75 ksi (295 MPa)

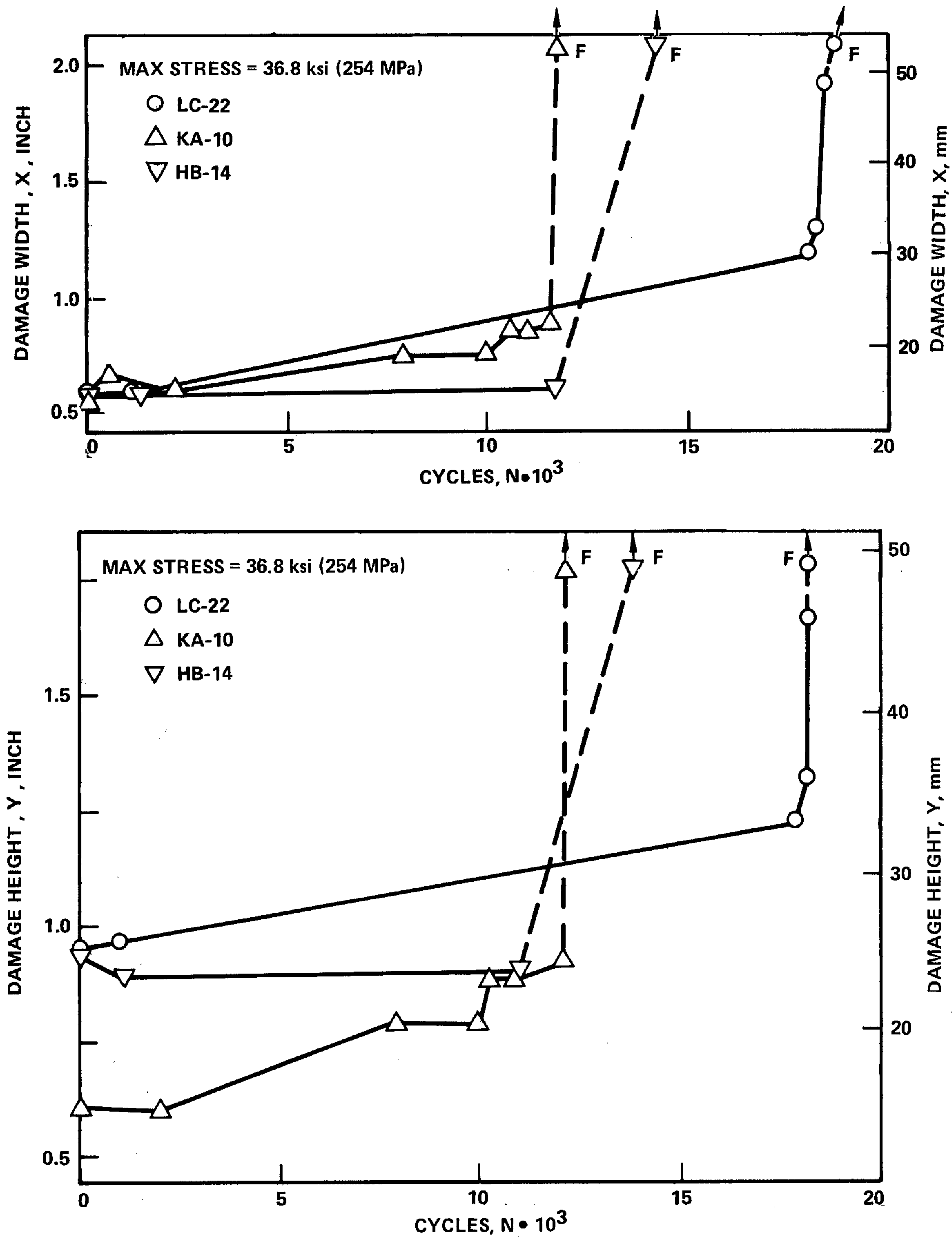

Figure 81a & b. Damage Growth Behavior of Impact Damaged 24-Ply 67% 0° Fiber T300/5208 Laminate Specimen, R = -1 σ_{max} = 36.8 ksi (254 MPa)

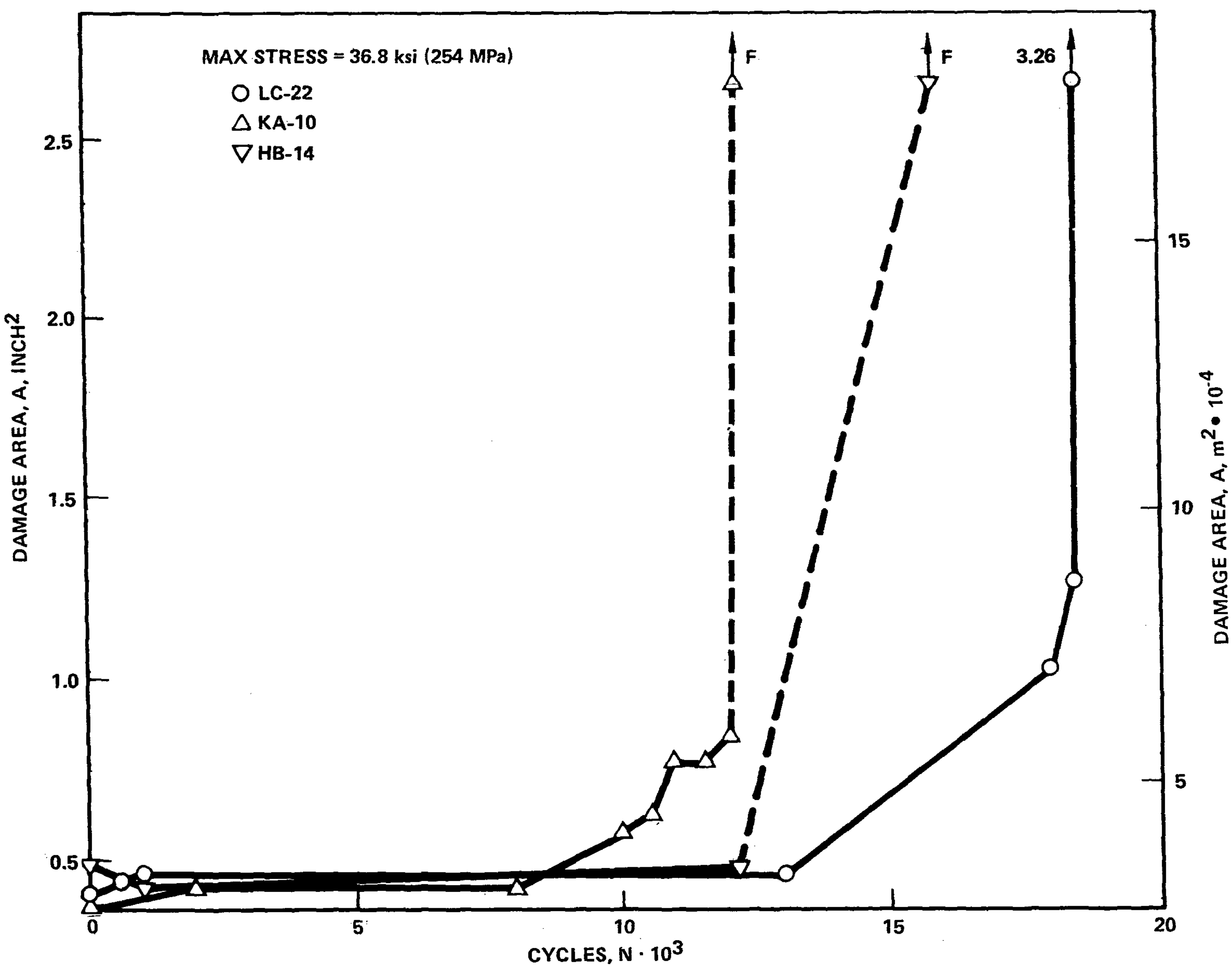

Figure 81c. Damage Growth Behavior of Impact Damaged 24-Ply 67% 0° Fiber Specimens, R = -1 σ_{max} = 36.8 ksi (254 MPa)

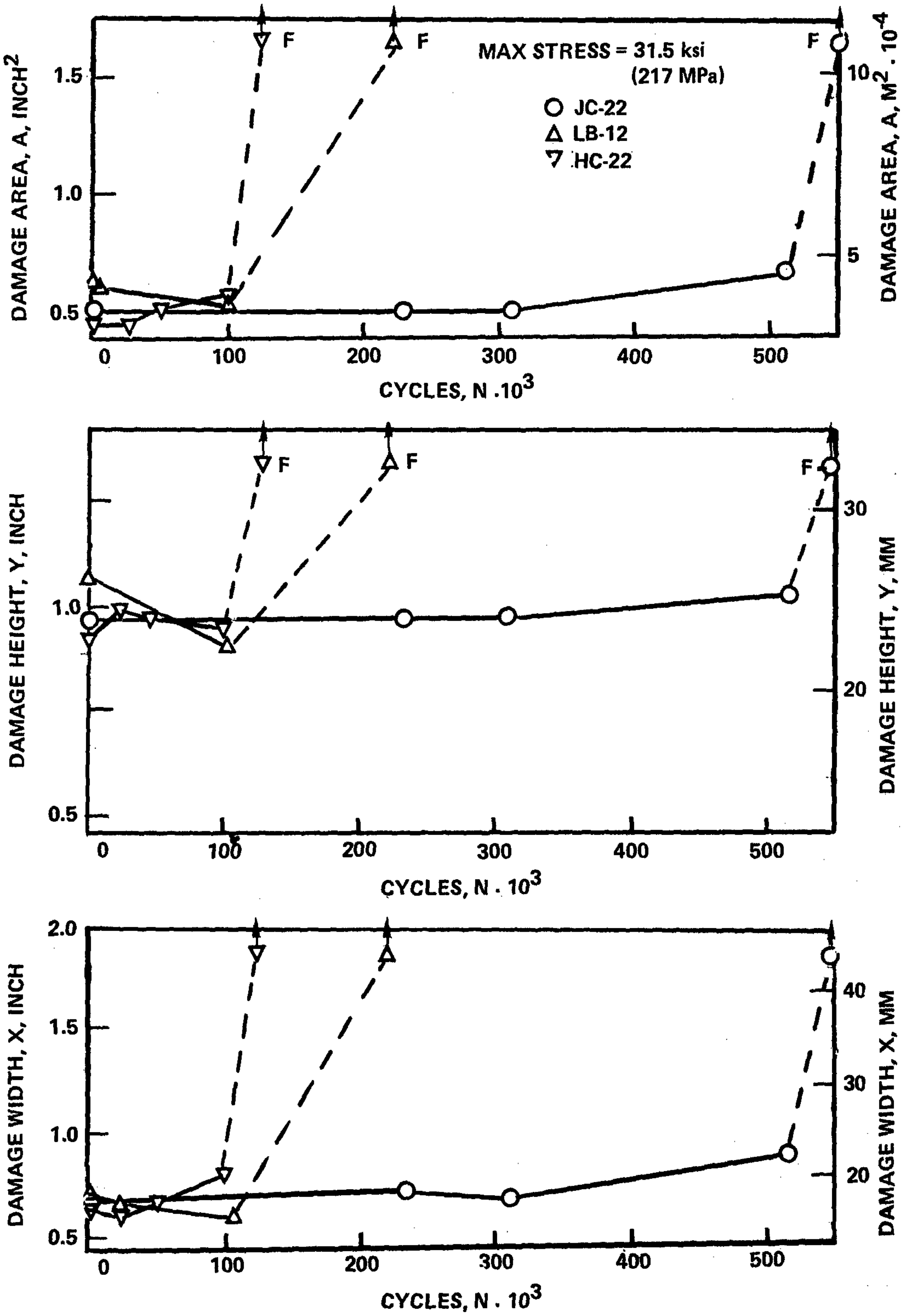

Figure 82. Damage Growth Behavior of Impact Damaged 67% 0° Fiber Specimens, R = -1, σ_{max} = 31.5 ksi (217 MPa)

appears on a consistent basis. The damage width, X, and damage area follow the same general trends. Typical damage growth results shown in Figures 83 through 85 show that the damage area would appear to be the more meaningful parameter. The balance of the specimen data is presented in Figure 86 in terms of the damage area. Representative damage growth data for each test condition are presented in Appendix C.

7.6 DAMAGE GROWTH IN THE 32 PLY LAMINATE WITH A DAMAGED HOLE

Results of the 32 ply quasi-isotropic laminate containing a damaged hole were plotted to compare the growth characteristics in terms of the three parameters, X, Y, and A vs. cycles to failure for the three replicate specimens at a given stress level. For all maximum stress levels the Y parameter was found to be constant or very slowly increasing, reflecting the general observation that for this laminate the overall height of the damage is essentially unchanging during fatigue, the damage primarily extending across the specimen width rather than in the direction of loading. Typical Y vs cycles data are shown in Figure 87.

As would be expected given that the overall damage height changes relatively little, the damage width and damage area characteristics parallel each other quite closely. Typical results, shown in Figures 88 through 89, show that the damage area parameter, A, and the damage width, X, exhibit similar trends, the main difference being that the area, A, continues to show a more definite slow growth region in the later stages of fatigue life than does the damage width. This is due to the added influence of the slowly increasing damage height which is reflected in the total damage area.

Careful examination of the damage width data for the high stress level tests (σ_{max} = 30 and 26 ksi) (207 and 179 MPa) shows the abrupt slowing in the damage growth rate to occur at a damage width of ~ 2.1 to 2.5 inch (0.05 to 0.06 m). This corresponds to a size where-upon the support fixture clamping at the edge of the specimen would provide not only added longitudinal support but also a thickness direction clamping effect. For this reason the slowing of the damage growth rate is not believed to be real, but rather a function of

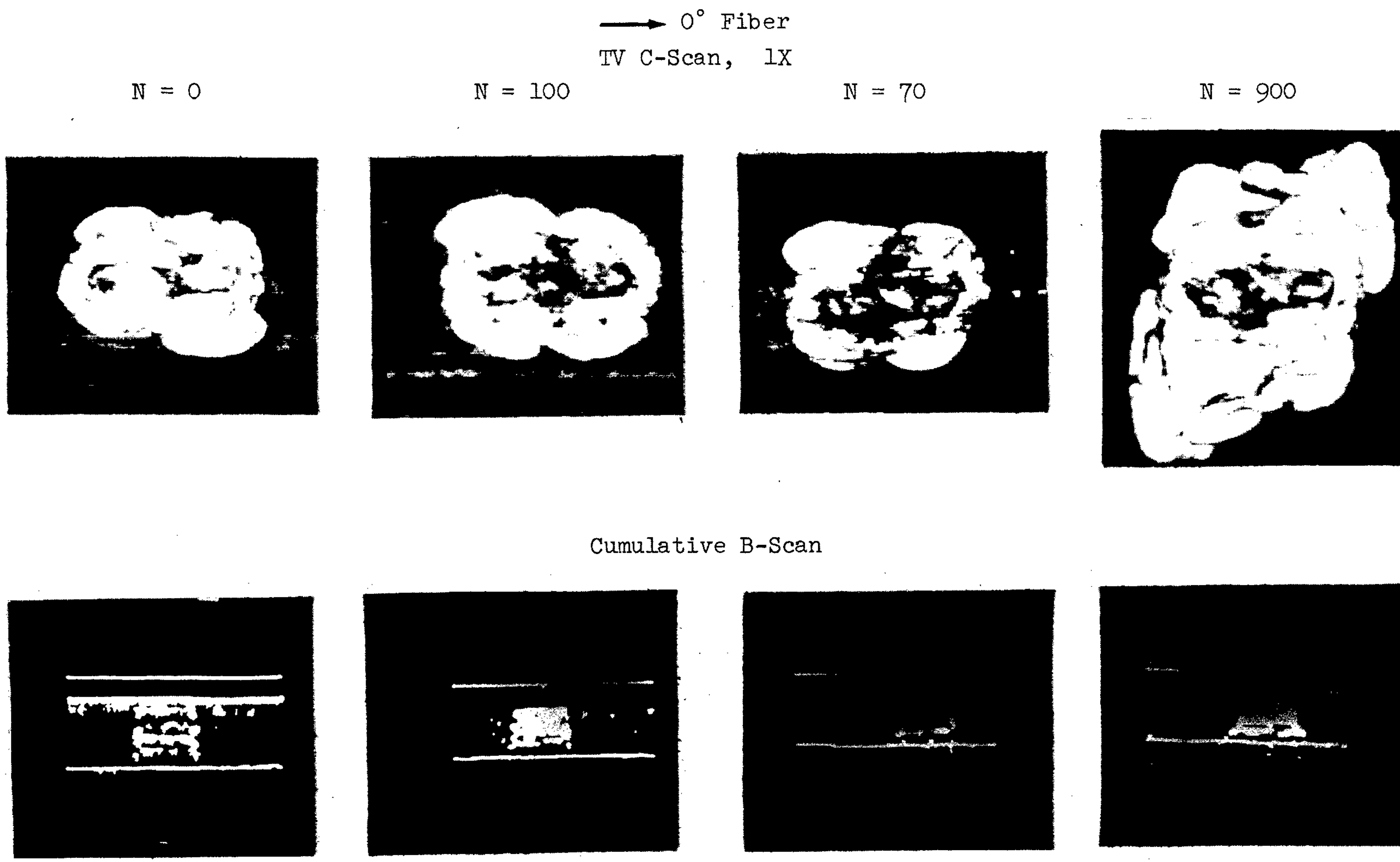

Figure 83. Damage Growth Characteristics of Impact Damaged Specimen JA-7, 24-Ply 67% 0° Fiber Laminate, $R = -1$, $\sigma_{max} = 42.75$ ksi (295 MPa)

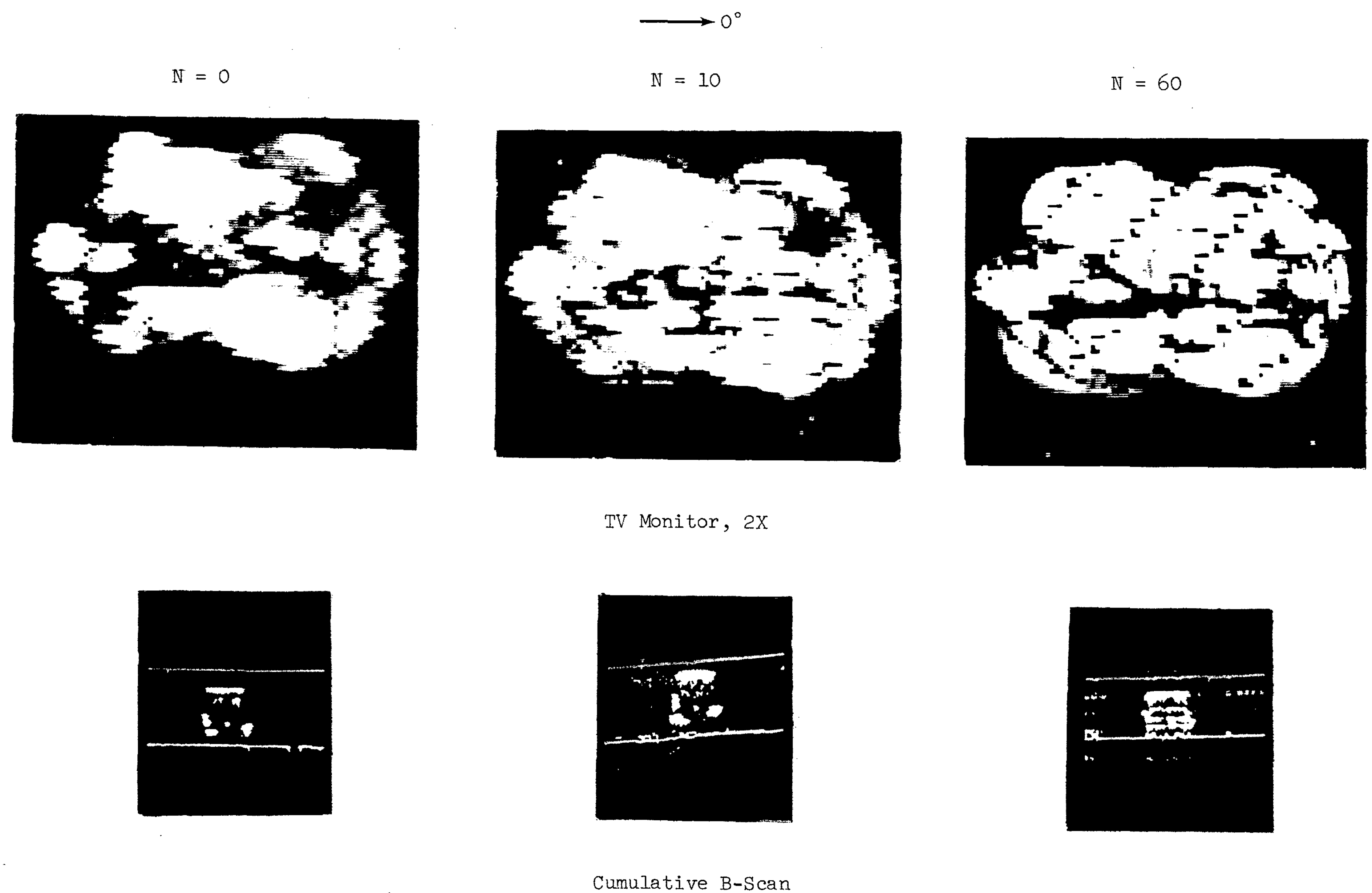

Figure 84a. Damage Growth Characteristics of Impact Damaged Specimen LC-22, 24-Ply 67% 0° Fiber Laminate, R = -1

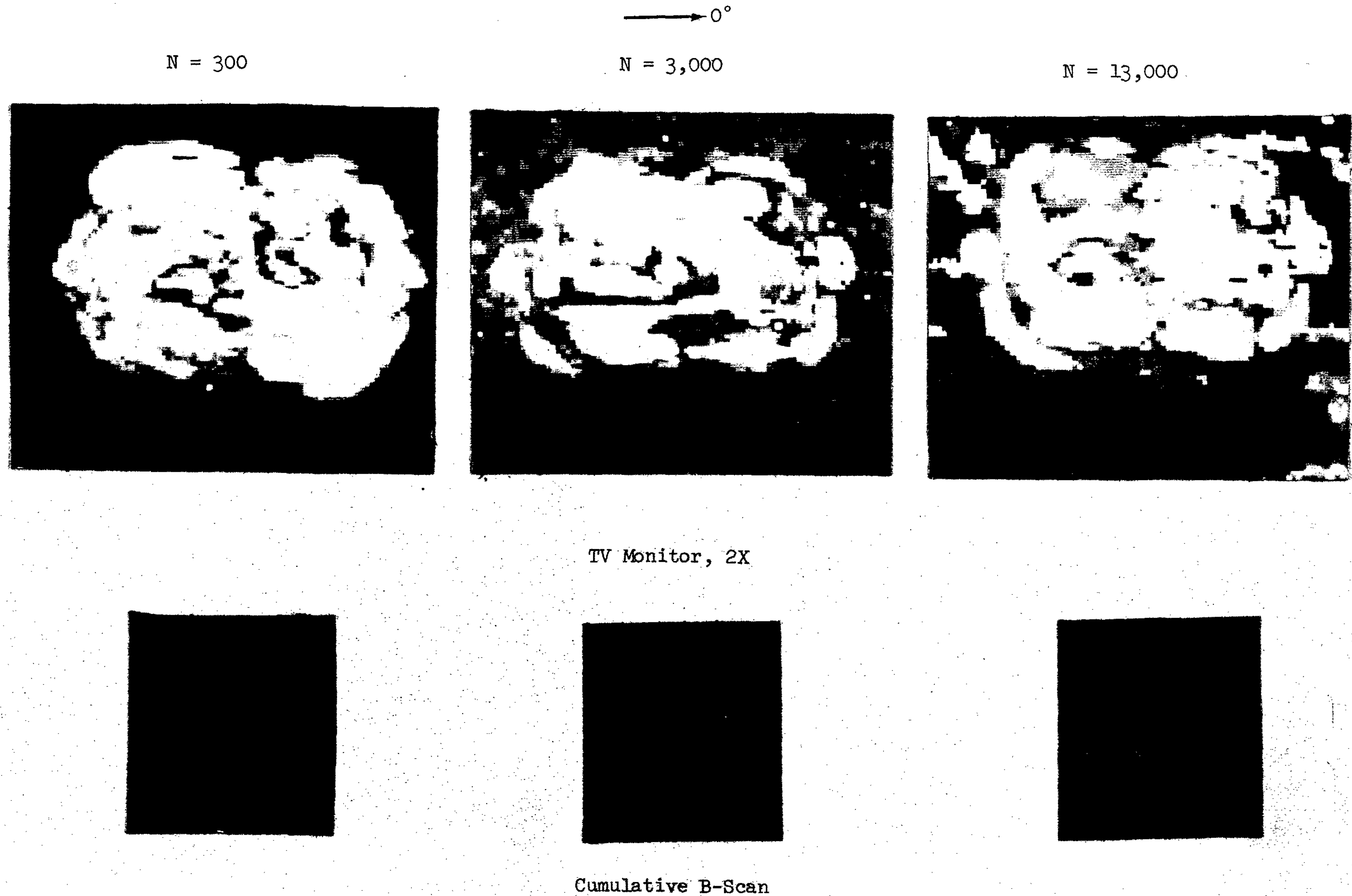

Figure 84b. Damage Growth Characteristics of Impact Damaged Specimen LC-22
24-Ply 67% 0° Fiber Laminate, R = -1

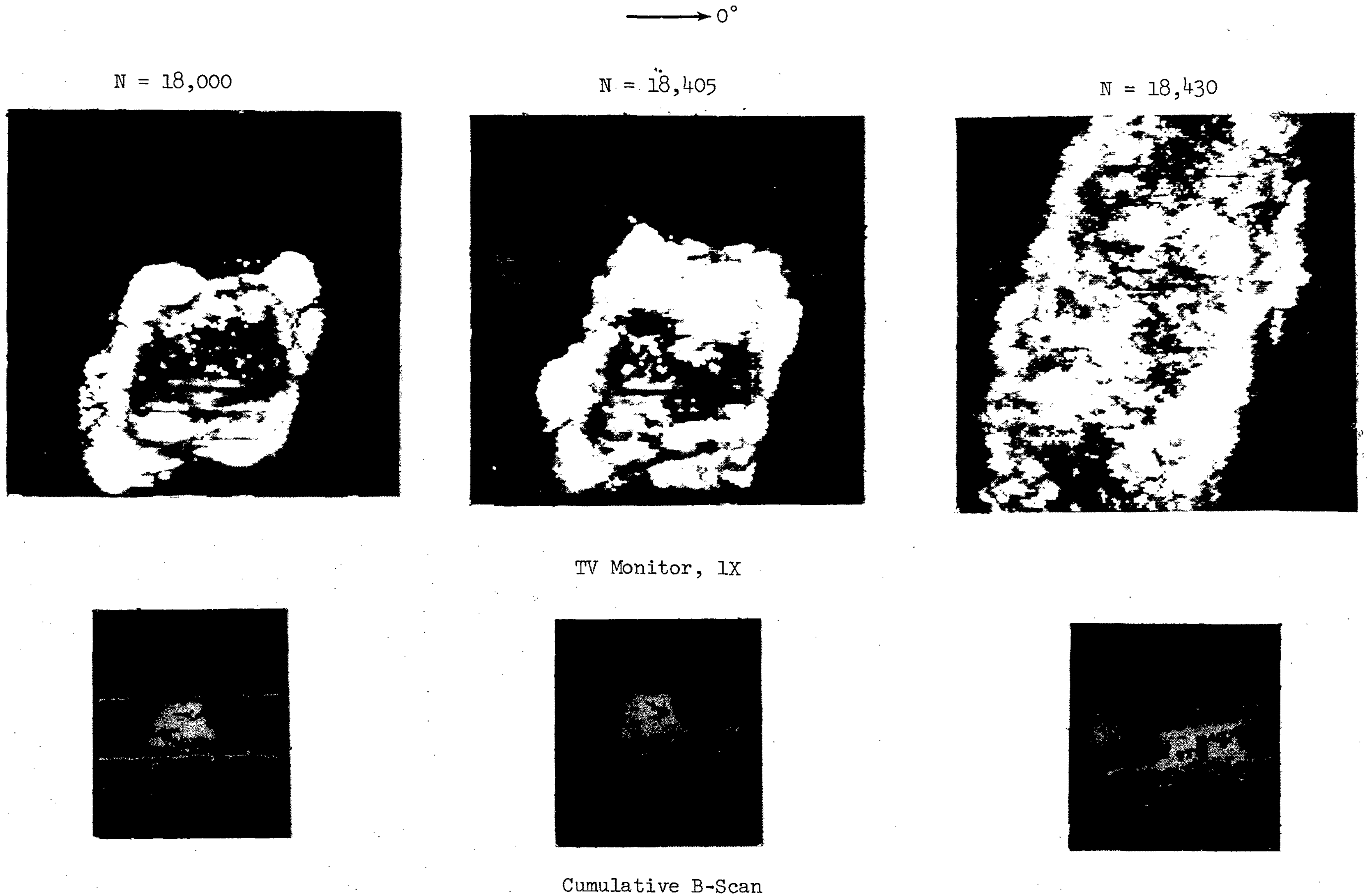

Figure 84c. Damage Growth Characteristics of Impact Damaged Specimen LC-22
24-Ply 67% 0° Fiber Laminate, R = -1

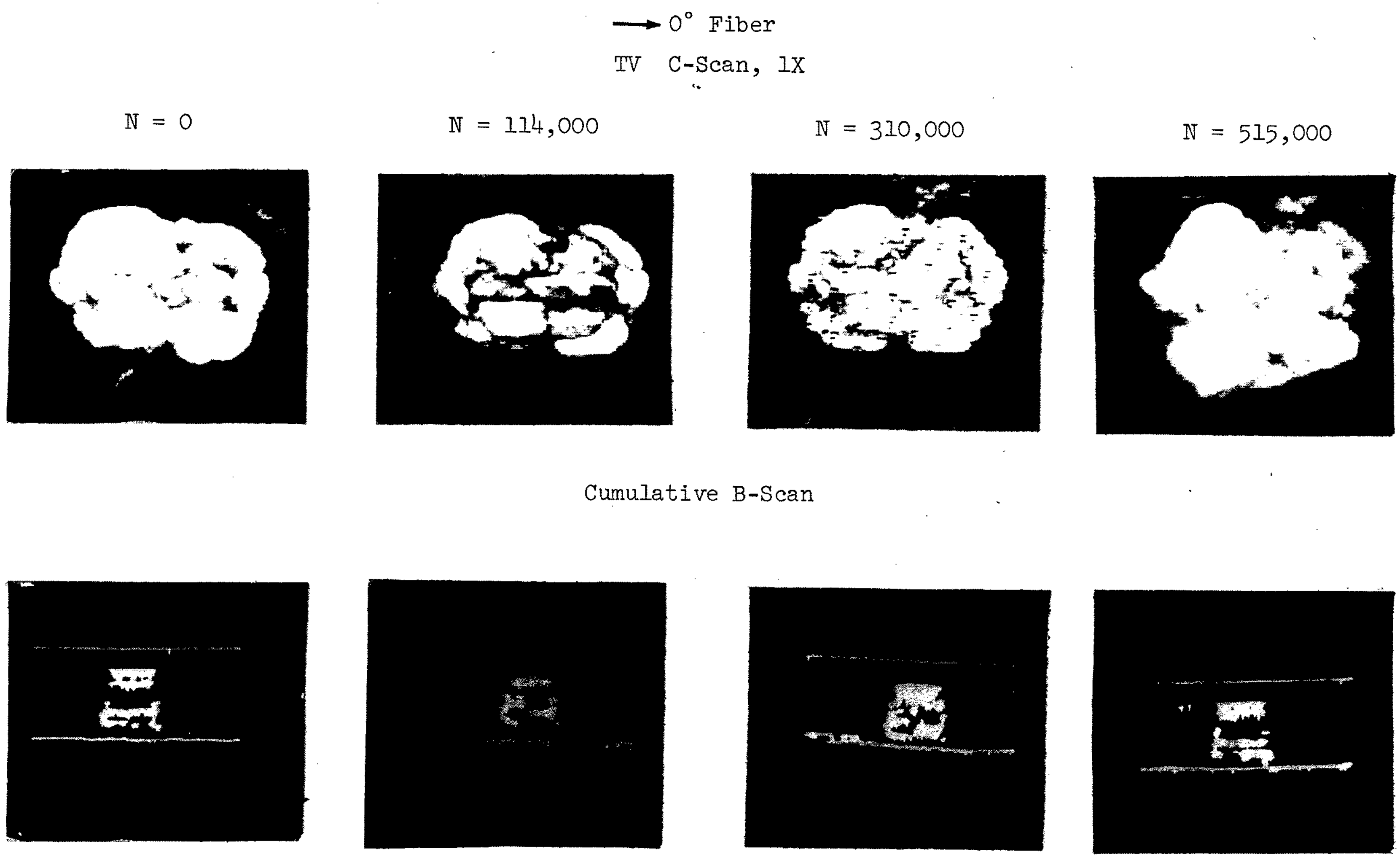

Figure 85. Damage Growth Characteristics of Impact Damaged Specimen JC-22, 24-Ply 67% 0° Fiber Laminate, R = -1, σ_{max} = 31.5 ksi

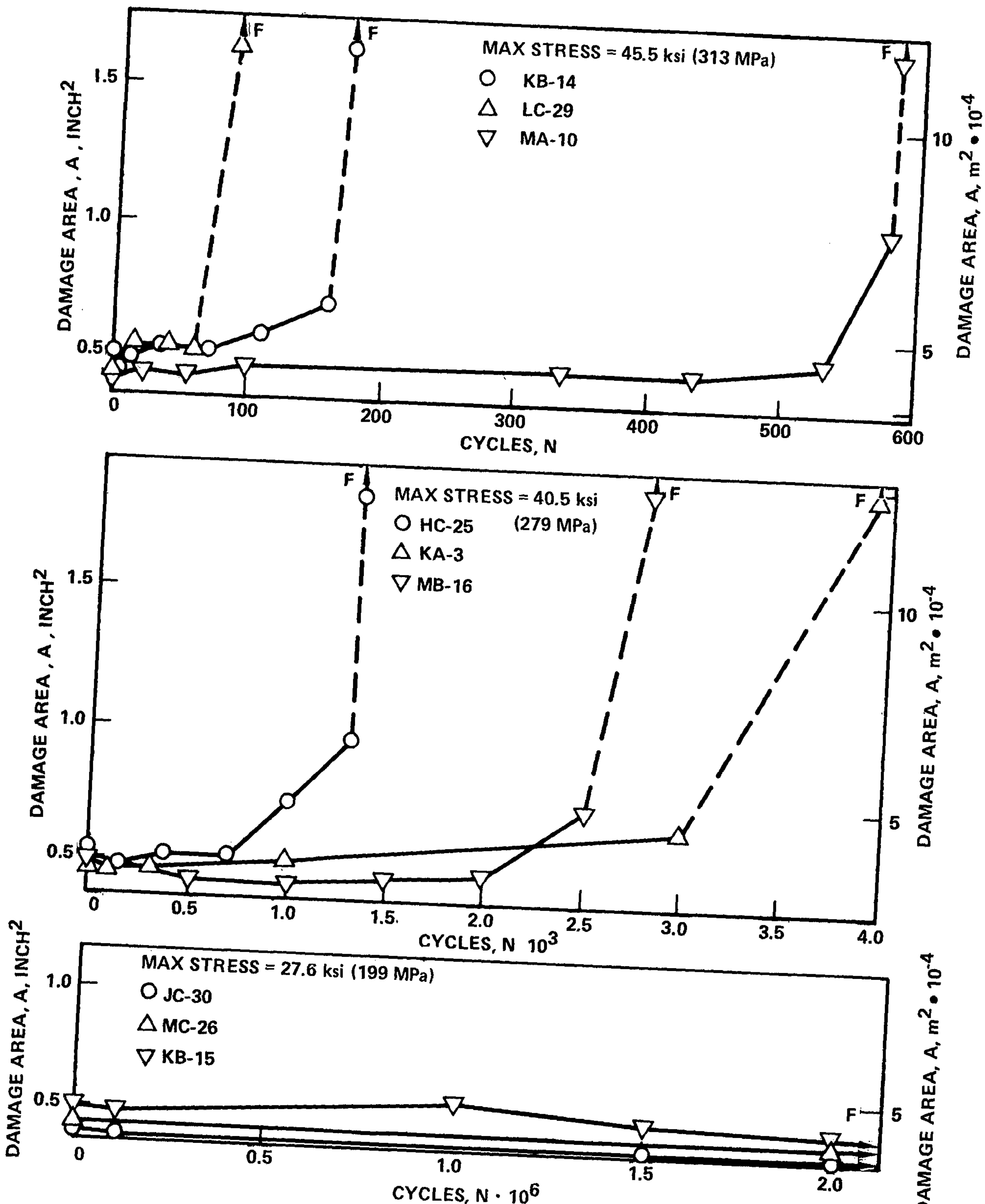

Figure 86. Damage Growth Characteristics of Impact Damaged 24-Ply Laminates, R = -1, σ_{max} = 45.5 ksi (313 MPa), 40.5 ksi (279 MPa) and 27.6 ksi (199 MPa).

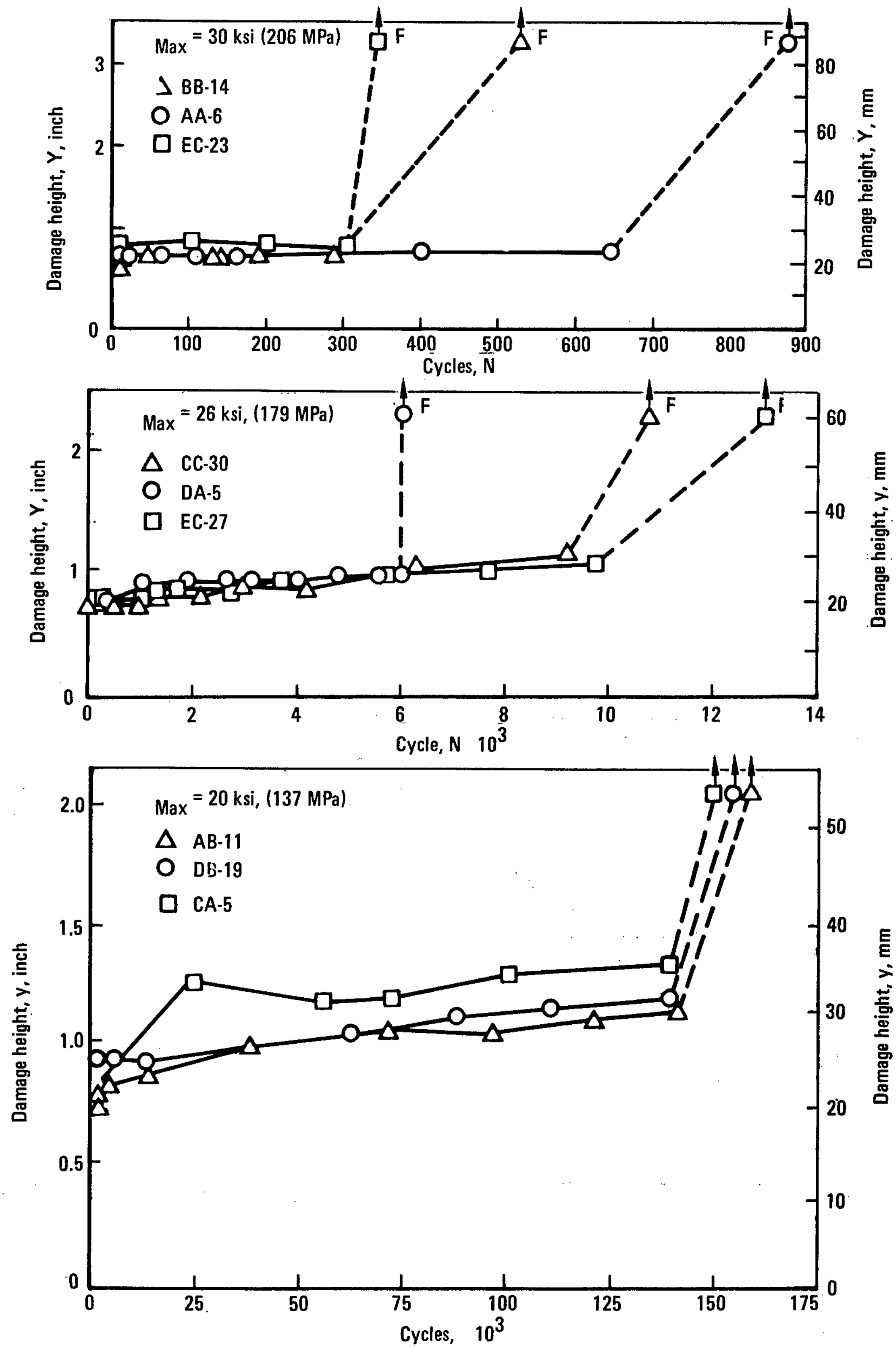

Figure 87. Typical Change in Maximum Damage Height, Y, vs Fatigue Cycles for Damaged Hole 32-Ply Quasi-Isotropic Laminates, R = -1

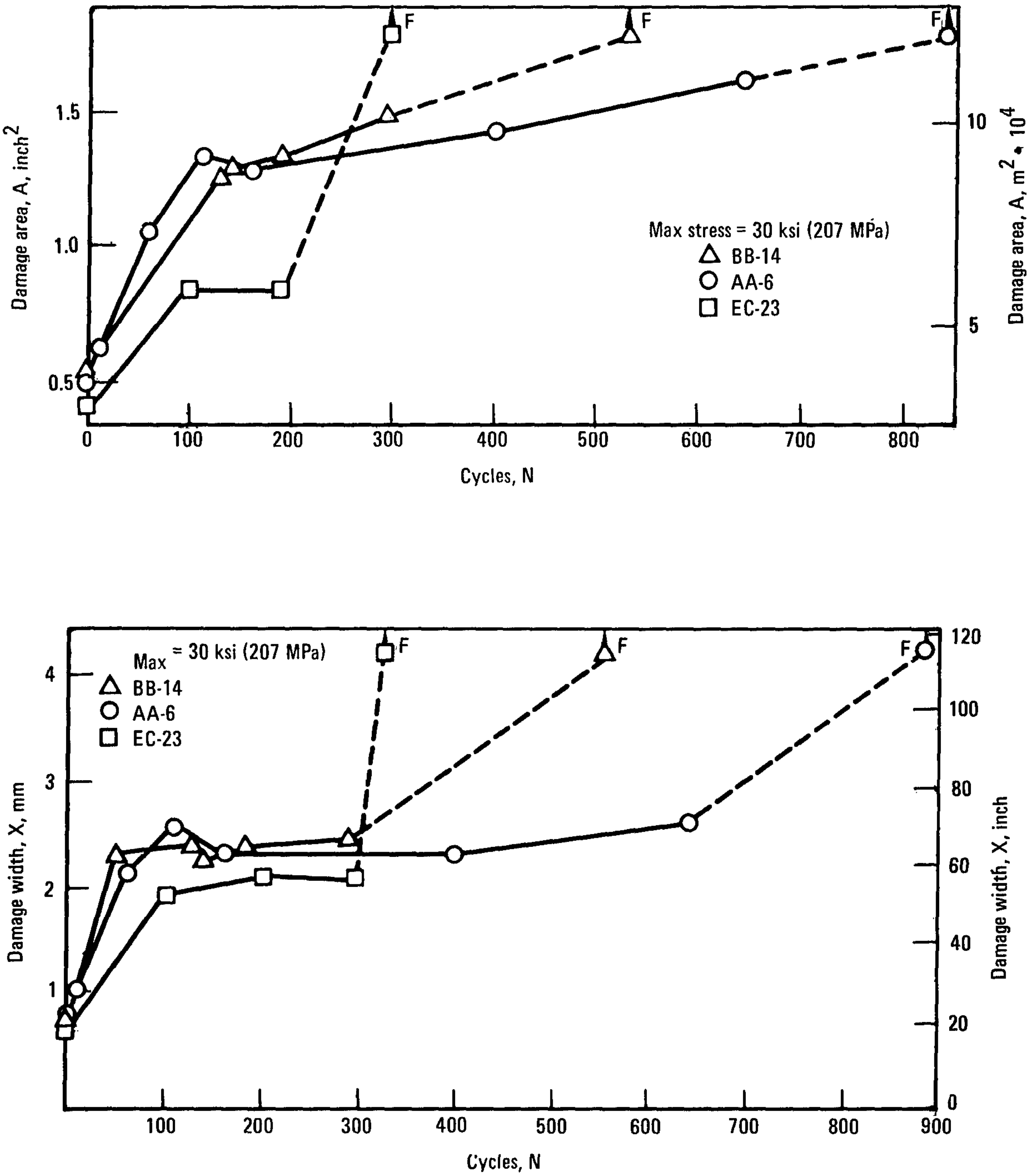

Figure 88. Comparison of Change in Damage Area and Damage Width for Damaged Hole 32-Ply Quasi-Isotropic Specimens, R =-1, σ_{max} = 30 ksi (207 MPa)

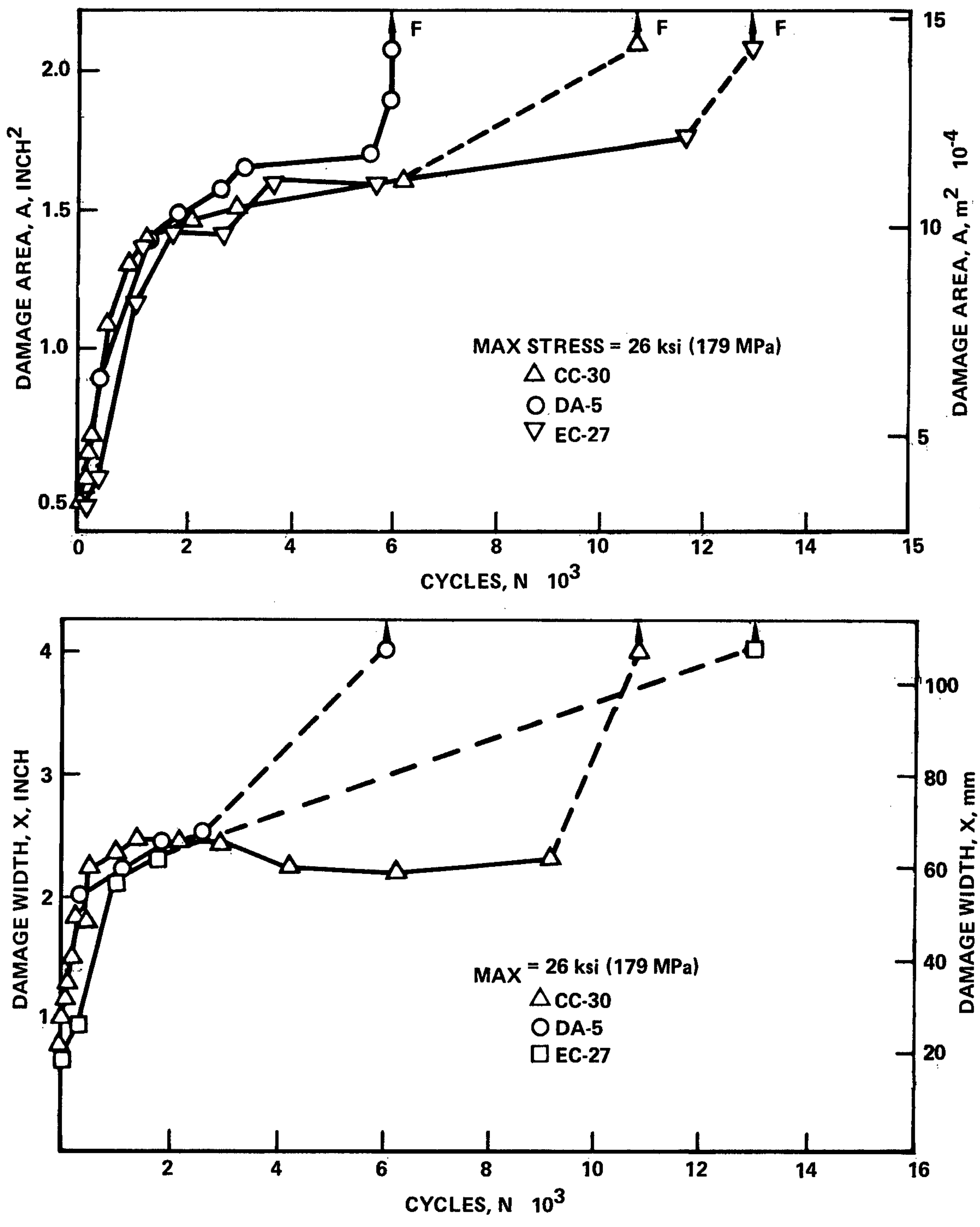

Figure 89. Comparison of Change in Damage Area and Damage Width for Damaged Hole 32-Ply Quasi-Isotropic Specimens, R = -1, σ_{max} =26 ksi (179 MPa)

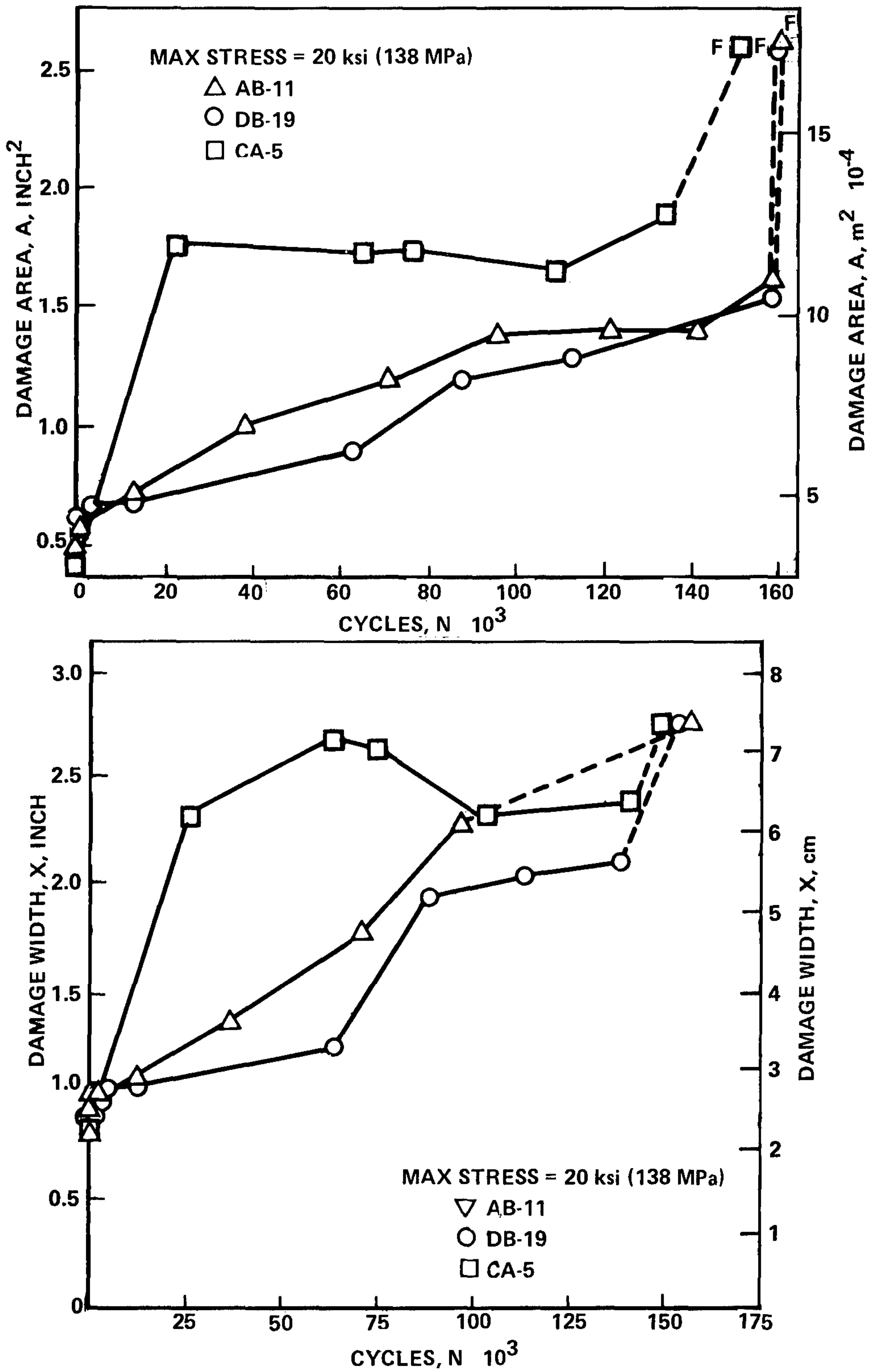

Figure 90. Comparison of Change in Damage Area and Damage Width for Damaged Hole 32 Ply Quasi-Isotropic Specimens, R = -1 σ_{max} =20 ksi (138 MPa)

the fatigue buckling guide configuration. At lower stress levels, (20 ksi (138 MPa) and below) the damage growth exhibits a much more constant rate until failure as shown typically in Figure 90. It should be noted that the stress levels of 26 ksi (179 MPa) and above are at a level greater than 73% of the average static strength and greater than 92% of the lowest of 10 static compression strength values. Also worthy of note is the observation that a definite damage growth threshold appears to exist for the 32-ply laminate in that no growth was observed for runout specimens. This, however, was not the case for the 24-ply laminate where damage extension was evident in specimens which had been cycled to the selected limit of 2×10^6 cycles without failure even at stress levels considerably below those required to produce runouts.

Typical damage growth results are presented in Figures 91 through 93. Additional data for other stress levels are presented in Appendix C.

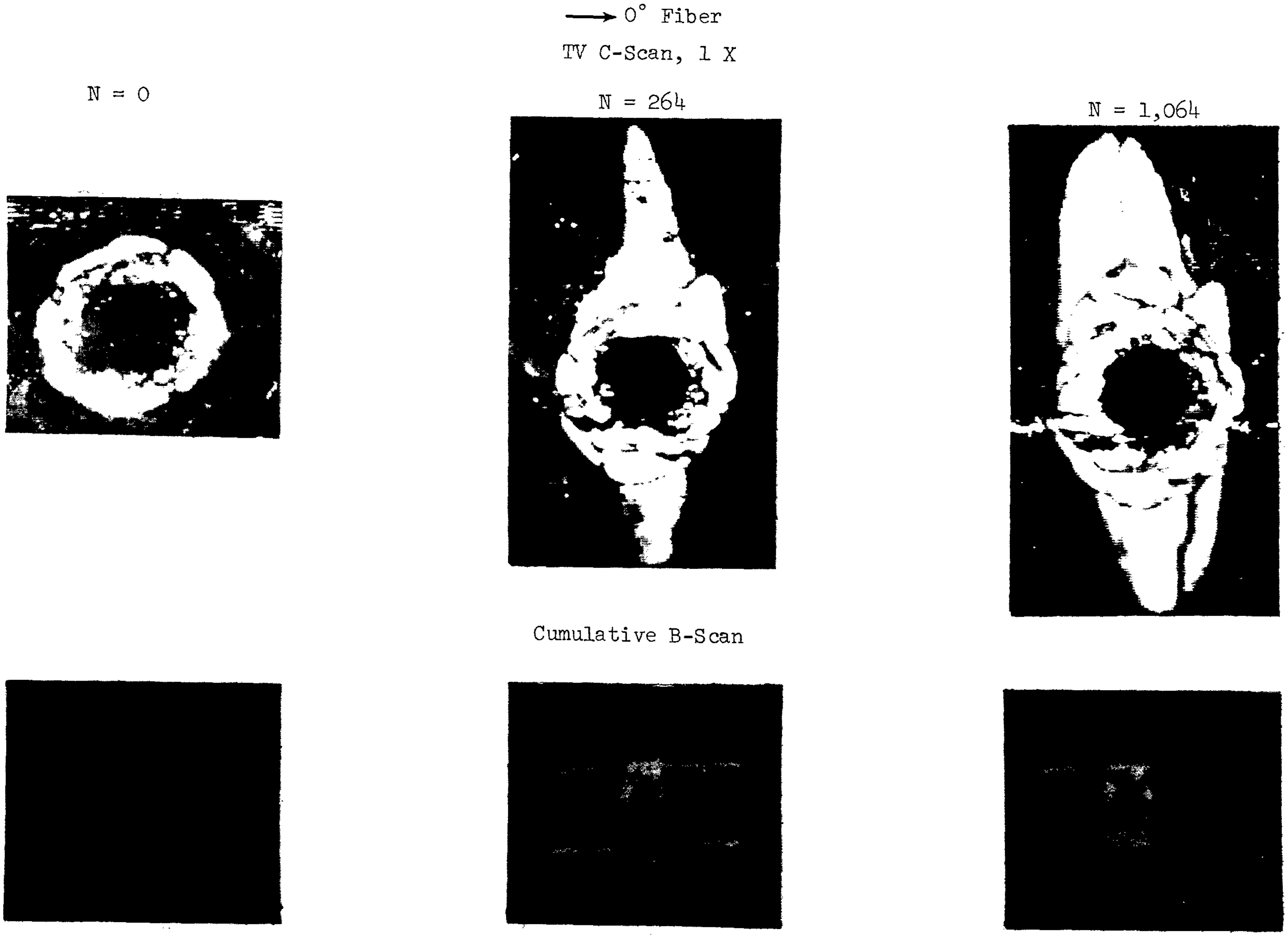

Figure 91a. Damage Growth Characteristics of Damaged Hole Specimen DA-5, 32-Ply Quasi-Isotropic Laminate, R = -1, σ_{max} = 26 ksi (179 MPa)

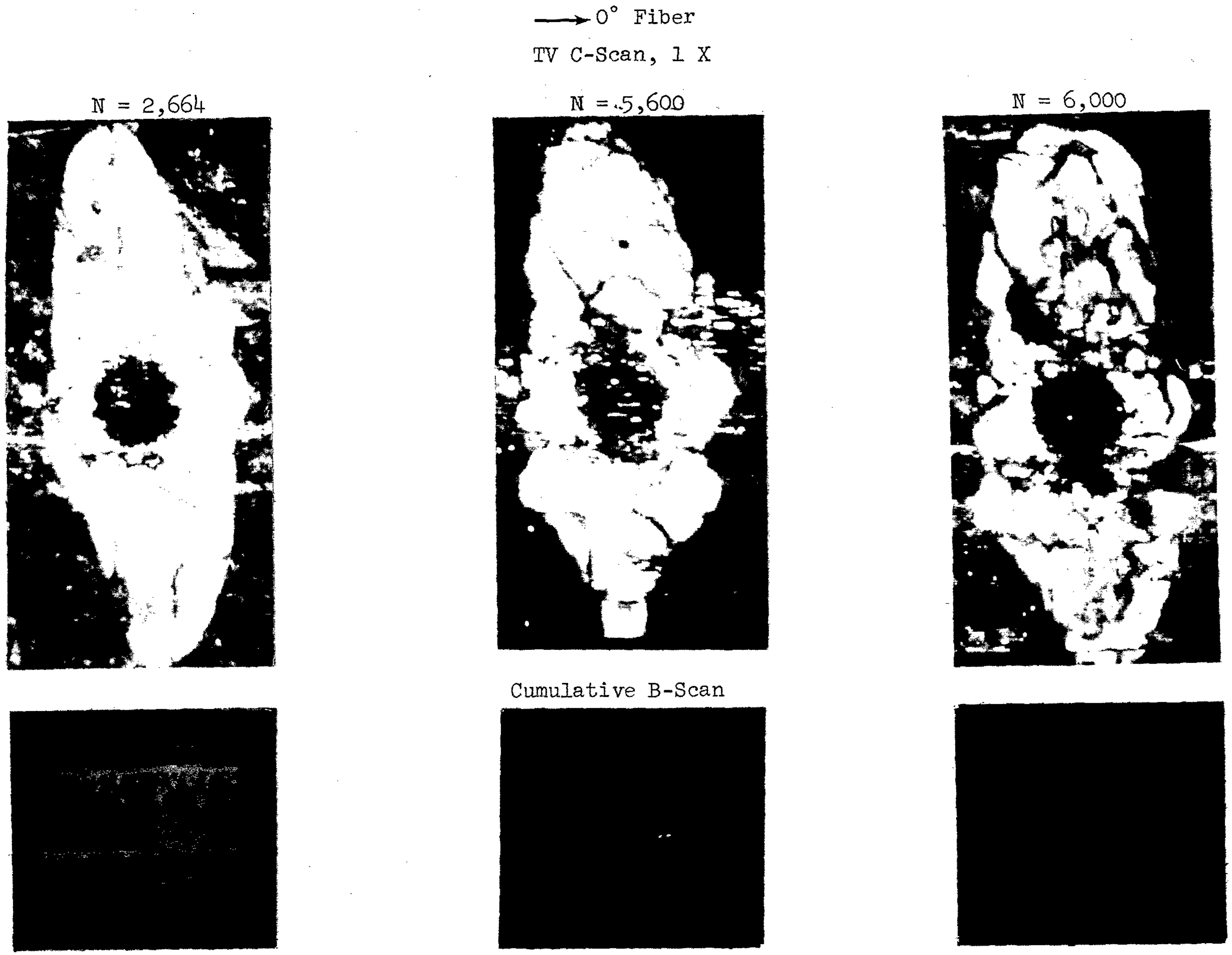

Figure 91b. Damage Growth Characteristics of Damaged Hole Specimen DA-5, 32-Ply Quasi-Isotropic Laminate, R = -1, σ_{max} = 26 ksi (179 MPa)

N = 0 N = 10 N = 60

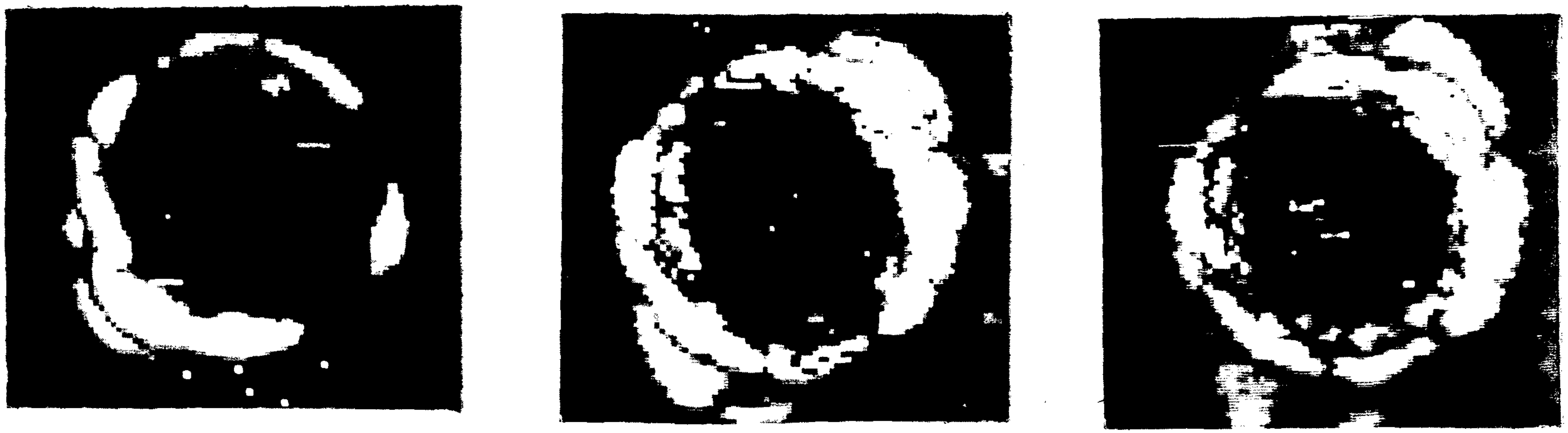

TV Monitor, 2X

Cumulative B-Scans

Figure 92a. Damage Growth Characteristics of Damaged Hole Specimen BC-28, 32-Ply Quasi-Isotropic Laminate, R = -1, σ_{max} = 23 ksi (158 MPa)

N = 3,000 N = 5,000 N = 10,000

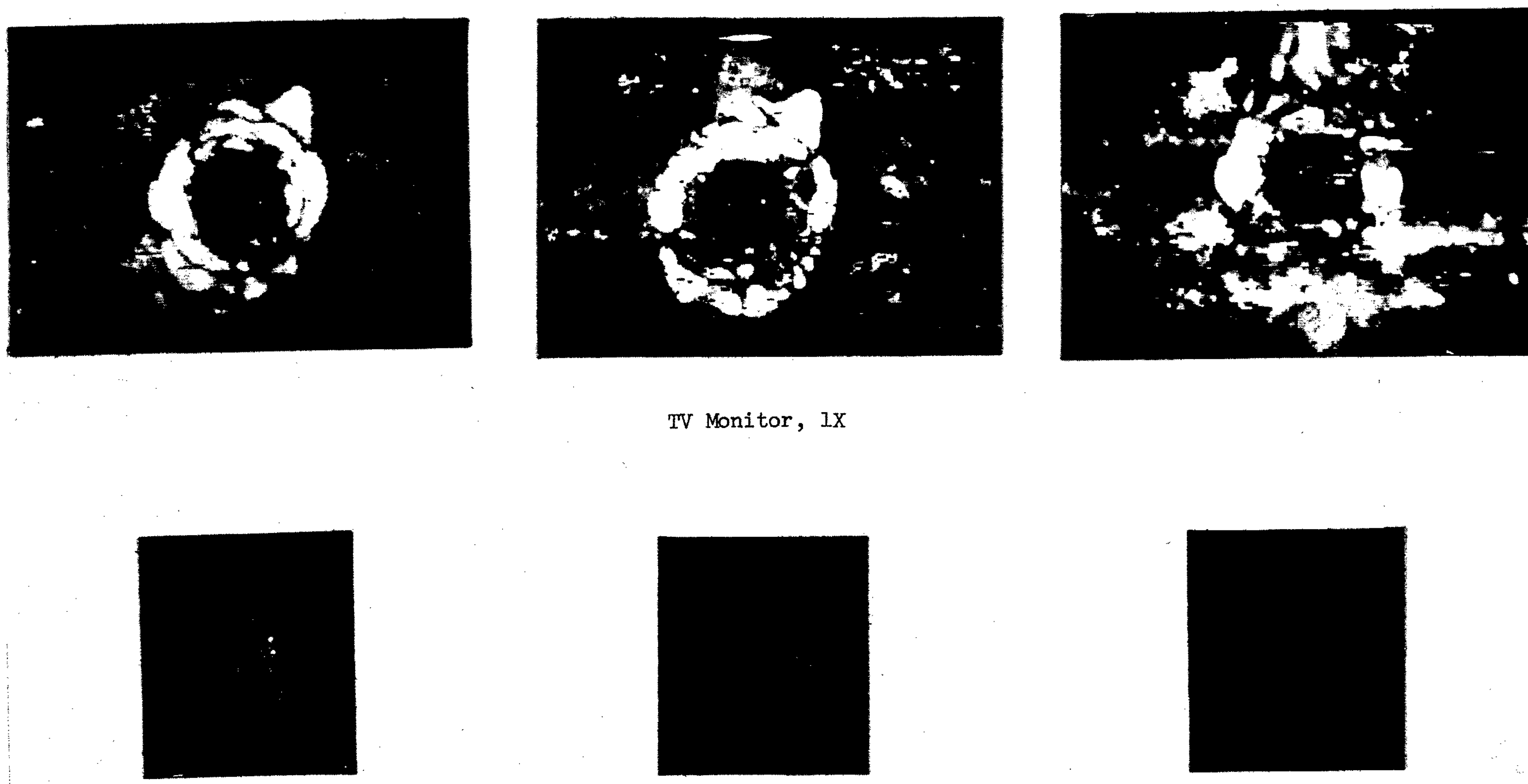

TV Monitor, 1X

Cumulative B-Scan

Figure 92b. Damage Growth Characteristics of Damaged Hole Specimen BC-28, 32-Ply Quasi-Isotropic Laminate, R = -1, σ_{max} = 23 ksi (158 MPa)

N = 17,000 N = 32,000 N = 39,000

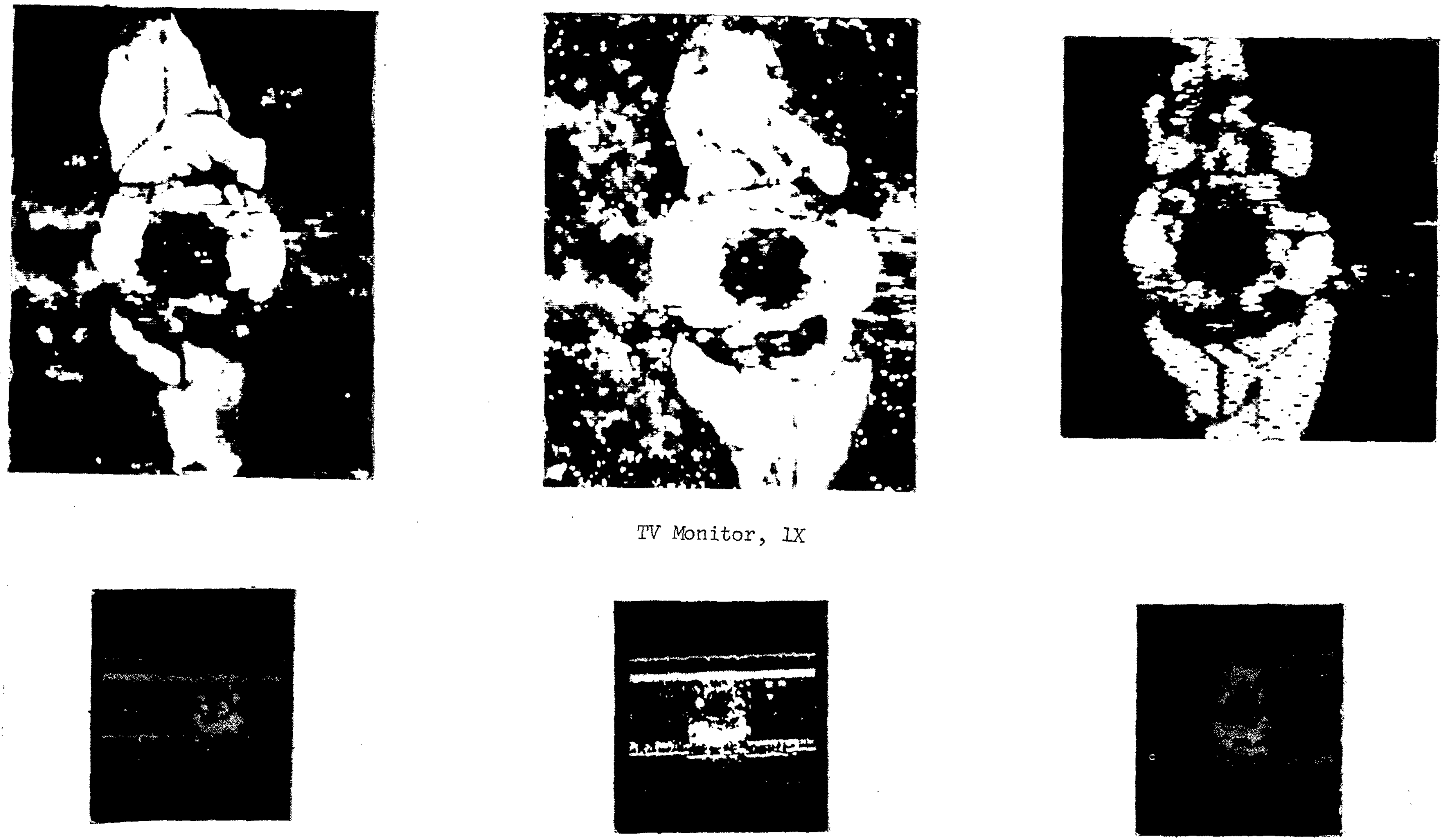

TV Monitor, 1X

Cumulative B-Scan

Figure 92c. Damage Growth Characteristics of Damaged Hole Specimen BC-28, 32-Ply Quasi-Isotropic Laminate, R = -1, σ_{max} = 23 ksi (158 MPa)

N = 42,000 N = 51,000 N = 54,222

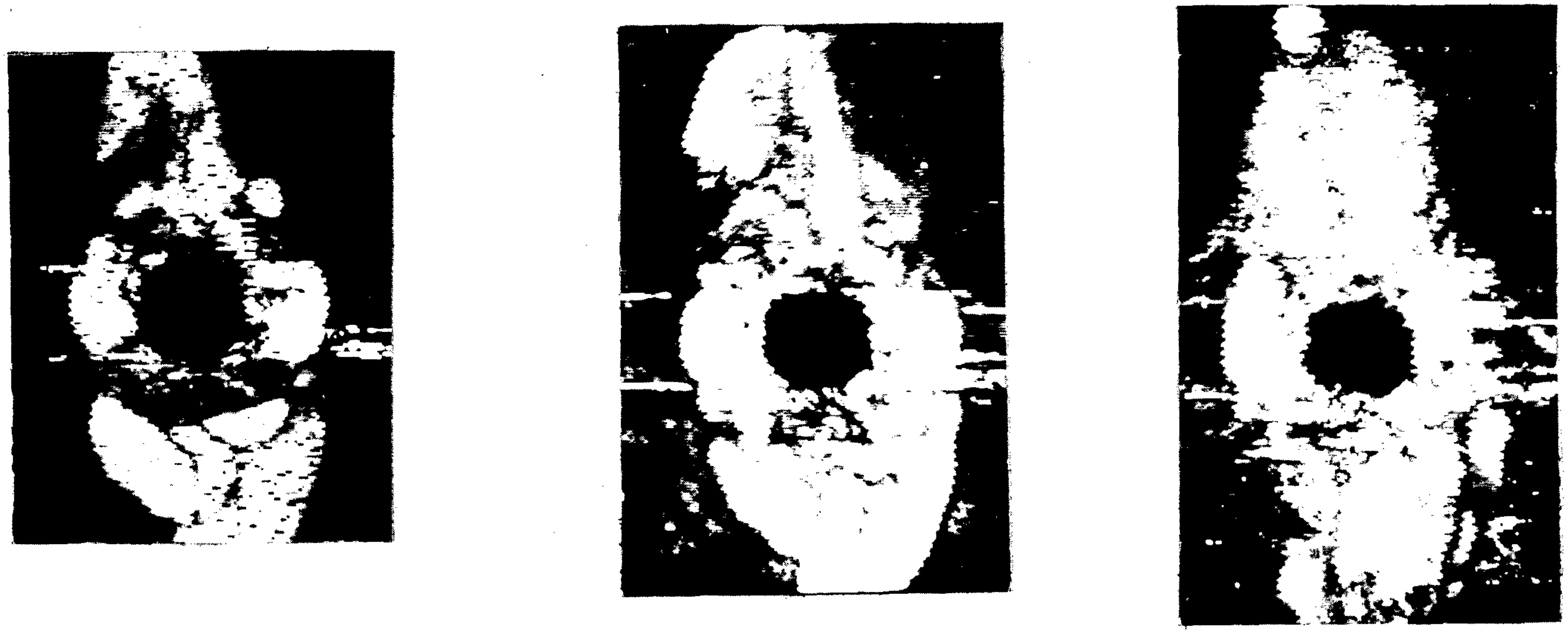

TV Monitor, 1X

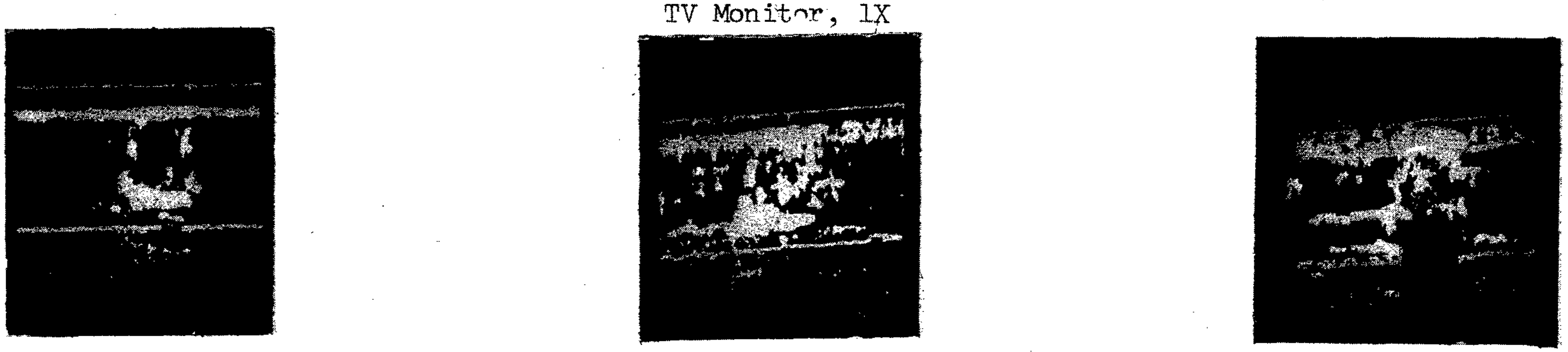

Cumulative B-Scan

Figure 92d. Damage Growth Characteristics of Damaged Hole Specimen BC-28, 32-Ply Quasi-Isotropic Laminate, R = -1, σ_{max} = 23 ksi (158 MPa)

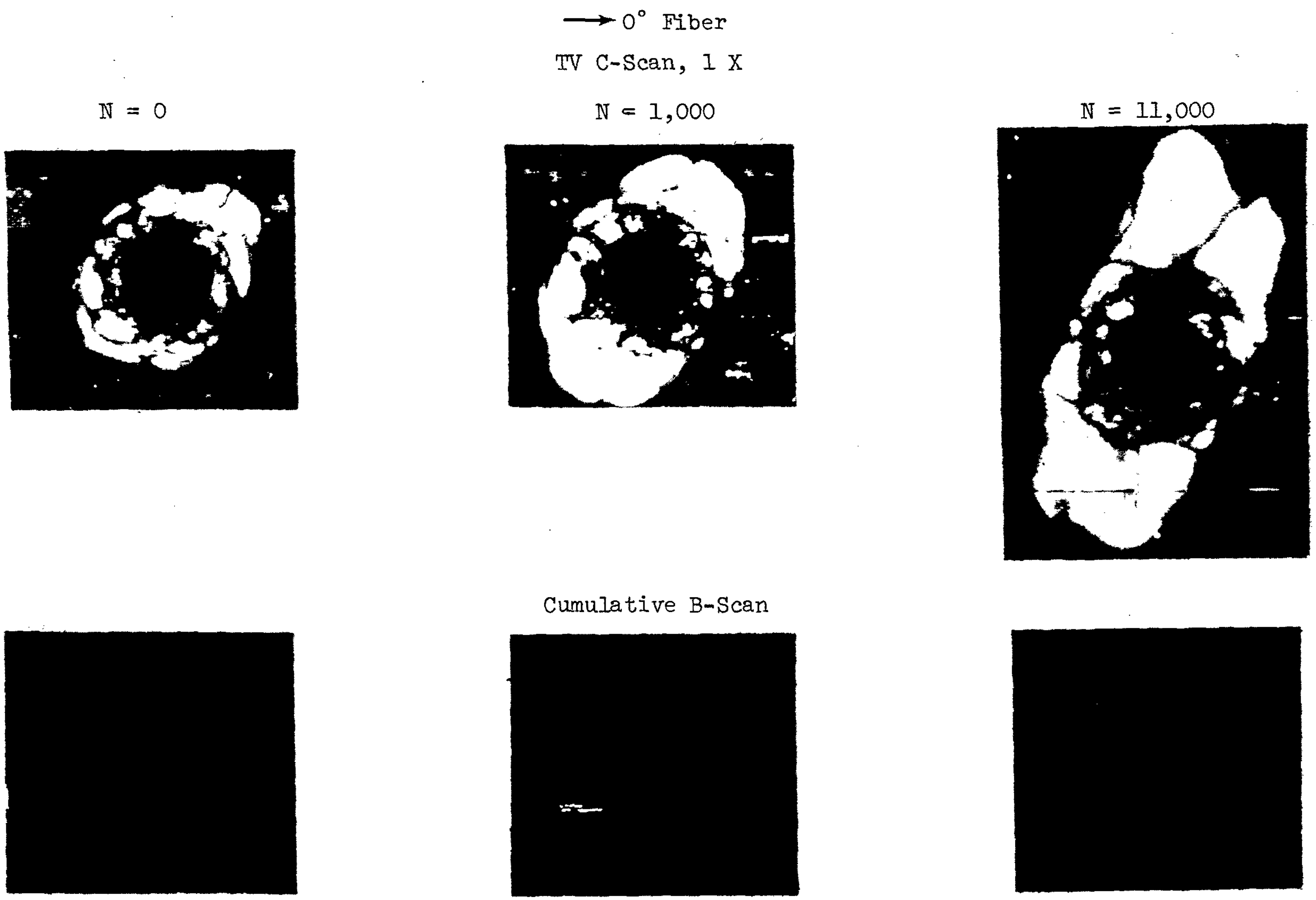

Figure 93a. Damage Growth Characteristics of Damaged Hole Specimen CA-5, 32-Ply Quasi-Isotropic Laminate, R = -1, σ_{max} = 20 ksi (138 MPa)

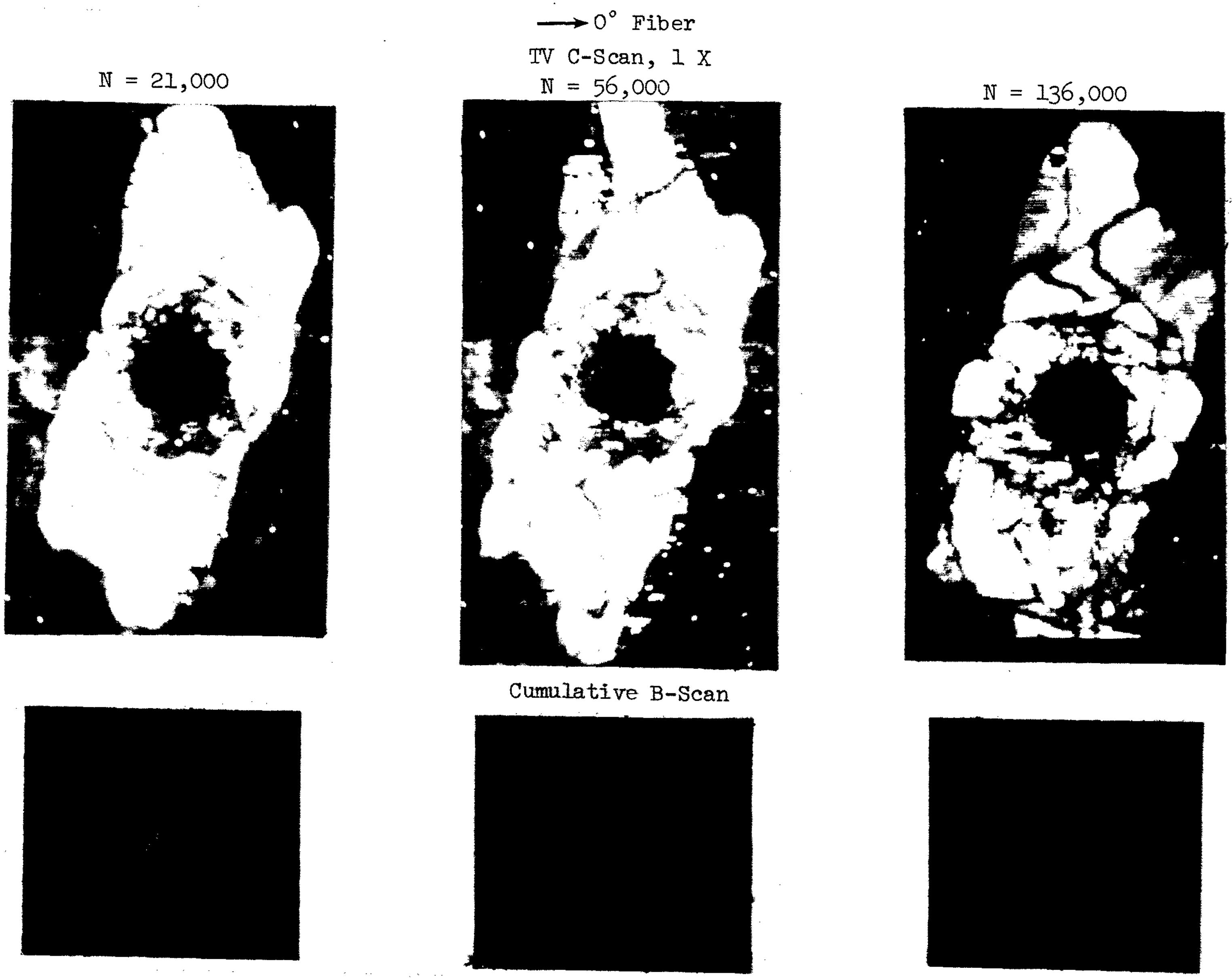

Figure 93b. Damage Growth Characteristics of Damaged Hole Specimen CA-5, 32-Ply Quasi-Isotropic Laminate, R = -1, σ_{max} = 20 ksi (138 MPa)

SECTION 8

EVALUATION OF X-RAY TECHNIQUE AND THE EFFECT OF TBE

In the current program a subset of specimens was identified for testing in static compression and R = -1 fatigue using TBE enhanced X-ray methods to evaluate the damage. The objectives of these tests are defined by the following questions:

1) What is the effect upon the damage indication when the period between TBE soak and X-ray exposure is varied?
2) Does prior exposure to TBE affect static compression strength and/or fatigue life?
3) What is the correlation between damage indications resulting from the X-ray and Holscan techniques employed?
4) Does periodic exposure to TBE affect the damage growth as recorded by the Holscan unit?

Since the impact conditions did not result in sufficient surface damage to allow ingress of the TBE, TBE tests were limited to the damaged hole condition for both laminates. The following sections present the results of this phase of the program.

8.1 X-RAY PROCEDURES

All TBE X-ray examinations were conducted using a Norelco 150 KV X-ray unit with a Be window and equipped with a micro focus spot. For this study the X-ray procedures used were those previously selected for use on damaged holes in graphite/epoxy material [27,28]. All specimens first received a 30-minute soak of the damage region in TBE. Two X-ray exposures were then taken, the first within two hours of the completion of the TBE soak and the second 20-24 hours after the completion of the TBE soak. The X-ray parameters used were a 25 KV constant potential at 5 mA for an exposure time of 10 seconds for the 24 ply laminate (13 seconds for the 32 ply laminate) at a one meter film focal distance. A fine grained film was used (Type D-4 or Type M) and the film developed in a Kodak Model B X-Omat film processor.

8.2 DELAYED TIME EFFECTS ON TBE DAMAGE INDICATIONS

Two X-ray exposures were taken per TBE exposure, the first within two hours of the completion of TBE soak and the second twenty to twenty-four hours after the completion of TBE soak. Figures 94 and 95 illustrate typical X-ray sets taken at the two and twenty-four hour time intervals. These figures are from static compression and R = -1 fatigue specimens respectively. On these prints black indicates a positive response to TBE presence. It should be noted that X-ray negatives are designed to be viewed as negatives and that positive prints from them, such as those contained within, are inferior to 'normal' positives. All analysis and data collection have been acquired from the original "X-ray negatives" since the behavior is most readily observed on the original X-ray negative.

Exposures at the two hour wait time typically revealed areas surrounding the hole which were well-defined. This inner, well defined area was surrounded by a halo-like band along the outer periphery of the damage indication, with rather ill-defined outer boundaries as illustrated in Figure 96. Exposures at the twenty-four hour wait period revealed the extension of the well-defined areas into the halo regions and a slight contraction of the outer halo.

The growth of these well-defined areas occurs as a dark-to-light (on the positives) transition. This would seem to indicate that the TBE is draining away from the center of the large delamination areas toward their edges. The extent to which the remaining halo regions are an indication of further delamination or matrix cracking was not determined.

In addition, Figure 95 shows an almost complete 'fade out' of damage indication at the N_5 cycle interval. The effect was noticed as typical for most of the fatigue specimens during the N_5 cycle exposure and will be discussed in later sections.

A comparison of all of the two and twenty four hour delay time X-ray results showed that in some cases no significant difference was noted while some variations were noted in others, the twenty four hour generally (but not always)

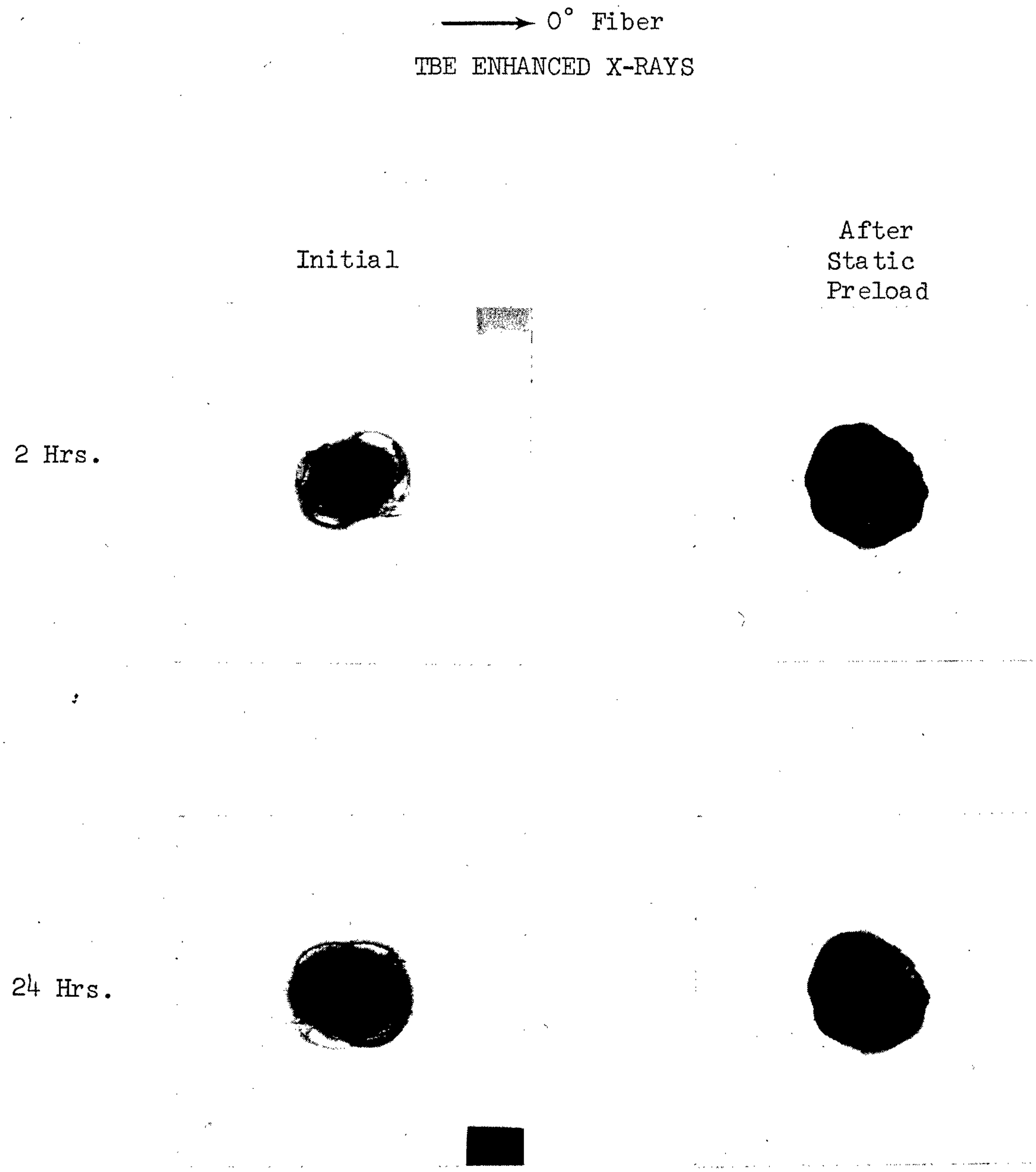

Figure 94. Effect of Delay in X-Ray Exposure after TBE Soak, Damage Hole Specimen LA-1, 24-Ply 67% 0° T300/5208 Laminate, Specimen Preloaded to 28 ksi, σ_u = 47.9 ksi

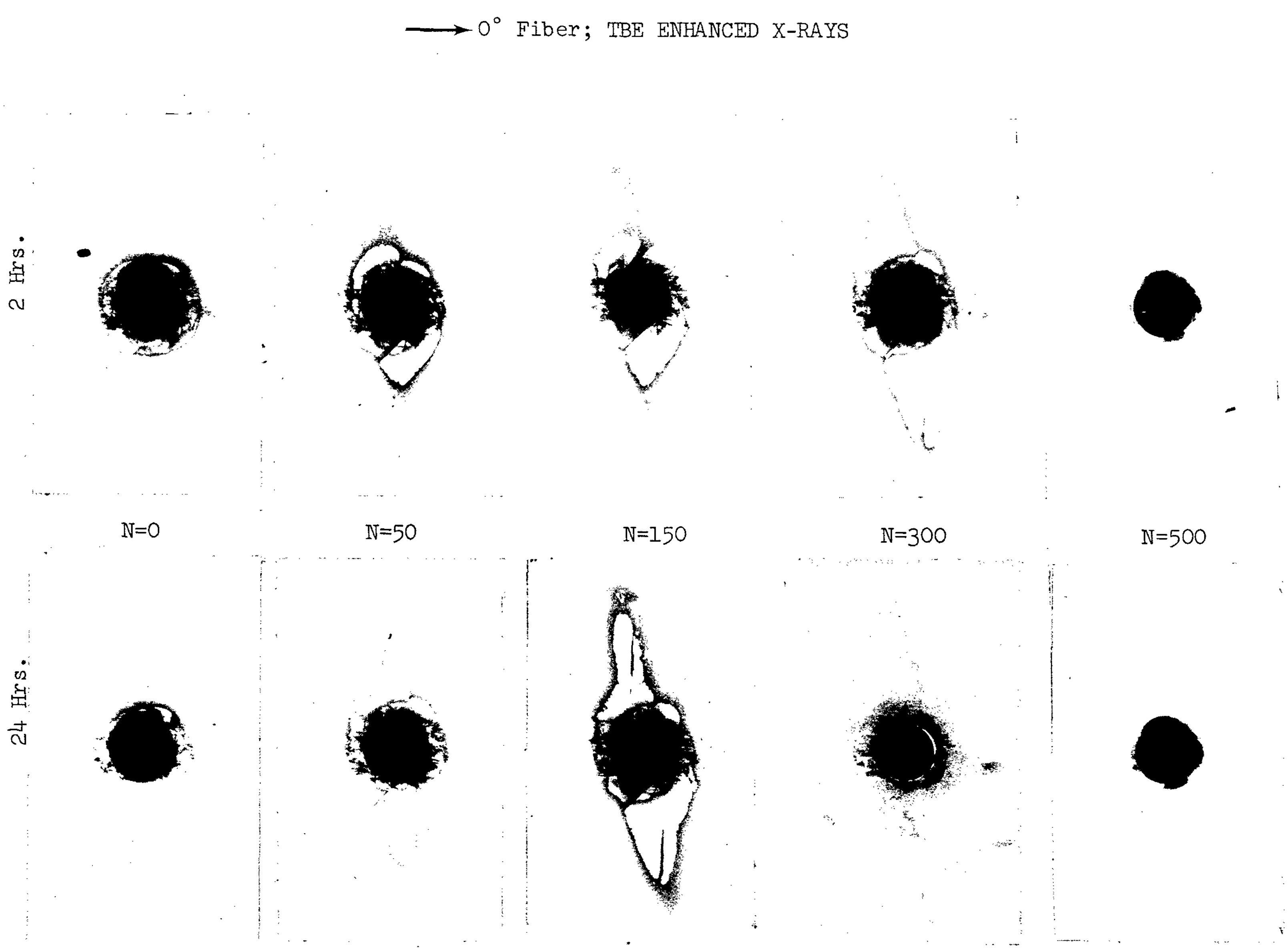

Figure 95. Effect of Delay in X-Ray Exposure after TBE Soak, Damage Hole Specimen BA-9, 32-Ply Quasi-Isotropic T300/5208 Laminate, R = -1, σ_{max} = 30 ksi (207 MPa), N_f = 1,709 Cycles.

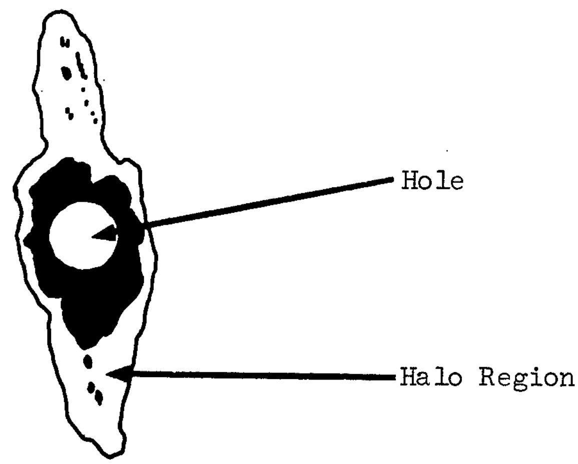

2 Hr.

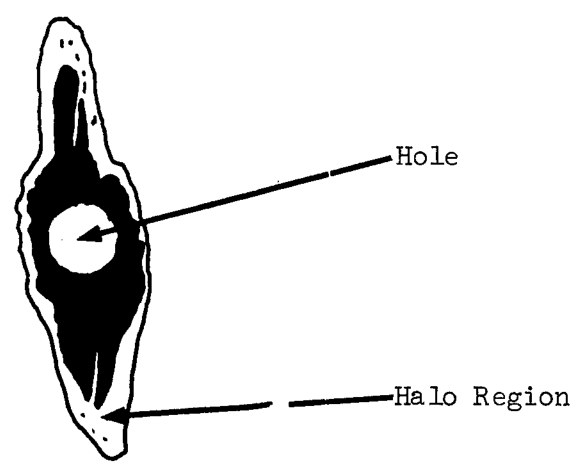

24 Hr.

Figure 96. Schematic of Typical TBE X-ray Damage Size Result.

showing the slightly larger damage size.

X-ray photographs contained hereafter were selected to give the reader the best idea of the damage areas without respect to time after TBE soak. When measurements were made from the X-rays, the exposures which showed the maximum damage areas were selected.

8.3 STATIC COMPRESSION AND FATIGUE PROCEDURES

In this evaluation nine specimens were randomly selected from each laminate. Three stress levels were then selected per laminate from the baseline damaged hole compression data which would provide (a) a stress level in the essentially linear region of the load vs deflection curve, (b) a stress level near the onset of significant non-linearity, and (c) a stress level equal to ~ 85 to 90% of the average static failure stress for the baseline tests, i.e., a level where damage growth may be occurring. All specimens were subjected to a 30 minute soak in TBE prior to the onset of testing. X-ray photographs were taken at two-hour and 24-hour intervals following exposure and the specimens returned for pre-loading. These specimens were pre-loaded to the selected stress level, (presented in Table XXXIII), using the same procedures used for the baseline static compression tests, unloaded and returned to the X-ray laboratory, and the TBE X-ray sequence repeated. Specimens were then returned for final testing to failure.

Triplicate specimens were randomly selected for fatigue testing at each of three selected stress levels per laminate. The eighteen specimens were first X-rayed using the TBE procedure previously used for the static tests and then returned for the first block of fatigue cycling. The fatigue stress levels and cycle intervals used are presented in Table XXXIV. Holscan ultrasonic measurements were also made at selected times for comparison with the TBE enhanced X-ray results.

8.4 EFFECT OF TBE ON COMPRESSION STRENGTH AND FATIGUE LIFE

Failure stresses under compression loading with the fatigue buckling guides for these specimens are given in Table XXXIII. If the failure stresses of these TBE exposed specimens are compared with the original baseline data,

TABLE XXXIII. STATIC COMPRESSION FAILURE STRESS LEVELS FOR DAMAGED HOLE SPECIMENS WHICH HAD BEEN PREVIOUSLY EXPOSED TO TBE

Specimen No.	Average Width, W		Average Thickness, T		Maximum Gross Preloaded Stress, σ		Gross Failure Stress, σ_{ult}	
	in	mm	in	mm	ksi	MPa	ksi	MPa
24 Ply								
HA-5	2.9969	76.121	0.1226	3.114	28.0	193	46.1	318
IA-1	2.9961	76.101	0.1227	3.117	28.0	193	47.9	330
IB-11	2.9963	76.106	0.1233	3.132	35.0	241	49.0	338
KC-24	2.9969	76.121	0.1232	3.129	35.0	241	46.9	323
MA-7	2.9965	76.111	0.1242	3.155	41.0	283	47.4	327
HA-3	2.9978	76.144	0.1209	3.071	41.0	283	47.5	328
						Average	47.5 + 1.5 - 1.4	328 + 10 - 10
32 Ply								
EC-25	2.9707	75.456	0.1665	4.230	17.5	121	34.8	240
CA-8	2.9601	75.187	0.1613	4.097	17.5	121	38.1	263
DA-1	2.9960	76.098	0.1638	4.161	22.0	152	36.7	253
AC-30	2.9504	74.940	0.1595	4.051	22.0	152	35.5	245
EC-29	2.9985	76.162	0.1643	4.173	27.0	186	31.8	219
BC-25	3.000	76.200	0.1592	4.044	27.0	186	36.2	249
						Average	35.5 + 2.6 - 3.7	245 + 18 - 26

TABLE XXXIV. FATIGUE HISTORY FOR TBE EXPOSED X-RAY STUDY SPECIMENS, R = -1

Specimen No.	Average Width, W		Average Thickness, T		Maximum Stress Level, σ_{max}		Total Fatigue Cycles Completed at Inspection						Total Cycles to Failure
	in.	mm	in.	mm	ksi	MPa	N_1	N_2	N_3	N_4	N_5	N_6	
24 Ply													
MB-13	2.9966	76.114	0.1244	3.160	41	283	0	100	400	1,000	2,000	3,420*F	3,420
JB-19	2.9966	76.114	0.1228	3.119	41	283	0	100	400	1,000	2,000	13,453*F	13,453
HC-24	2.9964	76.109	0.1208	3.068	41	283	0	100	400	1,000	1,500*F	-	1,500
MA-9	2.9956	76.088	0.1250	3.175	38	262	0	1,000	5,000	7,760F	-	-	7,760
KB-16	2.9966	76.114	0.1229	3.122	38	262	0	1,000	5,000	9,000	20,000	162,717*F	162,717
JB-20	2.9966	76.114	0.1241	3.152	38	262	0	1,000	5,000	15,000	30,000	132,814*F	132,814
LA-9	2.9962	76.103	0.1221	3.101	34	234	0	10,000	26,510*F	-	-	-	26,510
JA-6	2.9906	75.961	0.1237	3.142	34	234	0	10,000	27,800*F	-	-	-	27,800
LA-4	2.9962	76.103	0.1237	3.142	34	234	0	10,000	15,000	100,000	226,390*F	-	226,390
32 Ply													
BA-9	2.9860	75.844	0.1595	4.051	30	207	0	50	150	300	500	1,709*F	1,709
EB-12	2.9985	75.162	0.1654	4.201	30	207	0	50	90*F	-	-	-	90
CC-25	2.9604	75.194	0.1619	4.112	30	207	0	50	100	300	380*F	-	380
BA-1	2.9999	76.197	0.1582	4.018	26	179	0	500	1,500	5,000	5,970*F	-	5,970
AA-3	2.9993	76.182	0.1598	4.059	26	179	0	500	1.500	5,000	10,000	10,565*F	10,565
BB-17	2.9998	76.195	0.1599	4.061	26	179	0	500	1,500	5,000	10,000	11,856*F	11,856
CA-3	2.9964	76.109	0.1618	4.110	20	138	0	20,000	60,000	82,171*F	-	-	82,171
EB-13	2.9985	76.162	0.1660	4.216	20	138	0	20,000	60,000	110,000	160,000	392,584*F	392,584
DC-24	2.9977	76.142	0.1639	4.163	20	138	0	20,000	60,000	110,000	160,000	418,228*F	418,228

* Failed

the results are found to be well within the original data base scatter for both laminates. Thus it does not appear that the prior exposure to TBE had a significant effect on the subsequent static compression strength.

A comparison of the fatigue failures of the baseline laboratory air tests with the results of the TBE exposed specimens is presented in Figure 97 and Table XXXIV. The results indicate no significant effect of the TBE exposure on the fatigue behavior of the 32-ply quasi-isotropic laminate. Some effect does appear to exist in the lower stress, 34 ksi (234 MPa) region for the 24-ply 67% 0 ° fiber specimens, the lives of the three TBE exposed specimens being significantly shorter than those of the baseline specimens. Whether this is due to scatter cannot be determined from this limited data set, but the statistical fatigue life distribution study of Task II may clarify the apparent effect and resolve whether it is indeed real or an artifact due to normal scatter.

8.5 DAMAGE AS INDICATED BY TWO METHODS

The TBE enhanced X-rays for the static compression specimens are presented in Figures 98 and 99. Holscan records for these particular specimens were not available, however a comparison of the TBE enhanced X-ray results with the previously obtained Holscan ultrasonic results showed the indicated initial damage zones to be essentially equivalent in size. Results obtained using TBE enhanced X-ray following the pre-load cycle revealed a significant change in the damage X-ray indication due to the one cycle pre-load. The change in X-ray damage indication consisted of a marked increase in the intensity of the observed damage area for all pre-load levels. This is believed to be due to the localized buckling around the initial delamination damage which significantly opened up the delaminations. Thus on subsequent TBE exposure, more TBE was trapped in the delamination resulting in the change in the X-ray intensity indicated.

The TBE enhanced X-rays of the R = -1 fatigue specimens are presented in Figures 100 through 105. Included in these figures are the corresponding Holscan photographs. Holscan photographs were obtained for the last three

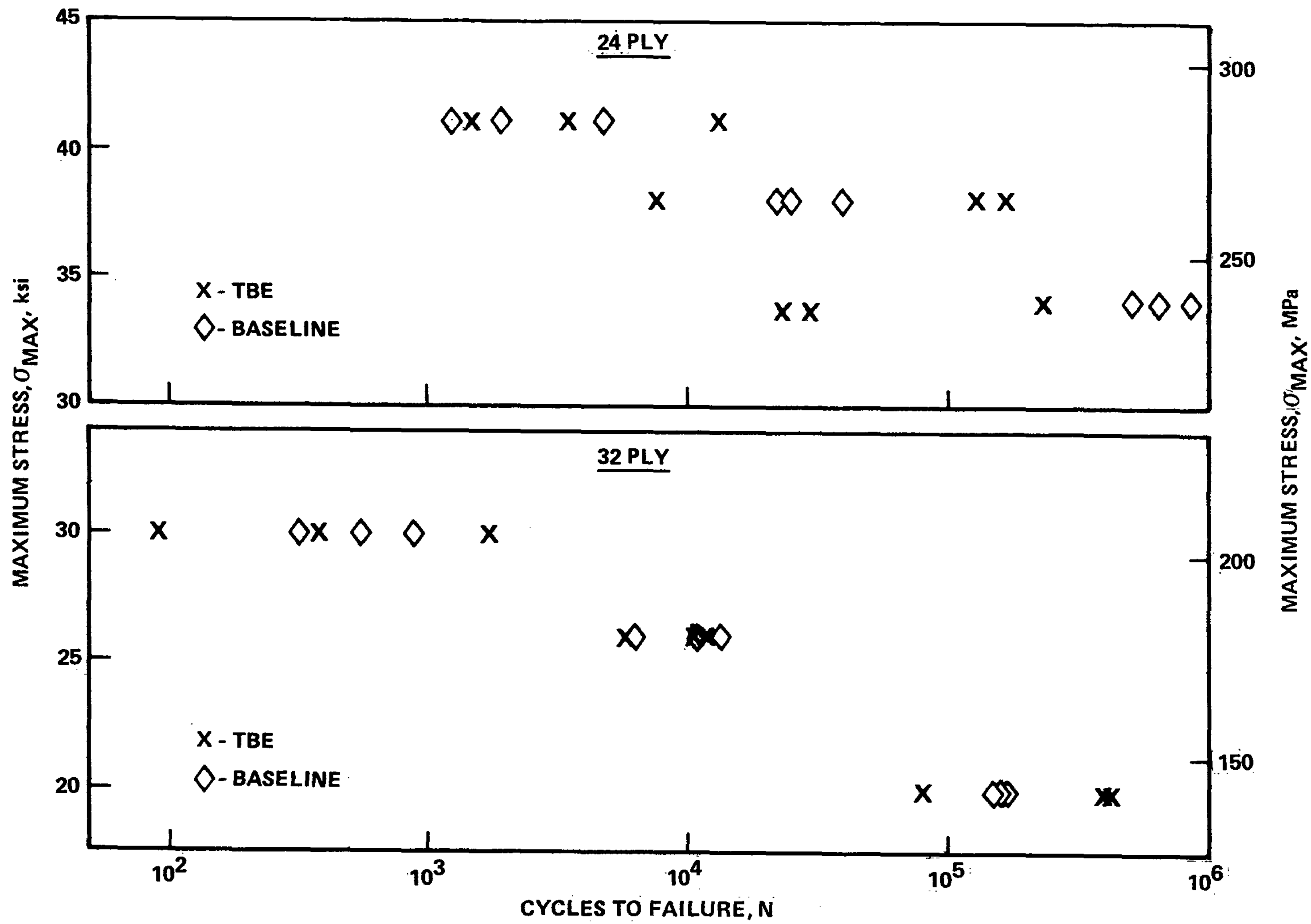

Figure 97. Comparison of Baseline and TBE Exposed Specimen Fatigue Results, R = -1, 5 Hz

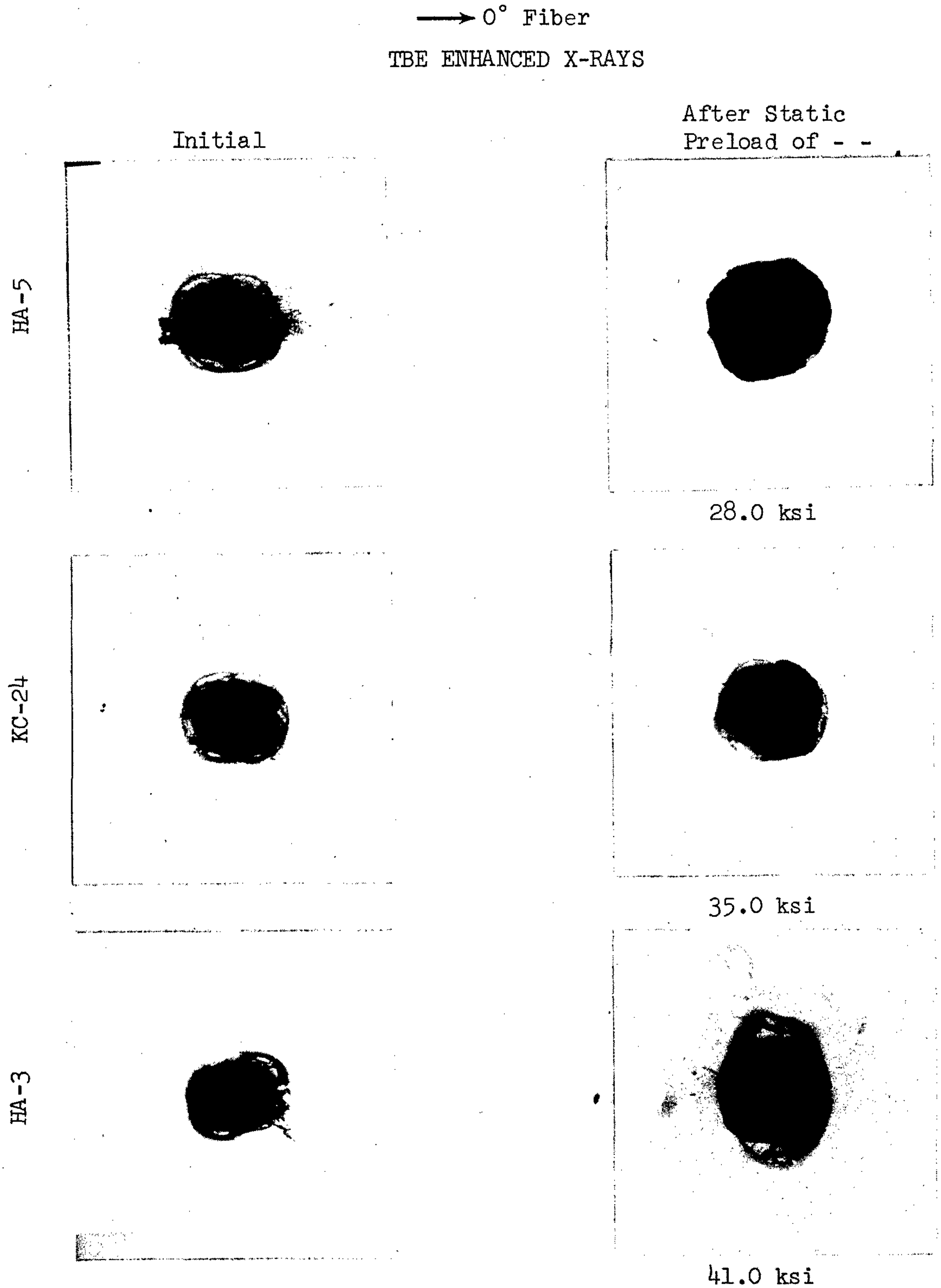

Figure 98. X-Ray Examination of Static Compression Specimens, 24-Ply 67% 0° Fiber Laminate; Specimens HA-5, KC-24, and HA-3

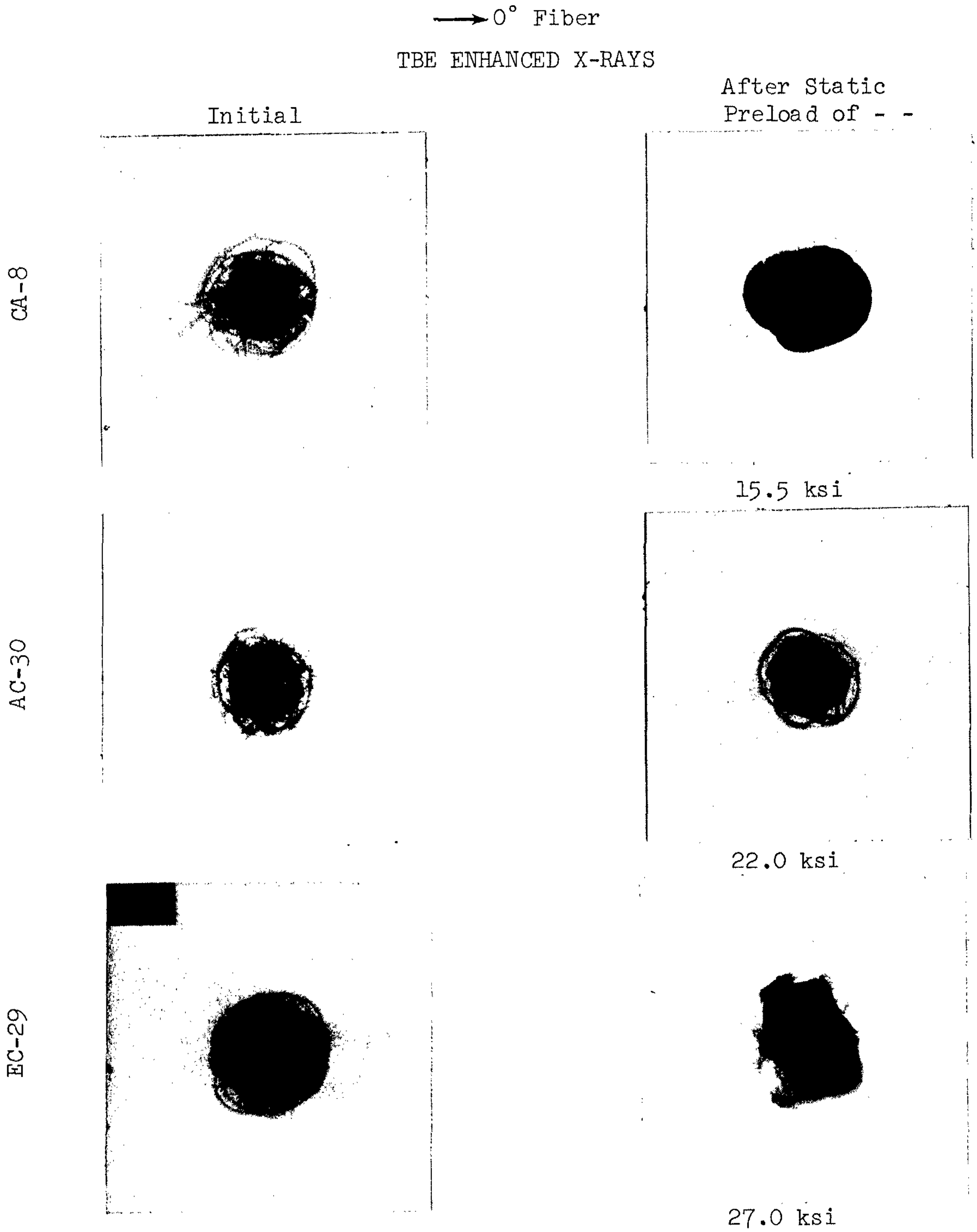

Figure 99. X-Ray Examination of Static Compression Specimens, 32-Ply Quasi-Isotropic Laminate; Specimens CA-8, AC-30, and EC-29 Preloads of 15.5, 22.0 and 27.0 ksi

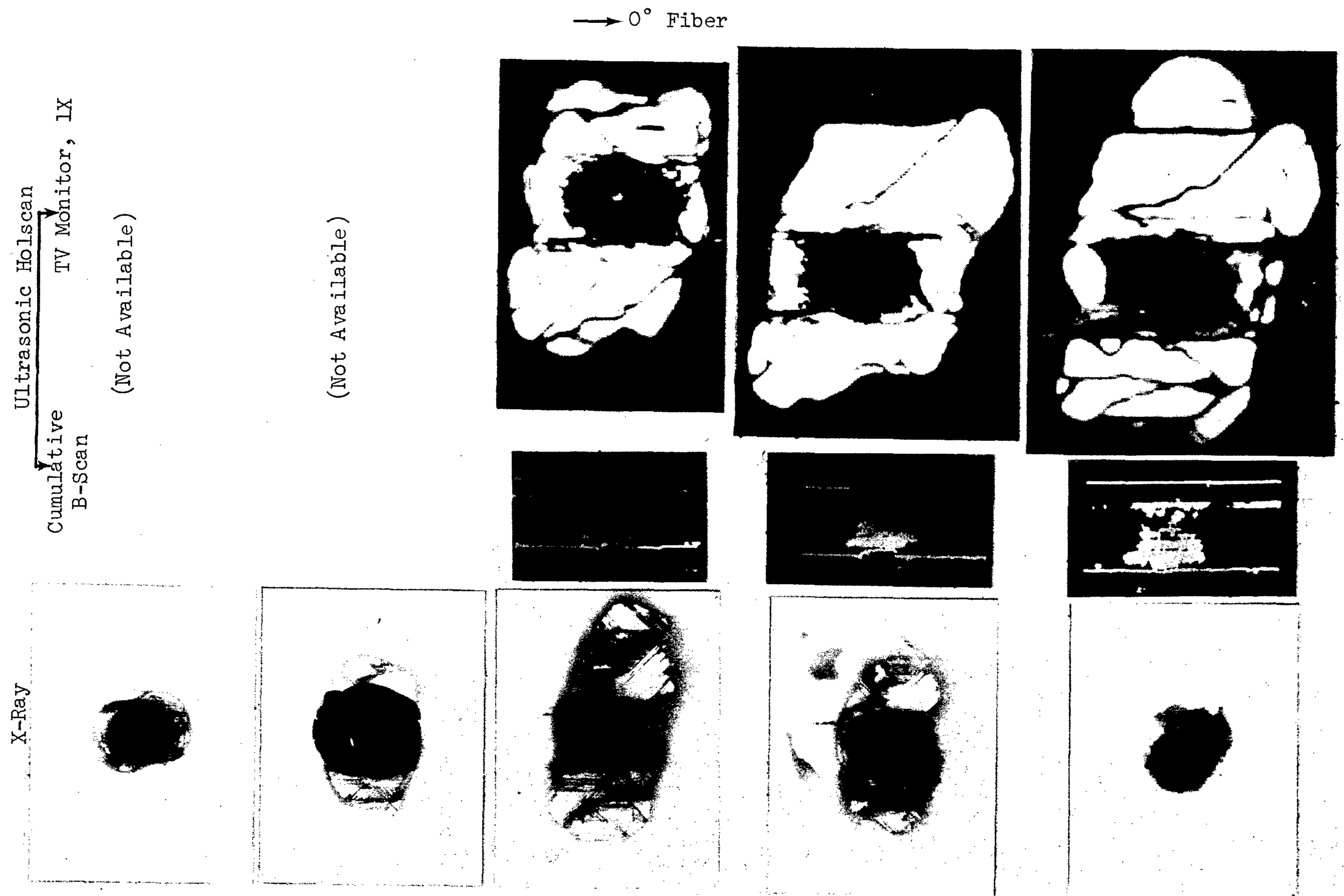

$N_1 = 0$ $N_2 = 100$ $N_3 = 400$ $N_4 = 1,000$ $N_5 = 2,000$

Figure 100. Fatigue Damage as Detected by Holscan and X-Ray for Specimen MB-13, 24-Ply 67% 0° Fiber Laminate, R = -1, σ_{max} =41 ksi (283 MPa), N_f = 3,420 Cycles

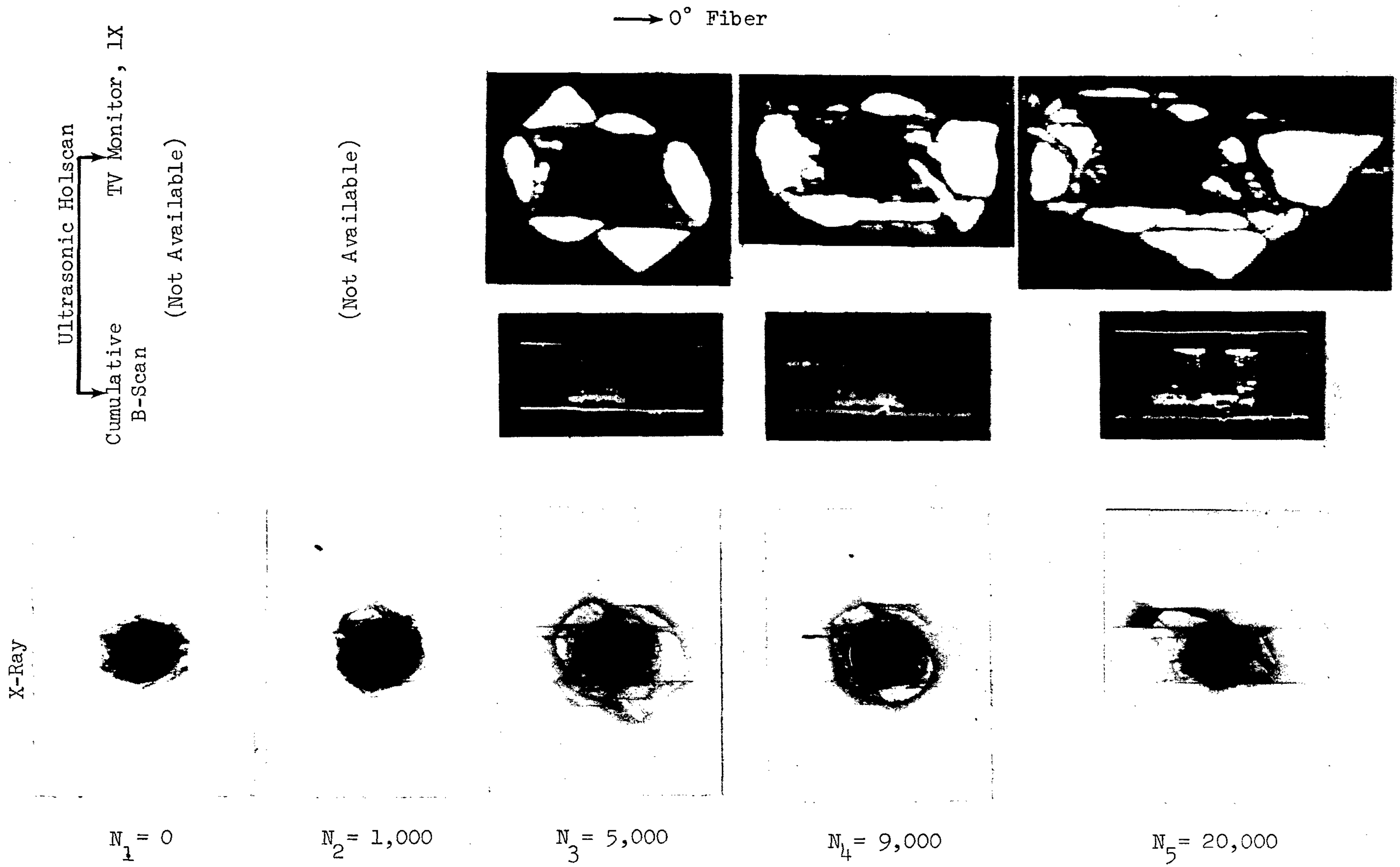

Figure 101. Fatigue Damage as Detected by Holscan and X-Ray for Specimen KB-16, 24-Ply 67% 0° Fiber Laminate, R = -1, σ_{max} = 38 ksi (262 MPa), N_f = 162,717 Cycles

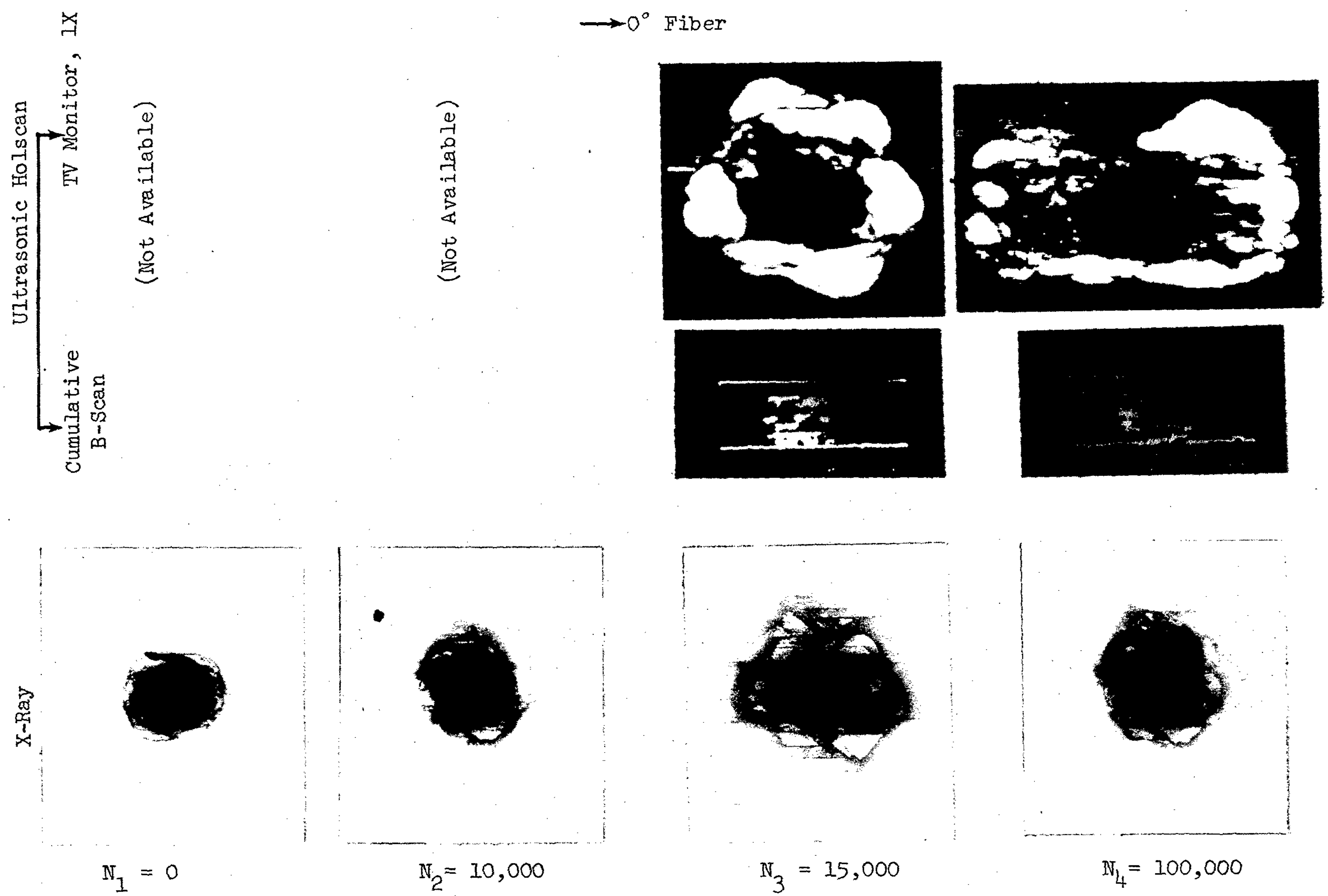

Figure 102. Fatigue Damage as Detected by Holscan and X-Ray for Specimen IA-4, 24-Ply 67% 0° Fiber Laminate, $R = -1$, $\sigma_{max} = 34$ ksi (234 MPa), $N_f = 226{,}390$ Cycles

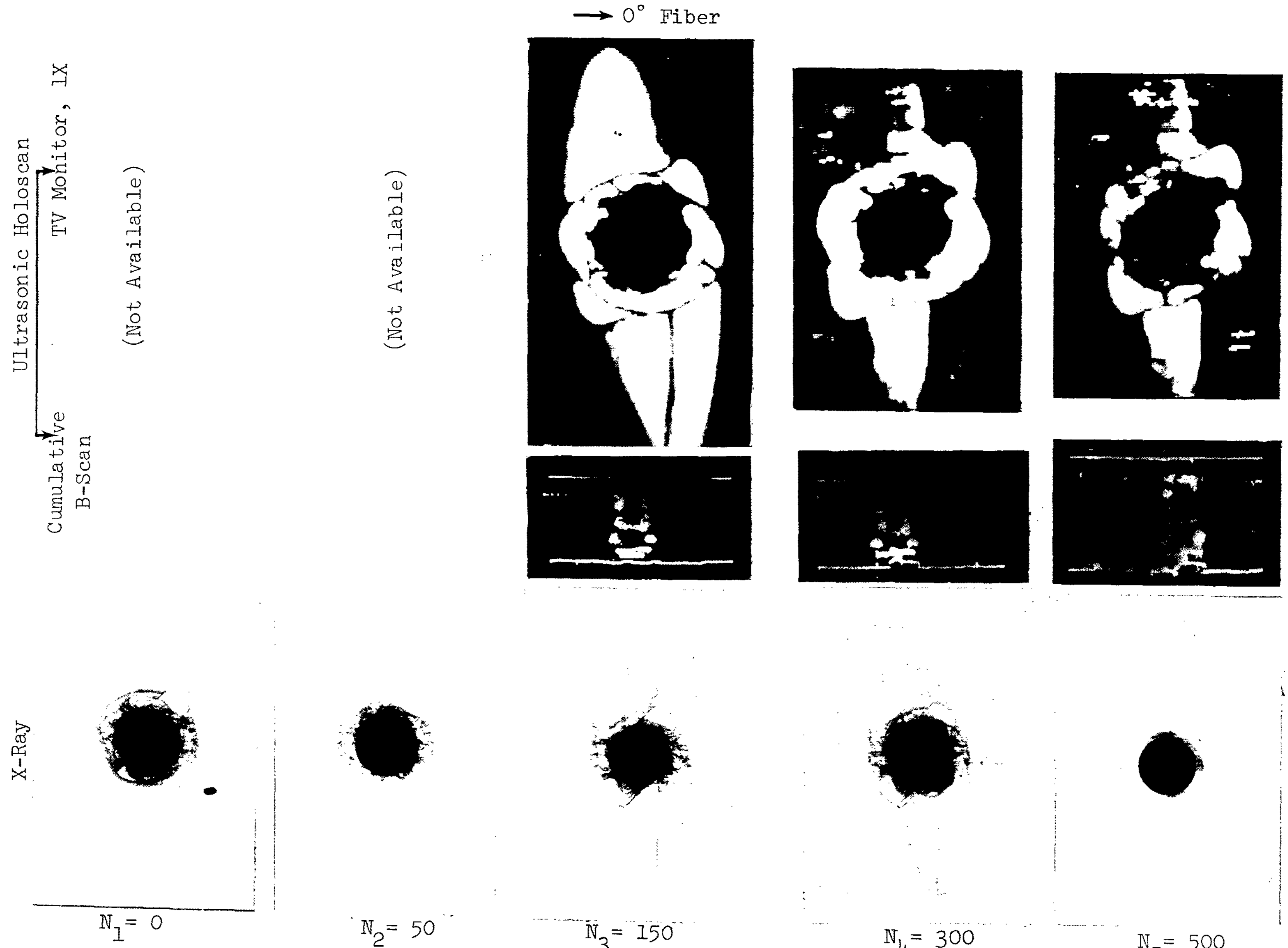

Figure 103 . Fatigue Damage as Detected by Holscan and X-Ray for Specimen BA-9, 32-Ply Quasi-Isotropic Laminate R = -1, σ_{max} = 30 ksi (207 MPa), N_f = 1,709 Cycles

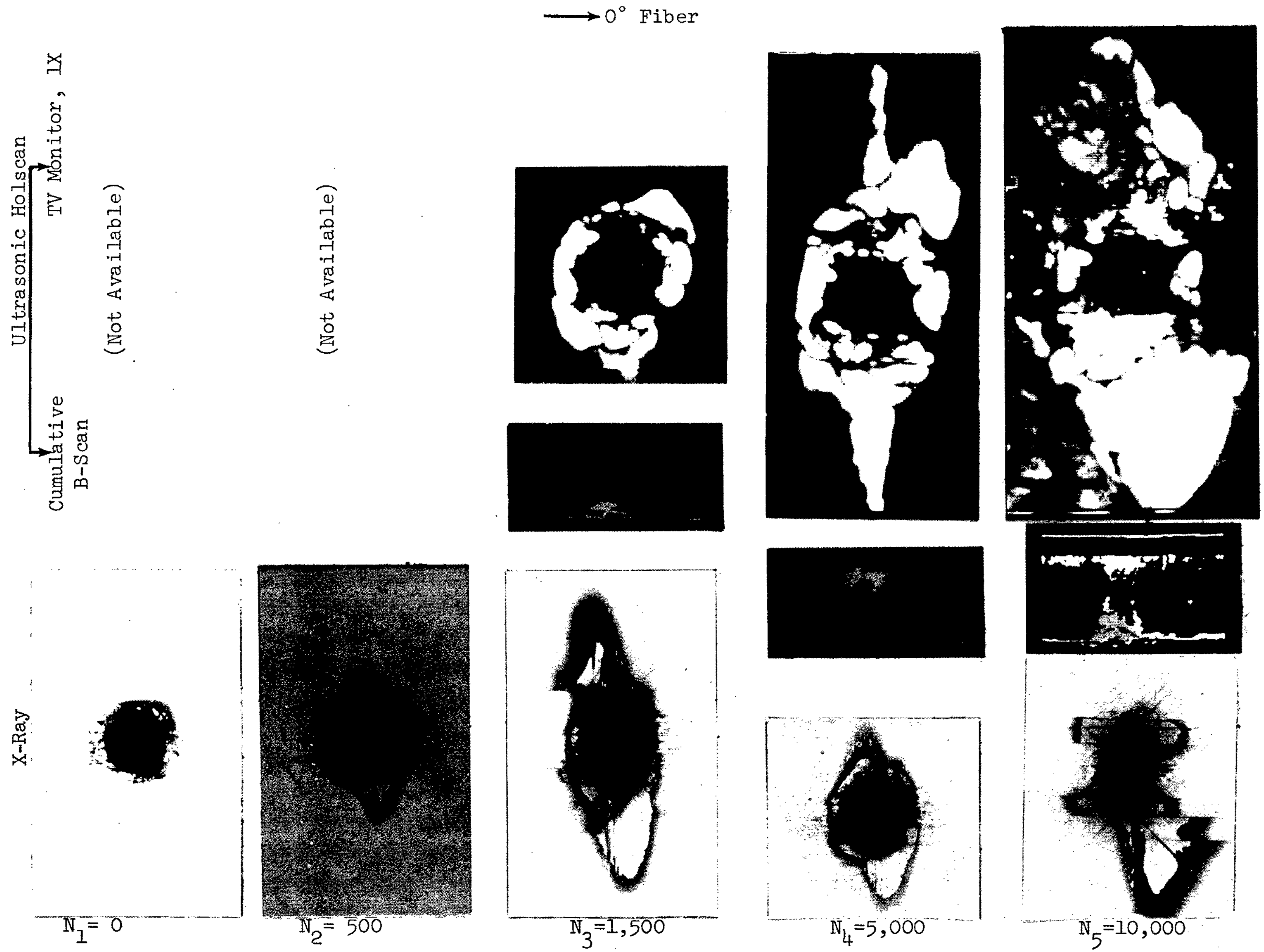

Figure 104. Fatigue Damage as Detected by Holscan and X-Ray for Specimen AA-3, 32-Ply Quasi-Isotropic Laminate R = -1, σ_{max} = 26 ksi (179 MPa), N_f = 10,565 Cycles

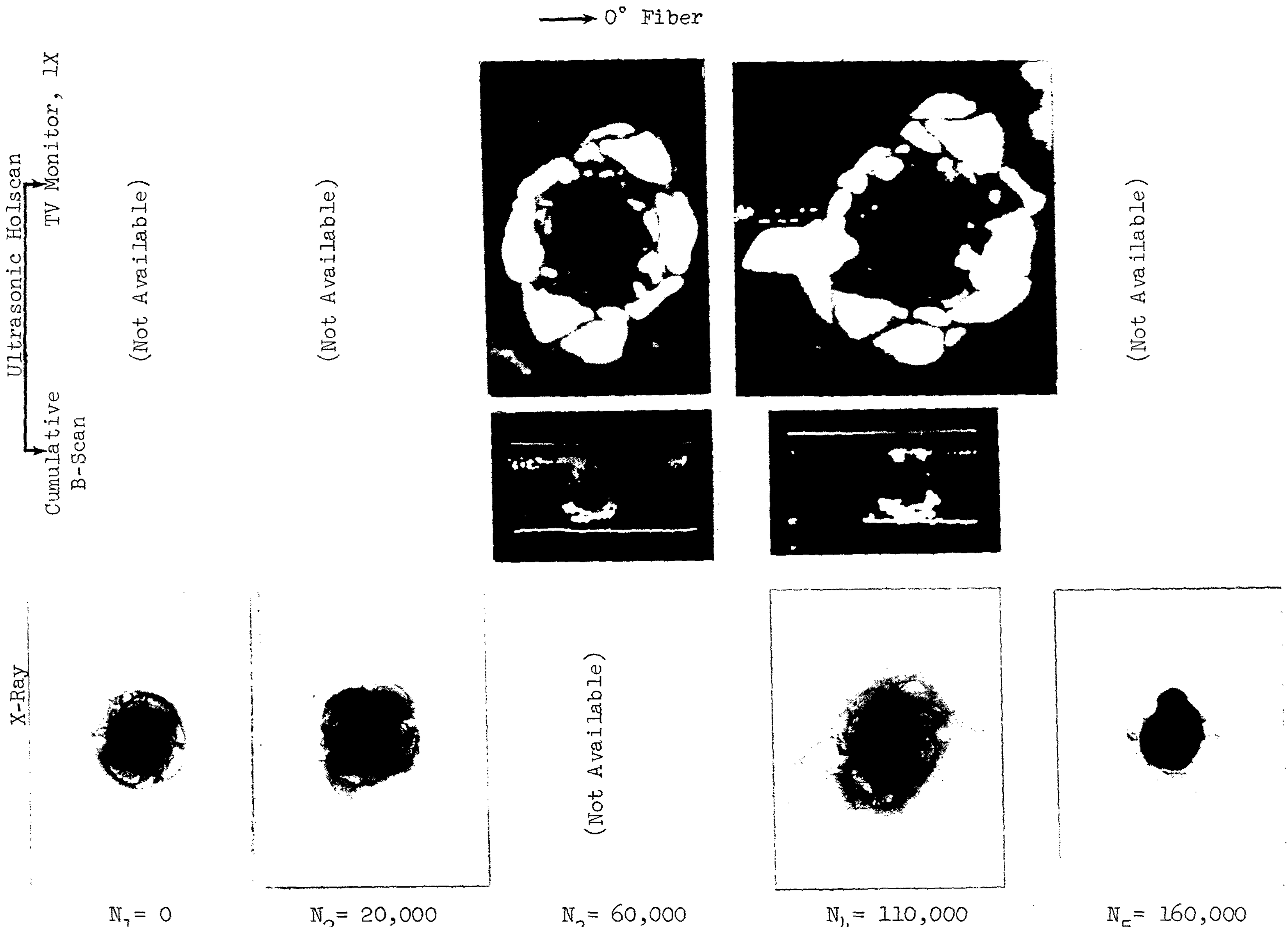

Figure 105. Fatigue Damage as Detected by Holscan and X-Ray for Specimen EB-13, 32-Ply Quasi-Isotropic Laminate, $R = -1$, $\sigma_{max} = 20$ ksi 138 MPa), $N_f = 392,584$ Cycles

cycle set intervals to permit a comparison to be made on the large damage growth indications.

In the X-ray series of photographs, there is an apparent peak in damage size at N_3 or N_4 at which point it begins to decrease. Twc possible explanations exist for this behavior. Since specimens (at the end of each cycle set, N_1, N_2, etc) were all X-rayed at the same time, it is possible that the X-ray technique for the last two cycle sets was inconsistent with that of the previous sets. At this time no variation in technique which could explain this behavior has been found since the same procedures and sequence were specified for all sets. The second possible explanation for this behavior is that as the fatigue damage continues something occurs which blocks the entrance of the TBE. This second explanation is supported by a continued decrease in damage indication size over two cycle sets rather than a complete loss of all damage indications. Inadequate removal of the molding clay from the hole is a possible source of variation, but does not appear to be visually significant.

In comparing the Holscan photographs with the X-rays a generally "good" correlation is found for both size and shape. (Note: Holscan photographs shown in the following figures are at a higher magnification than the X-ray photographs). In certain instances the correlation is extremely good, especially at cycle interval N_3. The correlation then tends to drop off in progressing from N_4 through N_5 due primarily to the previously noted behavior of the X-ray series.

Damage area was determined from both the X-ray and the Holscan photos plotted in Figures 106 through 111. These plots reflect the X-ray trend previously mentioned. Note should be made of the damage area correlations, especially in the earlier portions of the specimen lives. If the decreasing X-ray damage indications for N_4 and N_5 are discounted, the "small" data set remaining seems to suggest that damage size determination is roughly equivalent for both methods.

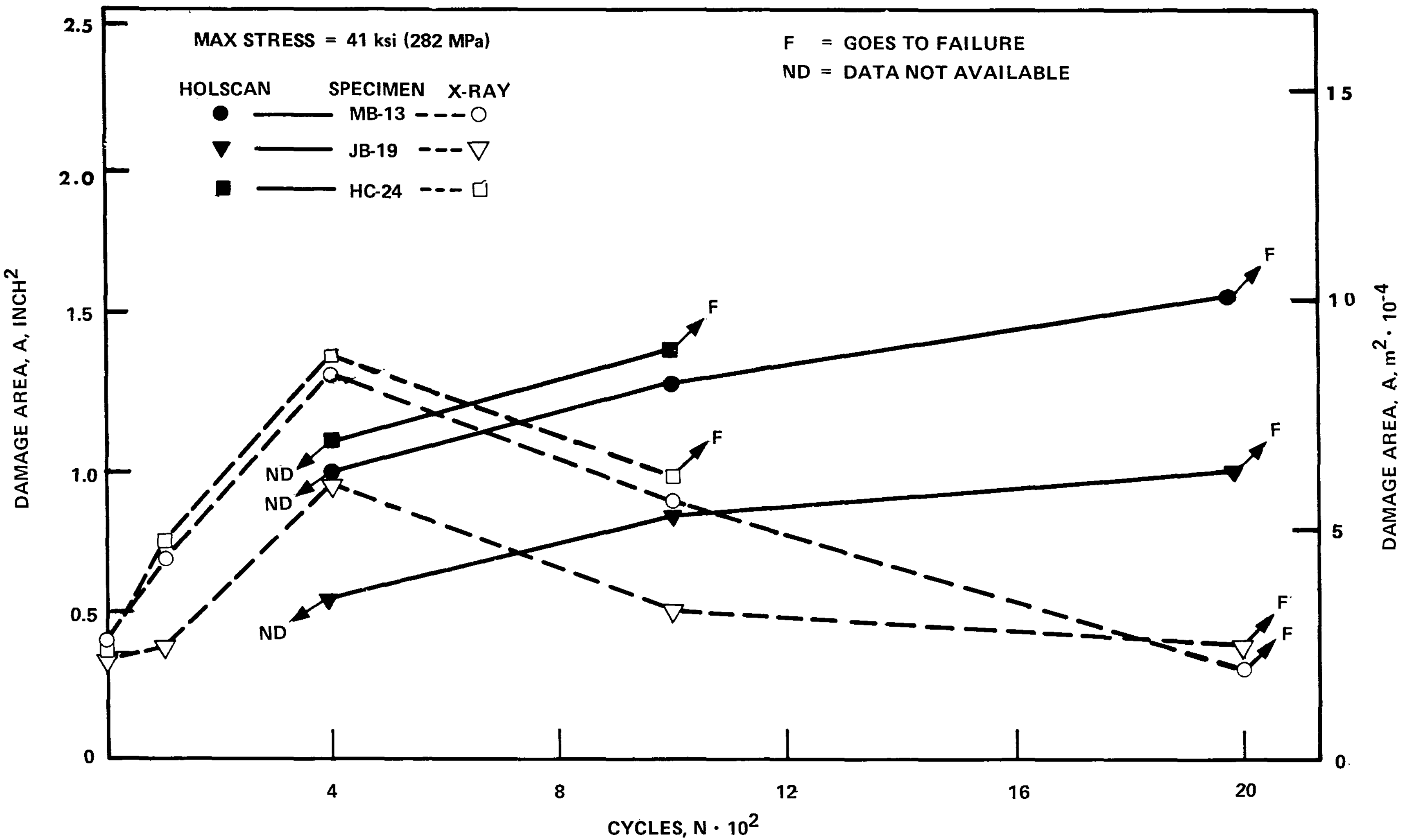

Figure 106. Damage Size Comparison From X-ray and Holscan Results, 24-Ply 67% 0° Fiber Laminate, σ_{max} = 41 ksi (282 MPa).

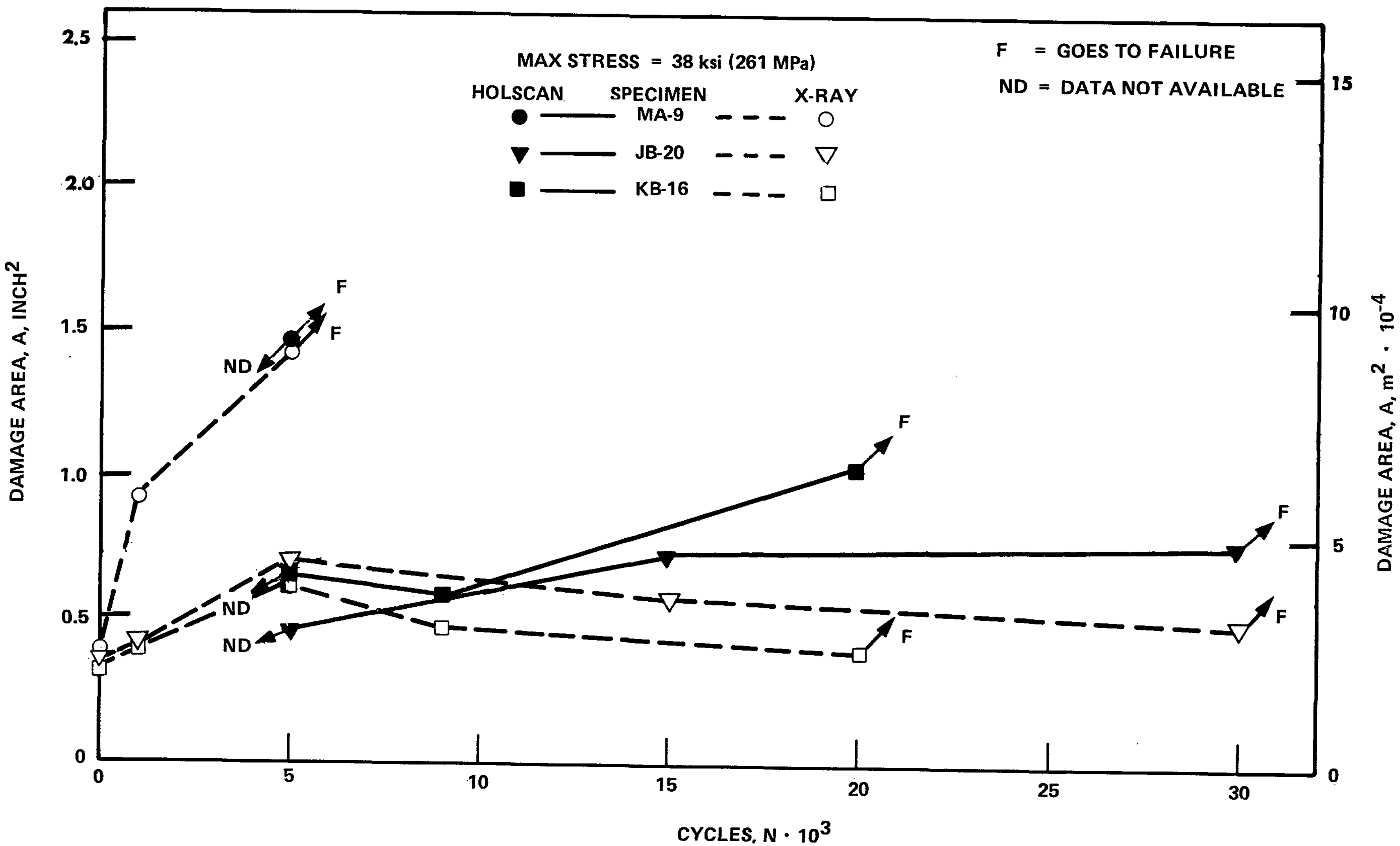

Figure 107. Damage Size Comparison From X-ray and Holscan Results, 24-Ply 67% 0° Fiber Laminate, σ_{max} = 38 ksi (261 MPa).

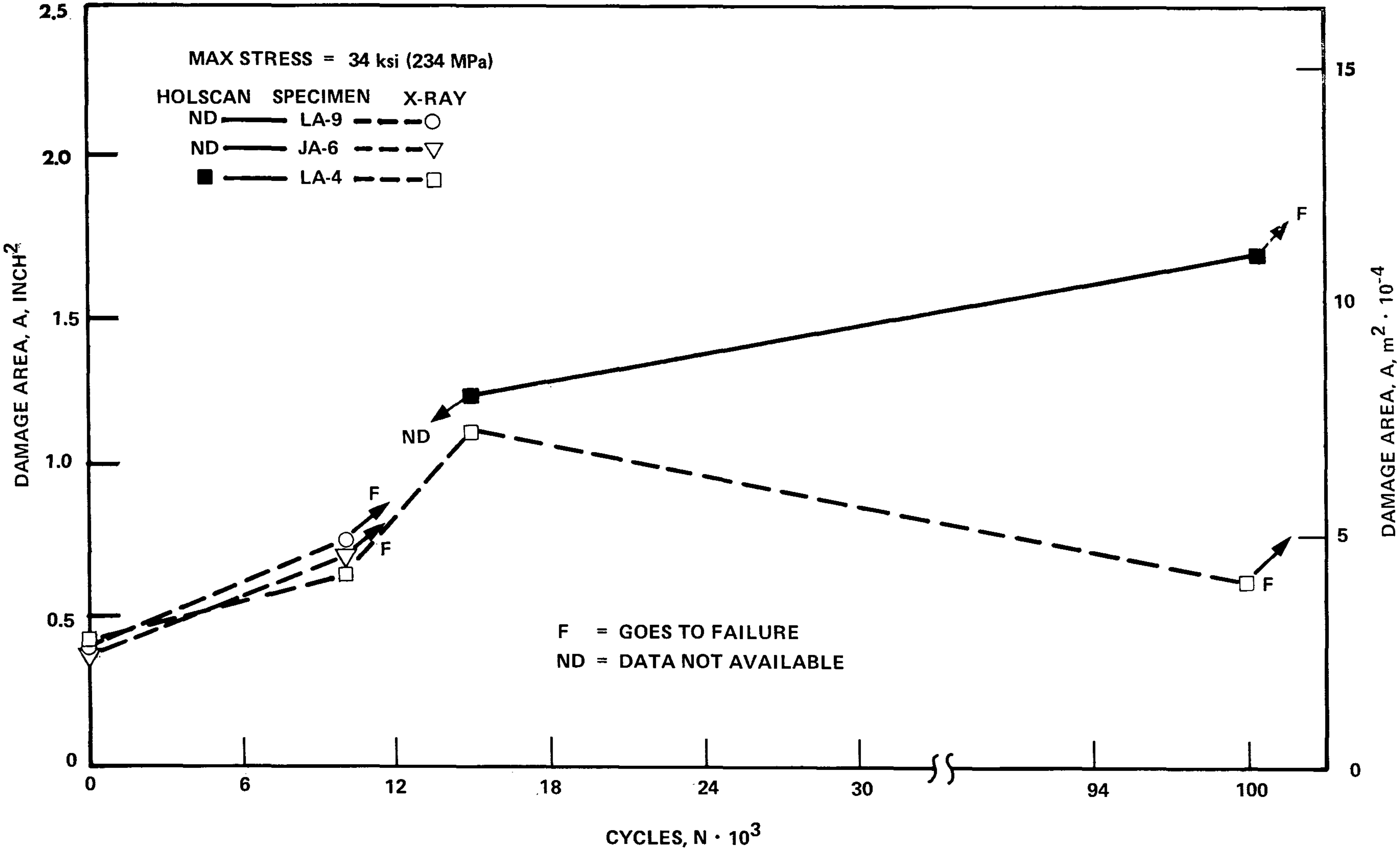

Figure 108. Damage Size Comparison From X-ray and Holscan Results, 24-Ply 67% 0° Fiber Laminate, σ_{max} = 34 ksi (234 MPa).

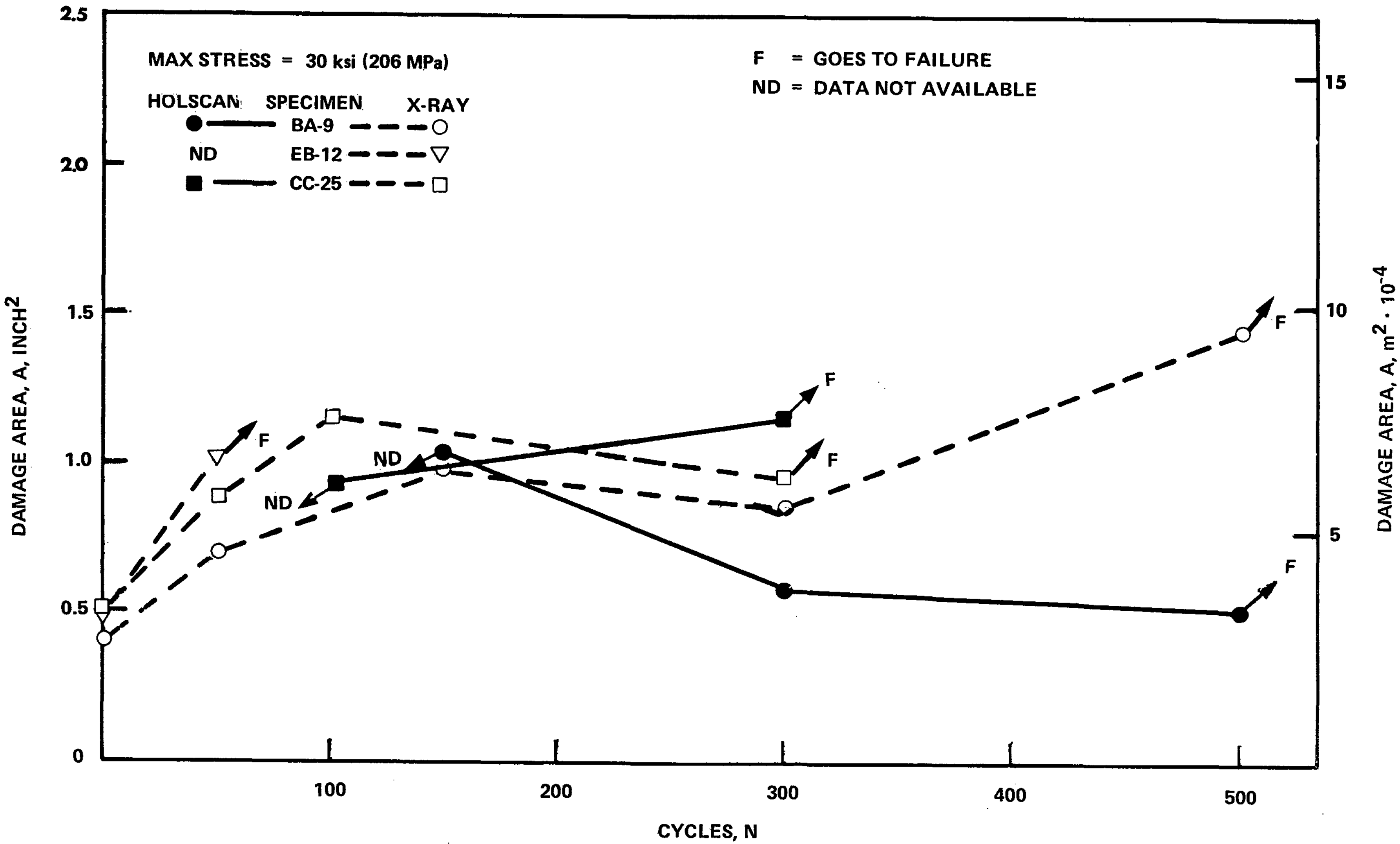

Figure 109. Damage Size Comparison From X-ray and Holscan Results, 32-Ply Quasi-Isotropic Laminate, σ_{max} = 30 ksi (206 MPa).

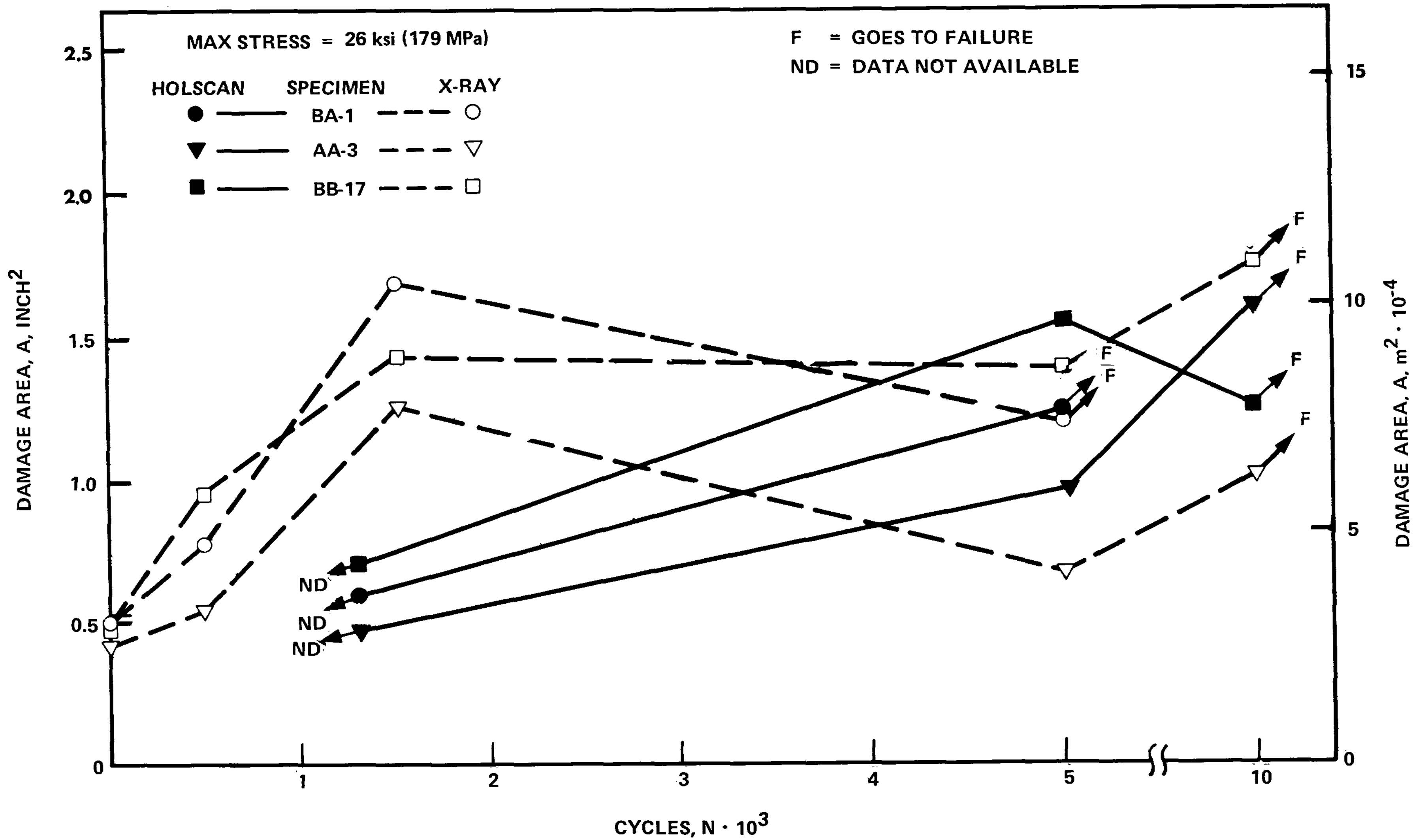

Figure 110. Damage Size Comparison From X-ray and Holscan Results, 32-Ply Quasi-Isotropic Laminate, σ_{max} = 26 ksi (179 MPa).

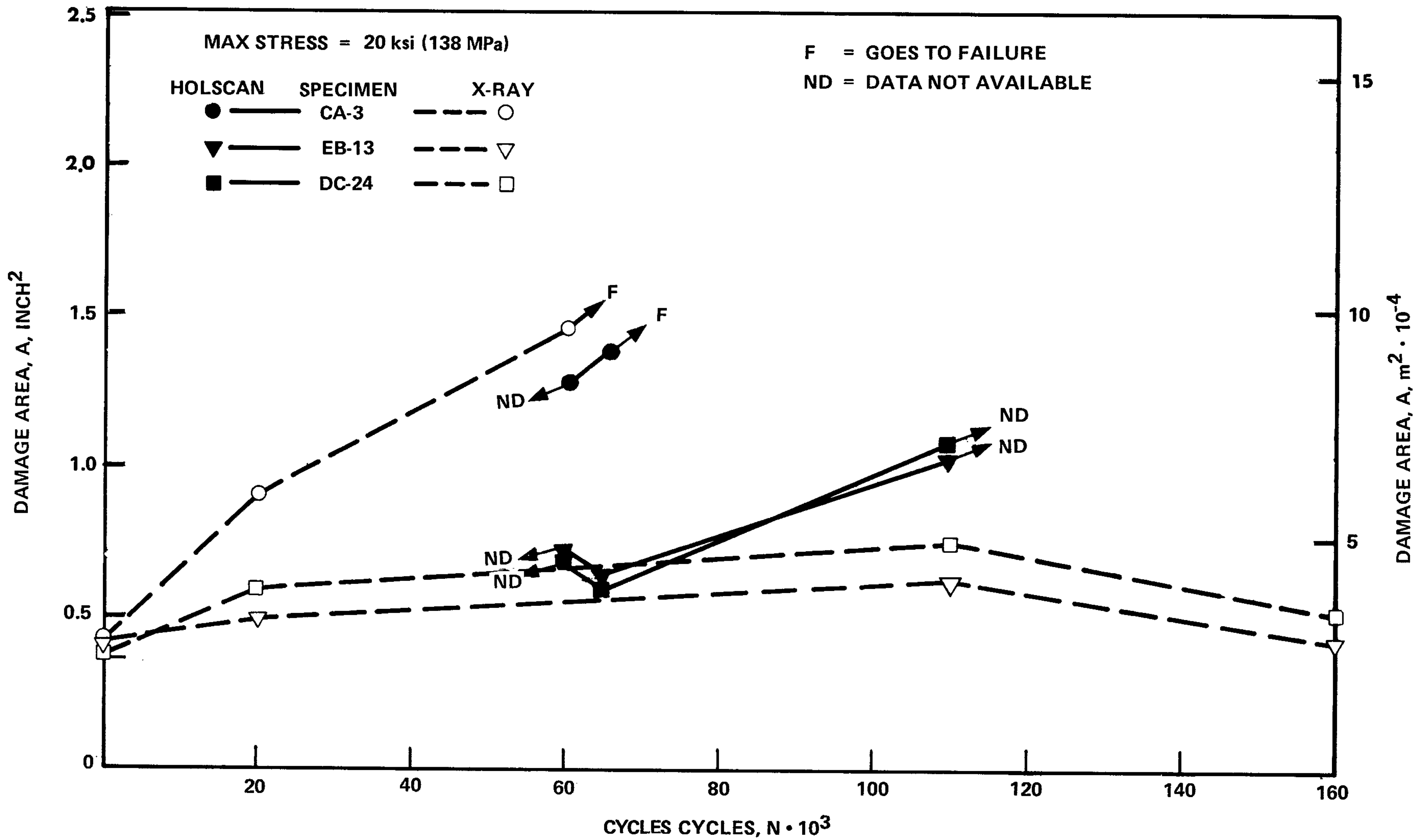

Figure 111. Damage Size Comparison From X-ray and Holscan Results, 32-Ply Quasi-Isotropic Laminate, σ_{max} = 20 ksi (138 MPa).

8.6 THE EFFECT OF TBE ON FATIGUE DAMAGE GROWTH

Damage area growth plots for baseline specimens are compared to those for specimens exposed to TBE in Figures 112 through 117 using the data obtained from the Holscan photographs to minimize the differences due to inspection method.

Growth data for TBE exposed 24-ply laminate specimens indicate the same general behavior as the baseline specimens at the same stress level when some allowance is made for the relative life of the specimens (i.e. typical scatter). Results for the 32-ply laminate show generally more erratic and inconsistent behavior for the TBE exposed specimens when compared to the baseline specimen data. Whether this is an indication of the true scatter in the results cannot be determined from the limited data set available.

From a consideration of all of these data sets, no clear evidence is seen to indicate any significant effect on the damage growth behavior due to the TBE exposure within the limitations of the current small data set.

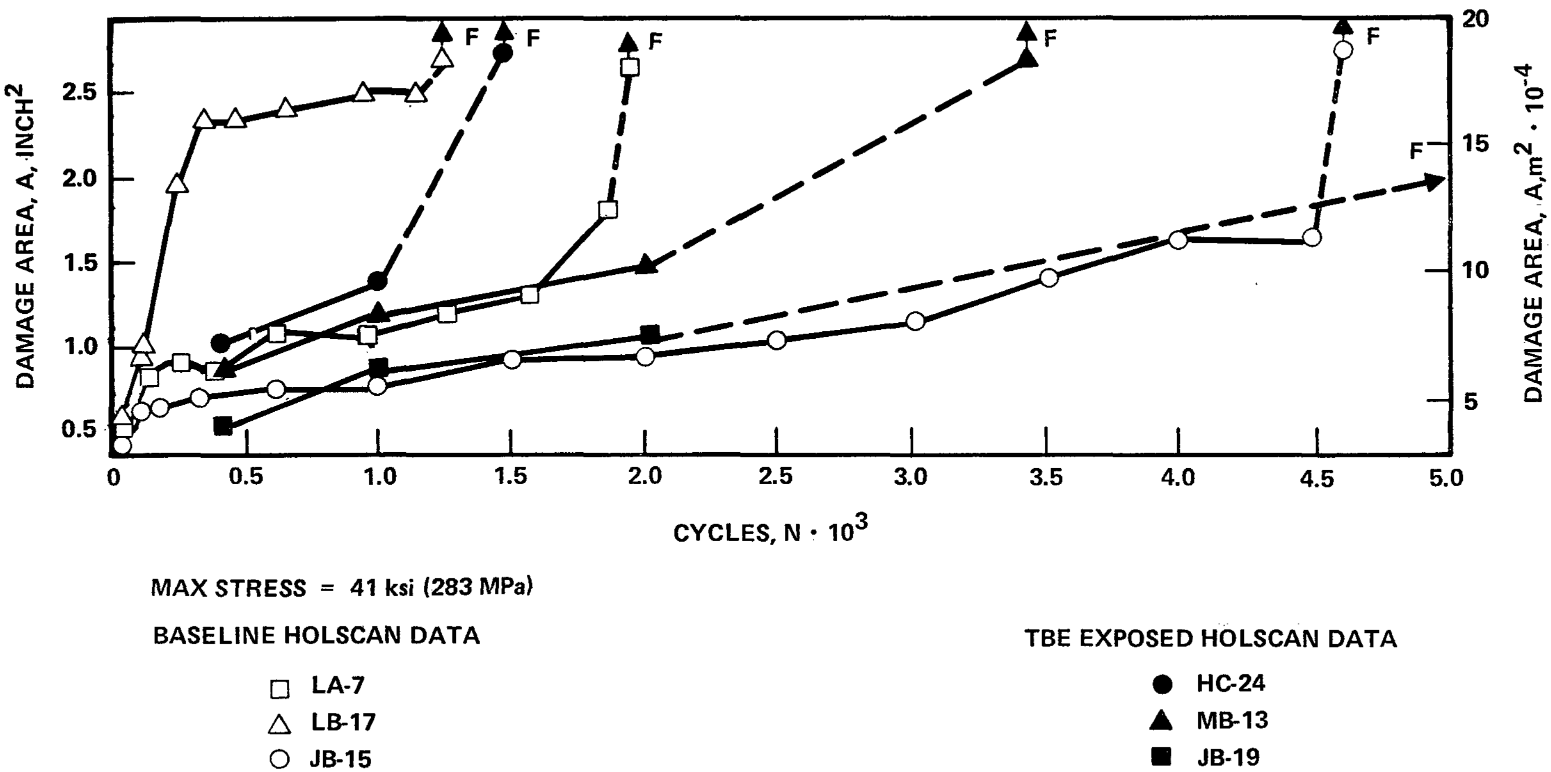

Figure 112. Comparison of Holscan Damage Size for Baseline Specimens and Specimens Exposed to TBE X-Ray Procedures, 24-Ply 67% 0° Fiber Laminate, σ_{max} = 41 ksi (283 MPa)

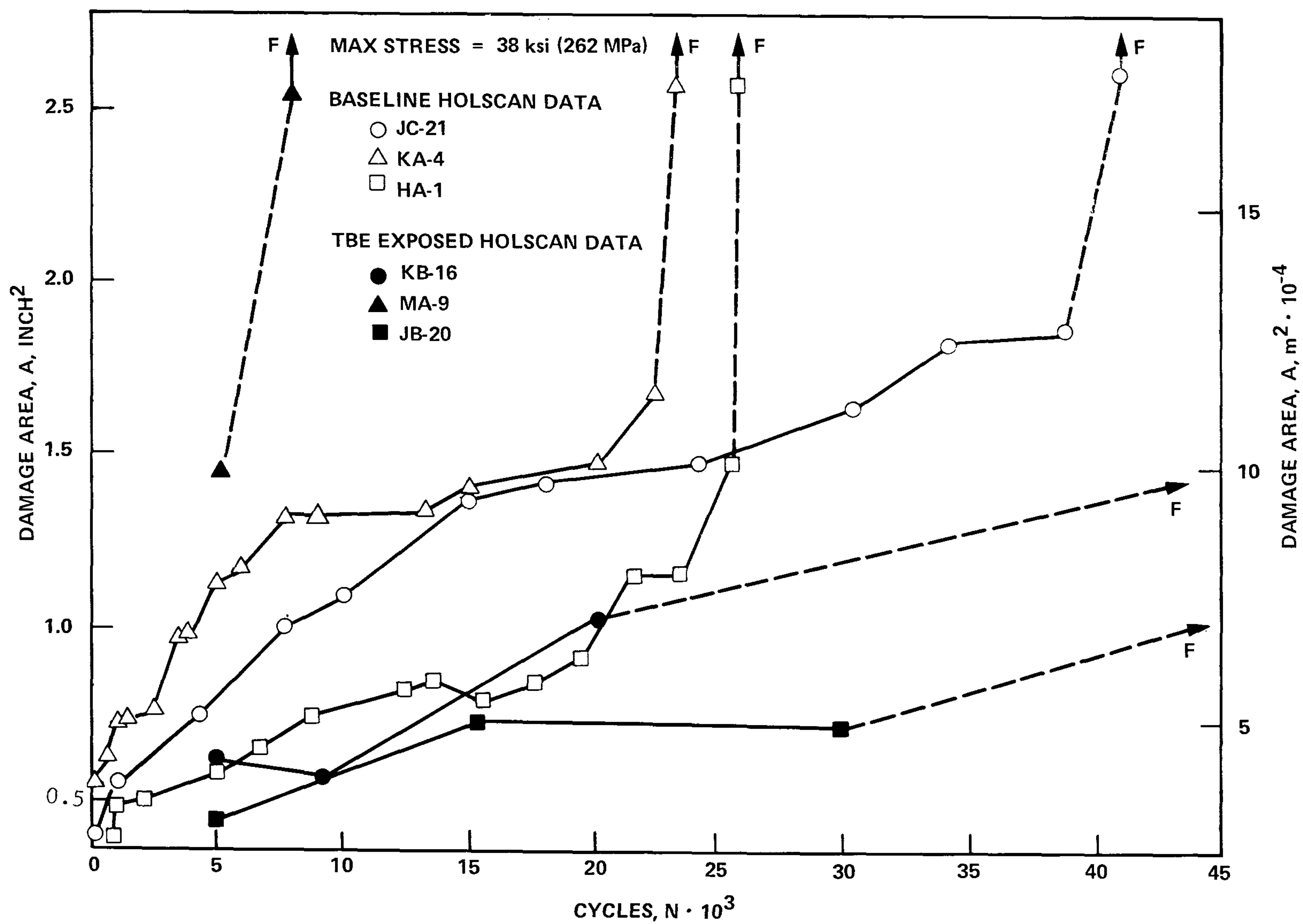

Figure 113. Comparison of Holscan Damage Size for Baseline Specimens and Specimens Exposed to TBE X-Ray Procedures, 24-Ply 67% 0° Fiber Laminate σ_{max} = 38 ksi (262 MPa).

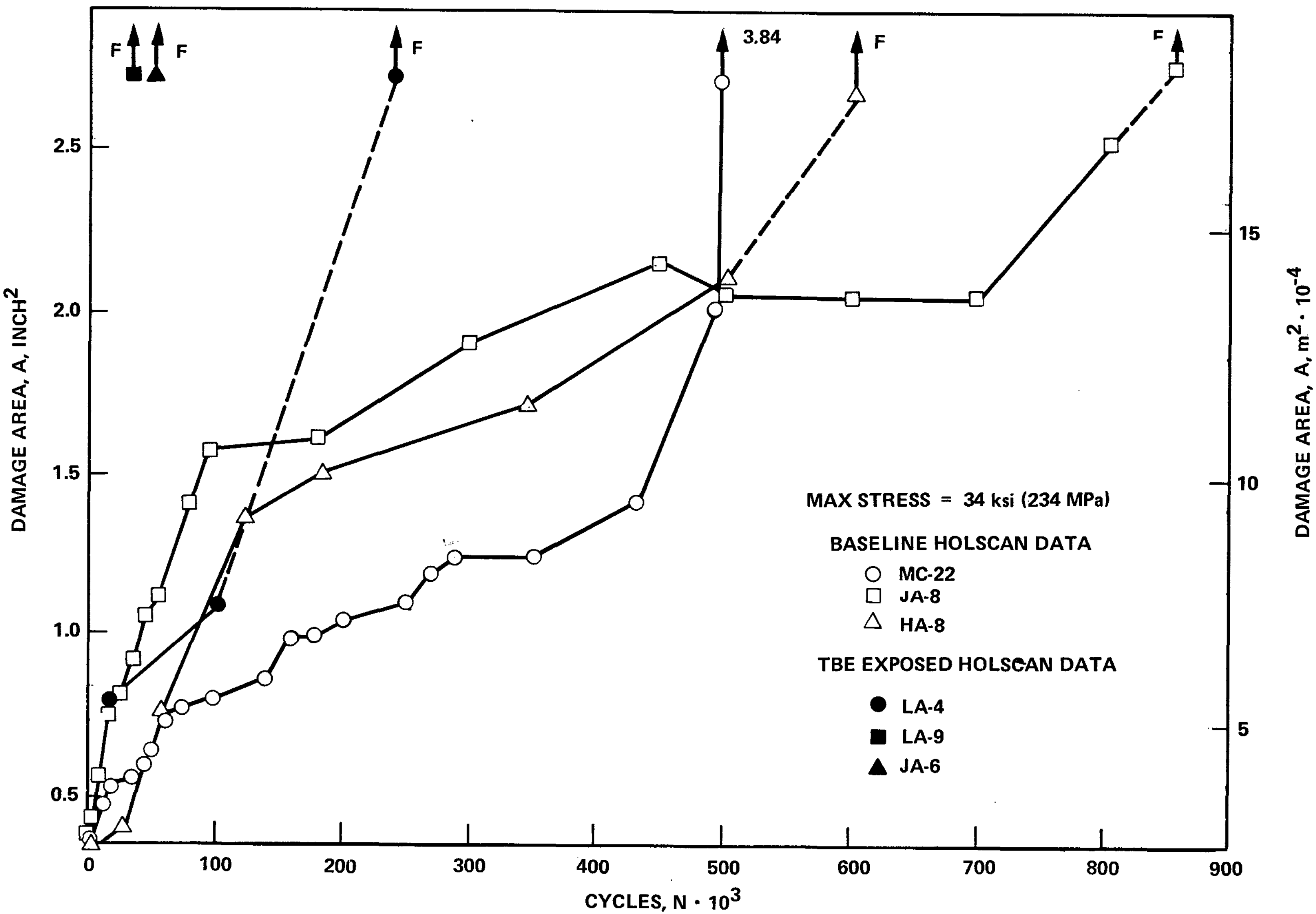

Figure 114. Comparison of Holscan Damage Size for Baseline Specimens and Specimens Exposed to TBE X-Ray Procedures, 24-Ply 67% 0° Fiber Laminate, σ_{max} = 34 ksi (234 MPa)

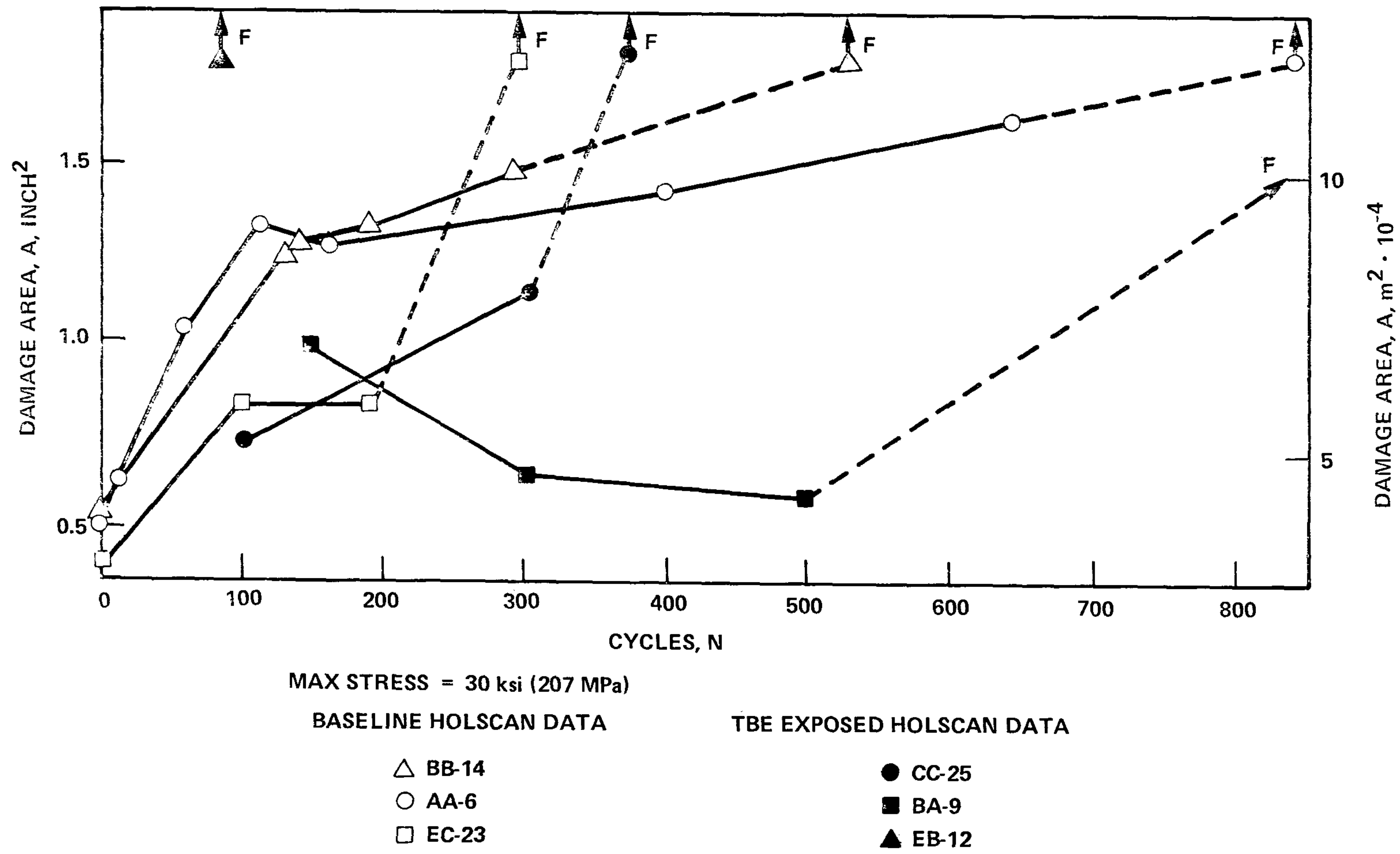

Figure 115. Comparison of Holscan Damage Size for Baseline Specimens and Specimens Exposed to TBE X-Ray Procedures, 32-Ply Quasi-Isotropic Laminate, σ_{max} = 30 ksi (207 MPa)

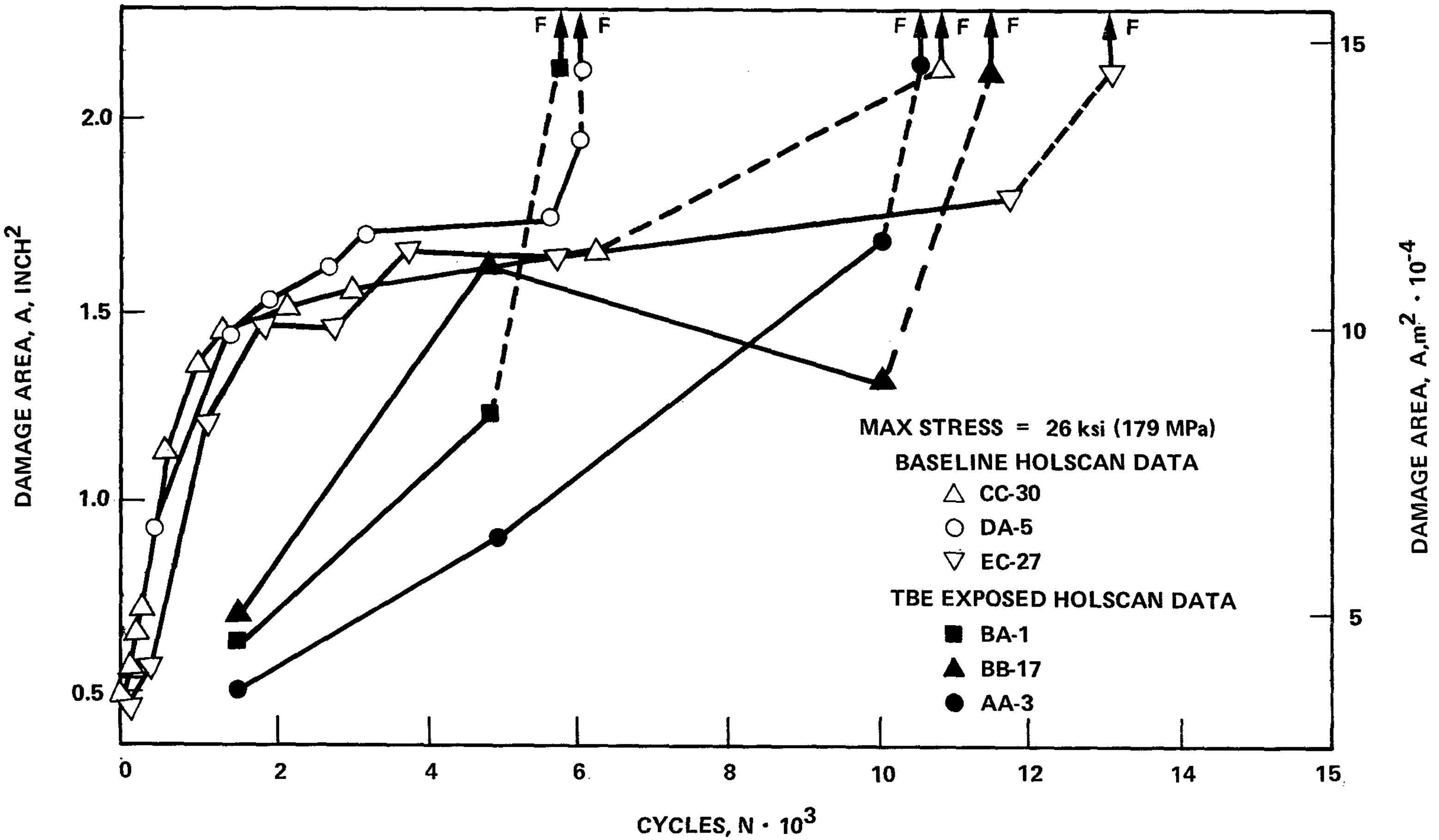

Figure 116. Comparison of Holscan Damage Size for Baseline Specimens and Specimens Exposed to TBE X-Ray Procedures, 32-Ply Quasi-Isotropic Laminate, σ_{max} = 26 ksi (179 MPa)

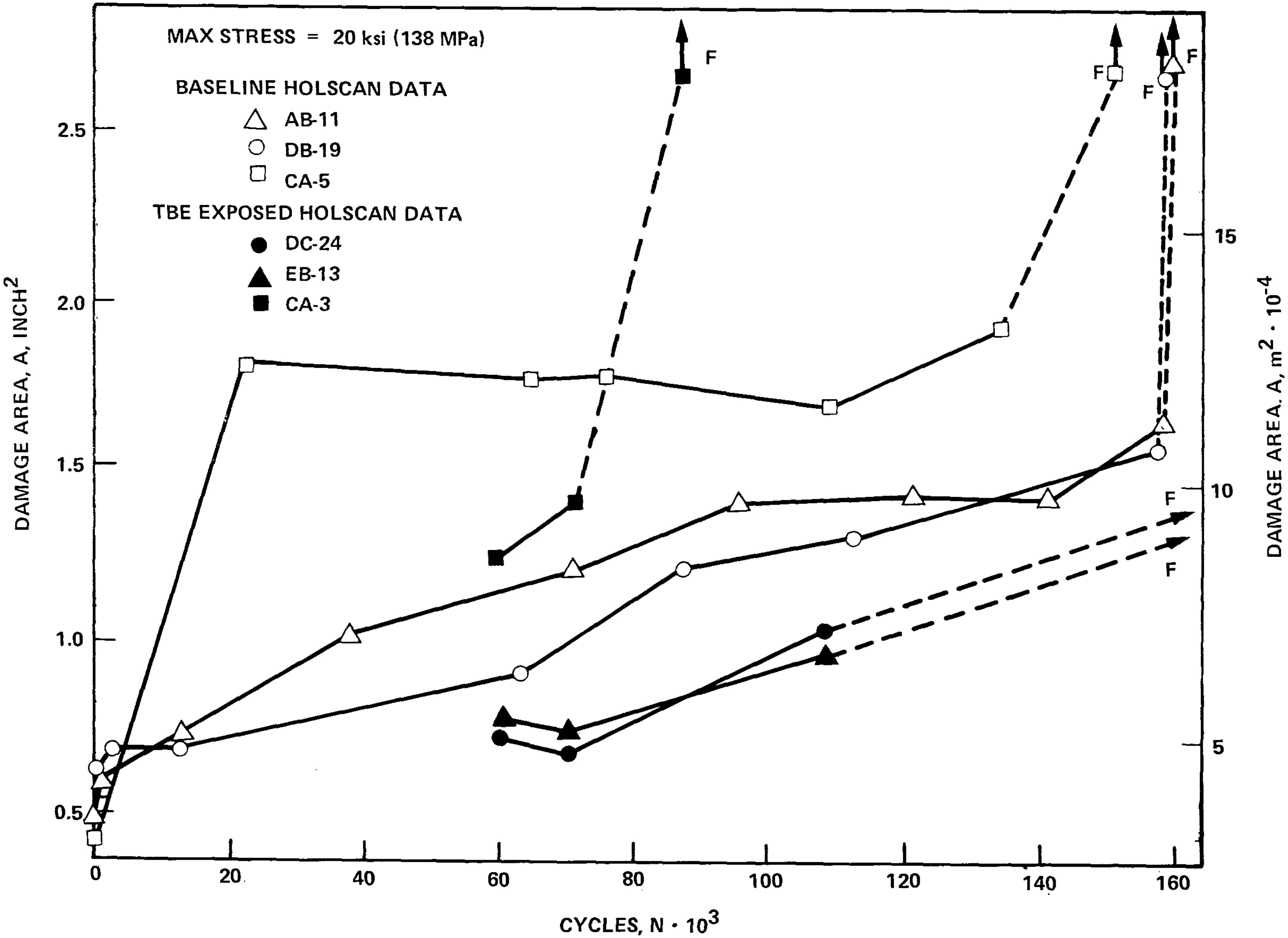

Figure 117. Comparison of Holscan Damage Size for Baseline Specimens and Specimens Exposed to TBE X-Ray Procedures, 32-Ply Quasi-Isotropic Laminate, σ_{max} = 20 ksi (138 MPa)

SECTION 9
SUMMARY OF TASK I RESULTS

In the following subsection, the results of each phase of the Task I study are summarized and the impact of the results on the selection of damage type, method of nondestructive damage monitoring and general approach to Task II: Damage Growth and Residual Strength Degradation Prediction, are presented.

9.1 INITIAL STATIC TENSION RESULTS

In the initial "as damaged" condition, the damaged hole condition was found to cause a significant ($\sim$ 48% for the 32-ply laminate and $\sim$53% for the 24-ply laminate) reduction in static strength. The initial impact damage condition showed no loss of static tension strength for the 24-ply laminate and from 0-25% reduction in strength for the 32-ply laminate, the results being strongly dependent on damage size with the greater reduction occuring at the larger end of the narrow range of damage sizes.

Initial static tension data indicate that while the damaged hole causes a major drop in static tension strength, the impact damage results in little if any reduction in strength.

9.2 INITIAL STATIC COMPRESSION RESULTS

As for the tension results, the damaged hole condition (tested using fatigue anti-buckling guides to provide maximum correlation with the fatigue results) showed a significant drop in static strength (note that since undamaged compression tests were not a part of this Task but rather are included in Task II, the undamaged tension strength is used as a reference). For the 24-ply laminate a relative loss of $\sim$ 69% was observed while the 32-Ply laminate revealed a $\sim$ 54% relative loss in strength.

The impact damaged 24-ply laminate displayed a similar loss in strength of $\sim$ 67% while the 32-ply laminate strength decreased only $\sim$ 30%. Thus both damage types produce a reduction in static compression strength of both laminates. The damaged hole resulting in a more severe loss of strength.

9.3 FATIGUE RESULTS

Results obtained to date for the 24-ply 67% 0° fiber damaged hole and impact damaged specimens exhibited a typical S-N curve for both damage types. Comparison of the results for the two damage types indicates distinct similarity in the general shape of the S-N curves.

Fatigue test results for the 32-ply quasi-isotropic specimens containing a single damaged hole again exhibit a typical S-N fatigue curve with what appears to be relatively small scatter, (i.e., less than an order of magnitude for any of three sets of triplicate specimens). Results for the impact damaged 32-ply quasi-isotropic specimens did not, however, show consistent damage growth or fatigue S-N behavior, a large number of the failures occurring away from the damage region. These data indicate that the impact conditions used for the 32-ply quasi-isotropic material produced damage too near the threshold size to result in a dominant cause of failure due to fatigue. Thus all damage/laminate conditions except the impact damaged 32-ply laminate condition were found to yield consistent S-N fatigue behavior.

9.4 DAMAGE GROWTH RESULTS

For the 24-ply 67% 0° fiber laminate specimens containing impact damage, the damage initially exhibited very slow growth (if any) for the first 60% to 70% of the specimen life. Growth then occured at an increasing rate during the later stages of the specimen life. The 24-ply 67% 0° fiber laminate specimens containing a damaged hole showed a somewhat different behavior. For these specimens the damage extended at a substantial rate during the initial 20% to 30% of specimen life. The damage growth rate then slowed to a significantly lower value until near the end of the specimen life where the rate of growth again accelerated until failure occurred.

Typical damage growth characteristics of the 32-ply quasi-isotropic laminate specimens containing a damaged hole at the higher stress levels revealed damage growth characteristics (as measured in terms of total damage area) comparable to those observed for the 24-ply damaged hole specimens in that the initial rapid damage growth slowed, progressing at the slower rate until near failure when the damage growth rate again accelerated.

9.4 DAMAGE GROWTH RESULTS (Continued)

At the lower stresses, however, the growth rates were more consistent over the entire life of the specimen. While few apparently valid failures were obtained for the impact damaged 32-ply laminates, the results showed a growth pattern similar to that observed for the 24-ply impact damaged specimens.

An important observation which is a factor in the examination of the significance of the damage growth data is the effect of the anti-buckling guide geometry. Carefull study of the data shows that at certain load ranges for a particular laminate/damage condition the damage may grow stably to the boundry of the anti-buckling guide opening. It is at this point the damage growth may be stopped or slowed due to the clamping effect of the guide. This in effect defines the limit of velocity of the damage growth rate data.

9.5 NDI COMPARISON RESULTS

A comparison of the TBE enhanced X-ray and Holscan ultrasonic method of monitoring and characterizing damage showed similar damage sizes on the subset of fatigue test coupons. Some variations in X-ray damage appearances were also observed with time after exposure to TBE. On occassion a loss of the X-ray indication was also observed, believed to be due to a failure to adequately remove the clay plug (needed to prevent water intrusion during the ultrasonic inspection) completely from the inside of the hole, thus blocking the entrance of the TBE. Test results showed no significant change in static compression strength following TBE examination. Effect of periodic TBE inspection also showed no significant effect on the subsequent fatigue behavior of the 32-ply laminate, but the results were less definitive for the 24-ply laminate where there is some indication of a possible shortening of the fatigue life at lower stresses. The limited sample size, however, is small enough that the results could be an artifact of the inherent scatter in fatigue which does appear to be greater for the TBE exposed specimen. Based on these results the Holscan ultrasonic unit was selected for use in subsequent tasks to characterize the damage.

9.6 CONCLUDING OBSERVATIONS

Based on the results of Task I, the preliminary Task II Test Plan was reviewed and finalized. The damage type selected for further study was that of a damaged hole since it provided generally more consistent behavior. The Holscan ultrasonic unit was also selected for use in Task II and III to monitor and characterize the damage. An overview of the Task II test plan is presented in the following section.

SECTION 10

TASK II TEST MATRIX OVERVIEW

Based on the results of Task I, the Task II Test Plan was prepared and was approved. This section presents a brief overview of the Task II Test Plan.

The approved Task II test matrix is presented in Table XXXV. Item 1 consists of basic panel Q.C. tension tests to assure panel quality. Items 2 and 4 are designed to provide the static tension and compression strength distribution of the damaged specimens. For both Items 2 and 4, fifteen replicates per test type/laminate condition will be tested to failure. A second set of four specimens per test type/laminate will be loaded to various percentages of ultimate and examined using ultrasonic inspection to define the damage zone growth characteristics. They will then be reloaded to failure and the results analyzed to determine if the unloading affected the final strength. Assuming no effect is seen in the nonparametric analysis, the combined sample set is thus 21 tests per laminate for both the tension and compression strength distributions. The strain rate tests in Item 3 are designed to provide additional information on the effect of higher strain rates on the fracture stress of the damaged laminates.

Twenty replicate specimens for each laminate will be fatigue tested to failure to determine the fatigue life distribution statistical parameters as shown in Item 5 of Table XXXV. A Holscan ultrasonic unit will be used to monitor the damage growth of each specimen at a minimum of ten times during its life. From these results a statistically based fatigue life distribution and damage growth rate distribution will be obtained. Also, five cycle levels will be selected for the residual strength study, based on the observed damage growth characteristics.

TABLE XXXV. TASK II TEST MATRIX

Item	Type of Test	Test Conditions	Replicate Per Condition	Data Required	Total Tests
1.	QA Tension Tests	2 Laminates, no damage = 2	2 per panel x 8 panels x 2 conditions	Basic Tensile Data	32
2.	Static Tension Strength Distribution	2 Laminates x 1 damage = 2	15 replicates x 2 conditions = 30	Damaged Tension Strength Distribution	30
			Plus 3 x 2 conditions = 6	Static Loading Damage Growth Characteristics	6
3.	Static Compression and Tension	2 Laminates x 1 damage = 2	5 replicates x 1 high strain rate x 2 tests x 2 conditions = 20	Strain rate effect	20
4.	Static Compression Strength Distribution	2 Laminates x 1 damage = 2	15 replicates x 2 conditions = 30	Damaged Compression Strength Distribution	30
			plus 3 x 2 conditions = 6	Static Load Damage Growth Characteristics	6
5.	Fatigue Life Distribution	2 Laminates x 1 damage = 2	20 replicates x 2 conditions = 40	Fatigue Life Distribution and Damage Growth Characteristics	40
6.	Tension Residual Strength	2 Laminates x 1 damage = 2	10 replicates x 5 cycles x 2 conditions = 100	Residual Strength at Five N Levels. Damage Zone Growth in Interval	100
7.	Compression Residual Strength	2 Laminates x 1 damage = 2	10 replicates x 5 cycles x 2 conditions = 100	Residual Compressive Strength at five N Levels. Damage Growth in Interval	100
8.	Destructive Inspection	2 Laminates x 1 damage = 2	3 replicates x 5 cycles x 2 conditions = 30	Destructive Definition of Damage Zone Characteristics	30
9.	Basic Material Tests	2 Laminates = 2	As required	As required by model	62
					456

Item 6, 7, and 8 constitute the residual strength portion of this task. Twenty-three specimens of each laminate will be initially inspected using the Holscan ultrasonic unit and then fatigue cycled to one of the five preselected cyclic N values, removed and again inspected using the Holscan. Three of the replicates will then be destructively analyzed to determine the damage zone characteristics. Both metallographic sectioning and matrix dissolution followed by SEM examination for fiber breakage will be used. Ten of the replicates will then be statically tested to failure in tension and in compression. This sequence will be repeated for each of the five selected cyclic N values. Item 9 tests are designed to provide basic material property data as required during the development of the model.

APPENDIX A

QUALITY CONTROL TEST RESULTS

APPENDIX A

QUALITY CONTROL TEST RESULTS

A.1 Chemical Analysis Results

Two samples for resin content analysis were randomly selected from the three resin content locations in each panel (i.e., one each from two of the three sub-panels). Triplicate specimens were then cut from each sample and the density, specific gravity, fiber content and resin contents determined.[29]

The procedures used to determine the reported values were as follows.

The fiber volume testing was conducted in accordance with ANSI/ ASTM D-3171-73, Procedure A: "Fiber Content of Reinforced Resin Composites," except as noted below:

a. Determinations for each strip were carried out in triplicate

b. Specimen size was approximately 1 gram rather than 0.3 grams.

c. The column of Nitric Acid used for digestion was increased from 30 milliliters to 100 milliliters because of the larger specimen mass used.

The specific gravity testing was conducted in accordance with ANSI/ ASTM D-792-66, Procedure A-1: "Specific Gravity and Density of Plastics by Displacement".

The resin content by weight was calculated using the following relationship:

$$\text{Resin, wt.\%} = \frac{w-W}{w} \times 100$$

Where: W = weight of fiber in composite

w = weight of initial composite specimen

All other calculations were conducted in accordance with the referenced specifications.

The following values were used for the fiber and resin densities:

$$D_f = 1.758 \text{ gm/ml}$$

$$D_r = 1.265 \text{ gm/ml}$$

Results of these analyses are reported in Tables A-1 and A-2. All results are within the range specified in the Quality Control Plan of 65 ± 2% for the fiber volume fraction and 1.58 ± 0.02 for the specific gravity results.

TABLE A-1. CHEMICAL ANALYSIS RESULTS

PANEL IDENTIFICATION		DENSITY gm/ml	AVERAGE DENSITY gm/ml, ±%	SPECIFIC GRAVITY	FIBER CONTENT BY WEIGHT %	AVERAGE FIBER CONTENT BY WEIGHT %	RESIN CONTENT, BY WEIGHT %	FIBER CONTENT BY VOLUME %
1TY1230DA	L	1.5708			71.98			
QC	M	1.5724	1.5730±0.17	1.5769	71.76	72.06±0.34	27.94	64.48±0.41
	R	1.5759			72.43			
1TY1230DB	L	1.5702			71.51			
QC	M	1.5693	1.5699±0.04	1.5738	71.41	71.59±0.24	28.41	63.93±0.24
	R	1.4703			71.86			
1TY1234MB	L	1.5714			71.40			
QC SPEC	M	1.4724	1.5726±0.08	1.5765	71.44	71.57±0.26	28.43	64.02±0.28
	R	1.5740			71.87			
1TY1234MC	L	1.5712			72.07			
QC SPEC	M	1.5721	1.5714±0.04	1.5753	71.52	71.73±0.30	28.27	64.12±0.29
	R	1.5709			71.61			
2TY1234LA	L	1.5742			72.60			
QC	M	1.5803	1.5760±0.24	1.5798	72.96	72.56±0.42	27.44	65.05±0.53
	R	1.5734			72.12			
2TY1234LB	L	1.5712			71.48			
QC SPEC	M	1.5755	1.5732±0.14	1.5774	72.00	71.84±0.32	28.16	64.29±0.38
	R	1.5739			72.05			
1TY1236JA	L	1.5712			71.16			
QC	M	1.5667	1.5670±0.26	1.5709	70.93	71.12±0.17	28.88	63.39±0.32
	R	1.5632			71.26			
1TY1236JB	L	1.5755			71.67			
QC	M	1.5727	1.5726±0.19	1.5764	71.41	71.41±0.27	28.59	63.88±0.36
	R	1.5696			71.14			

TABLE A-1. CHEMICAL ANALYSIS RESULTS (Continued)

PANEL IDENTIFICATION		DENSITY gm/ml	AVERAGE DENSITY gm/ml, ±%	SPECIFIC GRAVITY @23°C	FIBER CONTENT BY WEIGHT %	AVERAGE FIBER CONTENT BY WEIGHT %	RESIN CONTENT BY WEIGHT %	FIBER CONTENT BY VOLUME %
2TY1227CA	L	1.5766			73.32			
QC	M	1.5760	1.5746±0.19	1.5784	72.56	72.90±0.39	27.10	65.29±0.47
	R	1.5712			72.82			
2TY1227CC	L	1.5685			72.76			
	M	1.5764	1.5735±0.28	1.5774	73.13	73.11±0.34	26.89	65.44±0.49
	R	1.5757			73.43			
1TY1228BA	L	1.5802			73.31			
QC	M	1.5800	1.5794±0.08	1.5833	73.54	73.26±0.30	26.74	65.82±0.32
	R	1.5779			72.94			
1TY1228BB	L	1.5816			73.35			
QC	M	1.5810	1.5809±0.05	1.5848	73.24	73.22±0.15	26.78	65.84±0.17
	R	1.5800			73.06			
2TY1228AA	L	1.5821			72.76			
QC	M	1.5802	1.5790±0.25	1.5829	73.13	73.11±0.34	26.89	65.67±0.47
	R	1.5746			73.43			
2TY1228AC	L	1.5758			72.36			
QC	M	1.5761	1.5758±0.02	1.5797	72.57	72.58±0.23	27.42	65.06±0.22
	R	1.5756			72.81			
1TY1229EB	L	1.5644			71.68			
	M	1.5653	1.5658±0.11	1.5697	71.57	71.49±0.24	28.51	63.67±0.28
	R	1.5676			71.22			
1TY1229EC	L	1.5749			72.24			
	M	1.5719	1.5727±0.13	1.5766	71.59	71.74±0.44	28.26	64.18±0.48
	R	1.5713			71.40			

TABLE A-1. CHEMICAL ANALYSIS RESULTS (Continued)

PANEL IDENTIFICATION		DENSITY gm/ml	AVERAGE DENSITY gm/ml, ±%	SPECIFIC GRAVITY	FIBER CONTENT BY WEIGHT %	AVERAGE FIBER CONTENT BY WEIGHT %	RESIN CONTENT BY WEIGHT %	FIBER CONTENT BY VOLUME %
2TY1236KB	L	1.5735			71.87			
QC	M	1.5774	1.5760±0.14	1.5798	72.38	72.05±0.28	27.95	64.59±0.34
	R	1.5770			71.91			
2TY136KC	L	1.5785			72.84			
QC SPEC	M	1.5815	1.5785±0.19	1.5824	73.03	72.81±0.24	27.19	65.38±0.34
	R	1.5756			72.55			
1TY1238HA	L	1.5765			72.97			
QC	M	1.5844	1.5805_0.25	1.5844	73.60	73.24±0.33	26.76	65.85±0.46
	R	1.5807			73.14			
1TY1238HB	L	1.5789			72.68			
QC SPEC	M	1.5787	1.5785±0.03	1.5824	72.37	72.38±0.29	27.62	65.00±0.28
	R	1.5779			72.10			

TABLE A-2. VOID CONTENT RESULTS

IDENTIFICATION	VOID CONTENT %
2TY1227CA	0.98 ± 1.02
2TY1227CC	1.11 ± 1.01
1TY1228BA	0.79 ± 0.72
1TY1228BB	0.69 ± 0.37
2TY1228AA	0.76 ± 0.98
2TY1228AC	0.78 ± 0.51
1TY1229EB	1.04 ± 0.62
1TY1229EC	0.69 ± 1.07
1TY1230DA	0.78 ± 0.89
1TY1230DB	0.81 ± 0.55
1TY1234MB	0.64 ± 0.63
1TY1234MC	0.76 ± 0.68
2TY1234LA	0.76 ± 1.14
2TY1234LB	0.69 ± 0.83
1TY1236JA	0.83 ± 0.62
1TY1236JB	0.58 ± 0.97
2TY1236KB	0.59 ± 0.74
2TY1236KC	0.69 ± 0.88
1TY1238HA	0.72 ± 0.96
1TY1238HB	0.54 ± 0.65

APPENDIX B

INITIAL DAMAGE
DIMENSIONS

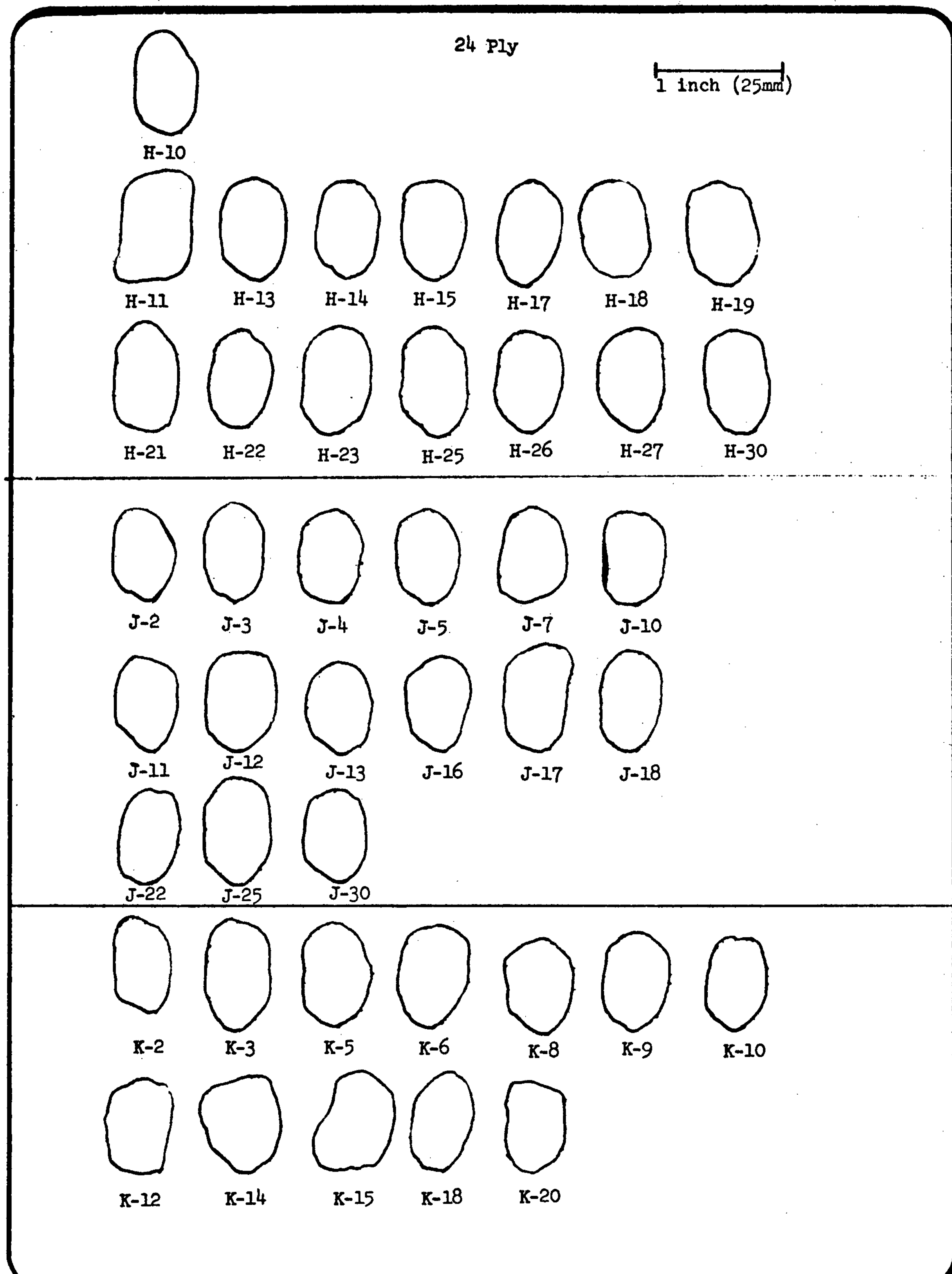

Figure 1a. Initial Impact Damage Dimensions for 67% 0° Fiber 24-Ply Laminate Specimens

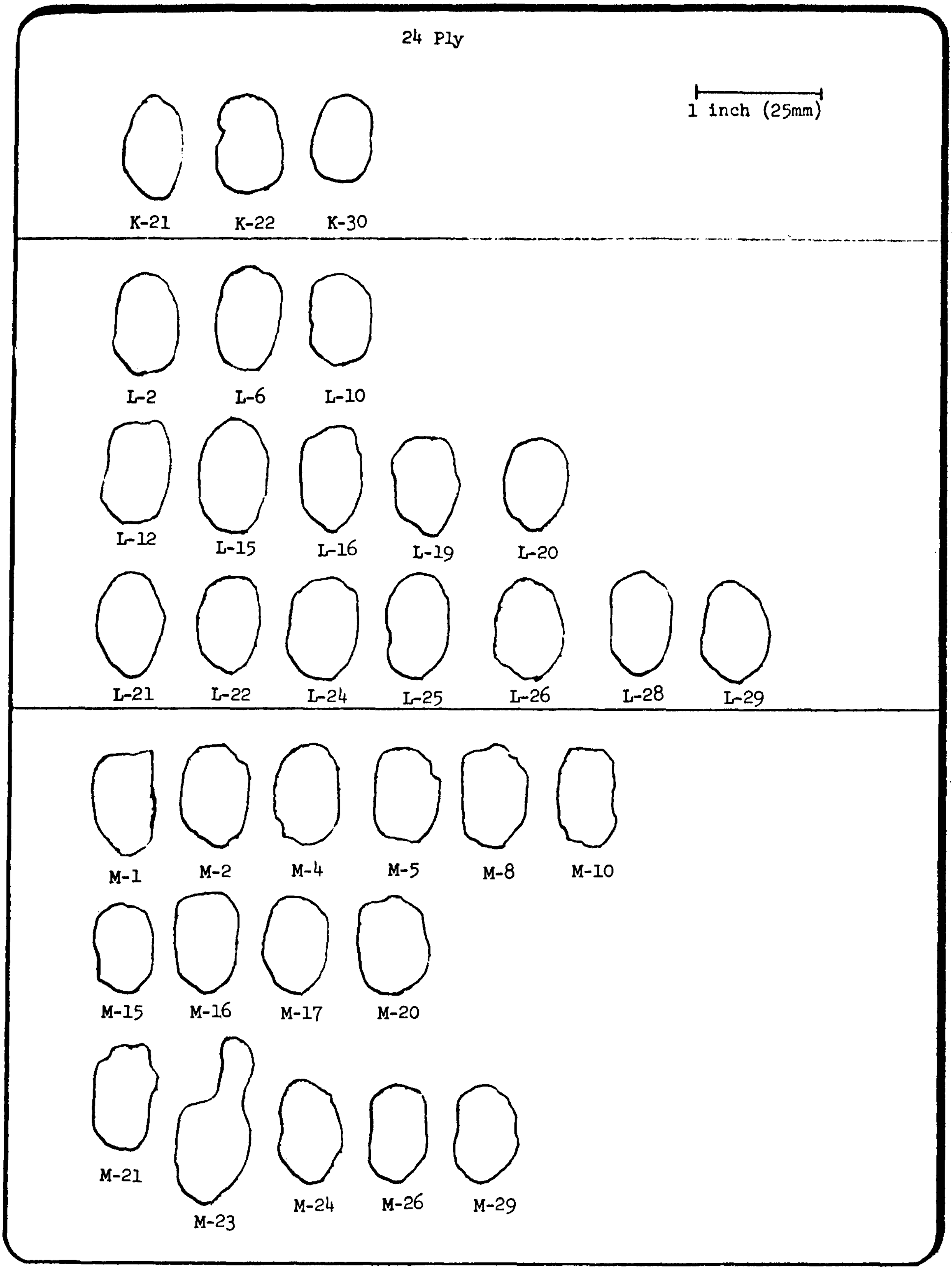

Figure 1b. Initial Impact Damage Dimensions for 67% 0° Fiber 24-Ply Laminate Specimens

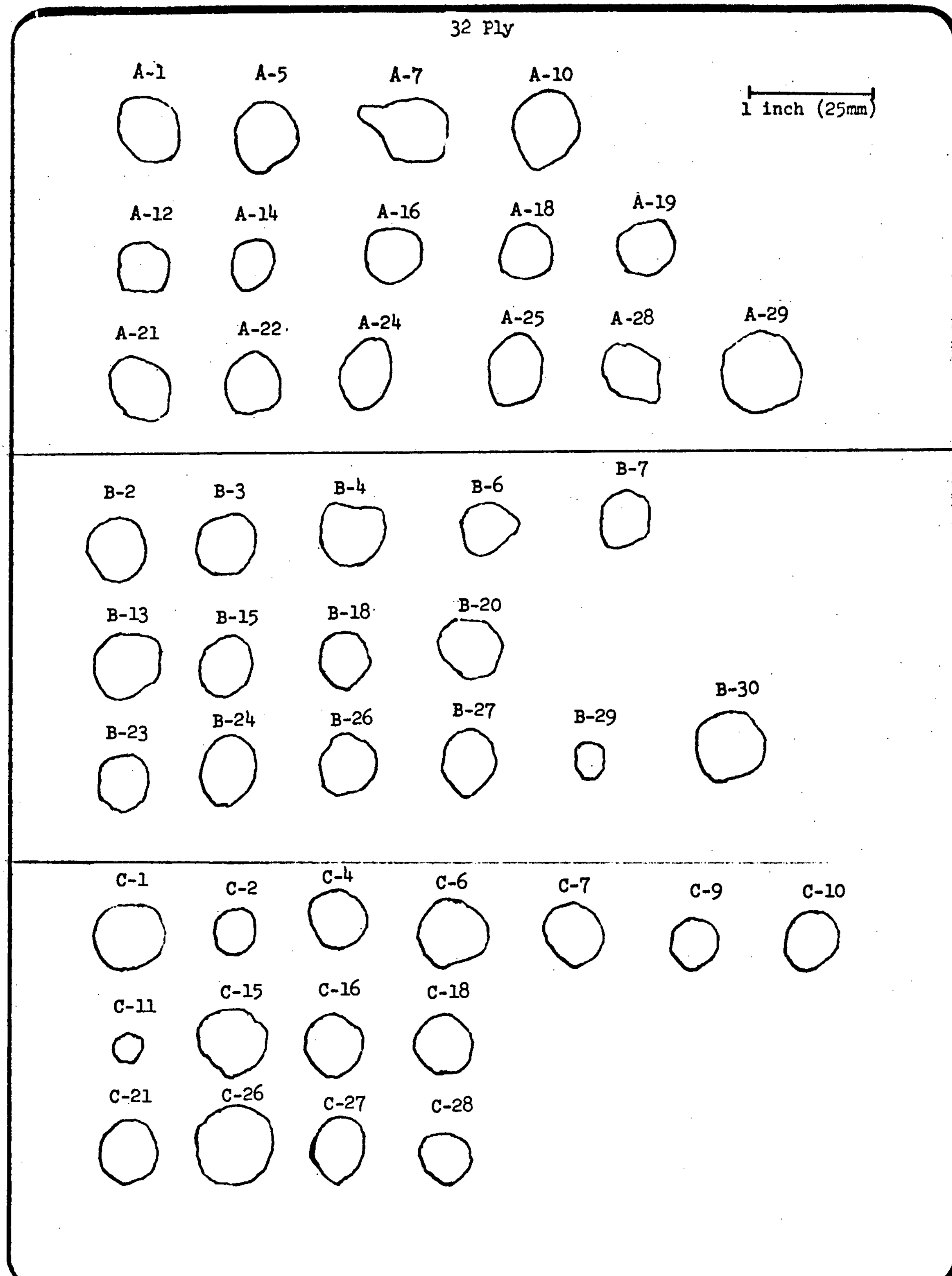

Figure 2a. Initial Impact Damage Dimensions for Quasi-isotropic 32-Ply Laminate Specimens

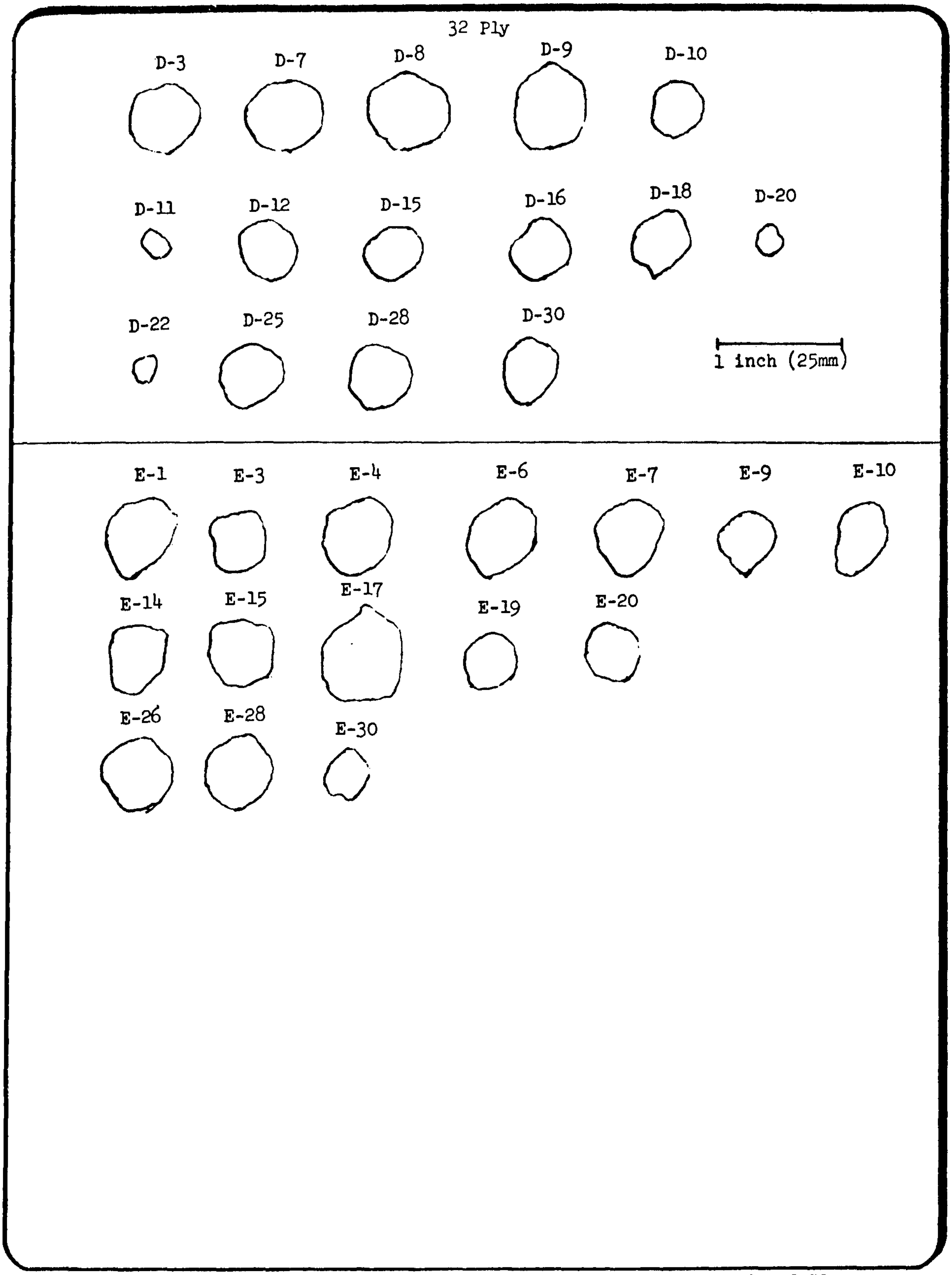

Figure 2b. Initial Impact Damage Dimensions for Quasi-isotropic 32-Ply Laminate Specimens

TV MONITOR, 2X

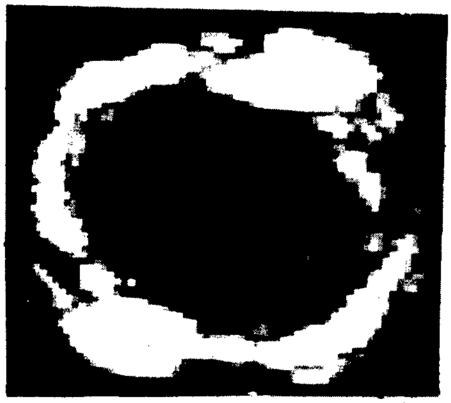

HA-6

IA-15

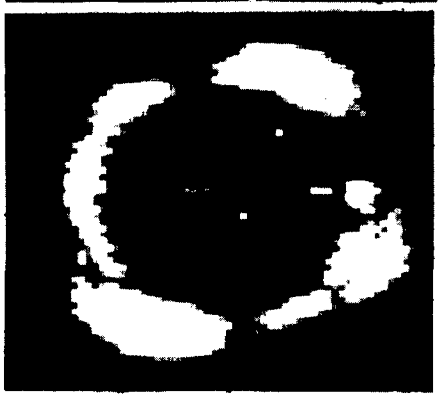

JC-26

IA-27

KB-19

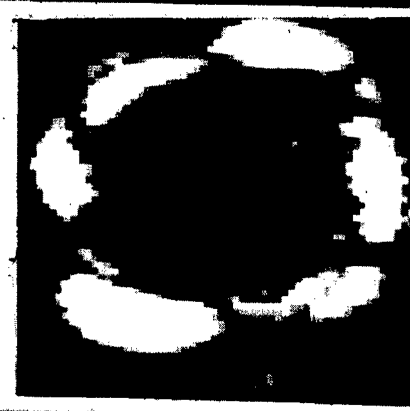

MA-6

KC-23

Figure 3. Typical Initial Damages for 24-Ply Laminate Specimens Tested in Static Tension

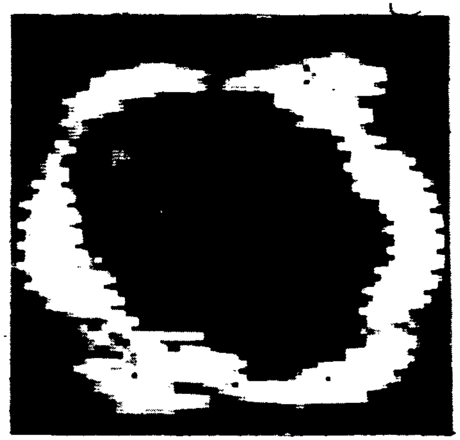

H-6

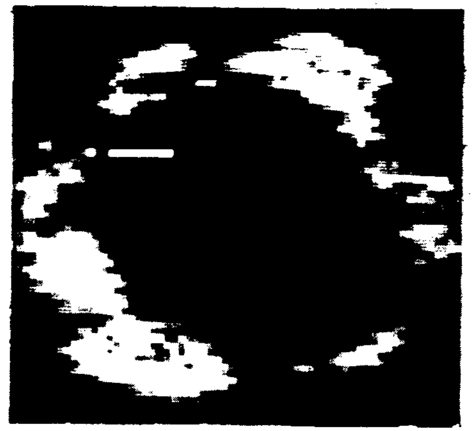

HB-16

J-24

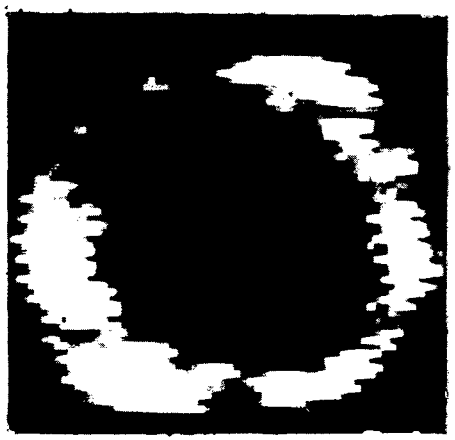

L-3

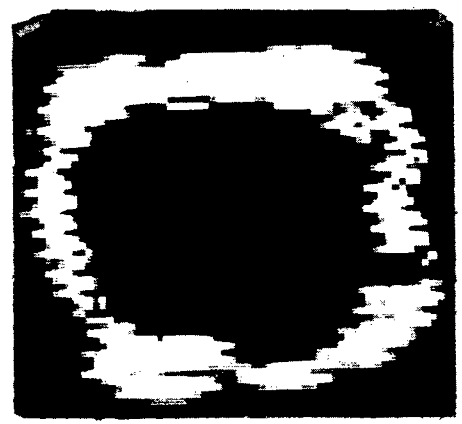

L-18

TV MONITOR, 2X

Figure 4. Typical Initial Damages for 24-Ply Laminate Specimens Tested in Static Compression

TV MONITOR, 2X

AB-20

AC-23

BA-10

Figure 5a. Typical Initial Damages for 32-Ply Laminate Specimens Tested in Static Tension

TV MONITOR, 2X

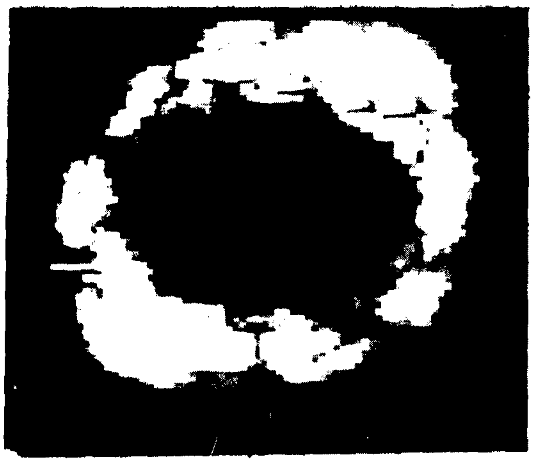

BA-5

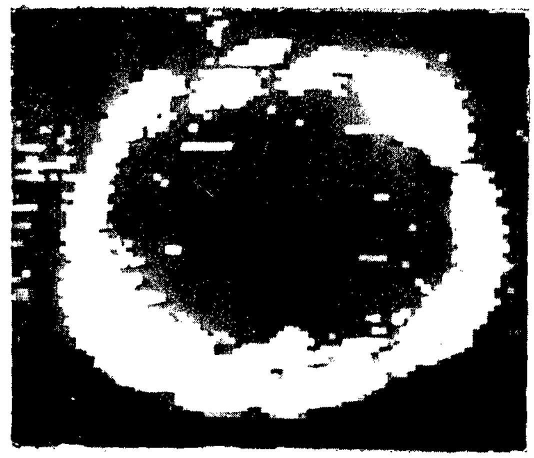

DC-12

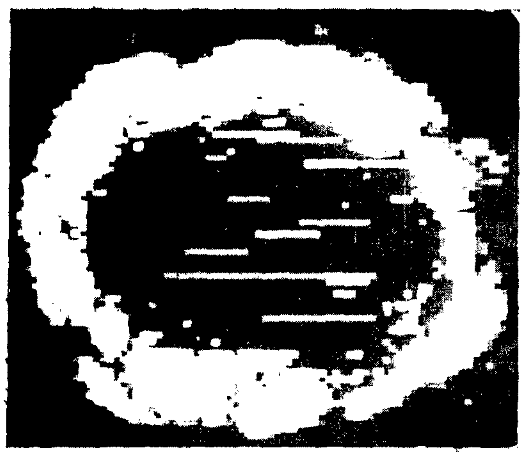

CC-23

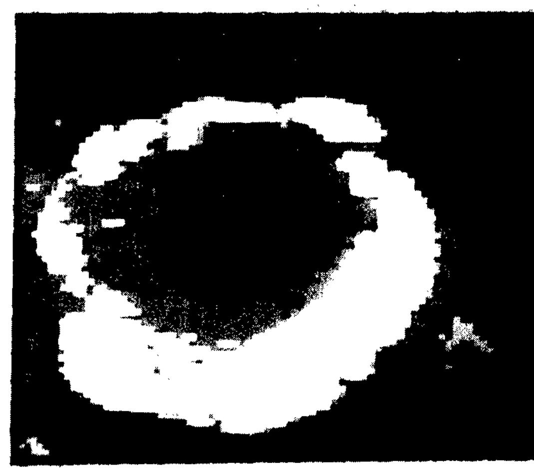

EB-16

CC-29

EC-12

Figure 5b. Typical Initial Damages for 32-Ply Laminate Specimens Tested in Static Tension

TV MONITOR, 2X

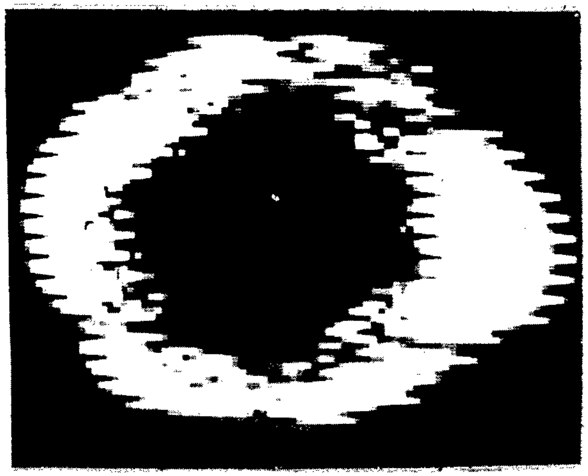

A 9

A-17

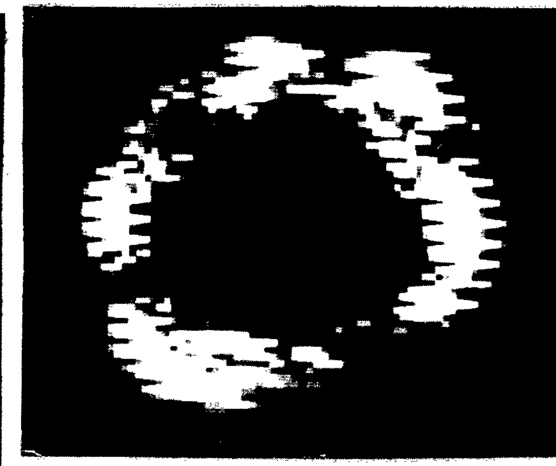

B-21

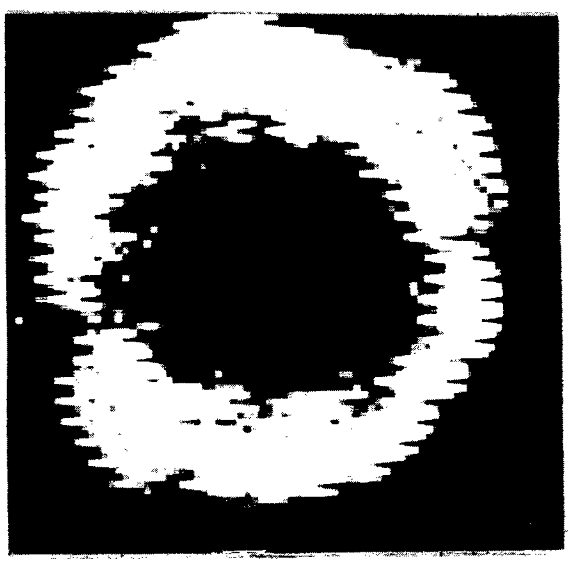

C-20

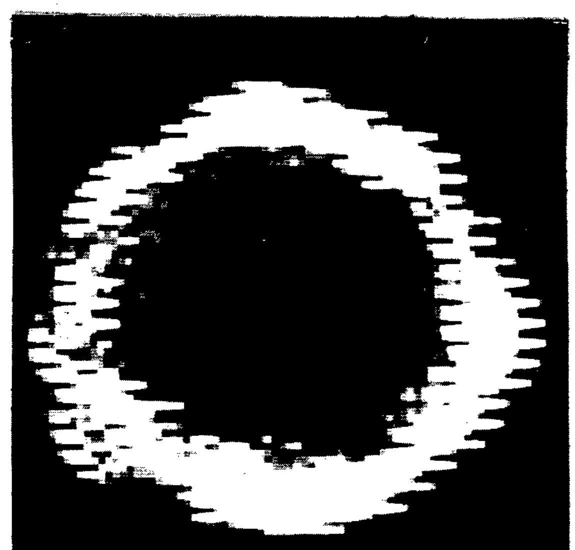

D-13

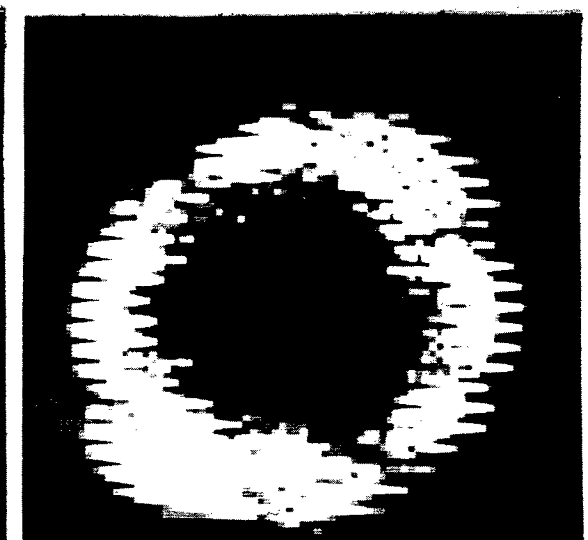

E-22

Figure 6. Typical Initial Damages for 32-Ply Laminate Specimens Tested in Static Compression

APPENDIX C

TYPICAL DAMAGE GROWTH RESULTS

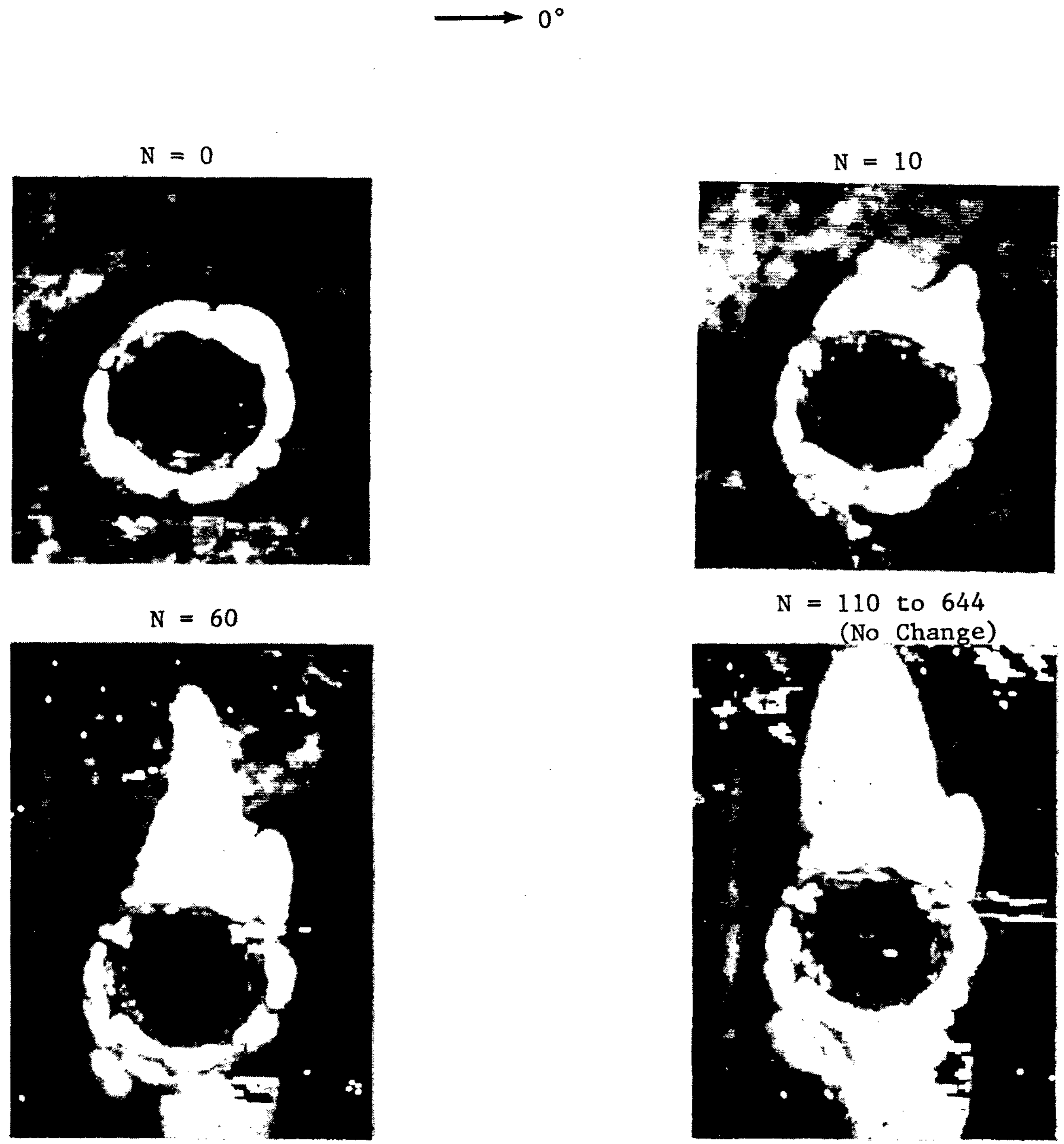

Figure 1. Damage Growth Results for 32 ply Specimen AA-6 Containing a Damaged Hole. Maximum Stress = 30 ksi (207 MPa), R = -1

See Figure 91 - In Text

Figure 2. Damage Growth Results for 32-ply Specimen DA-5 Containing a Damaged Hole, Maximum Stress = 26 ksi (179 MPa), R = -1

See Figure 92 - In Text

Figure 3. Damage Growth Results for 32 ply Specimen BC-28 Containing a Damaged Hole. Maximum Stress = 23 ksi (158 MPa), R = -1

See Figure 93 - In Text

Figure 4. Damage Growth Results for 32 ply Specimen CA5 Containing a Damaged Hole. Maximum Stress = 20 ksi (138 MPa), R = -1

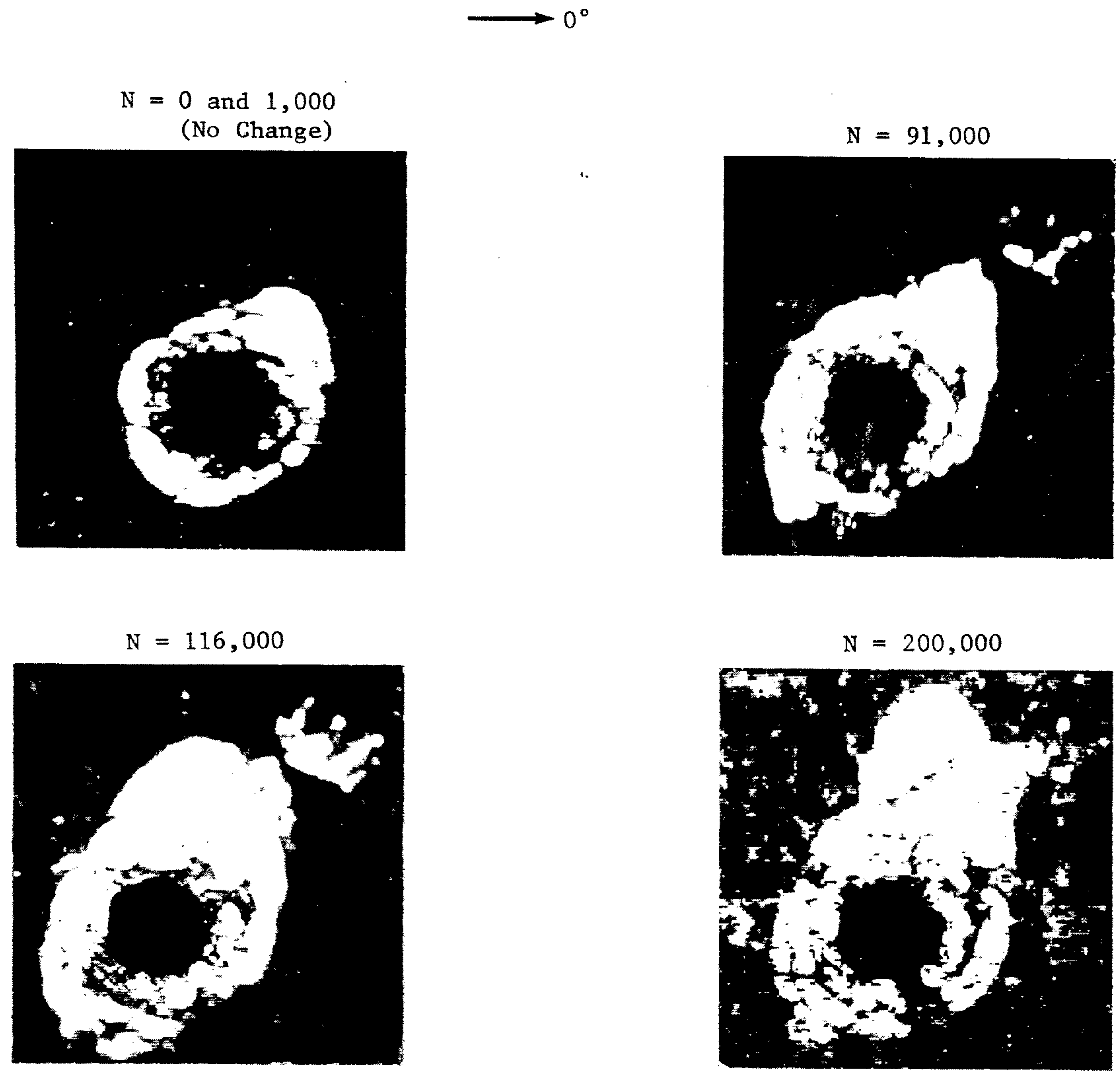

Figure 5A. Damage Growth Results for 32 ply Specimen CB-12 Containing a Damaged Hole. Maximum Stress = 17 ksi (117 MPa), R = -1

→ 0°

N = 422,000 N = 833,661 N = 1,065,000 N = 1,244,266

Figure 5B. Damage Growth Results for 32 ply Specimen CB-12 Containing a Damaged Hole. Maximum Stress = 17 ksi (117 MPa), R = -1 (Continued)

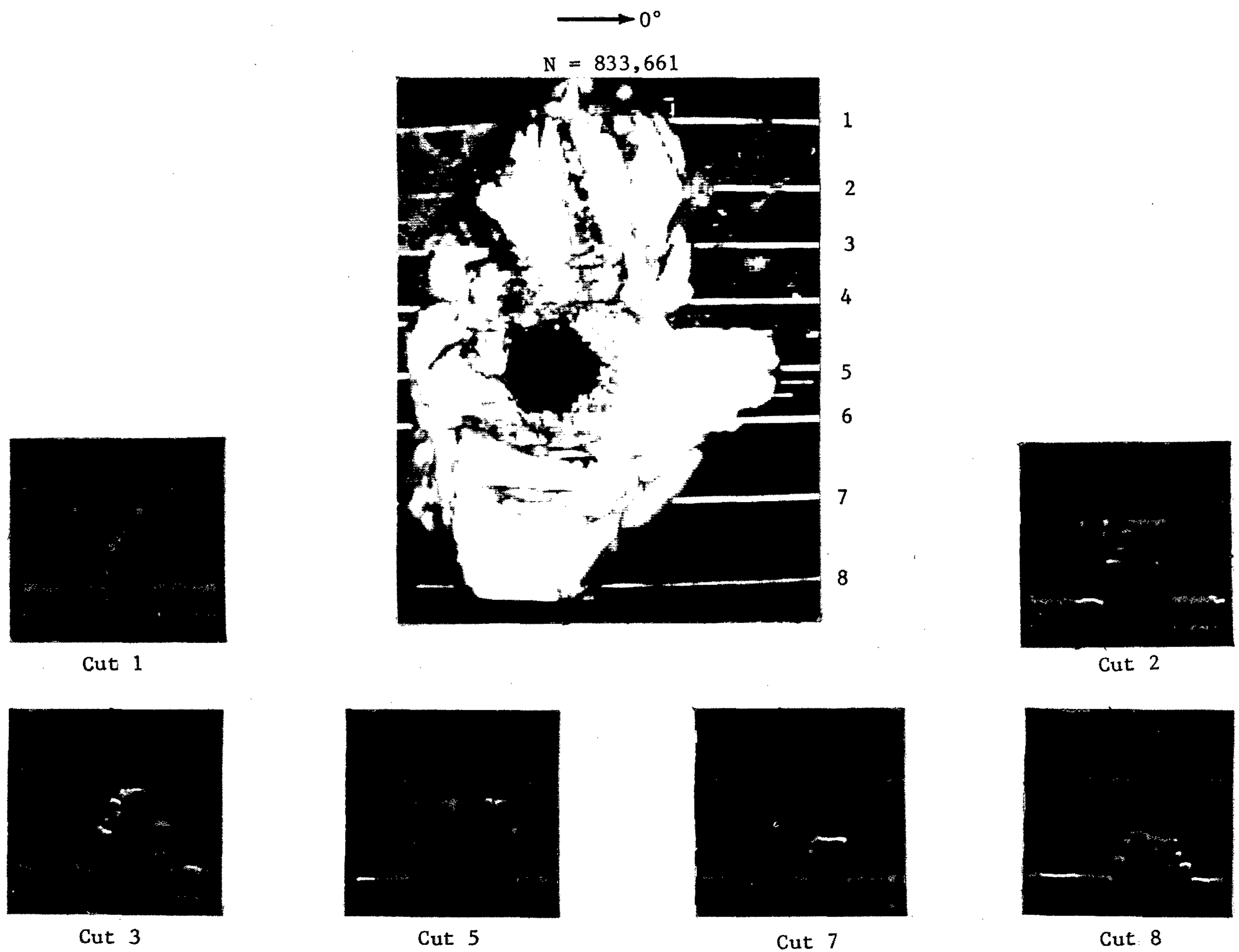

Figure 5C. Damage Growth Results for 32 ply Specimen CB-12 Containing a Damaged Hole. Maximum Stress = 17 ksi (117 MPa), R = -1

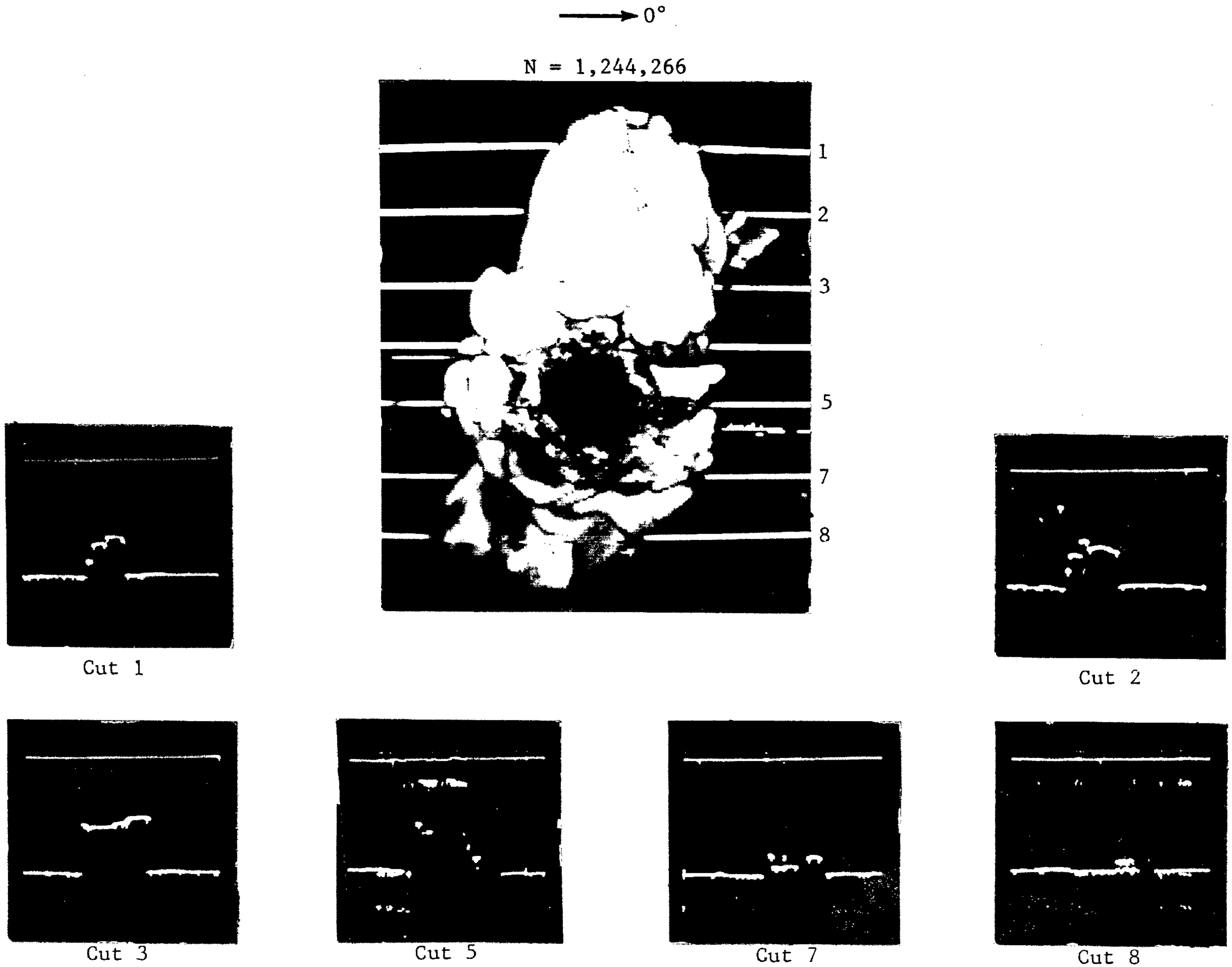

Figure 5D. Damage Growth Results for 32 ply Specimen CB-12 Containing a Damaged Hole. Maximum Stress = 17 ksi (117 MPa), R = -1

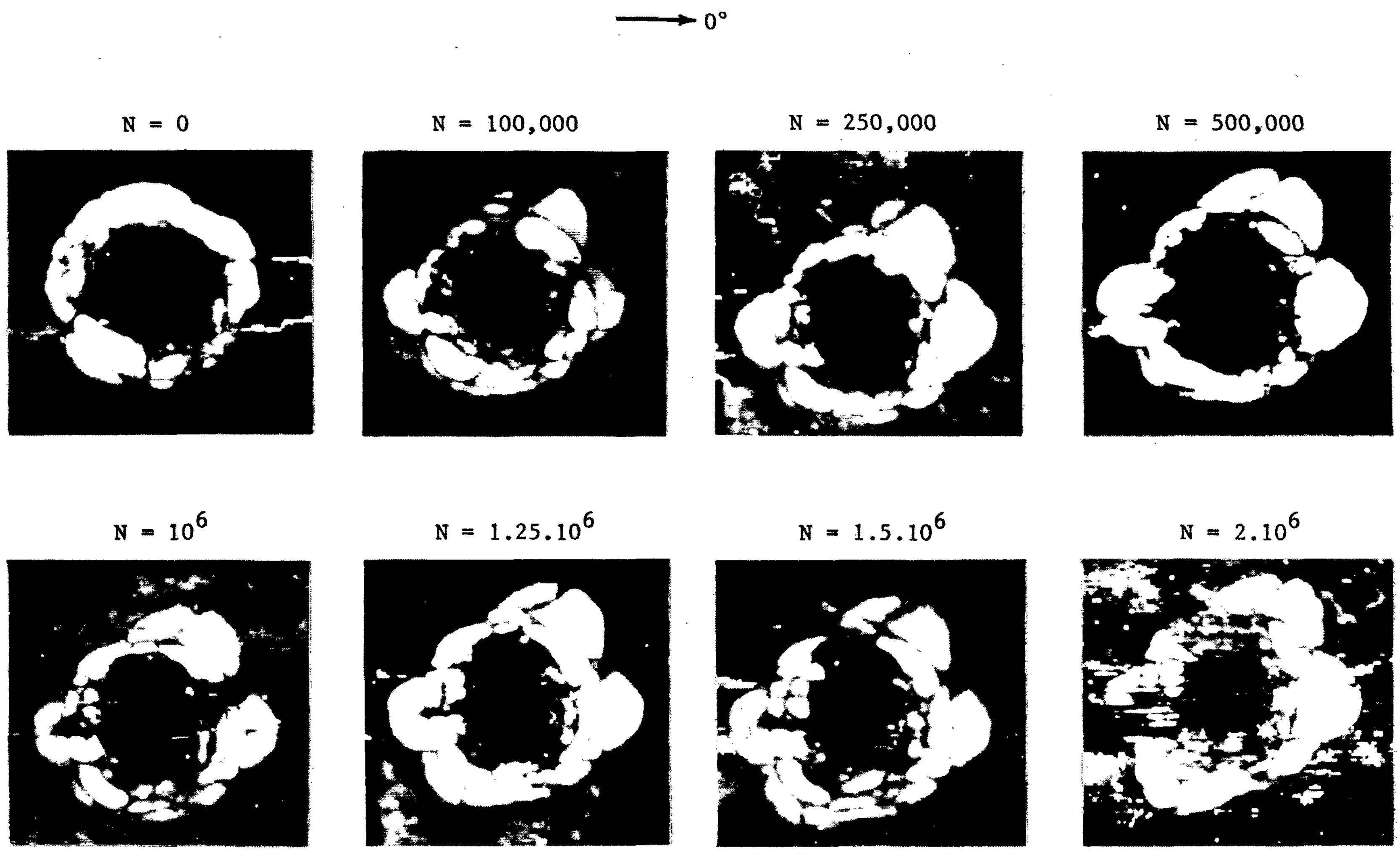

Figure 6A. Damage Growth Results for 32 ply Specimen AA-4 Containing a Damaged Hole. Maximum Stress = 14 ksi (96 MPa), R = -1

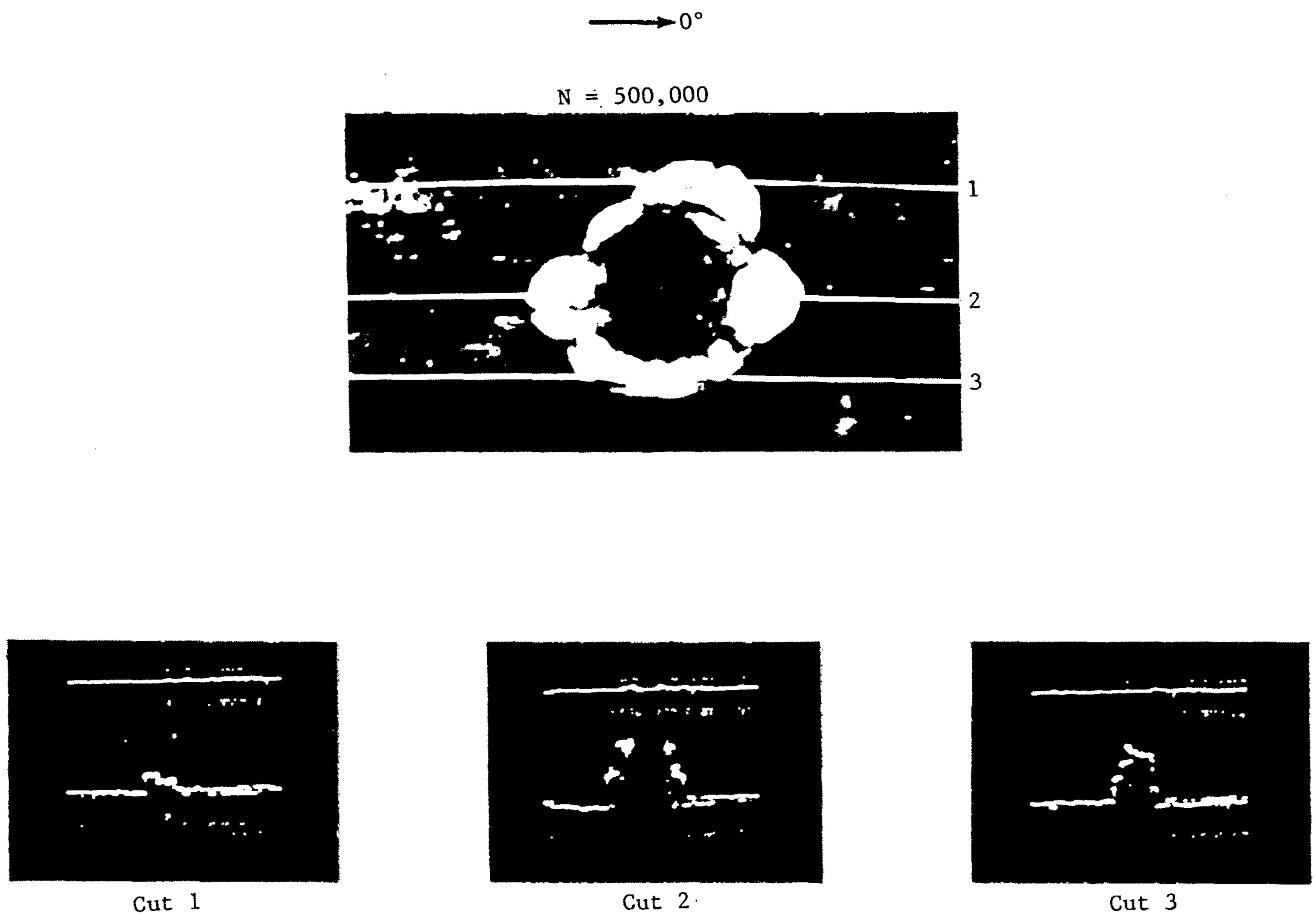

Figure 6B. Damage Growth Results for 32 ply Specimen AA-4 Containing a Damaged Hole. Maximum Stress = 14 ksi (96 MPa), R = -1

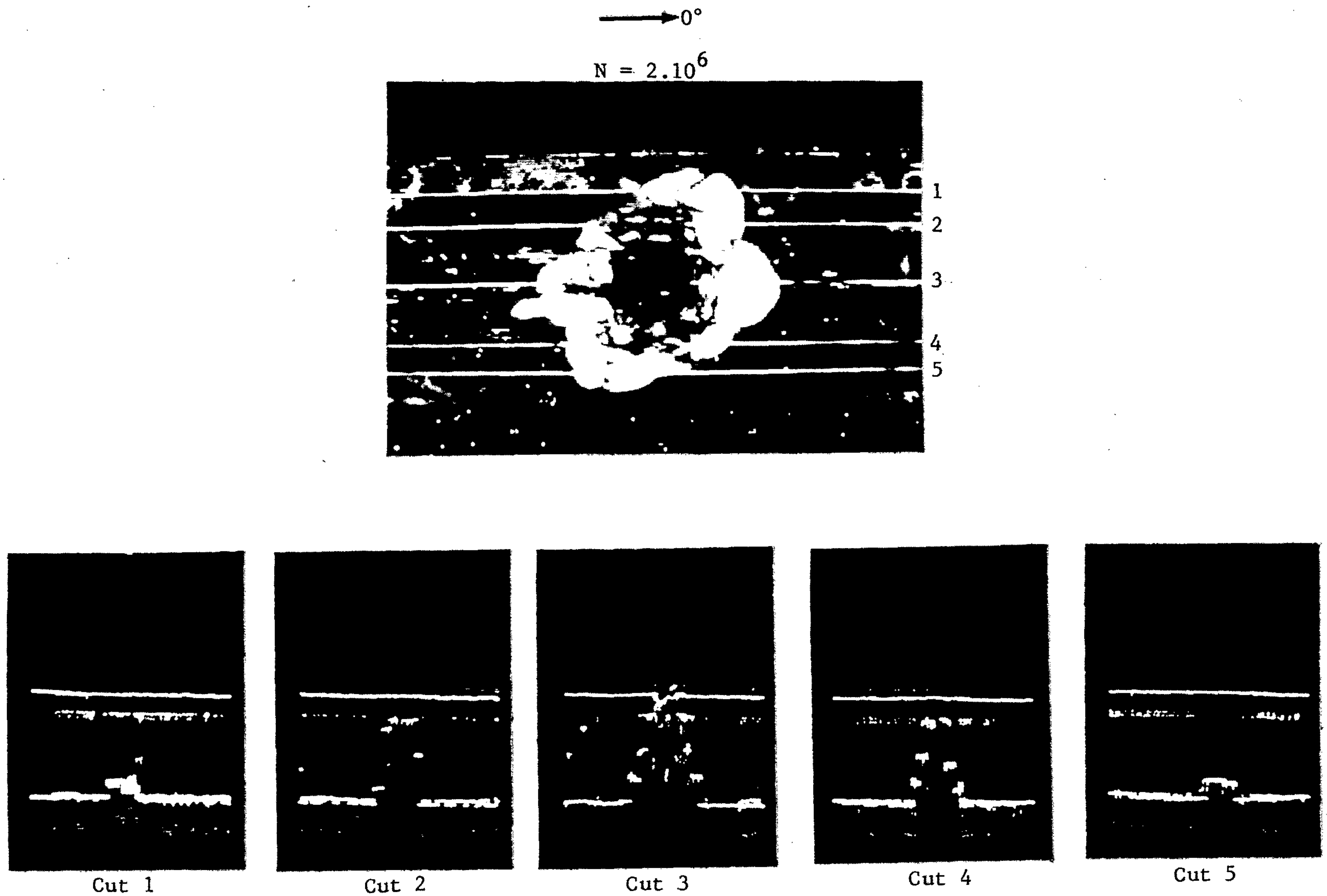

Figure 6C. Damage Growth Results for 32 ply Specimen AA-4 Containing a Damaged Hole. Maximum Stress = 14 ksi (96 MPa), R = -1

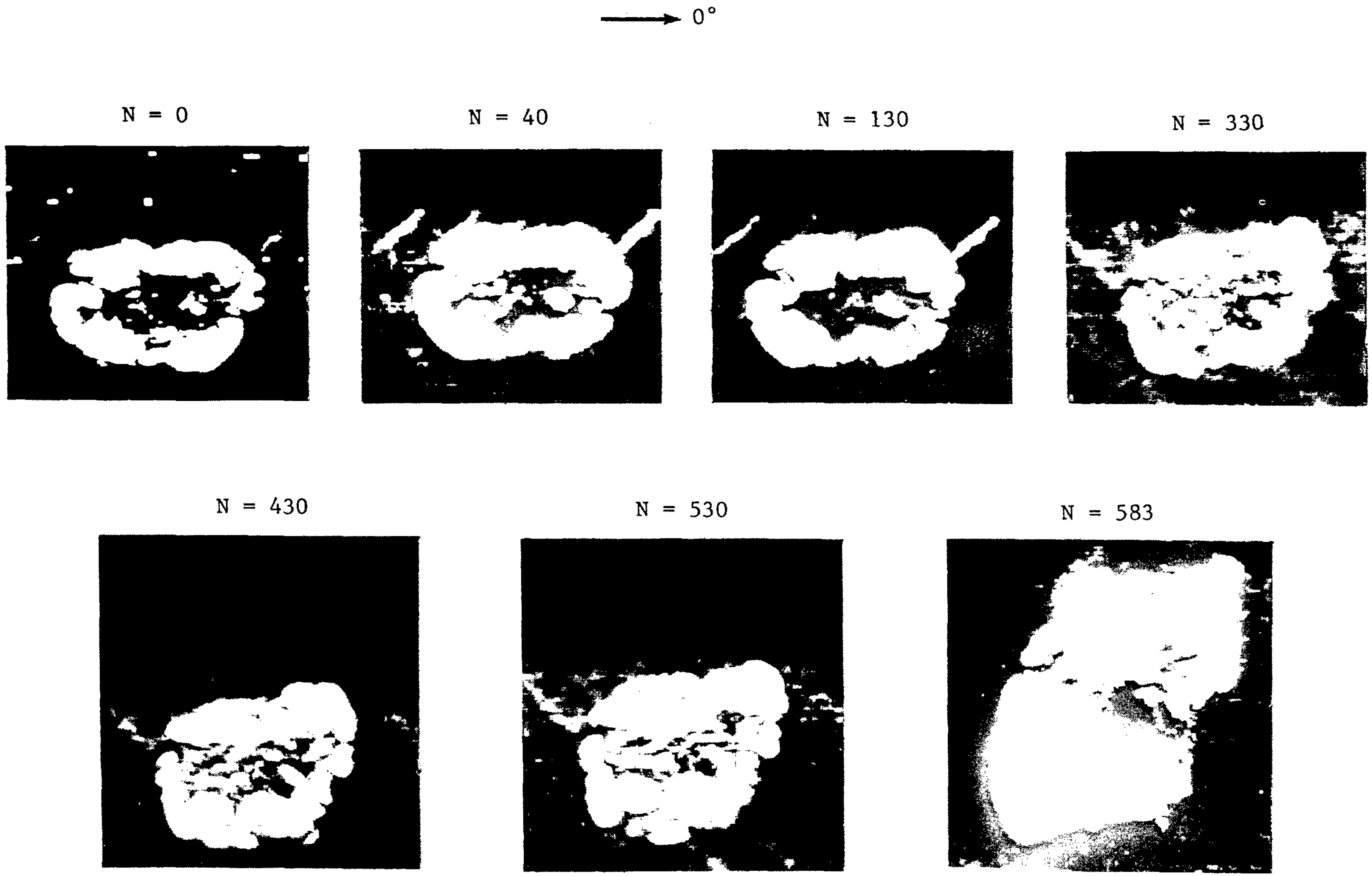

Figure 7A. Damage Growth Results for 24 ply Specimen MA-10 Containing Impact Damage. Maximum Stress = 45.5 ksi (313 MPa), R = -1

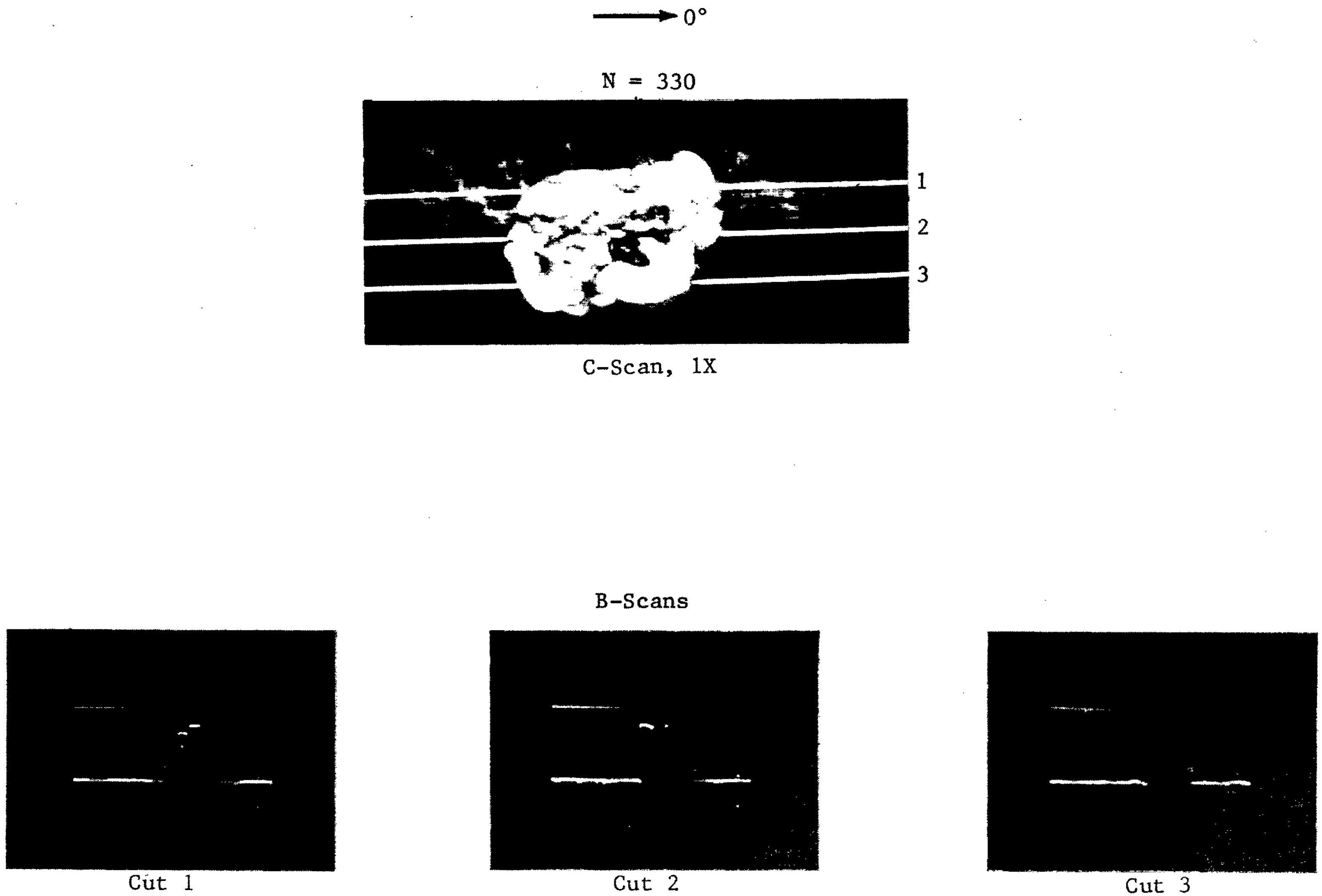

Figure 7B. Damage Growth Results for 24 ply Specimen MA-10 Containing Impact Damage. Maximum Stress = 45.5 ksi (313 MPa), R = −1

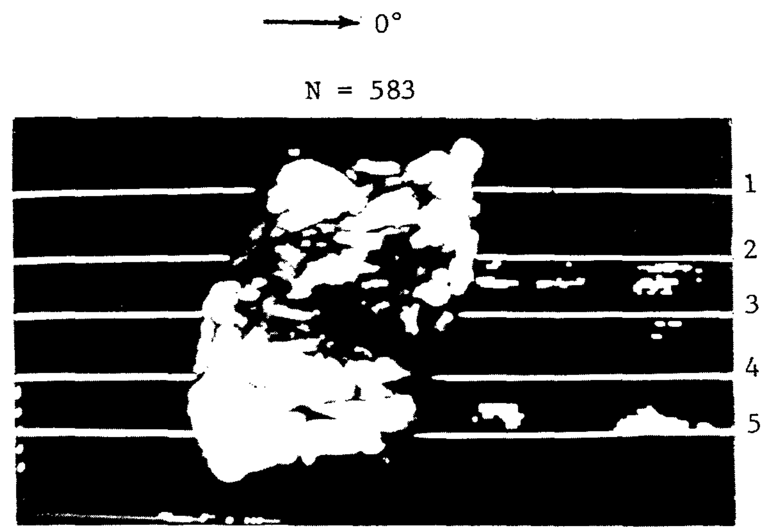

C-Scan, 1X

B-Scans

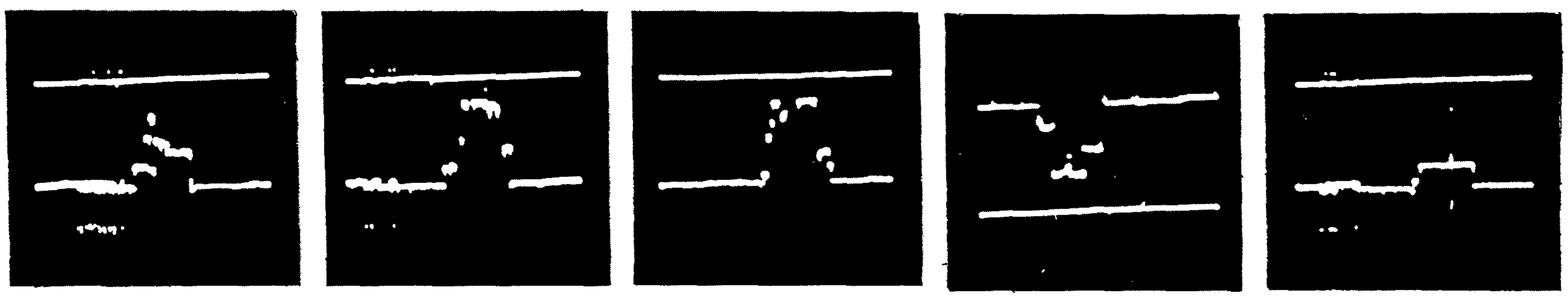

Cut 1 Cut 2 Cut 3 Cut 4 Cut 5

Figure 7C. Damage Growth Results for 24 ply Specimen MA-10 Containing Impact Damage, Maximum Stress = 45.5 ksi (313 MPa), R = -1

See Figure 83 - In Text

Figure 8. Damage Growth Results for 24-Ply Specimen JA-7 Containing Impact Damage. Maximum Stress = 42.75 ksi (295 MPa), R = -1

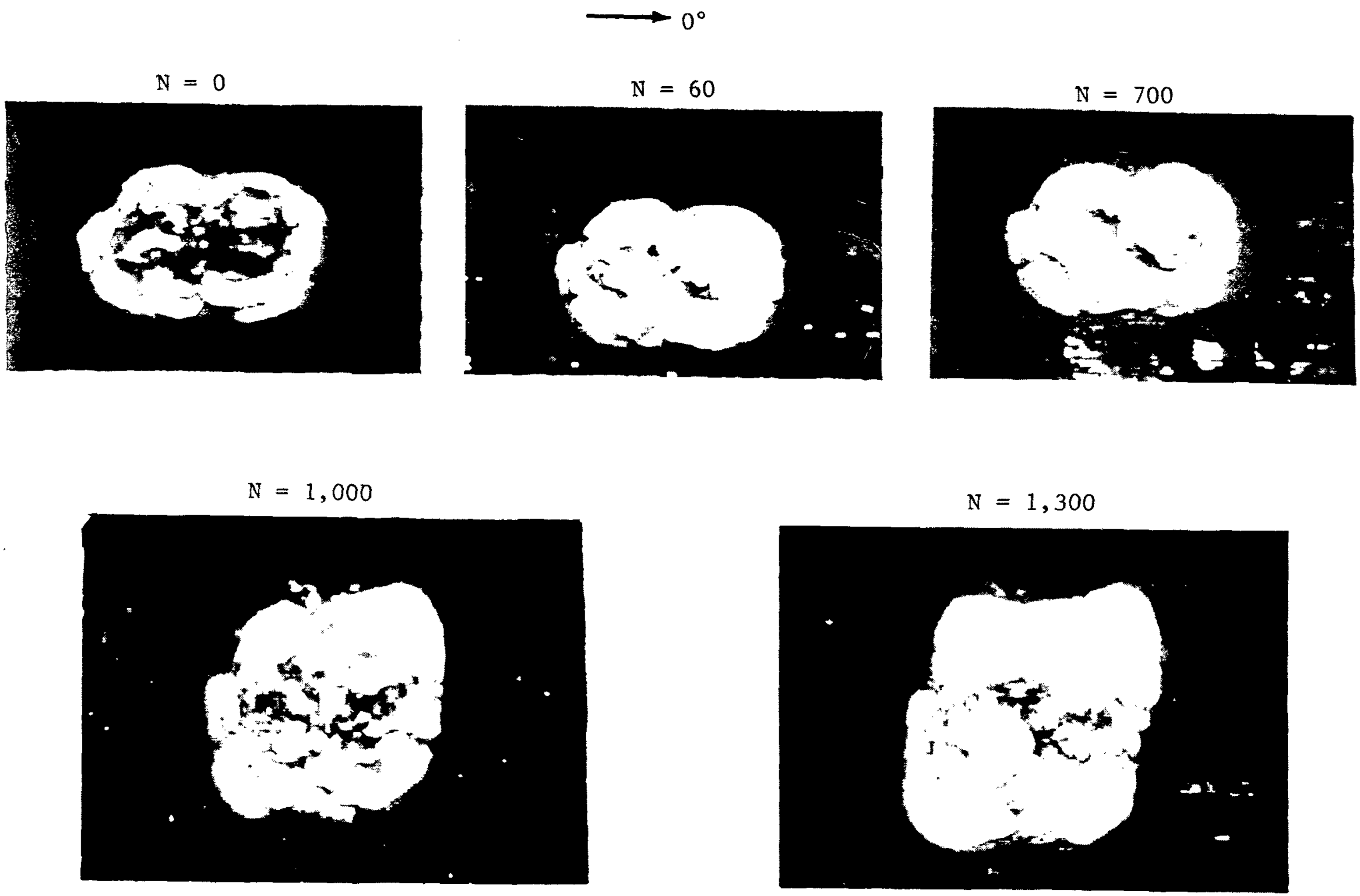

Figure 9A. Damage Growth Results for 24 ply Specimen HC25 Containing Impact Damage. Maximum Stress = 40.5 ksi (279 MPa), R = -1

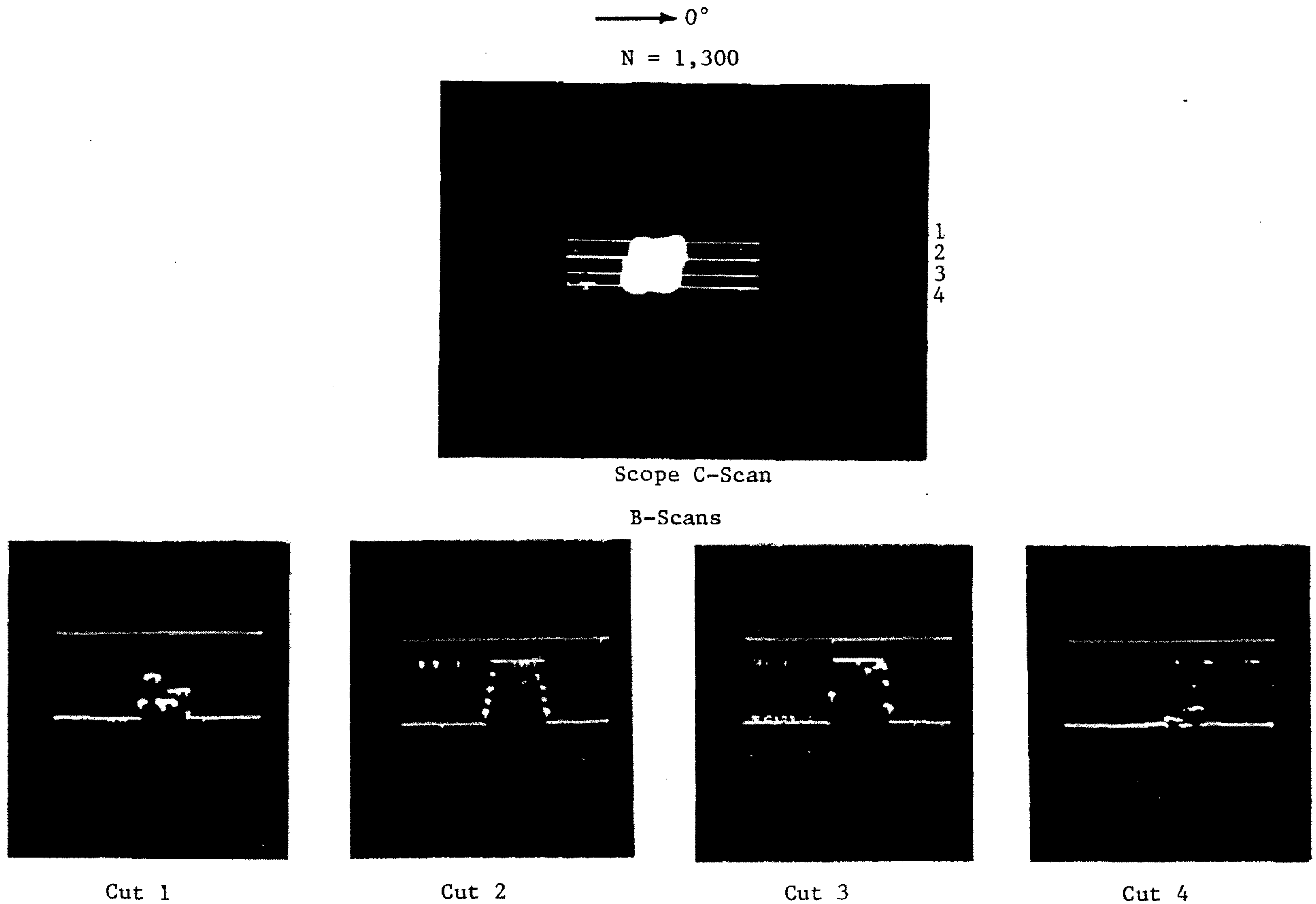

Figure 9B. Damage Growth Results for 24 ply Specimen HC25 Containing Impact Damage. Maximum Stress = 40.5 ksi (279 MPa), R = -1

See Figure 84 - In Text

Figure 10. Damage Growth Results for 24-Ply Specimen LC-22 Containing Impact Damage. Maximum Stress = 36.8 ksi (254 MPa), R = -1

See Figure 85 - In Text

Figure 11. Damage Growth Results for 24-Ply Specimen JC-22 Containing Impact Damage. Maximum Stress = 31.5 ksi (217 MPa), R = -1

0°

N = 0 N = 2,050,000

Figure 12. Damage Growth Results for 24 ply 67% 0° Fiber Specimen Containing Impact Damage, Maximum Stress = 27.6 ksi (190 MPa), R = -1

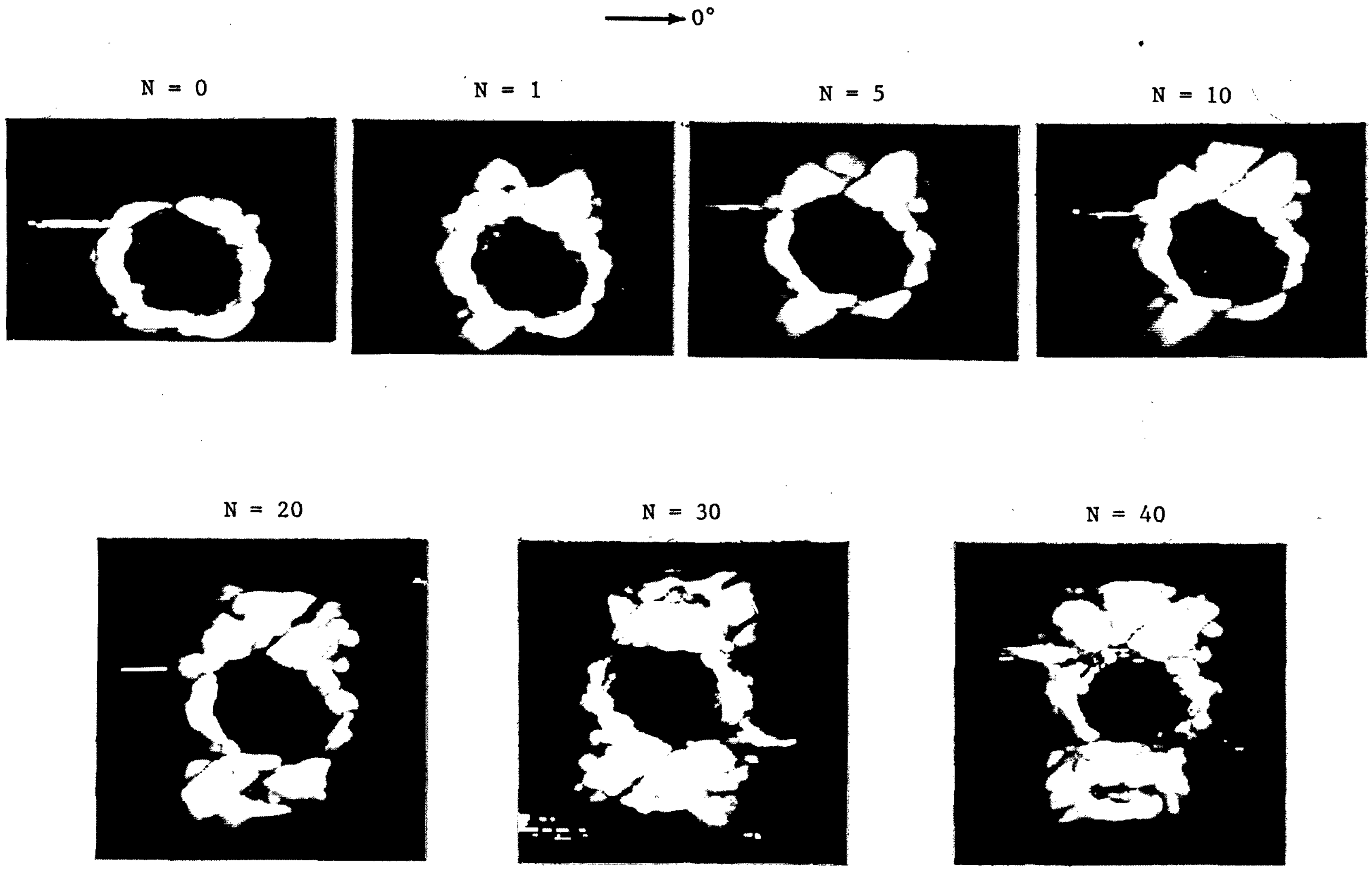

Figure 13A. Damage Growth Results for 24 ply Specimen JB-14 Containing a Damaged Hole. Maximum Stress = 44 ksi (303 MPa), R = -1

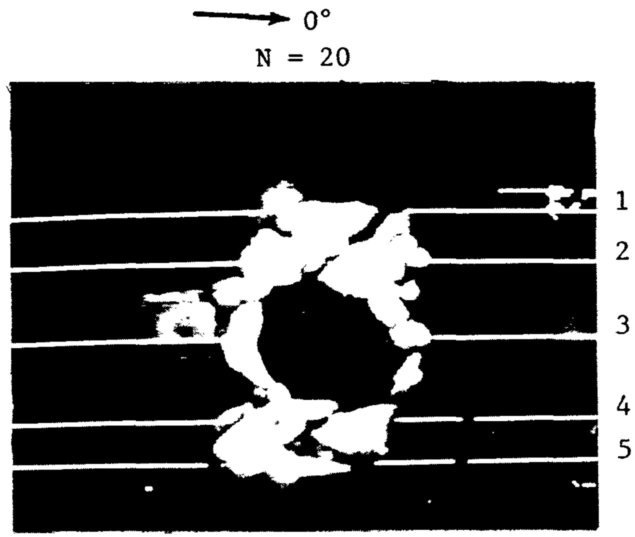

C-Scan, 1X

B-Scans

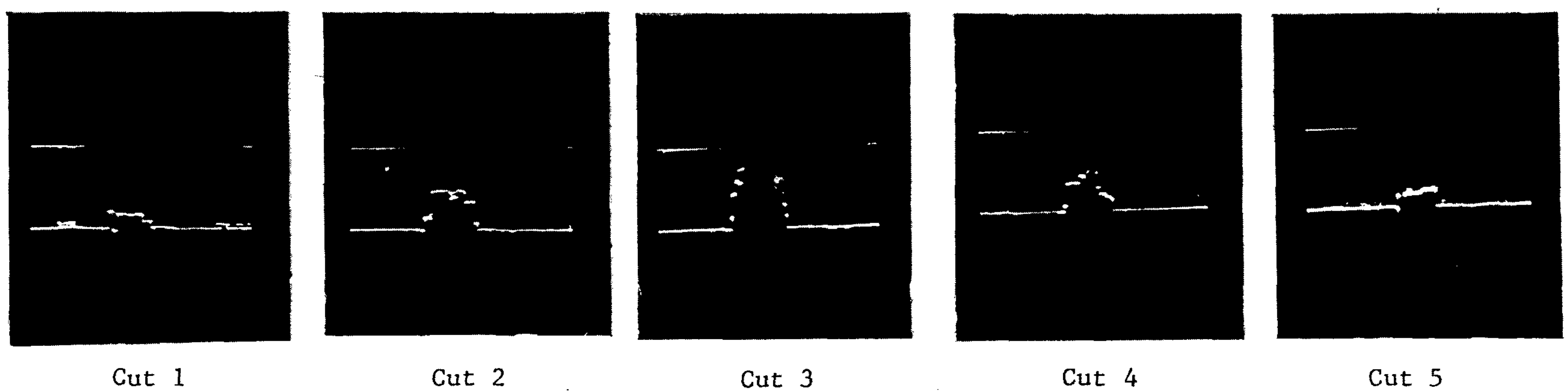

Figure 13B. Damage Growth Results for 24 ply Specimen JB-14 Containing a Damaged Hole. Maximum Stress = 44 ksi (303 MPa), R = -1

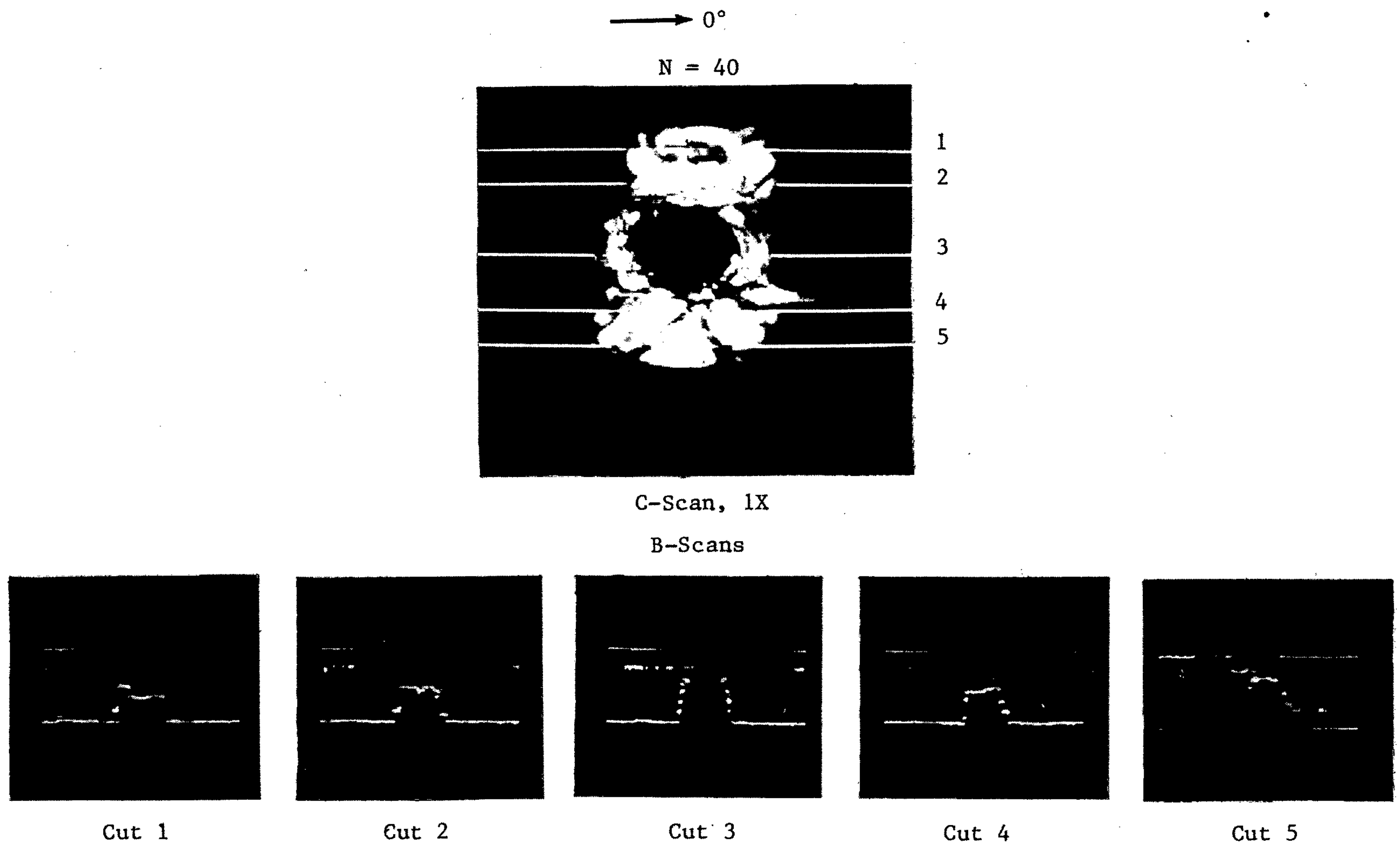

Figure 13C. Damage Growth Results for 24 ply Specimen JB-14 Containing a Damaged Hole. Maximum Stress = 44 ksi (303 MPa), R = -1

See Figure 76 - In Text

Figure 14. Damage Growth Results for 24-Ply Specimen LA-7 Containing a Damaged Hole. Maximum Stress = 41 ksi (283 MPa), R = -1

See Figure 71 - In Text

Figure 15. Damage Growth Results for 24-Ply Specimen JC-21 Containing a Damaged Hole. Maximum Stress = 38 ksi (262 MPa), R = -1

See Figure 75 - In Text

Figure 16. Damage Growth Results for 24-Ply Specimen JA-8 Containing a Damaged Hole. Maximum Stress = 34 ksi (234 MPa), R = -1

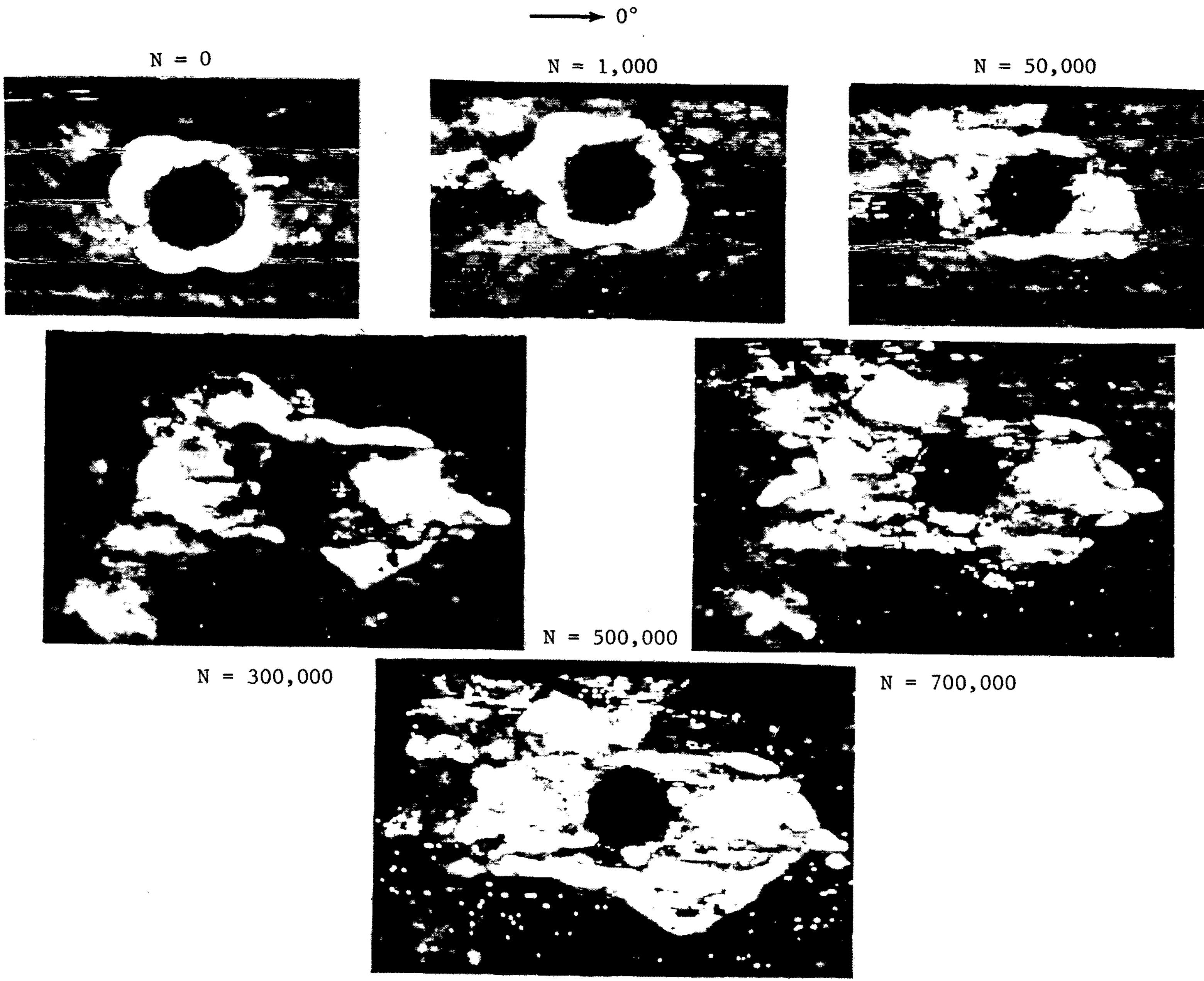

Figure 17A. Damage Growth Results for 24 ply Specimen LC-23 Containing a Damaged Hole. Maximum Stress = 30 ksi (207 MPa), R = -1

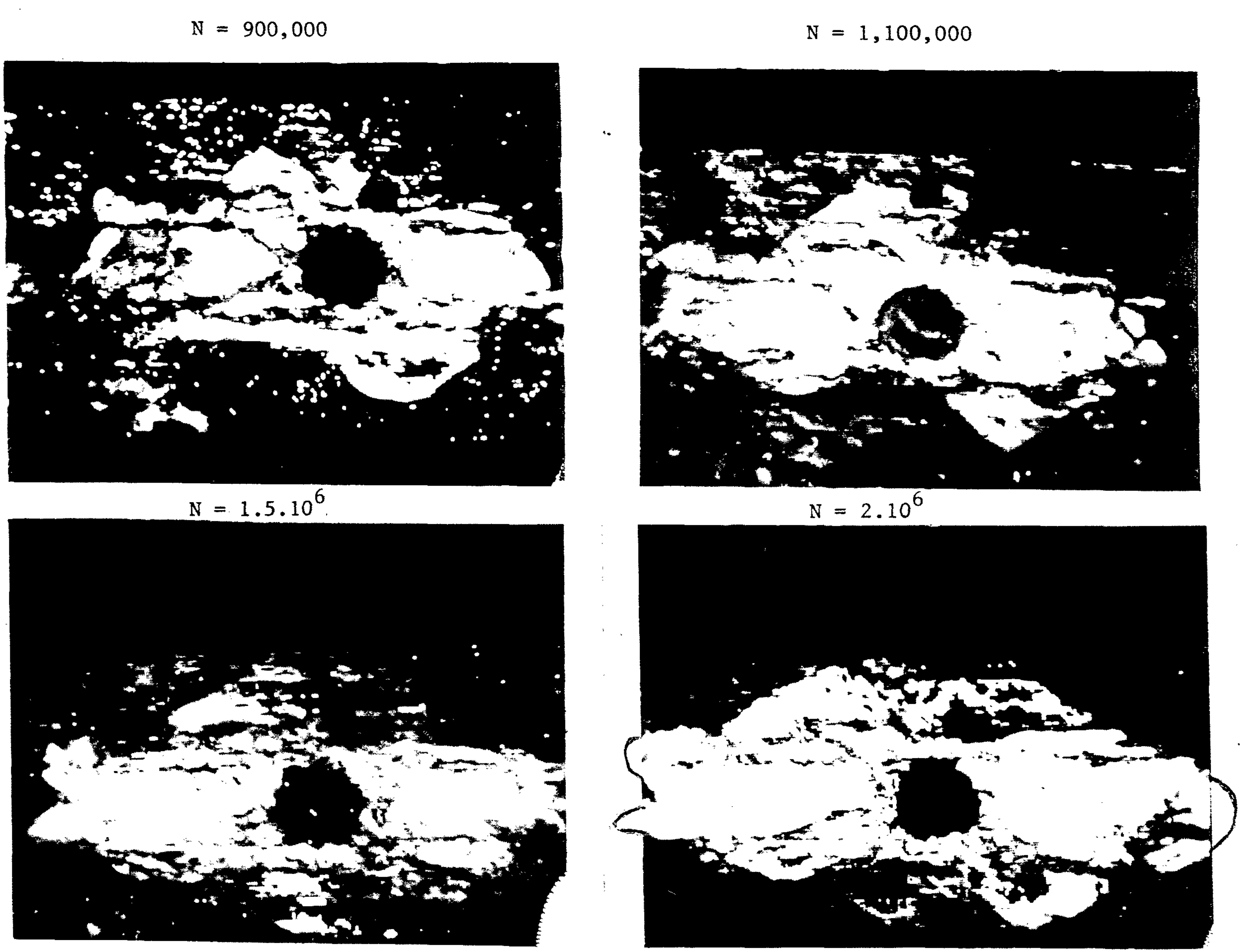

Figure 17B. Damage Growth Results for 24 ply Specimen LC-23 Containing a Damaged Hole. Maximum Stress = 30 ksi (207 MPa), R = -1

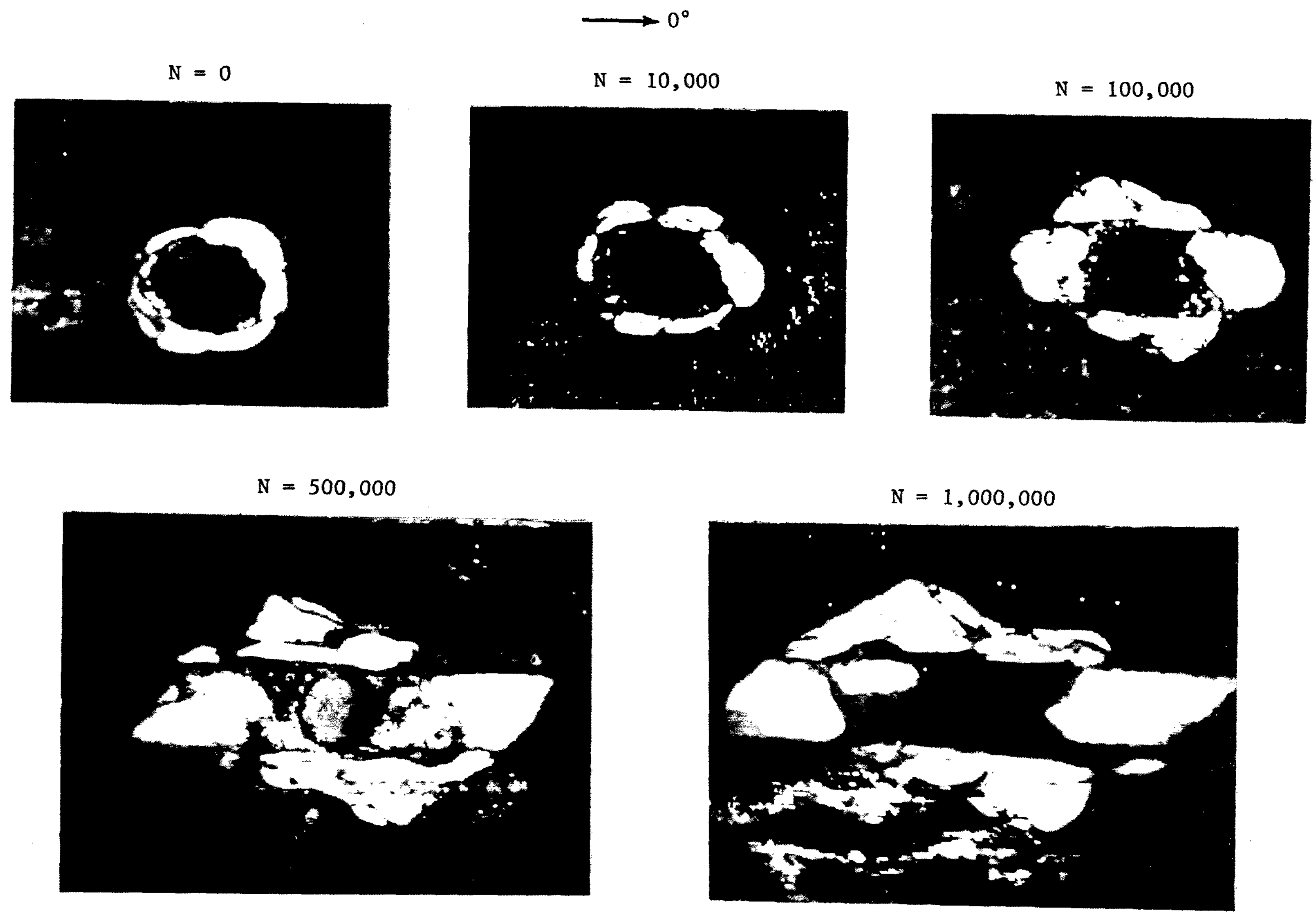

Figure 18A. Damage Growth Results for 24 ply Specimen MC-25 Containing a Damaged Hole. Maximum Stress = 26 ksi (179 MPa), R = -1

$\longrightarrow 0°$

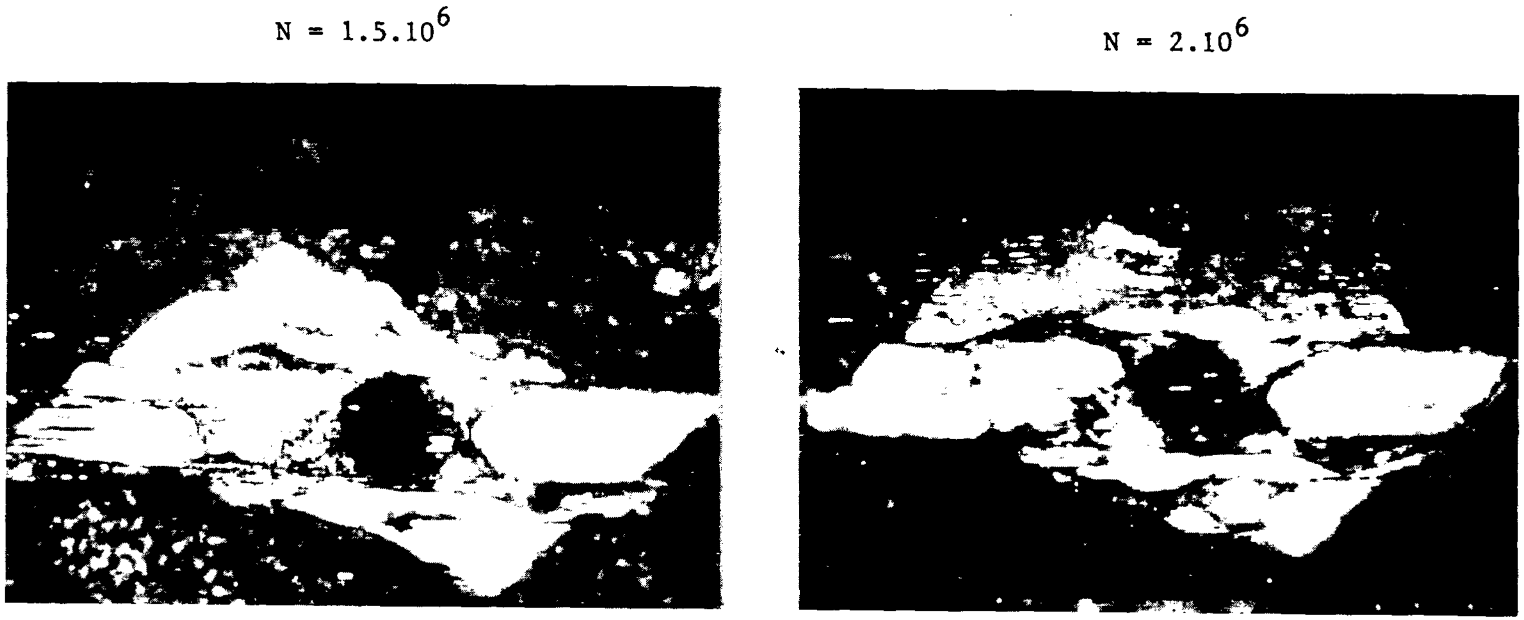

Figure 18B. Damage Growth Results for 24 ply Specimen MC-25 Containing a Damaged Hole. Maximum Stress = 26 ksi (179 MPa), R = -1

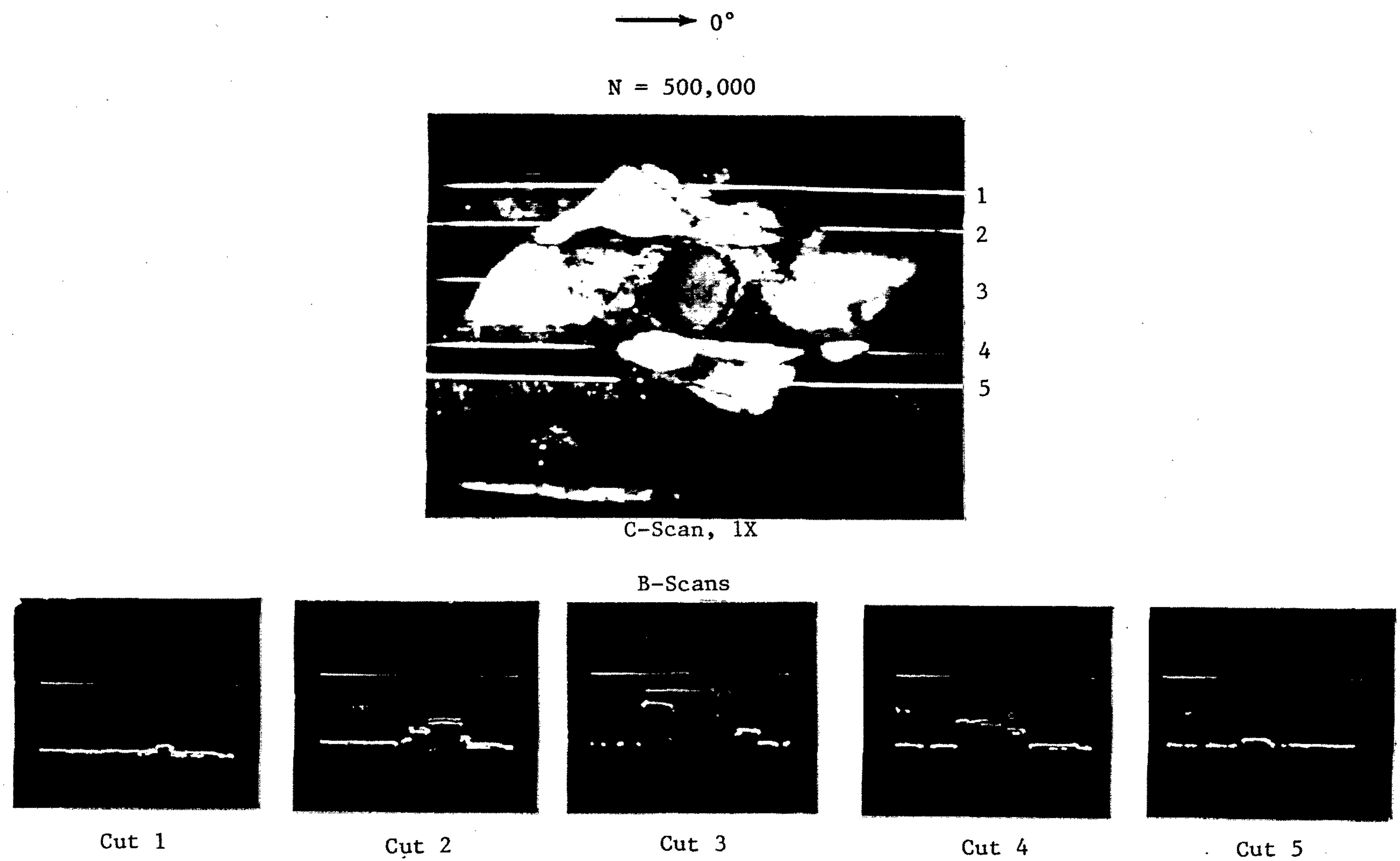

Figure 18C. Damage Growth Results for 24 ply Specimen MC-25 Containing a Damaged Hole. Maximum Stress = 26 ksi (179 MPa), R = -1

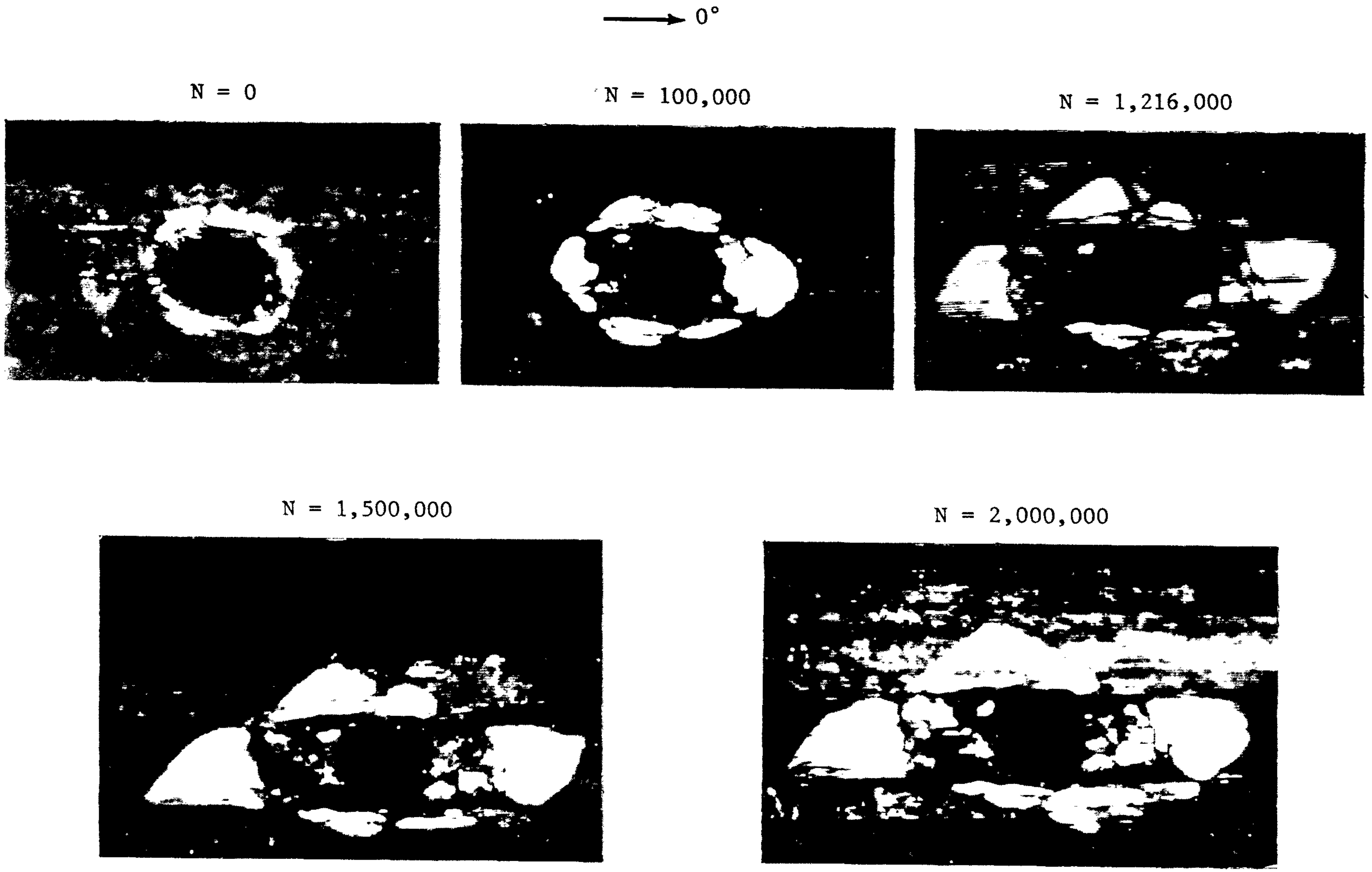

Figure 19A. Damage Growth Results for 24 ply Specimen JC-29 Containing a Damaged Hole. Maximum Stress = 23.0 ksi (158 MPa), R = -1

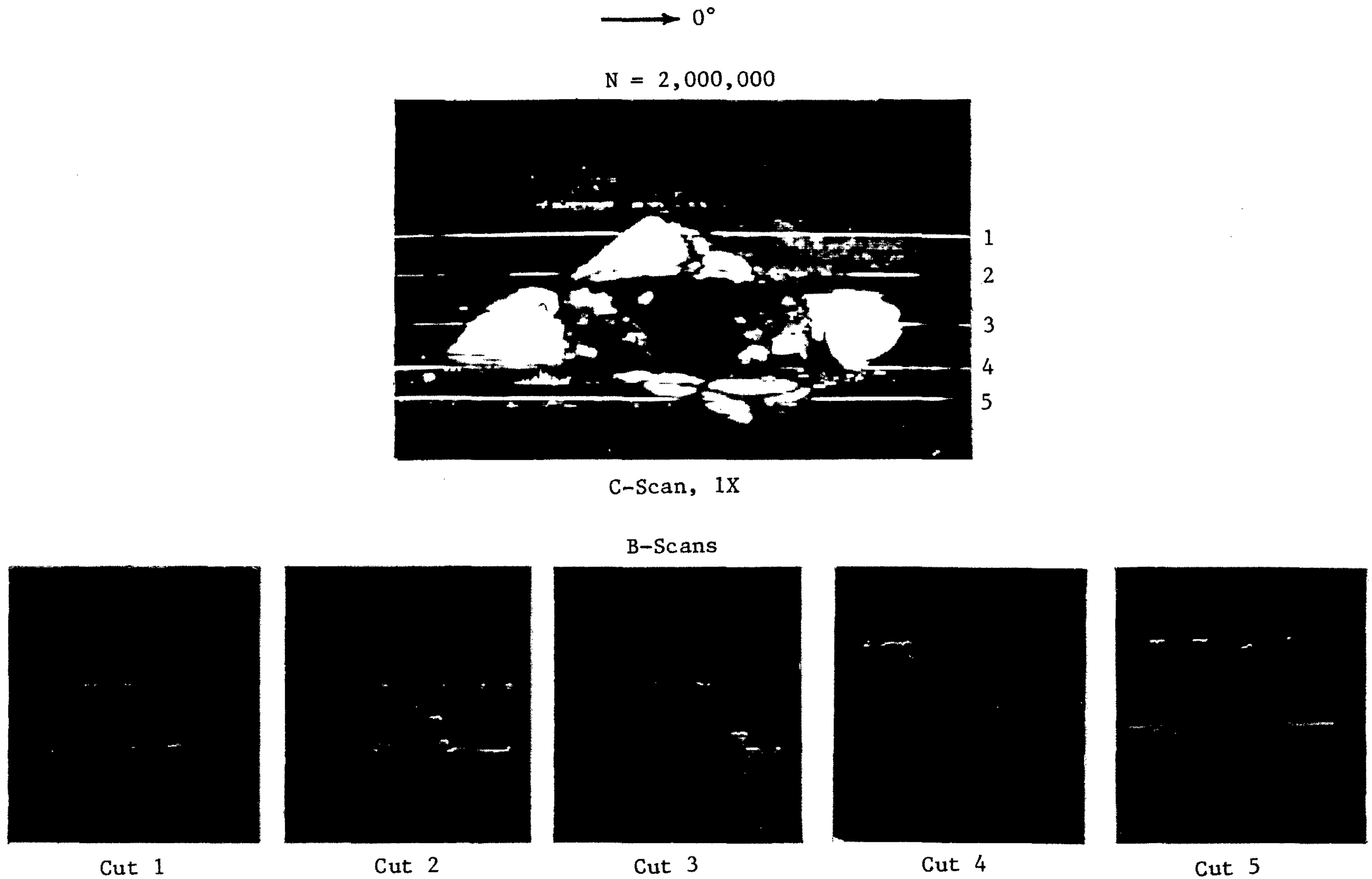

Figure 19B. Damage Growth Results for 24 ply Specimen JC-29 Containing a Damaged Hole. Maximum Stress = 23.0 ksi (158 MPa), R = -1

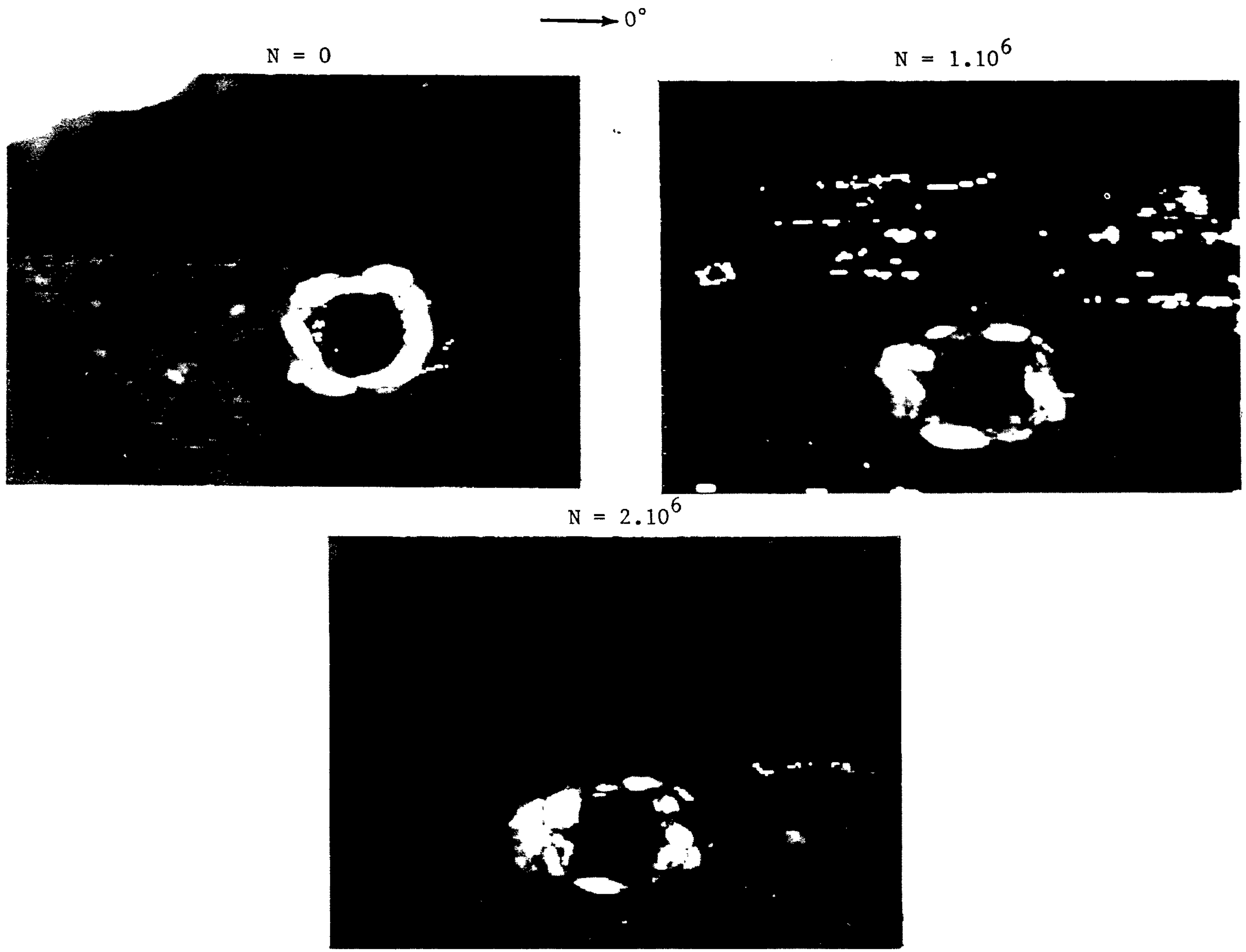

Figure 20. Damage Growth Results for 24 ply Specimen KC-29 Containing a Damaged Hole. Maximum Stress = 21 ksi (145 MPa), R = -1

REFERENCES

1. Pagano, N. J. and Pipes, R. B., "Some Observations on the Interlaminar Strength of Composite Laminates," Int. J. Mech. Sci., 1973, Vol. 15.

2. Ryder, J. T., and Walker, E. K., "Ascertainment of the Effect of Compressive Loading on the Fatigue Lifetime of Graphite Epoxy Laminates for Structural Applications," AFML-TR-76-241, Dec. 1976.

3. Pipes, R. Byron and Pagano, N. J., "Interlaminar Stresses in Composite Laminates Under Uniform Axial Extension," J. Comp. Materials, Vol. 4 (1970), p. 538.

4. Wang, A.S.D., and Crossman, F. W., "Some New Results on Edge Effect in Symmetric Composite Laminates," J. Comp. Materials, Vol. 11 (1977), p. 92.

5. Whitney, J. M. and Nuismer, R. J., "Stress Fracture Criteria for Laminated Composites Containing Stress Concentrations," J. Comp. Materials, Vol. 8, (1974), p. 253.

6. Daniel, I. M., Rowlands, R. E., and Whiteside, J. B., "Effects of Material and Stacking Sequence on Behavior of Composite Plates with Holes," Experimental Mechanics, Vol. 14 (1974), p. 1.

7. Altman, J., Konishi, D., Burroughs, B., Nodler, M. "Advanced Composites Servicibility Quarterly Progress Report," Rockwell International Corp., NA-76-783-1, Jan 1977.

8. Sendeckyj, G. P., Stalnaker, H. D., Kleismet, R. A., "Effect of Temperature on Fatigue Response of Surface Notched $(0/\pm 45/0)_{s\ 3}$ Graphite/Epoxy Laminate," Presented at ASTM D30 and E-9 Symposium on Fatigue of Filamentary Composite Materials, Denver, Colorado, Nov. 1976 (to be published as ASTM STP).

9. Pettit, D. E., "Experimental Techniques: Impact Damage of Composite Materials," Lockheed Report in progress, LR 28001, to be published.

10. Ligge, I. E., Hinshaw, J., Roy, P. A. and Olster, E. F., "Low-Weight Impact-Resistant Helicopter Drive Shafts," Composite Materials Testing and Design, ASTM STP 546 American Society for Testing and Materials, 1974, p. 651.

11. Nevadunsky, J. J., Lucas, J. J. and Salkind, M. J., "Early Fatigue Damage Detection in Composite Materials," J. Comp. Materials, Vol. 9 (1975) p. 394.

12. Chang, F. H., Gordon, D. E., and Gardner, A. H., "A Study of Fatigue Damage in Composites by Nondestructive Testing Techniques," Fatigue of Filamentary Composite Materials, ASTM STP 636, K. L. Reifsnider and K. N. Lauraitis, Eds., American Society for Testing and Materials, 1977, pp. 57 - 72.

13. Roderick, G. L. and Whitcomb, J. D., "Fatigue Damage of Notched Boron/ Epoxy Laminates Under Constant Amplitude Loading," Presented at ASTM E-9 and D30 Symposium on Fatigue of Filamentary Composite Materials, Denver, Colorado, Nov. 1976 (to be published as ASTM STP).

14. Phillips, E.P., "Effects of Truncation of a Predominantly Compression Load Spectrum on the Life of a Notched Graphite/Epoxy Laminate" Presented at ASTM D30 and E-9 Symposium on Fatigue of Composite Materials, San Francisco, Calif., 1979 (to be published as ASTM STP).

15. Knollman, G. C. et al., "Acoustic Imaging Techniques for Real-Time Nondestructive Testing," in Acoustical Holography (Plenum Press, New York, 1975), Vol. 6, p. 637.

16. Knollman, G. C., Weaver, J. L. Hartog, J. J., and Bellin, J. L., "Real-Time Ultrasonic Imaging Methodology in Nondestructive Testing," J. Acoust-Soc. Amer. 58, 455 (1975).

17. Sendeckyj, G. P., "Fatigue Damage Accumulation in $(0/\pm 45/90)_{2S}$ Graphite-Epoxy Laminates," Presented at ASTM Symposium on Fatigue of Fiberous Composite Materials," San Francisco, CA, May 22-23, 1979.

18. Pettit, D. E., "Characterization of Impact Damage in Composite Materials," Presented at ASTM - "Nondestructive Evaluation and Flow Criticality for Composite Materials Symposium," Oct. 10, 1978, Philadelphia, PA (To be published in STP.

19. Gumbel, E. J., Statistics of Extremes, Columbia University Press, New York, 1958.

20. Pettit, D. E., "Residual Strength Degradation for Advanced Composites," Interim Technical Quarterly Report, LR 28360-1, Lockheed-California Company, Burbank, CA, Nov. 11, 1977.

21. Certified Test Report No. 34255 Narmco Materials Inc., Costa Mesa, California, Sept. 16, 1977.

22. Quality Control Test Report for Laboratory Request No. 343931, Lockheed California Company, Burbank, California, October 13, 1977.

23. Pettit, D. E., "Experimental Techniques: Impact Damage of Composite Materials," Lockheed Report in progress, LR 28001, to be published.

24. Lauraitis, K. N., "Effect of Environment on the Compressive Strength of Laminated Epoxy Matrix Composites," Mechanics of Composites Review, U.S. AF., 25-27 Oct., 1977.

25. Lauraitis, K. N., "Effect of Environment on the Compressive Strengths of Laminated Epoxy Matrix Composites," Interim Technical Quarterly Report, LR 28508-1, Lockheed-California Company, Burbank, California, February 20, 1978.

26. Nuismer, R. J., and Whitney, J. M., "Uniaxial Failure of Composite Laminates Containing Stress Concentrations," Fracture Mechanics of Composites, ASTM STP 593, American Society for Testing and Materials, 1975, pp. 117-142.

27. Pengra, J. J., "Study of the Influence of Hole Quality on Composite Materials," Quarterly Progress Report, Contract NAS 1-15599, February 1979.

28. Wood, R. E., "Study of the Influence of Hole Quality on Composite Materials,", IR 28865, May 1979.

29. Test Report T15629, Delsen Testing Laboratories, Inc., Glendale, California August 31, 1978.

☆ U.S.Government Printing Office: 1982 — 559-005/4058